AD-A072 910 ROSENBLATT (M) AND SON INC NEW YORK F/G 13/10
EXAMINATION OF SERVICE AND STRESS DATA OF THREE SHIPS FOR DEVEL--ETC(U)
APR 79 J F DALZELL, N M MANIAR, M W HSU N00024-75-C-4324
UNCLASSIFIED SSC-287 NL

1 OF 3
ADA 072910

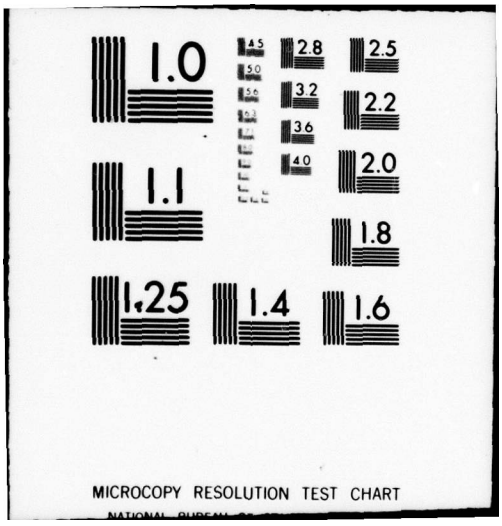
1.0
1.1
1.25
1.4
1.6
1.8
2.0
2.2
2.5
2.8
3.2
3.6
4.0
4.5
5.0
MICROCOPY RESOLUTION TEST CHART

SSC-287

LEVEL II

EXAMINATION OF SERVICE AND STRESS DATA OF THREE SHIPS FOR DEVELOPMENT OF HULL GIRDER LOAD CRITERIA

AD A022910

DDC FILE COPY

DDC RECEIVED AUG 21 1979 C

This document has been approved for public release and sale; its distribution is unlimited.

SHIP STRUCTURE COMMITTEE

1979

79 08 17 009

SSC-287 EXAMINATION OF SERVICE AND STRESS DATA

Member Agencies:
United States Coast Guard
Naval Sea Systems Command
Military Sealift Command
Maritime Administration
United States Geological Survey
American Bureau of Shipping

Ship Structure Committee

An Interagency Advisory Committee
Dedicated to Improving the Structure of Ships

Address Correspondence to:
Secretary, Ship Structure Committee
U.S. Coast Guard Headquarters,(G-M/82)
Washington, D.C. 20590

SR-1227

JUNE 1979

The development of a rational procedure for determining the loads which a ship's hull must withstand is a primary goal of the Ship Structure Committee. The long-term goal is to bring about a stage of ship design in which load criteria can be established directly from analysis of the expected seaway, the strength and flexibility characteristics of the hull, and the interaction between the ship structures and the sea.

Considerable research activity has been devoted to theoretical studies on the prediction of hull loads and to measurements of response, both on models and on ships at sea. A first effort into the synthesis of the results of these diverse efforts into a rational load criteria was published in 1973 as SSC-240, *LOAD CRITERIA FOR SHIP STRUCTURAL DESIGN*.

Subsequently, the Ship Structure Committee undertook the present project to apply the statistically based load predictions to those ships for which actual stress records and service repair histories were available. This report describes the results of that project.

Henry H. Bell
Rear Admiral, U.S. Coast Guard
Chairman, Ship Structure Committee

UNCLASSIFIED

SECURITY CLASSIFICATION OF THIS PAGE (When Data Entered)

REPORT DOCUMENTATION PAGE	READ INSTRUCTIONS BEFORE COMPLETING FORM
1. REPORT NUMBER: SSC-287	2. GOVT ACCESSION NO. / 3. RECIPIENT'S CATALOG NUMBER
4. TITLE (and Subtitle): EXAMINATION OF SERVICE AND STRESS DATA OF THREE SHIPS FOR DEVELOPMENT OF HULL GIRDER LOAD CRITERIA.	5. TYPE OF REPORT & PERIOD COVERED: FINAL REPORT.
	6. PERFORMING ORG. REPORT NUMBER: SF 43 422 703
7. AUTHOR(s): J. F. Dalzell, N. M. Maniar and M. W. Hsu	8. CONTRACT OR GRANT NUMBER(s): N00024-75-C-4324
9. PERFORMING ORGANIZATION NAME AND ADDRESS: M. Rosenblatt & Son, Inc. New York, N.Y. 10013	10. PROGRAM ELEMENT, PROJECT, TASK AREA & WORK UNIT NUMBERS
11. CONTROLLING OFFICE NAME AND ADDRESS: Department of the Navy Naval Ship Engineering Center Washington, D.C. 20362	12. REPORT DATE: April 1979 / 13. NUMBER OF PAGES: 180
14. MONITORING AGENCY NAME & ADDRESS (if different from Controlling Office): Ship Structure Committee U. S. Coast Guard Headquarters Washington, D.C. 20690	15. SECURITY CLASS. (of this report): UNCLASSIFIED / 15a. DECLASSIFICATION/DOWNGRADING SCHEDULE
16. DISTRIBUTION STATEMENT (of this Report): UNLIMITED	62543N
17. DISTRIBUTION STATEMENT (of the abstract entered in Block 20, if different from Report): UNLIMITED	F43422
18. SUPPLEMENTARY NOTES	
19. KEY WORDS (Continue on reverse side if necessary and identify by block number)	
20. ABSTRACT (Continue on reverse side if necessary and identify by block number): This is a follow-on project to SSC-240, "Load Criteria for Ship Structural Design", which proposed methods for the estimation and superposition of the primary loads and performed sample calculations for one conventional dry cargo ship. It involved the following bending moments: 404 192 (cont.)	

DD FORM 1 JAN 73 1473 EDITION OF 1 NOV 65 IS OBSOLETE S/N 0102-014-6601

UNCLASSIFIED

SECURITY CLASSIFICATION OF THIS PAGE (When Data Entered)

SSC-287

FINAL REPORT

on

Project SR-1227

"Load Criteria Application"

EXAMINATION OF SERVICE AND STRESS DATA OF THREE SHIPS FOR DEVELOPMENT OF HULL GIRDER LOAD CRITERIA

by

J. F. Dalzell

Stevens Institute of Technology

and

N. M. Maniar and
M. W. Hsu

M. Rosenblatt & Son, Inc.

under

Department of the Navy
Naval Ship Engineering Center
Contract No. N00024-75-C-4324

This document has been approved for public release and sale; its distribution is unlimited.

U. S. Coast Guard Headquarters
Washington, D.C.
1979

- Still-water due to weight and buoyancy;
- Ship's own wave train;
- Quasi-static wave-induced, vertical and lateral combined;
- Dynamic loads, including slamming, whipping and springing; and
- Thermal effects.

Here the service and full-scale stress data of three larger and/or faster ships (Containership SL-7, Bulk Carrier FOTINI-L and very large Crude Carrier UNIVERSE IRELAND) are examined for the purpose of the eventual development of hull-girder criteria. The examination is limited to extreme midship bending moment loads which are related to the ultimate strength.

An assessment is made of the compatibility between the service and stress data of the distinctly different study ships and the analysis methods of SSC-240 and their assumptions for cargo ship type.

Considerable insight is obtained into the probable correct mathematical approximations of the loads and their interrelationships.

It appears that still-water bending moments can be approached probabilistically, however, considerable additional information on experienced loading conditions must be gathered to determine the statistical distributions.

Additional effort is required to determine the suitable probabilistic expression and a synthesis method for the contribution of vibration to the extreme load.

Accession For
NTIS GRA&I
DDC TAB
Unannounced
Justification
By
Distribution/
Availability Codes
Dist | Avail and/or special
A

79 08 17 009

METRIC CONVERSION FACTORS

Approximate Conversions to Metric Measures

Symbol	When You Know	Multiply by	To Find	Symbol
	LENGTH			
in	inches	*2.5	centimeters	cm
ft	feet	30	centimeters	cm
yd	yards	0.9	meters	m
mi	miles	1.6	kilometers	km
	AREA			
in^2	square inches	6.5	square centimeters	cm^2
ft^2	square feet	0.09	square meters	m^2
yd^2	square yards	0.8	square meters	m^2
mi^2	square miles	2.6	square kilometers	km^2
	acres	0.4	hectares	ha
	MASS (weight)			
oz	ounces	28	grams	g
lb	pounds	0.45	kilograms	kg
	short tons (2000 lb)	0.9	tonnes	t
	VOLUME			
tsp	teaspoons	5	milliliters	ml
Tbsp	tablespoons	15	milliliters	ml
fl oz	fluid ounces	30	milliliters	ml
c	cups	0.24	liters	l
pt	pints	0.47	liters	l
qt	quarts	0.95	liters	l
gal	gallons	3.8	liters	l
ft^3	cubic feet	0.03	cubic meters	m^3
yd^3	cubic yards	0.76	cubic meters	m^3
	TEMPERATURE (exact)			
°F	Fahrenheit temperature	5/9 (after subtracting 32)	Celsius temperature	°C

*1 in = 2.54 (exactly). For other exact conversions and more detailed tables, see NBS Misc. Publ. 286, Units of Weights and Measures, Price $2.25, SD Catalog No. C13.10:286.

Approximate Conversions from Metric Measures

Symbol	When You Know	Multiply by	To Find	Symbol
	LENGTH			
mm	millimeters	0.04	inches	in
cm	centimeters	0.4	inches	in
m	meters	3.3	feet	ft
m	meters	1.1	yards	yd
km	kilometers	0.6	miles	mi
	AREA			
cm^2	square centimeters	0.16	square inches	in^2
m^2	square meters	1.2	square yards	yd^2
km^2	square kilometers	0.4	square miles	mi^2
ha	hectares (10,000 m^2)	2.5	acres	
	MASS (weight)			
g	grams	0.035	ounces	oz
kg	kilograms	2.2	pounds	lb
t	tonnes (1000 kg)	1.1	short tons	
	VOLUME			
ml	milliliters	0.03	fluid ounces	fl oz
l	liters	2.1	pints	pt
l	liters	1.06	quarts	qt
l	liters	0.26	gallons	gal
m^3	cubic meters	35	cubic feet	ft^3
m^3	cubic meters	1.3	cubic yards	yd^3
	TEMPERATURE (exact)			
°C	Celsius temperature	9/5 (then add 32)	Fahrenheit temperature	°F

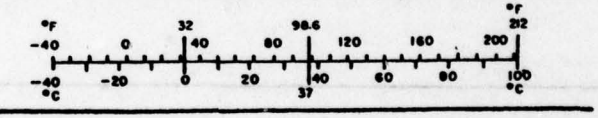

SHIP STRUCTURE COMMITTEE

The SHIP STRUCTURE COMMITTEE is constituted to prosecute a research program to improve the hull structures of ships and other marine structures by an extension of knowledge pertaining to design, materials and methods of construction.

RADM H. N. Bell (Chairman)
Chief, Office of Merchant Marine Safety
U. S. Coast Guard Headquarters

Mr. P. M. Palermo
Assistant for Structures
Naval Ship Engineering Center
Naval Sea Systems Command

Mr. W. N. Hannan
Vice President
American Bureau of Shipping

Mr. M. Pitkin
Assistant Administrator for Commercial Development
Maritime Administration

Mr. R. B. Krahl
Chief, Branch of Marine Oil and Gas Operations
U. S. Geological Survey

Mr. C. J. Whitestone
Chief Engineer
Military Sealift Command

LCDR T. H. Robinson, U. S. Coast Guard (Secretary)

SHIP STRUCTURE SUBCOMMITTEE

The SHIP STRUCTURE SUBCOMMITTEE acts for the Ship Structure Committee on technical matters by providing technical coordination for the determination of goals and objectives of the program, and by evaluating and interpreting the results in terms of structural design, construction and operation.

U. S. COAST GUARD

Cdr. J. C. Card
Lcdr S. H. Davis
Capt C. B. Glass
Dr. W. C. Dietz

NAVAL SEA SYSTEMS COMMAND

Mr. R. Chiu
Mr. R. Johnson
Mr. G. Sorkin
Mr. J. B. O'Brien (Contracts Admin.)

MARITIME ADMINISTRATION

Mr. F. J. Dashnaw
Mr. N. O. Hammer
Mr. F. Seibold
Mr. M. Touma

NATIONAL ACADEMY OF SCIENCES
SHIP RESEARCH COMMITTEE

Mr. O. H. Oakley - Liaison
Mr. R. W. Rumke - Liaison

SOCIETY OF NAVAL ARCHITECTS & MARINE ENGINEERS

Mr. A. B. Stavovy - Liaison

WELDING RESEARCH COUNCIL

Mr. K. H. Koopman - Liaison

MILITARY SEALIFT COMMAND

Mr. T. W. Chapman
Mr. A. B. Stavovy
Mr. D. Stein
Mr. J. Torresen

AMERICAN BUREAU OF SHIPPING

Dr. H. Y. Jan
Mr. D. Liu
Mr. I. L. Stern
Mr. S. G. Stiansen (Chairman)

U. S. GEOLOGICAL SURVEY

Mr. R. Giangerelli
Mr. J. Gregory

INTERNATIONAL SHIP STRUCTURES CONGRESS

Prof. J. H. Evans - Liaison

AMERICAN IRON & STEEL INSTITUTE

Mr. R. H. Sterne - Liaison

STATE UNIV. OF NEW YORK MARITIME COLLEGE

Dr. W. R. Porter - Liaison

U. S. COAST GUARD ACADEMY

Capt W. C. Nolan - Liaison

U. S. NAVAL ACADEMY

Dr. R. Battacharyya - Liaison

U. S. MERCHANT MARINE ACADEMY
Dr. Chin-Bea Kim - Liaison

NOTES

CONTENTS

LIST OF FIGURES

LIST OF TABLES

APPENDIX A

APPENDIX B

Table	Description
B-24	UNIVERSE IRELAND - Ballast (Mean Draft 39.59 Ft.) 15.0 Knots Vertical Bending Moment Response Operators At Amidship Calculated from SCORES Ship Motion Program (Ft/Tons/Ft)
B-25	UNIVERSE IRELAND - Full (Mean Draft 81.70 Ft) 10.0 Knots Vertical Bending Moment Response Operators At Amidship Calculated from SCORES Ship Motion Program (Ft/Tons/Ft)
B-26	UNIVERSE IRELAND - Full (Mean Draft 81.70 Ft.) 15.0 Knots Vertical Bending Moment Response Operators At Amidship Calculated from SCORES Ship Motion Program (Ft/Tons/Ft)

APPENDIX C

LIST OF TABLES IN APPENDIX C

LIST OF FIGURES IN APPENDIX C

TABLE OF NOMENCLATURE

A_j	Conceptual Environmental Parameters
a	Weibull Parameter
B	Ship Breadth
C	Peak Compression
C_b	Block Coefficient
C_R	Main Extreme in Compression of Combined Stress
C_W	Main Extreme of Wave-Induced Compression
f_p	Nominal Permissible Longitudinal Stress
$f_{ij}(a,b...)$	Long-Term Joint Probability Density
H_e	Effective Height of Standard Wave
L	Ship Length
L_1	Length Between Perpendiculars
M_{BH}	Horizontal Bending Moment
M_c, M_s, M_{sv}	Still-water Bending Moments
M_t	Total Longitudinal Bending Moment
M_w, M_H, M_{BV}	Wave-Induced Bending Moment
m	Weibull Parameter
$P_j(a,b)$	*Joint Probability Density or* Conditional Density
R	Rayleigh Parameter
SM	Section Modulus
SWBM	Still-water Bending Moment
T	Peak Tension

T_R	Main Extreme in Tension of Combined Stress
T_W	Main Extreme in Tension of Wave-Induced Stress
V	Vibration Double Amplitude
WIBM	Wave-Induced Bending Moment
X	Dimensional Variate
Z_o	Section Modulus
z	Combined Stress
δ^+, δ^-	Vibration Produced Increments to Wave-Induced Main Stress Extremes
ε	Spectrum Broadness Parameter
$\hat{\varepsilon}$	Fitted Spectrum Broadness Parameter
η	Reduced Variate, X/R
σ_j	Stress Components or Stress
$\sigma_L \sigma_B$	Permissible Stresses
σ	Process RMS or Square Root of Variance
$\hat{\sigma}$	Fitted Process RMS
σ^2	Variance

1. INTRODUCTION

1.1 Background and Objectives of Project

The Ship Structure Committee is committed to the development of rational procedures for the design of the main hull girder of ships. Rational procedures imply the capability of predicting the loads and structural response based on theory and statistical data with minimum reliance on experiments and experience factors or factors of ignorance. This goal is being pursued by improving analytical methods, conducting model experiments, gathering full-scale data, correlating their results and comparing them with existing design procedure.

This project is devoted to extreme midship bending moment loads which are related to the ultimate strength of the main hull girder of ships. Its purpose was to perform calculations using recently developed statistically based load-prediction techniques and to compare the results with actual values and with service experience.

Essentially, the study is a follow-up to the Ship Structure Committee Project SR-198 published as SSC-240 report, "Load Criteria for Ship Structural Design", (1)*. The heart of SSC-240 was the set up of the ultimate load criterion for the main hull girder involving the following bending moments:

- o Still-water due to weight and buoyancy
- o Ship's own wave train
- o Quasi-static wave-induced, vertical and lateral combined
- o Dynamic loads, including slamming, whipping and springing
- o Thermal effects

Determination of each of the loads was reviewed and the methods of combining loads, all expressed in probability terms, were considered in the SSC-240 project. Finally, calculations of loads were carried out for a typical cargo ship, the S.S. WOLVERINE STATE, by application of the methods developed. The results were compared with the standards under which the ship was designed.

This meant that the procedures for analytical predictions and load superposition presented were validated for one particular ship type. For universal application of these procedures, it was necessary to determine their applicability to markedly different ship types.

Consequently, the broad objective of this project was to perform similar calculations and comparisons of results for three ships, namely a modern containership, a bulk carrier and a very large crude carrier. Since this project was limited to ultimate strength, it was necessary to focus attention on maximum loads, their superposition and their probability of occurrence.

Throughout the study the philosophy maintained was that the first priority should be given to obtaining maximum insight into the correct mathematical

---

*Numbers in parenthesis refer to references listed in Section 8.

approximation of the loads and their relationships and the second priority should be given to the accomplishment of the actual numerical calculations. The reason for this attitude was that there would always remain an element of doubt in the results of the calculations and consequently, their value would be lessened if they involved unproven hypotheses. In all the tasks a point was made to identify the gaps in the rational design procedure which should be filled in with follow-on projects. The philosophy also intended to shed light on the probable limitations, if there be any, of the practicality of a completely rational procedure and to what extent it must be combined with empiricism.

One of the intrinsic and important responsibilities of this study was to examine the validity of the available full-scale data and to determine if the analysis methods of SSC-240 and their assumptions for conventional dry cargo ships were compatible with service and stress data of the three larger or faster ships.

1.2 Selection of Study Ships

It was desirable that the project select three different ship types which represented the latest trends in ship design. The ship types should be:

a. A large, high-speed containership
b. An ocean-going dry bulk carrier, and
c. A very large crude carrier (VLCC)

From a practical viewpoint it was necessary that specific ships be selected for which service data and full-scale stress data existed and would be available.

The choice of the SL-7, the SEA-LAND McLEAN, was an obvious choice for the containership. It is certainly a ship of today and at least the near future. The full-scale stress data for its first and second seasons of operation were available at the initiation of the study (2, 3). Further, published reports were available on theoretical and experimental estimates of the SL-7 waveloads (4, 5, 6).

The bulk carrier selected for the study was the FOTINI-L. Full-scale stress data was collected for the ship in October 1967 to December 1969 and considerable analysis of this data had already been performed (7, 8). This ship reportedly experiences springing type vibrations. Subsequent to full-scale measurements, the vessel had been converted to a self unloader and the old operations information was not available. However, the logbooks of the sister ship, MARKA-L, which continues to operate as a bulk carrier, were obtained.

Amongst the VLCC's the SS UNIVERSE IRELAND had the most to offer as a study ship. Full-scale data were available similar to the FOTINI-L (7). In addition, both theoretical and experimental information on bending moment was available including response amplitude operators (9, 10).

1.3 Tasks and Overview

Once the study ships were selected, parallel effort was devoted to three main areas, viz.,

a. Compilation and analysis of Still-water Bending Moment (SWBM)

b. Calculations of Wave-Induced Bending Moment (WIBM)
c. Analysis of dynamic loads

In the SWBM task, it was intended to calculate the moments at midship for actual loading conditions experienced at sea; further, to deduce the variation of the SWBM during voyages and to determine the distribution (magnitude vs. number of occurrences). Lastly, it was necessary to estimate for each ship the SWBM for superposition of loads in probabilistic or deterministic terms, as indicated by the data. To the surprise of the investigators, in the case of all three ships, it was found that the logbook data was inadequate and/or the data on the actual loading conditions unretrievable to establish the weight distribution along the length of the ship necessary to calculate the SWBM. In view of this predicament, efforts were made to combine the information in the loading booklets with the measured stress data to generate the probable experienced total SWBM. This effort was not fruitful. However, most valuable insight was obtained from the full-scale data in the variation of the SWBM during voyages.

The tasks of WIBM was divided into two parts, namely short-term and long-term predictions. The former was rather straight-forward. Response RAO's were compiled from existing sources and calculated as necessary. Inputs for the wave spectra were derived from published observed wave data on the trade routes for each ship. The pre-requisite of the long-term predictions of the WIBM was the validation of the compatibility of its assumptions with the method for superposition of loads as they apply to the ships in question. This task was combined with the task on dynamic bending moment.

The primary objective of the task on dynamic moments was to examine the full-scale stress data with the view of developing empirical or analytical representation of the contribution of vibration (slamming, whipping, springing) upon the ultimate loads of the study ships. A great portion of the effort was devoted to the establishment of the reliability of the data and the investigation of the probability distributions of the stress components.

The project did not reach the point of performing all the numerical calculations of each of the bending moments' loads and their superposition.

The hull girder design criteria of 4 classification societies were examined and applied to the study ships as a review of the current design practices.

The owners of each of the study ships were questioned with regard to any hull girder damage of whatever nature - major, minor or incipient, that might be attributed to high bending moment. It was hoped that damage can be correlated with specific full-scale stress data. The owners reported no pertinent damage.

2.0 STILL-WATER BENDING MOMENTS AND THERMAL EFFECTS

2.1 Introduction

Still-water bending moment (SWBM) loads and thermal effects on the hull girder have distinct identities and normally they have to be handled separately; however, in this report it was found convenient to present them in one section mainly because in case of both items extensive reference is made to the same full-scale stress data, as will be seen later.

Initially, the investigations of the still-water loading were to involve the following:

i. Calculations of the SWBM at midship for all the different loading conditions experienced by each ship over a period of 6-9 months, preferably during the instrumented voyages.

ii. Reconstruction of the time history of the SWBM at midship and the determination of the distribution (magnitude verses number of occurrences).

iii. Comparison of the calculated moments for the experienced loadings with the design moments and moments for the sample loading conditions in the loading booklets.

iv. Estimation of SWBM for superposition of loads in probabilistic or deterministic terms, as indicated by the data.

In case of the SL-7 containership and UNIVERSE IRELAND, the owners would only supply the loading booklets. Subsequent to the instrumented voyages, the bulk carrier FOTINI-L was converted to a self-unloader. The new owner did not save the old files. As an alternative, the actual loading conditions and the logbook data were obtained for the sister ship MV OREMAR (ex-MARKA-L). Unfortunately, the information provided only the total cargo, ballast and consumables on board at the beginning and end of the voyages, and did not include the distribution along the length of the ship to develop the weight curves.

In brief, the investigators did not have the data required to calculate the SWBM based on actual experience for any of the three ships. The next hope was to examine the full-scale stress data and determine if they could be correlated with typical loading conditions in the loading booklets. Putting it another way, the question was whether the total variation of the mean for each instrumented voyage was comparable to that for sample voyages in the loading booklet. The results of this examination were negative. If the results had been positive, then some picture could have been formed of the distribution of total SWBM by combining the sample loading conditions and the stress data.

It is, of course, a disappointment that no determination could be made of the experienced total SWBM. However, in retrospect it is believed that most valuable insight has been obtained in the variation of SWBM during voyages by examination of the full-scale stress data. This is a significant component of the SWBM regarding which very little is known.

This is illustrated in Figures 2-1, 2-2 and 2-3, Typical Voyage Variations of the Relative Still-water Bending Stresses (SWBS), for the SL-7, FOTINI-L, and the UNIVERSE IRELAND, respectively. The data are from the actual full-scale stress measurements (2), (3), (7). It should be clarified that the variations do not reflect stress changes due to weight and buoyancy only which account for SWBM. There was no way to separate the various components of the mean stress and consequently the plots are for total stress variation whatever the cause may be such as ballast changes, reduction of consumables, thermal effects and ship's own wave train. The instrumentation was adjusted to zero at the beginning of each voyage and the plots are values of the mean stress relative to this zero during each watch or interval represented in the TMR (Teledyne Material Research) tapes. It can be seen that the variation of the mean and the diurnal changes is significant, at least for the FOTINI-L and the UNIVERSE IRELAND, a tanker and a bulk carrier, respectively.

Until quite recently, design practices called for calculating the SWBM for probable loading conditions at the beginning and end of voyages, and indicating in the loading booklet the extremes (generally in terms of stress numerals) within which the master must load his vessel. Now it can be seen from Figures 2-1, 2-2 and 2-3 that even though the master may follow the loading booklet in keeping the stress at departure within the allowable limits, the variation during the voyages may result in exceeding these limits.

Another interesting observation that can be made from the sample plots is that the variation of the mean and diurnal changes appear to have a random nature; based on this, one may conjecture that the estimation of the SWBM could be approached statistically to a certain extent.

The recent work of Ivanov and Madjoarov (11) states that the SWBM can and should be approached probabilistically. It claims that: (a) the maximum SWBM's have normal distribution, and the probability of exceeding some given value of SWBM may be estimated, (b) for ships which have on-board means of controlling the SWBM, the normal distribution can be truncated, implying that the extreme values can be controlled.

Mano et. al. (12) examined logbooks of 10 containerships and 13 tankers in their work related to the statistical character of the demand on the longitudinal strength and long-term distribution of still-water bending moments. They found that the SWBM can be described approximately by a normal distribution. Further, that the containerships travel in nearly full-load conditions and that the coefficient of variation of SWBM is about 30%. For tankers in ballast the coefficient of variation was found to be about 100% and in full load about 35%. It is significant to note that Figures 2-1, 2-2 and 2-3 tend to substantiate these findings in a gross way.

In this project it was desired to obtain a rational method for the estimation of SWBM in order to perfrom the superposition of loads. It was important that the proposed method reflect the actual experience of the study ships and their full-scale stress data. Basic to the data examination was to determine if the SWBM's lend themselves to a complete or partial probabilistic description, or if they should be approached deterministically.

Ship: SEA-LAND McLEAN
Trip: 25E Route North Atlantic
Date: 9/23/73 - 9/26/73
TMR Tapes: 101 & 103

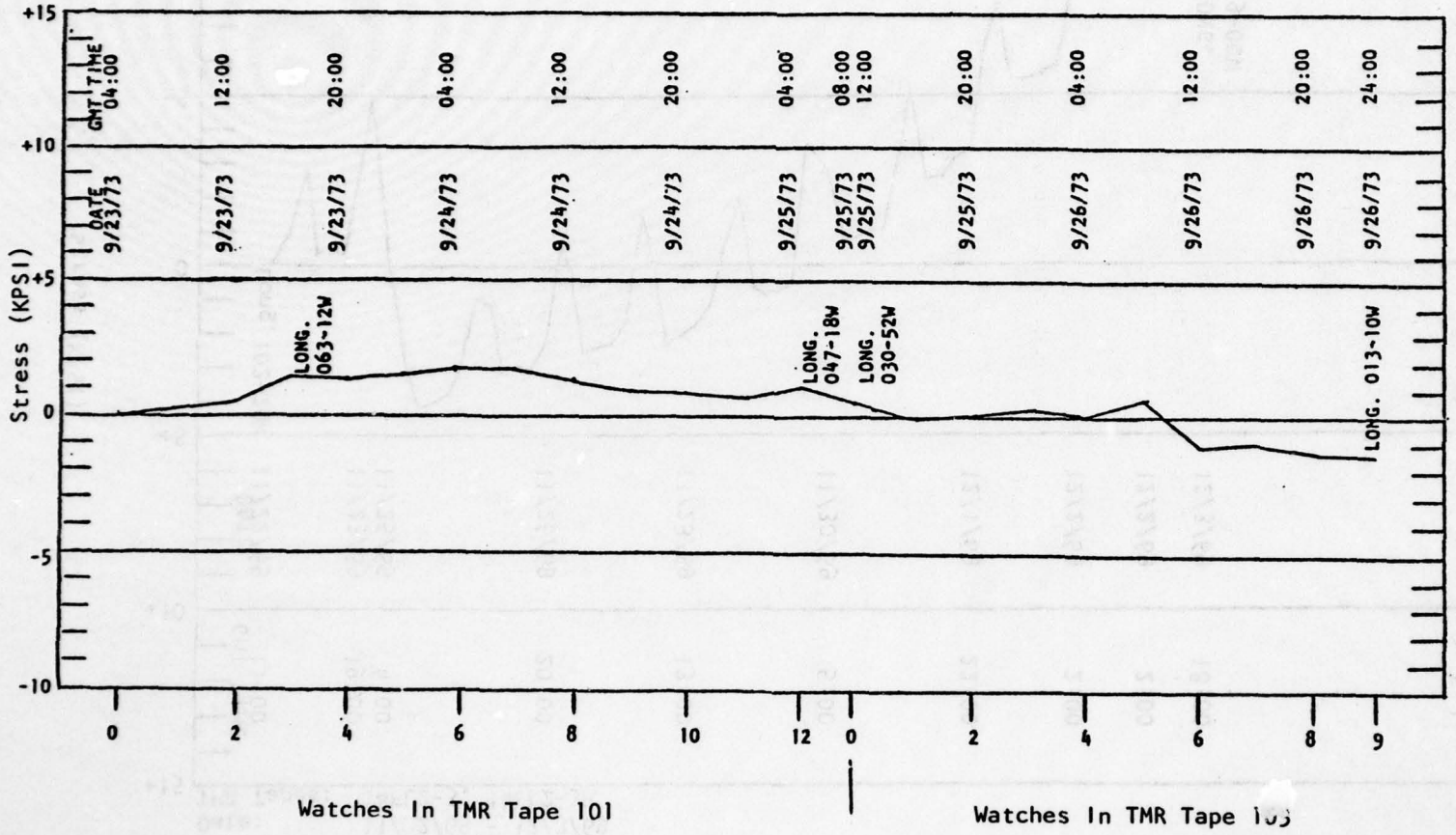

Figure 2-1 SL-7 - Typical Voyage Variation Of The Relative Still-Water Stresses

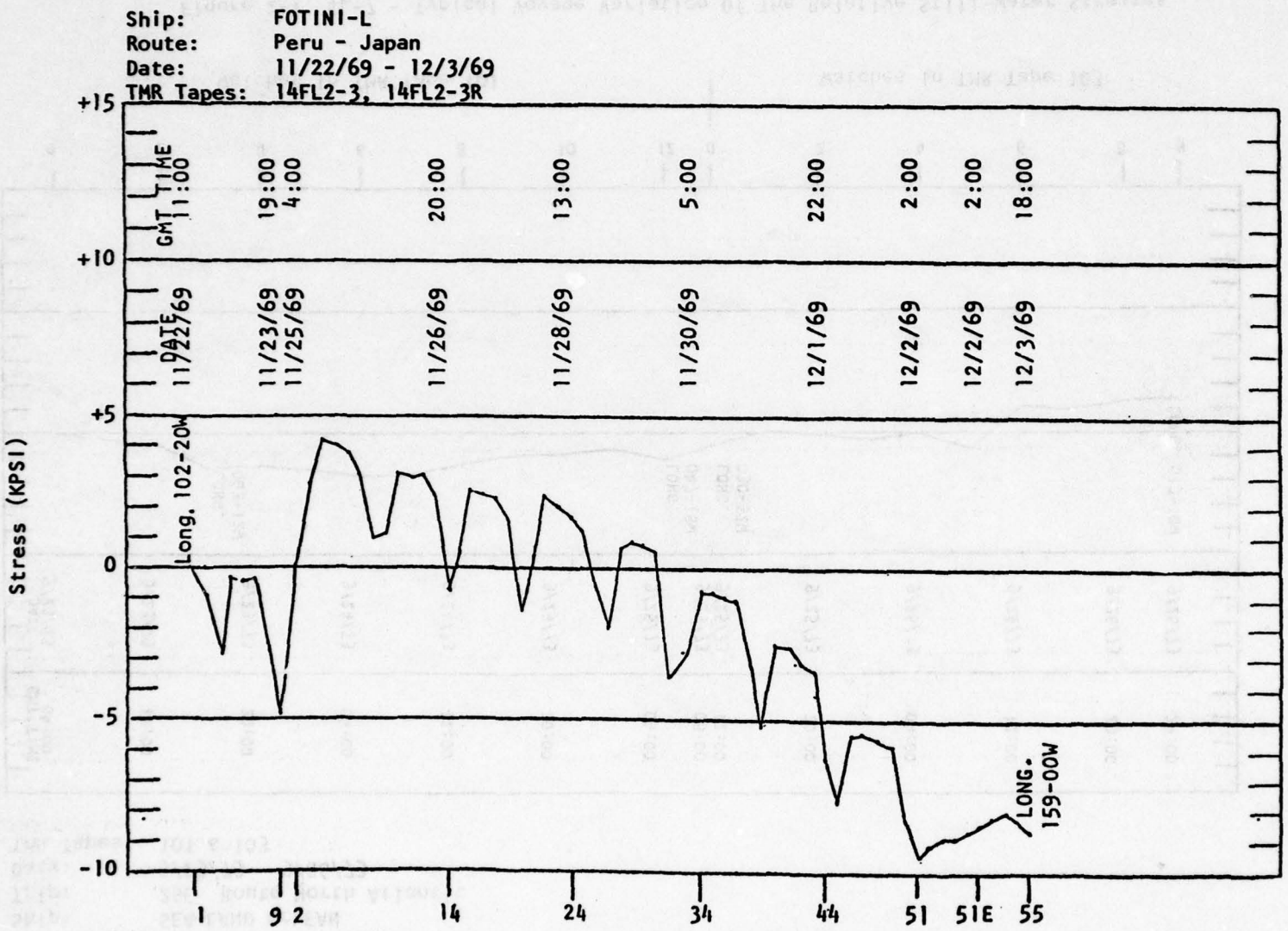

Figure 2-2 FOTINI-L - Typical Voyage Variation Of The Relative Still-Water Stresses

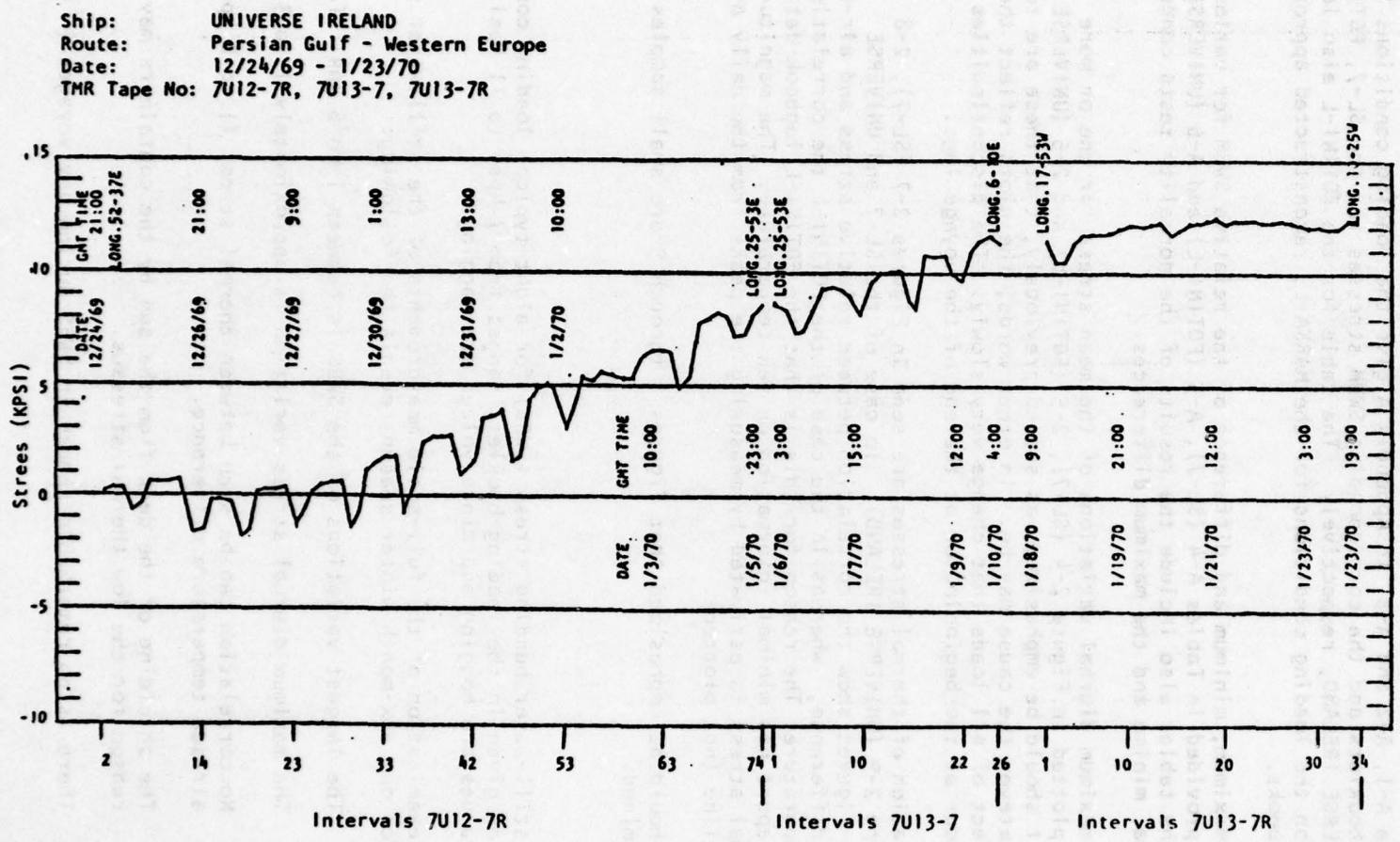

Figure 2-3 UNIVERSE IRELAND - Typical Voyage Variation Of The Relative Still-Water Stresses

2.2 Analysis of Data

Table A-1, A-2 and A-3, in Appendix A give the loading conditions from the loading booklets and the corresponding SWBM stresses for the SL-7, FOTINI-L and the UNIVERSE IRELAND, respectively. The table for the FOTINI-L also includes information on the loading conditions for the MARKA-L, reconstructed approximately from the logbooks.

The maximum, minimum and difference of the relative SWBM for various voyages are provided in Tables A-4 (SL-7), A-5 (FOTINI-L) and A-6 (UNIVERSE IRELAND). The tables also include the results of the normality tests conducted on the maxima, minima and the maximum differences.

The maximum diurnal variations of the mean stress for one or more voyages are plotted in Figure 2-4 (SL-7), 2-5 (FOTINI-L) and 2-6 (UNIVERSE IRELAND). It should be emphasized, as stated previously, that these are total variation whatever the cause may be. In other words, the plots reflect the combined effect of all loads that change very slowly. The discontinuities in the plots occur at the beginning or at the end of the voyage legs.

Variation of thermal stresses are seen in Figures 2-7 (SL-7), 2-8 (FOTINI-L) and 2-9 (UNIVERSE IRELAND). In case of the SL-7 and UNIVERSE IRELAND, the figures show the correlation between relative stress and air-sea temperature difference, whereas in the case of the FOTINI-L the correlation is with air temperature. The reason for this is that the FOTINI-L logbook data in Teledyne's report has minimal information on sea temperature. The magnitude of the thermal stress is estimated by measuring the peaks from the daily average mean stress line (not plotted).

It should be emphasized that Figures 1 through 9 are small samples of all the data examined.

SL-7

The still-water bending stress (SWBS) for eight typical loading conditions, (Table A-1) as given in the loading booklet, ranges from 7 kpsi to 11 kpsi, where plus values are hogging and minus values are sagging.

The examination of the full-scale measurements of the still-water stress variations for one six-month winter season reveals the following:

i. The largest variations of the SWBS is between 1 to 6 kpsi (Table A-4).

ii. The maximum diurnal stress variation is approximately 1 to 3 kpsi.

iii. No correlation can be seen between thermal stress (1 to 2 kpsi) and air-sea temperature difference.

iv. The shielding of the deck from the sun by the containers may be the reason for the low thermal stresses.

v. There is no remarkable change in SWBS during any voyages in question.

Ship: SEA-LAND McLEAN
TMR Tape: 101, 103, 105, 107, 109, 111, 113, 115, 117 & 119
Route: North Atlantic

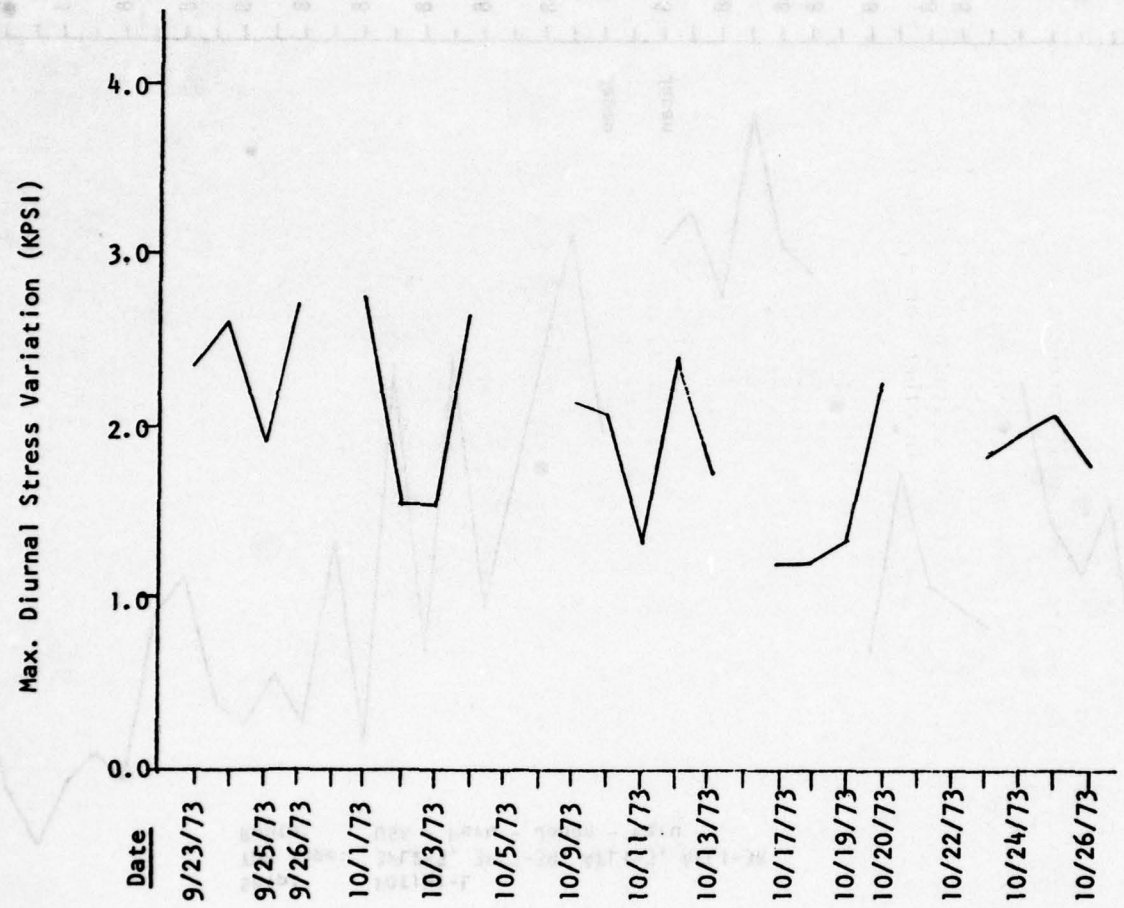

Figure 2-4 SL-7 Maximum Diurnal Stress Variation

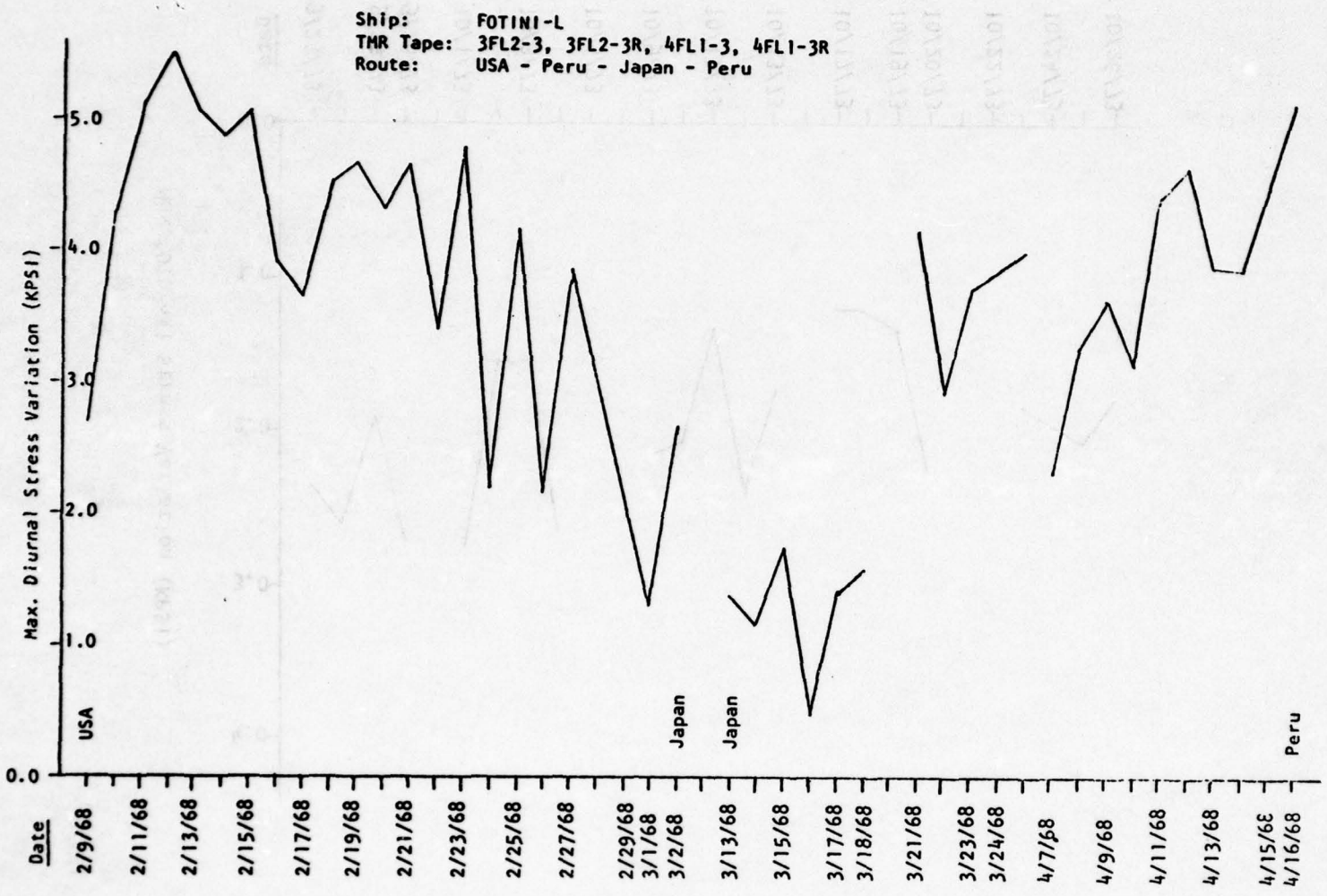

Figure 2-5 FOTINI-L Maximum Diurnal Stress Variation

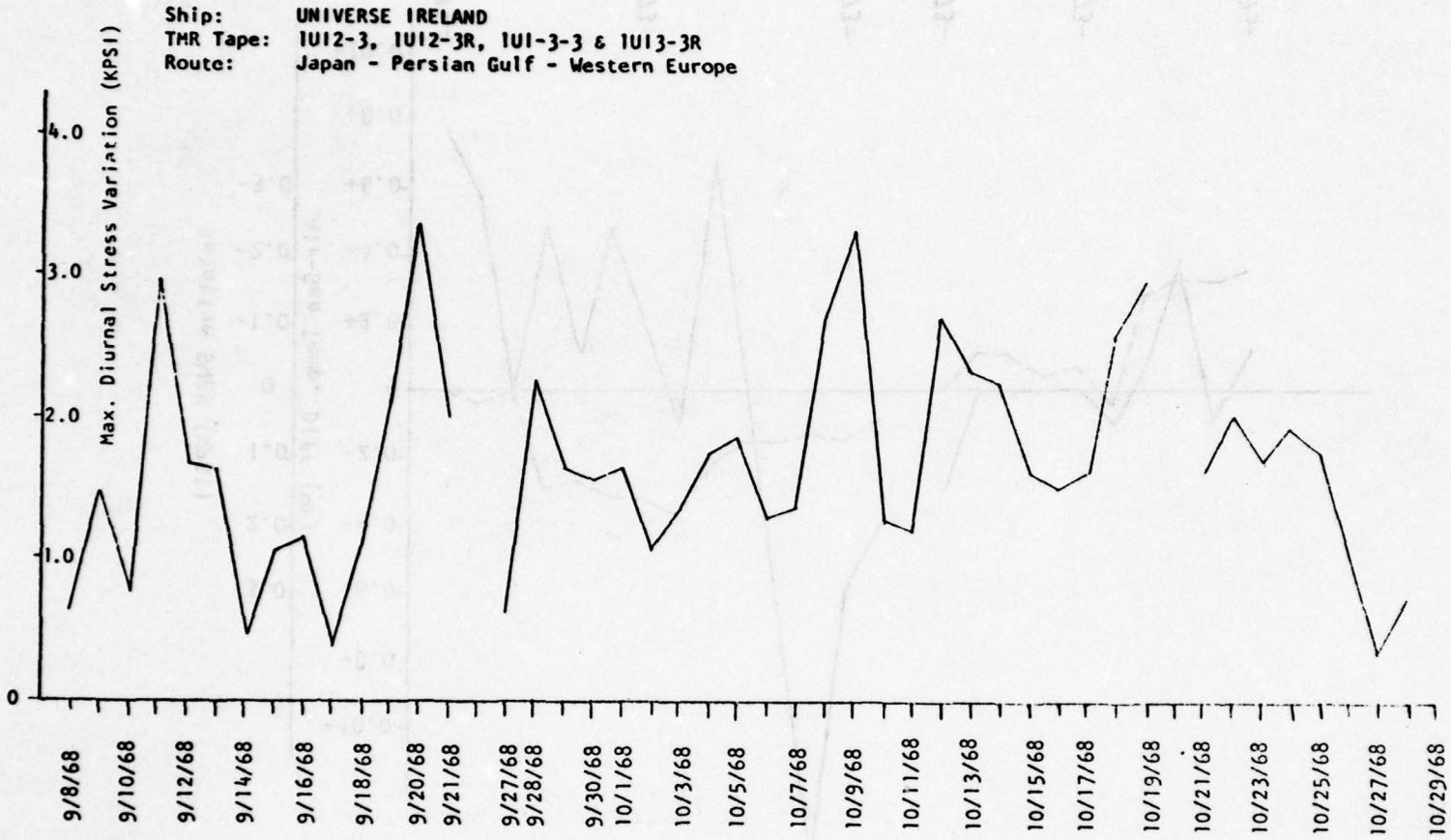

Figure 2-6 UNIVERSE IRELAND Maximum Diurnal Stress Variation

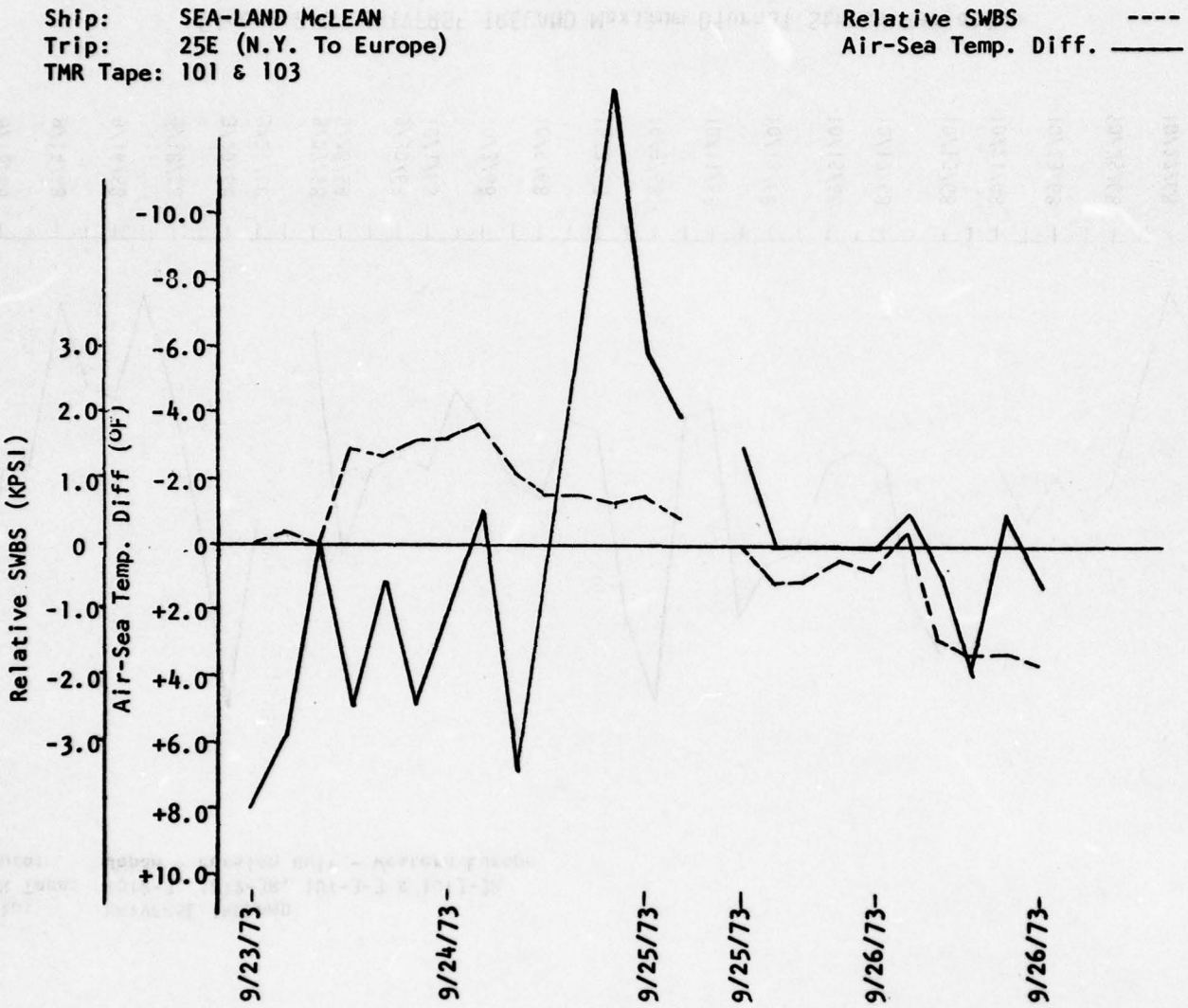

Figure 2-7 SL-7 Correlation Between Relative SWBS And Air-Sea Temperature Difference From TMR's Data

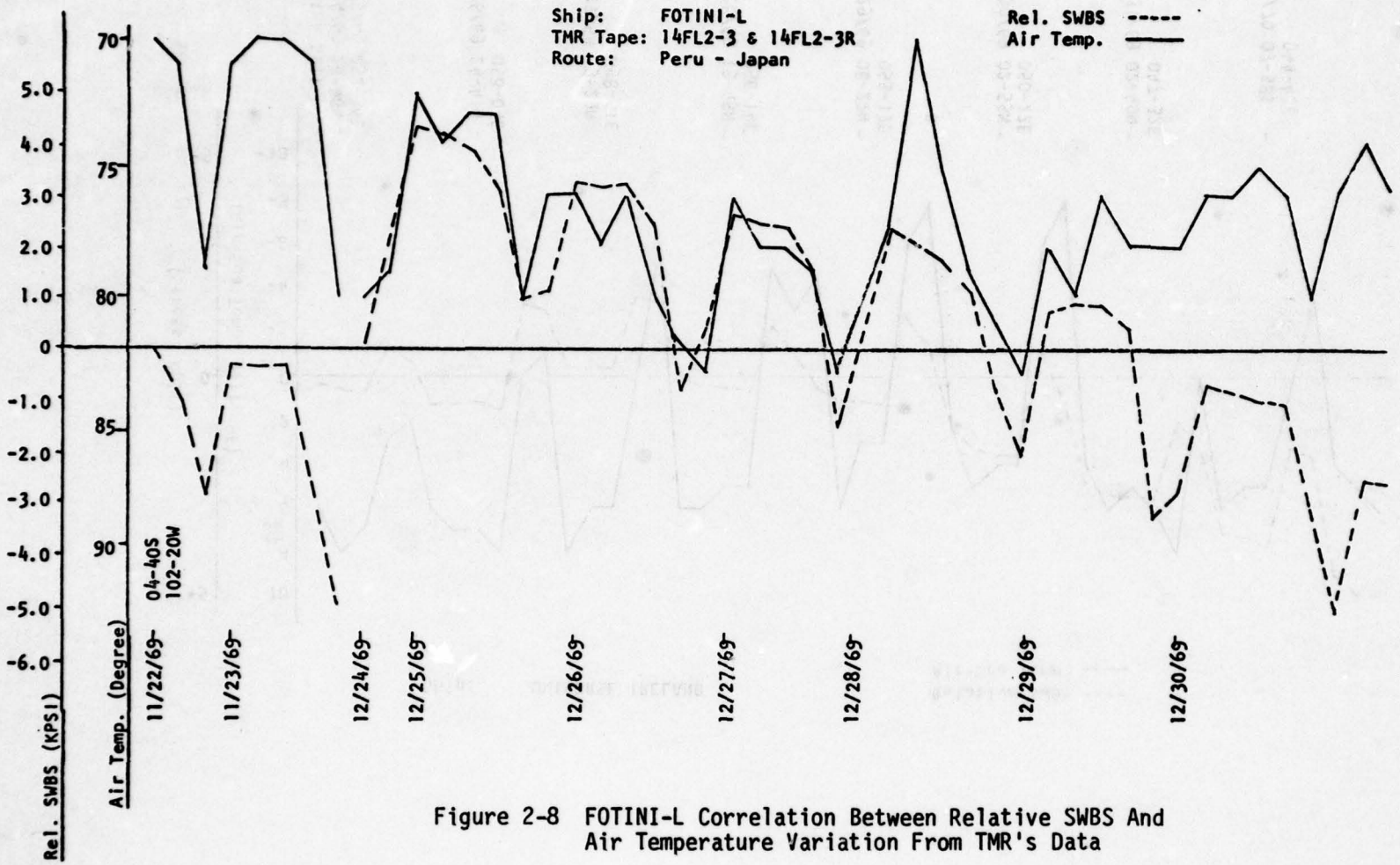

Figure 2-8 FOTINI-L Correlation Between Relative SWBS And Air Temperature Variation From TMR's Data

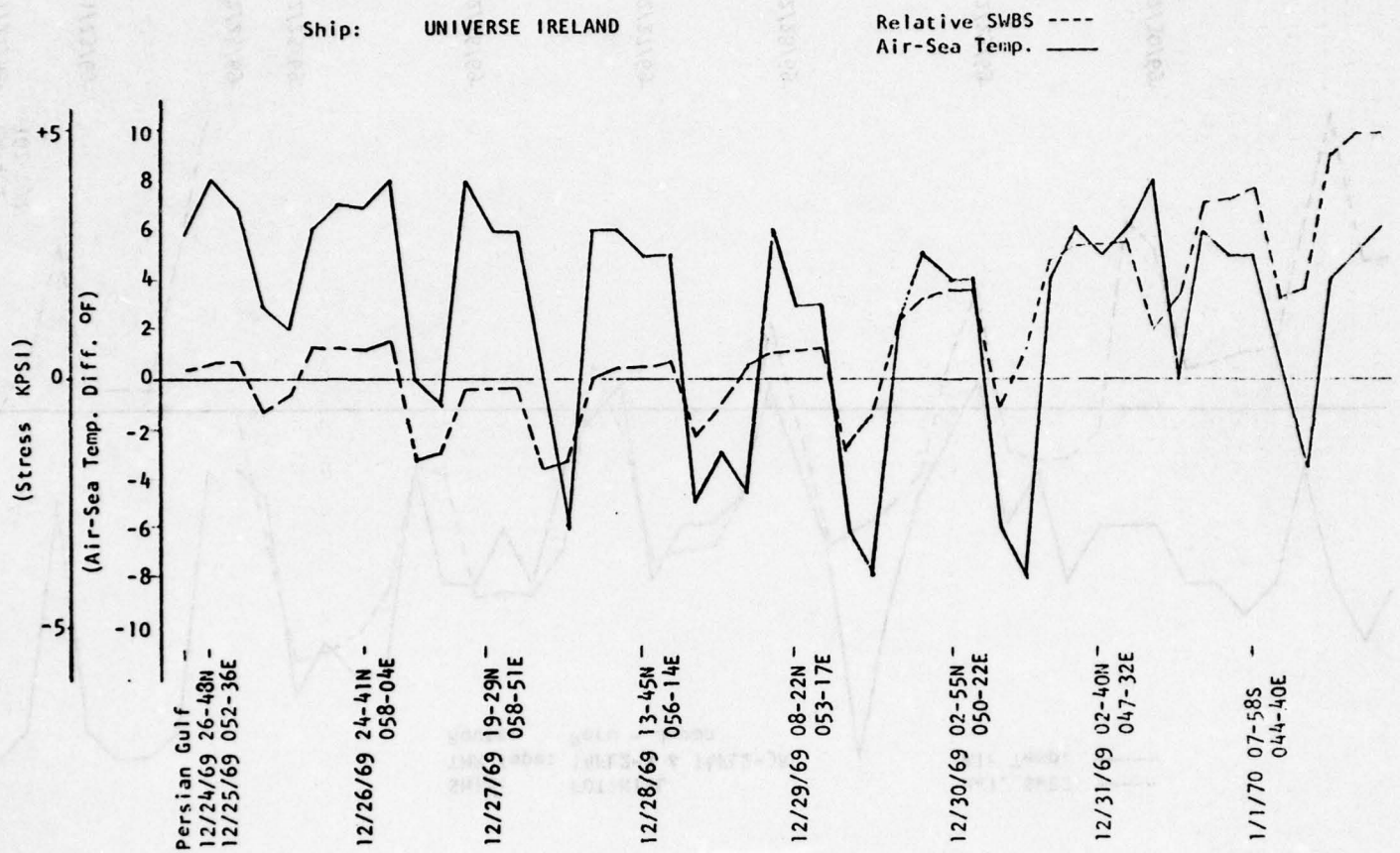

Figure 2-9 **UNIVERSE** IRELAND Correlation Plot Between Relative SWBS And Air-Sea Temperature Difference From TMR's Data

The probable explanation for the low variation in stress during the voyages is the extensive shore-side control, and detailed instructions provided to the master. This practice appears to be consistent with the operators of modern containerships. If it can be confirmed that containerships are loaded within the stress range allowed by the loading booklets and the variation during voyages is as low as observed for the SL-7, then it would appear that an estimate of the SWBM for design could be made from a truncated statistical distribution, or even deterministically. A word of caution should be added that the instrumentation which recorded stress at specific time intervals only may not have picked up abrupt stress changes in course of ballast adjustments which could be significant.

FOTINI-L

Table A-2a and A-2b show the summary of the loading conditions and their corresponding SWBS taken from the loading booklet. In addition, it includes summary of loading conditions reconstructed from the logbook for the sister ship MARKA-L. This was accomplished by distributing the total cargo, ballast, fuel oil and consumables along the length of the ship to suit the fore and aft drafts. In the loaded conditions (with cargo) the stress range is 5.2 (sagging) to 2.5 (hogging) kpsi, whereas, in the ballast condition the range is -2.5 to 3.8 kpsi.

As for typical bulk carriers, the bending moment curves for the FOTINI-L supplied in the loading manual have several peaks. When loaded with coal or bauxite, the maximum sagging stress occurs approximately 10% aft of midship. In the ballast conditions, peaks of the hogging stress appear at the quarter points and those for the sagging occur in the neighborhood of amidships.

Examination of the full-scale records for midship stress show that the diurnal stress varies from about 1 to 6 kpsi with an average variation of 3 kpsi over a one-year period. The diurnal stress variation from the daily average could be considered as thermal effects. It can be seen in Figure 2-8 that the stress levels are related to the air temperature variation.

The maximum stress variation during the instrumented voyages range from 2 to 17 kpsi (Table A-5). This, of course, is a sizable variation. The maxima of the relative SWBS during these voyages passed the normality tests whereas the minima and the differences failed the normality tests. No comment can be made on the statistical distribution of the SWBM since the bending moment at beginning and end of the voyages are not known.

UNIVERSE IRELAND

According to the owners of the UNIVERSE IRELAND, the vessel is loaded very much in accordance with the loading manual. The loaded conditions (with cargo) and heavy ballast conditions, always have sagging stress that ranges from -3 to -9.3 kpsi, (Table A-6). In the normal ballast condition, there is a hogging stress of approximately 6.5 to 7.3 kpsi. The maximum stress occurs within approximately 10% of midship.

The variation of the relative SWBS for the instrumented voyages was found to be quite high, i.e. 4 to 19 kpsi. The data show abrupt changes of 5 to 13 kpsi in the mean of the SWBS. This can only be caused during the period when

the tanks were being cleaned or it could be due to malfunction of the measuring instruments. (It should be noted that in the case of the UNIVERSE IRELAND and the FOTINI-L, the instrumentation was unattended.) The results of the normality tests and the relative maxima, minima and differences are not consistent; however, they tend to favor a normal distribution.

The full-scale stress records show maximum diurnal variation of 2 to 6 kpsi and there is strong correlation between relative SWBS and air-sea temperature differences as seen in Figure 2-9. It will be noted that when the thermal effects result in a sagging stress they will generally add to the SWBS which is also sagging. In case of UNIVERSE IRELAND and the FOTINI-L the stress data were examined to determine if the level of the mean in any way correlates with the geographical area or the ambient temperature. No particular correlation was recognized.

It should be reiterated that both the UNIVERSE IRELAND and the FOTINI-L show large variation of the mean stress and much of it can be attributed to ballast shifts and consumption of fuel.

3. WAVE-INDUCED BENDING MOMENTS

3.1 Introduction

The estimation of wave-induced bending moment (WIBM) is generally approached in two parts, the first part being short-term prediction and the second part being the application of the short-term prediction results to make long-term predictions. The long-term predictions are required for the superposition of loads. The scope of each part can be summarized as follows:

Short-Term Prediction:

i. Derivation of the Response Amplitude Operators (RAO's) for a range of headings and frequencies (from existing calculations and model test data or new calculations).

ii. Compilation of observed wave data on the trade routes for each ship. Selection of range of combinations of significant wave heights and mean periods for generation of wave spectra for irregular short-crested seas.

iii. Combination of (i) and (ii) to obtain short-term response in irregular short-crested seas. (Bending moment response for each wave spectrum.)

Long-Term Prediction:

i. Calculation of the probability density function of WIBM for range of weather conditions (or wave height groups) using the short-term predictions.

ii. Estimate of the distribution of sea conditions or the probability of occurrence of each wave height group.

iii. Combination of (i) and (ii) to obtain long-term prediction for the life time of ships.

The procedure for the calculation of long-term prediction and its combination with other loads, particularly dynamic or vibration-induced loads (1) require validation of certain key assumptions. The method of approach followed by the investigators for this validation was linked closely with the assessment of the dynamic loads. Consequently, the presentation of the work accomplished in the area of long-term prediction is presented in the section on Dynamic Bending Moments.

The task on short-term WIBM prediction was performed in parallel to the tasks on still-water bending moments and dynamic bending moments. When, in due course, it was recognized that the superposition of loads could not be accomplished in the project in view of the problems encountered in the other tasks, this particular task was terminated essentially after completing the sub-tasks related to wave data and Response Amplitude Operators. Limited effort was devoted to obtaining the short-term prediction. The procedure for the short-term prediction is well established and straight forward. Therefore it was deemed more worthwhile to divert the effort to other problem areas particularly since the results of the short-term prediction would remain unused in this project.

3.2 Short-Term Prediction

3.2.1 Wave Data

The statistics of the ocean waves for each one of the individual trade routes of the study ships was compiled using References 13 and 14. The wave data are available in a tabulated form and it gives the frequency of occurrence of different combinations of significant wave height and mean wave period in different parts of the world.

Hogben and Lumb (13) provide data for 50 areas of the Atlantic Ocean. They refer to different seasons and different wave directions and cover wave periods ranging from 0.0 to 20.0 seconds in 1 second increments and wave heights from 1.0 to 62.0 ft. in 30 different increments. These data are based on almost 2 million sets of observations recorded from ships over a period of 8 years. Wave data for 54 sub-zones of the North Pacific Ocean are given by Yamanouchi and Ogawa (14). They also refer to different seasons and different wave directions. They cover periods ranging from 0.0 to 17.0 seconds and wave heights ranging from 0.0 to 10.0 meters, both in 7 increments each.

For the purpose of limited short-term WIBM calculations, 10 mean-wave periods and corresponding 10 significant wave heights were selected from the table of pertinent wave data to generate 10 two-parameter spectra each for the SL-7 and the FOTINI-L. Extremes of wave period bracketed some 99 percent of the occurrences for each of the 10 mean-wave periods. The significant wave height selected was the one which had the highest occurrence for the wave period in question.

Table B-1 thru B-5 of Appendix B summarize the wave-data compilation.

3.2.2 Response Calculations

SL-7

Theoretical calculations for the short-term WIBM of the SL-7 were available from References 4 and 5 and the experimental values were available from Reference 6. The only pertinent information missing from these references was for zero speed.

Several accepted computer programs are available for WIBM calculations. The project employed the program SCORES (15), developed for the Ship Structure Committee. Calculations were performed for the heavy-load condition at zero speed and seven headings with respect to the waves. The input for the two-parameter spectrum used in the SCORES program was based on the compiled wave data. The results are shown in Table B-6 and B-7.

A decision has to be made as to which of the existing information on short-term WIBM for all other conditions should be used in the follow-on calculations for long-term prediction. Theoretical calculations of wave loads have been made by Kaplan et. al (4) and Kim (5). Experimental wave loads have been obtained by Dalzell and Chiocco (6). It is known that the particular version of SCORES used by Kaplan gave questionable results in the case of SL-7 at high speed, and correlation with the experimental results was unsatisfactory. On the other hand, calculations at all speeds based on Kim's program showed good correlation with

the experimental results. For this reason, it seems appropriate to use Kim's work for the short-term prediction for high speeds, or to use the mean between Kim's results and the experimental value.

FOTINI-L

The short-term WIBM prediction for the FOTINI-L, a medium-speed bulk carrier, was accomplished by employing the SCORES program (15). Calculations were made for three loading conditions (ballast, full load with coal, and full load with iron ore), 2 speeds and 7 headings. The drafts were selected by reference to the logbooks of the sister ship, OREMAR (ex-MARKA-L). Speeds were selected by reference to Teledyne's logbook information. As in the case of the SL-7, input for the wave spectra was based on the compiled data. Table B-8 thru B-18 summarizes the calculations.

UNIVERSE IRELAND

All the necessary response amplitude operators for the UNIVERSE IRELAND were supplied by the Webb Institute of Naval Architecture and they are reproduced in Table B-19 thru B-26. Additional pertinent information related to full-scale stress analysis, long-term prediction, and model tank experiments are found in References 7, 9 and 10.

4. DYNAMIC BENDING MOMENTS

4.1 Introduction

Reference 1 summarizes and extends the work of the last two decades toward "rational" structural design. The fundamental attitude in this work has been that all the major components of the demand on the structure as well as those of its capability are random to a greater or lesser extent. The ultimate objective in rational design is thus to be able to balance the statistics of demand and capability within the constraint of an acceptable risk of structural failure. Within this framework the ultimate objective of work on the demand or load side of the problem is to enable the synthesis of a "long-term" probability density function of demand. (By "long term" is meant time spans of the order of ship lives.)

As noted in Section 1, the present project was oriented toward "ultimate" longitudinal bending loads as defined in Ref. 1. Among the five load components included in the definition there are two which involve the response of the structure in some sense. These components are "thermal effects" and "the dynamic loads due to slamming, springing or whipping". In the case of thermal effects there is no external mechanical load which produces stress changes in the hull girder, and this difficulty was surmounted by defining an effective bending moment (a moment which would produce the equivalent stress according to simple beam theory). In a similar way the effects of slamming or whipping upon longitudinal bending stress were converted into an effective moment. In this latter case the structural dynamics of the ship come into play in a major way so that the effective slamming or whipping moments also might be considered a step removed from actual mechanical loads. Thus the "ultimate load" definition of Ref. 1 may be alternately and usefully thought of as a definition for the "ultimate stress" response of the structure.

It was pointed out in Ref. 1 that it is possible that the relatively short duration of stress peaks induced by slamming or whipping increases the effective capability of the structure to withstand damage; this is, that there is a possible interaction between the bending load as defined and the capability of the structure. The magnitude of this interaction is unkown. Thus, as a practical matter, the stance taken in Ref. 1 in the context of ultimate loads, was to consider an instantaneous peak combined stress as a meaningful demand on the structure regardless of the frequency of application.

The time scale of variations of three of the stress components noted in Section 1 (SWBM, Forward Speed, Thermal) is typically between hours and days, that of the other two (wave induced and vibratory) is between minutes and seconds. Wave-induced and vibratory stresses appear in the short-term as being superimposed upon a sensibly constant mean stress which is thought of as being made up of the sum of the first three slowly varying components. Essentially, the present state of knowledge suggests that stresses due to weight and buoyancy distribution, those due to thermal loads, the stress induced by the ship's own wave system, and those due to waves and vibrations do not interact directly with one another. Thus the combined stress occurring in a relatively short time interval in the ship life is considered to be a simple sum of five random variables.

σ_t = combined stress (all components)

$$= \sum_{i=1}^{5} \sigma_i \qquad (4.1)$$

and:

σ_1 = stress due to SWBM

σ_2 stress due to steady state waves generated by forward speed of the vessel

σ_3 stress due to thermal effects

σ_4 stress directly induced by waves (quasi-static response)

σ_5 stress induced by slamming, whipping, etc. (the vibratory response of the structure to a variety of loads)

Each of the stress components enumerated is considered to be a function of other random variables which define the long-term environment and operation of the ship. Thus the problem of the synthesis of the long-term probability density of σ_t, $f_t(\sigma_t)$ say, centers about the synthesis of the joint long-term density of the five stress components and the variables of which they are functions:

$$f(\sigma_1, \sigma_2, \sigma_3, \sigma_4, \sigma_5, A_1, A_2 \ldots\ldots)$$

where A_1, A_2, etc., are the (conceptual) random variables defining the long-term environment and operation, and the marginal joint density of $\sigma_1 \ldots \sigma_5$ is found by integrating out the A's.

As implied by the above expression, in at least a minor way, all the components of stress are influenced by all the environmental and operational parameters so that the ideal problem of finding the marginal density of the σ's assumes a dimension beyond reason for present state of the art. This dimension is reduced to a relatively tractable size in Ref. 1 by reasonable engineering arguments. The first argument is that the variability of SWBM is dictated largely by operational factors and human judgement. Apart from an occasional change in ballast to ease the vessel in heavy weather, the parameters controlling SWBM of commercial vessels operate nearly independently of the environment, and consequently SWBM is considered to be statistically independent. Generally similar arguments were advanced for the ship's own wave and thermal stress components. The net effect was that the overall structure of the problem was simplified by assuming independence of various sets of variables, with the result that the joint long-term density becomes a product of joint densities of smaller dimension, conceptually:

$$f(\sigma_1, \sigma_2, \sigma_3, \sigma_4, \sigma_5, A_1, \ldots)$$

$$\approx f_1(\sigma_1, A_1)\ f_2(\sigma_2, A_2)\ f_3(\sigma_3, A_3)$$

$$\cdot\ f_{45}(\sigma_4, \sigma_5, A_4, A_5 \ldots)$$

In this form the marginal densities of σ_1, σ_2 and σ_3 may be obtained in separate integrations. The wave-induced (σ_4) and vibratory stresses (σ_5) are conceptually functions of the same set of parameters.

The last of the four joint densities is the subject of the present section of the report. Both the fourth and fifth stress components may be considered "dynamic", their characteristic time durations are of the same order, and it is natural to consider them together to the extent which is possible.

The objective of the present task was to examine the available "dynamic" stress data for the three study ships with the view toward:

1. Gathering information on the statistics of σ_5, the slamming, whipping or springing-induced stress.

2. Attempting to synthesize this information in a useful way.

3. Verifying, as feasible, the basic assumptions in state of the art or proposed prediction methods for both wave-induced and vibratory stresses as applied to the study ships.

4.2 Wave-induced and Vibratory-Stress Response: Generalities

Considering the long-term joint density of wave-induced and vibratory stress separately, some further reduction can be effected by introducing conditional densities:

$$f_{45}(\sigma_4,\sigma_5,A_4,A_5\ldots) = P_{45}(\sigma_4,\sigma_5|A_4,A_5\ldots)\ P_A(A_4,A_5\ldots) \quad (4.3)$$

where

$P_{45}(\sigma_4,\sigma_5|A_4,A_5\ldots)$ is the conditional joint density of σ_4, σ_5 given the enviromental variables A_4, $A_5\ldots$

$P_A(A_4,A_5\ldots)$ is the joint density of the environmental variables

A special interpretation of the above expression is fundamental to most of the known state-of-the-art synthesis methods. The interpretation is that the conditional joint density ($P_{45}(\ldots)$) represents the short-term joint stress response(given particular values of the environmental variables, $A_4\ldots$). Since the overall objective is to synthesize peak stresses, the further interpretation is made that $P_{45}(\sigma_4,\sigma_5|A_4,A_5\ldots)$

is the short-term conditional density of the maxima of the (σ_4,σ_5) process which is defined by the variables $(A_4,A_5\ldots)$ and assumed to be statistically stationary. The overall physical justification is again based upon time scales. Enviromental and operational parameters (wave heights, etc.) fluctuate much more slowly than dynamic stresses, and are assumed to be sensibly constant in the short term. "Short term" in this constant means times in the order of half an hour.

With respect to a prediction of the combined wave-induced and vibratory stress the above treatment implies the following procedure:

Let $z = \sigma_4 + \sigma_5$ = the combined stress.

Then:

$$P_z(z) = \iint\ldots\int P_{45}(\sigma_4, z-\sigma_4 | A_4\ldots)\ P_A(A_4\ldots)\, d\sigma_4 dA_4\ldots dA_n \tag{4.4}$$

Where the limits of the integrals are infinite. If σ_4 and σ_5 are statistically independent for given choices of parameters, the problem is only slightly simplified because of the integrations over the (assumed common) enviromental parameters.

The approach to this problem in Ref. 1 appears to have involved rather different assumptions. If it is considered that vibratory response is filtered out over the lifetime of the ship (or that the ship is rigid) the stress remaining is σ_4, the wave-induced stress. In the notation of the general treatment above, the long-term density of σ_4 alone would be:

$$P_w(\sigma_4) = \int\ldots\int p_4(\sigma_4 | A_4\ldots)\ P_A(A_4\ldots) dA_4\ldots dA_n \tag{4.5}$$

This was predicted in ref. 1. In a presumably similar fashion, estimates were made of the long-term density of σ_5. The values of σ_4 and σ_5 corresponding to low probabilities of occurrence (return periods corresponding to ship lives) were found and the results were added to form an estimate of long-term combined wave-induced and vibratory stress. Intuitively, the approach seems conservative.

Clearly the reason for the approach taken in Ref. 1 was that systematic procedures for the prediction of the joint density, $P_{45}(\sigma_4,\sigma_5,A_4\ldots)$, in Eq. 4.4 were not available for the ships studied in that reference. Reliance had to be placed upon empirical stress data for the vibratory part of the problem. Consequently, the assumptions made and the procedures developed were a function of the available information for the particular study ship of Ref. 1. The present task involving ships of different types was a direct outgrowth.

Thus in examining the stress data for the present task it had to be borne in mind that not only the marginal statistics of σ_5 was of

importance; but also that the basic approach to the combination of wave-induced and vibratory stresses of the present three ships might have to be quite different.

4.3 Full-Scale Stress Data Bases

Insofar as long-term statistical generalizations are concerned, validation of methods are dependent upon the amount of data available and its representativeness. Appendix C-1 describes the available data bases utilized in the study. Since the majority of available data dealt with the average of port and starboard midship deck-edge stresses, only this measure of stress response was considered. This response may be thought of as the midshipdeck stress response due only to body vertical bending loads. The data bases for the UNIVERSE ISLAND and the FOTINI-L appear quite representative of a realistic long-term situation. The data from these ships involve a sampling of longitudinal bending stresses in one-half to one-third of the sea watches naturally occurring over a 2 1/2 or three year period. The data base for the SL-7 is biased toward severe weather conditions since it corresponds to a sampling of about 2/3 of the sea watches occurring in about 270 days of exposure to winter North Atlantic weather.

With respect to an additive vibratory component of stress response (σ_5) the extent to which the available data have been reduced was not thought adequate for all three ships. Accordingly, representative data sub-sets were chosen for the FOTINI-L and the SL-7. As described in Appendix C-1, a digital representation of the original stress-time history for each sample was thereby made available for detailed analyses.

4.4 Examination of Maximum Vibratory-Stress Double-Amplitude Data for the UNIVERSE IRELAND

Since the primary data reduction methods noted in Ref. 16 have been carried out on all the available data, it was reasonable to begin the inquiry into vibration response with the measures of response already available.

The only significant measure of vibratory response available was the maximum isolated double amplitude of vibration in each 20-minute record in the data base. The vibration in each record had been isolated by filtering such that the wave-induced components were eliminated. The resulting maximum double amplitude of vibratory stress (or maximum "burst" stress as it is sometimes called) is thus not correlated with the short-term maxima of the wave-induced stresses. Since it is just the maximum in a short-term sample, it can have meaning only in a longer term sense.

It should be emphasized that the maximum double amplitude of vibratory stress is <u>not</u> the vibratory-stress increment (σ_5) of Sections 4.1 and

4.2. However, intuitively, half the maximum vibratory stress as developed could be numerically equal to the maximum value of σ_5 in a record. A quite possibly conservative upper bound on combined stress might be formed by summing half the maximum vibration double amplitude and the maximum wave-induced stress (tension or compression) in a record. Accordingly, the maximum "burst" data, though not exactly in the form desired, was of considerable pertinence.

The details of the examination of the maximum vibration double-amplitude data for the UNIVERSE IRELAND (and an initial examination for the other two ships) are contained in Appendix C-2, where correlations of this data with Beaufort wind strength, ship speed and ship-wave heading are described.

The fundamental result for the UNIVERSE IRELAND was the absence of any firm trends. The reason was that maximum vibration double amplitudes were reported as zero if they were below 1 kpsi; coupled with the fact that in the vast majority of records the vibration double amplitudes were below this threshhold. It is difficult to do much with zeros.

However, it was noted that all of the 1900 maximum vibration double amplitudes in the data base except for 4 were below 3.4 kpsi, that none of those four were associated with exceptionally severe weather for such a large ship and that all four were above 6.5 kpsi. Owing to the nature of the statistic, the data-reduction method and the suspicious gap in observed magnitudes (between 3.4 and 6.5 kpsi) it appeared permissible to assume that the isolated highest points were spurious. On this basis it appeared reasonable to take the position that the effect of vibratory response from all causes in the UNIVERSE IRELAND could conservatively be taken care of by assuming an increment to wave-induced tension or compression of 1.0 or 1.5 kpsi for all conditions.

The absolute magnitude of the maximum vibration appeared to be so small in relation to the potential wave-induced and SWBM contributions, that there seemed little point in delving deeper into the UNIVERSE IRELAND data and this was not attempted.

4.5 Analyses of Maximum Vibratory-Stress Double-Amplitudes for the FOTINI-L and the SL-7

4.5.1 Trends

An initial examination of the available data on maximum vibratory-stress double-amplitudes for the FOTINI-L and the SL-7 was carried out as for the UNIVERSE IRELAND and is described in Appendix C-2. As in the case of the UNIVERSE IRELAND there were also thresholds involved in the original reduction of this data, but the magnitudes of vibration were generally higher and some general trends could be seen.

The data for both the FOTINI-L and the SL-7 indicated mild upward trends of vibration with Beaufort number (and by implication, with wave severity) and as heading varies from following to head seas. Both data bases involve a relatively low incidence of reduced speed. The consequence was that maximum vibration double amplitudes appeared independent of speed on the average.

As far as magnitudes of maximum vibration double amplitudes were concerned, there were a quite significant number of double amplitudes between 3 and 10 kpsi in the SL-7 data, and a few ranging up to 15 kpsi. The FOTINI-L data showed many points between 3 and 8 kpsi and some isolated points ranging up to 11 kpsi.

The presence of trends with operational parameters and the relatively high magnitudes of stress variation indicated that more detailed studies of the vibratory response of both the FOTINI-L and the SL-7 were in order. In order to accomplish this more detailed examination, representative data subsets were selected from the available data bases (details of the selection are to be found in Appendix C-1). What was intended was to re-analyze the original stress records in various ways alternate to those which had been previously employed.

There are two worthwhile routine operations which are common to any analysis of random time histories. The first is a qualitative visual inspection of the original time histories, and the second is to estimate and analyze the scalar spectrum of each record. In the present case, digital methods of separating wave-induced from vibratory stresses similar to the analog methods of Ref. 16 also had to be devised. The detail of those operations and some results are summarized in Appendix C-3.

The result of most interest from the analysis of the scalar spectra was the difference between the FOTINI-L and the SL-7 stress spectra with respect to the relative contributions of vibratory and wave-induced stresses to the whole. In the SL-7 case the spectral peak corresponding to vibration was rarely more than 10% of the peak in the wave-induced frequency range. Vibration contribution to the spectra was not prominent (in fact barely visible) in cases where overall stress response was large. In contrast, the spectral peak due to vibration was much more prominent in the FONTINI-L spectra, and in fact, upon occasion, was larger than the peak in the wave-induced frequency range. Given the small differences between the magnitudes of maximum vibration for the two ships, and the not enormously larger wave-induced stresses for the SL-7, this qualitative difference was initially surprising.

Detailed examination of short samples of the original stress time histories showed that the completely automatic determination of maximum vibration double amplitudes (Ref.16) did not always produce a reliable statistic. Upon

occasion, sudden pulses without subsequent vibratory decay were observed. These could not be accepted as representing something which actually happened aboard ship.

The incidence of those stray phenomena in the SL-7 data sub-set was relatively low -- only six out of 198 records were rejected on this basis.

A much higher incidence of oddities was observed on the FOTINI-L data sub-set. In the end, 78 out of 168 records were rejected. In addition to the stray-pulse problem, occasional evidence of saturation of the initial magnetic-tape record was found. (This was due to large changes in SWBM).

Examination of the remaining records indicated that the superimposed vibration was consistently qualitatively different for the two ships. For the FOTINI-L the vibration had the appearance of springing when the vibration was appreciable. On the other hand, when the vibratory response of the SL-7 is large, it appears to be impact induced. Judging by the timing of the initiation of vibration relative to the wave-induced stress, both forward-bottom slamming and the flare-shock phenomenon originally associated with aircraft carriers (Ref. 17) appear to be present. Qualitatively, the vibratory response of neither ship appears exactly similar to that of the study ship of Ref. 1.

Because the data sub-set for the FOTINI-L had been selected in part so that it contained most of the unusually high vibratory response (Appendix C-1), it was of interest to re-examine the trends initally found in Beaufort number/speed/heading classifications of the data after discarding points strongly suspected to be spurious. Details of this re-examination and revision of the data base are indicated in Appendix C-6. The significant result of this re-examination was that the majority of the original exceptionally high maximum double amplitudes of vibration were thrown out. In the revised FOTINI-L data base there are just 19 instances where the maximum double amplitude of vibration fell between 3 and 8 kpsi and only one in excess of 8 kpsi. Effectively, 98.6% of the FOTINI-L maximum vibration double amplitudes are below 3 kpsi.

A further examination of the 1.4% of data above 3 kpsi disclosed that at least two of the 20 high values were of suspicious origin though this could not be confirmed. It appears that 98% of the data base for the FOTINI-L implies an allowance for vibratory addition to wave-induced stress not appreciably higher than that previously suggested for the UNIVERSE IRELAND. However, the revised data base also suggests that real maximum vibration double amplitudes above about 3 kpsi are nearly always associated with Beaufort wind strengths above 6.

A comparable re-examination was carried out on the SL-7 data base. In this case the 3 kpsi level of double amplitudes is exceeded in 12% of the records.

Though the result must be partly due to the bias in the SL-7 data base toward severe conditions, vibration double amplitudes above 3 kpsi appear to be 8 or 10 times more likely in the SL-7 than the FOTINI-L.

4.5.2 Fitted Distributions

As has been pointed out, the statistics of the isolated vibratory stress are not exactly what is wanted in the development noted in Sections 4.1 and 4.2. However, they are of pertinence (especially if no clear results can be obtained for what is really wanted). Thus it was of interest to see if the maximum vibration double amplitudes could be fitted by some convenient semi-analytical ("long-term") distribution function.

It is reasonable in such an effort to begin with an examination of the short-term statistics of the process from which the sample maximum is found, since the general form of the long-term distribution is influenced by the short-term distribution, and because there is the possibility of developing a synthesis method similar to that implied in Secion 4.2. A brief investigation was undertaken of the short-term vibratory response in the data sub-sets for both the FOTINI-L and SL-7. The details are indicated in Appendix C-6.

The spectral analyses had indicated the isolated vibratory responses to be quite narrow banded. In addition, it was possible to count the number of vibration double amplitudes in each record of the data subsets. In each case the number of vibrations was nearly equal to the number which would be expected if the ships were always in continuous vibration at the frequency of the longitudinal two-noded mode.

Those facts suggested that the short-term distribution of vibratory maxima might be the Rayleigh. Under this hypothesis a simple statistical hypothesis test was devised to see if the maximum vibratory amplitude in each record was generally what would be expected if the parameter of the Rayleigh distribution (RMS vibratory response) was known. If the assumption was generally true it was expected that the test would be failed in about 10% of the records of each data sub-set. The rate of failure for the SL-7 was 64%, that for the FOTINI-L 37%. The detail of each test disclosed that when the tests were failed the problem was that the maximum vibration double amplitude was always <u>higher</u> relative to the RMS vibration than expected.

The same test procedures were applied under the hypothesis that the short-term distribution of vibration double amplitudes was exponential. In this case, when a test failure occurred it always implied that the maximum vibration was <u>lower</u> than expected relative to the RMS. The results indicated that the short-term distribution of vibratory maxima was somewhat closer to exponential than to Rayleigh since the failure rate for the SL-7 was 15% and that for the FOTINI-L was 27%.

The results also implied that construction of long-term trends of maximum vibration from short-term estimates of RMS may not be wholly within current state of the art. In the case of suspected springing response of the FOTINI-L, current state of the art implies a zero mean Gaussian vibratory response, and consequently a Rayleigh distribution of maxima. For the suspected flare shock and slamming response of the SL-7 it is not clear what distribution current state of the art implies. In either case, it was suspected that vibrations due to propeller excitation were confusing the situation.

With respect to the problem of fitting some distribution to the long-term statistics of maximum vibratory double amplitudes, the unconvincing results for the short-term situation suggested that the next best assumption might be one of the asymptotic extreme-value distributions. For reasons detailed in Appendix C-6, a variation of the third asymptotic form as used in Ref. 18 (the Weibull distribution) was assumed to be appropriate.

Fits to the Weibull distribution were made of all the maximum vibration double-amplitude data in both the SL-7 and FOTINI-L data bases. From the graphical point of view, both fits appeared reasonable, the SL-7 fit appearing better than that for the FOTINI-L. Chi-square tests for goodness-of-fit were applied to both sets of data. The results of these tests indicated that the FOTINI-L data fit very well indeed, the SL-7 data not so well. For reasons explained in Appendix C-6 the test procedure for the SL-7 were probably biased toward a failure of the test. The net result was that it appears reasonable to accept the Weibull distribution as a reasonable long-term representation of the empirical data for both ships, and the derived parameters of the distribution for each ship are given in Appendix C-6.

It was of interest to see if reasonable fits to the Weibull distribution could be made for various sub-groupings of the data base; that is for the various headings, speeds, Beaufort number, etc. The reason for this interest was the hope that some leads on an alternate synthesis method might emerge. Efforts made in this direction are detailed in Appendix C.

The effort in this direction made with the FOTINI-L maximum "burst" data can only be described as having resulted in no credible answers. The basic problem has to do with the 1 kpsi analysis threshold of the original data reduction, Ref. 16. Of the 1455 seconds in the revised FOTINI-L data base there are only 140 records having maximum vibration double amplitudes above the threshold. Thus the maximum vibration is reported as zero (less than 1 kpsi) 90% of the time. In the process of producing sub-groups of data for given combination of Beaufort number, etc., the 140 non-zero points are split so many ways that practically no credible fits could be made.

A similar, though not so severe condition influenced the efforts with the SL-7 maximum burst data. Despite a revision of the grouping rules, no credible fits could be obtained for a three-way (Beaufort number, speed and heading) classification of data. However, some reasonable fits were obtained for

two two-way classifications (wave height-heading) and(speed-heading). Numerical results for the Weibull parameters are cited in Appendix C-6. Reasonably sensible variations of the Weinbull parameters were obtained for variations in ship speed, heading and wave height.

4.6 Analyses of the Statistics of Short-Term Wave-Induced Stresses For the FOTINI-L and the SL-7

It was one of the general objectives of the present task to develop the statistics of the amount by which the combined stress exceeds the wave-induced stress. (In the notation of Section 4.2 this is σ_5.) Since this quantity is not necessarily half of the maximum vibration double amplitude treated in Sections 4.4 and 4.5, it was necessary to make a direct approach to the problem utilizing the original stress records contained in the data sub-sets described in Appendices C-1 and C-3.

The original stress records are combined stresses so that in order to extract information about an addition to wave-induced stresses, it is necessary that the wave-induced stresses be first derived, and their statistics understood.

Within the current state of understanding, the wave-induced stresses are zero mean and are superimposed in the short term on a constant-stress bias due to slowly varying loads. Thus, insofar as data reduction is concerned, the position of zero wave-induced stress is taken to be the record mean. For both practical and conceptual purposes the wave-induced and vibratory stresses are separated by a filtering operation which removes frequency components due to ship vibration. Methods employed in the present study are discussed in Appendix C-3.

It is worthwhile to review some of the additional assumptions made in state-of-art long-term prediction methods for wave-induced stresses. The general guide-lines for developing these methods were that it be possible to synthesize a long-term distribution for a specific ship in a specific trade route. The fundamental assumption is that the wave-induced stresses are a linear function of suitably defined wave elevations and that the stress spectrum may be estimated from hydromechanic theory or model tests, given the input wave spectrum. A consequence of this assumption is that the wave-induced stress process must be a zero mean random Gaussian process. A further consequence is that the process must be statistically symmetrical; for instance, the short-term statistics of stress maxima in the tensile direction (hogging in the present case) are assumed to be the same as those in the compressive direction. Finally, under the above conditions the theoretical probability density function of the maxima of the process is known. (The derivation is variously ascribed to Rice or Cartwright and Longuet-Higgins, see Ref. 35; it is referred to herein as the CLH Distribution because the Cartwright/Longuet-Higgins notation has been utilized).

In the prediction methods of Ref 1 (as well as in a somewhat different approach, Ref 18) an additional assumption is made. This is that in the short-term the wave-induced stress process is always sufficiently narrow banded so that the theoretical distribution of maxima may <u>always</u> be represented

by the Rayleigh distribution. This was an approximation substantiated empirically, principally from data acquired on ships similar to the study ships of Ref. 1. The Rayleigh distribution has one parameter, which is taken equal to the predicted standard deviation (square root of the predicted stress spectrum) times a constant which depends upon the conventions employed with respect to normalization of spectral areas and the definition of the analytical expression for the Rayleigh distribution. For present purposes the Rayleigh parameter will be denoted R and taken equal to the process RMS. "R" is a function of a host of random operational variables (wave properties, spectral shape, ship speed, heading, etc.). Under the Rayleigh assumption the long-term density of wave-induced stress, Eq. 4.5, may be written:

$$P_w(\sigma_4) = \int \cdots \int P_4(\sigma_4 | R)\, P_e(R | A_4, A_5 \ldots)\, P_a(A_4, A_5)\, dR dA_4 \ldots \tag{4.6}$$

where $p_e(R\, A_4, A_5)$ is the conditional density of R given the environmental variables $A_4 \ldots$.

If the long-term probability, $Q(\sigma_4)$, of σ_4 exceeding some value X is desired:

$$Q(\sigma_4 > x) = \int_x^\infty P_w(\sigma_4)\, d\sigma_4$$

$$= \int \cdots \int \mathrm{Exp}\,(-X^2 / 2R^2)\; P_e\,(R \mid A_4 \ldots.)\; P_a\,(A_4 \ldots)\; dR dA_4 \ldots \tag{4.7}$$

after substitution of the analytical form of the Rayleigh density function for $p_4(\sigma_4)$. Eq. 4.7 is the fundamental long-term prediction equation utilized in the methods of Ref. 1 as well as Ref. 18; the difference in methods being the procedure and order of the integration over the range of environmental variables, and the form of the resulting density of R. Because the limits of the R integration are infinite (or at least very large) there are always contributions for large values of X from moderate and low values of R. Thus the answer obtained depends in part upon the validity of the "tail" of the Rayleigh distribution.

There are thus two consequences of the basic short-term assumptions which are of fundamental importance to the validity of state-of-art prediction procedures and which could be checked against the data in the data

sub-sets for both the FOTINI-L and the SL-7. These are that in the short-term:

1) The wave-induced stresses are always statistically symmetrical.

2) The distribution of the stress maxima is always Rayleigh.

Appendix C-4 describes the work accomplished in this direction and Appendix C-5 summarizes some of the statistical techniques employed.

The first test of symmetry discussed in Appendix C-4 involved a graphical comparison of the maximum tensile wave-induced stress in each record with the maximum compressive stress. The maximum instantaneous stresses in a 20-minute record are not particularly stable statistics so that there was much scatter. The maximum tensile (hogging) stress in a record may be larger or smaller than the maximum compressive (sagging) stress. However, viewing the data sub-sets as a whole it appears that the maximum wave-induced tensile and compressive stresses for the FOTINI-L are <u>on average</u> nearly the same; statistical symmetry appears to be a good assumption. The assumption for the SL-7 appeared not nearly so good; on average the ratio of sagging to hogging stresses appeared to be in the vicinity of 1.2.

As may be noted from the material presented in Appendix C-3, real wave-induced stress-time histories do not always appear to be narrow banded. The Rayleigh assumption colors much of what is done to cope with this situation in the data-reduction methods of Ref 16. For present purposes, many of the same procedures were followed. Using the sample mean as a reference, a "main extreme" in tension was defined as the largest tensile stress observed during a stress excursion in the tensile direction, and a main extreme in compression as the largest compressive stress observed in a stress excursion in the compressive direction. The algebraic sum of main extremes found in adjacent tensile and compressive stress excursions is defined to be a "double amplitude". These definitions are exactly compatible with very narrow-band processes and produce, it is thought, a series of maxima, minima and double amplitudes from an approximately equivalent narrow-band process. These conventions were followed in developing, for each record in both data sub-sets, arrays of succeeding maxima, minima and double amplitudes which were considered to be samples from the underlying process.

From samples of the maxima and minima of a Rayleigh process it is possible to make two estimates of the Rayleigh parameter, one estimate from the maxima and one from the minima. These estimates were compared graphically for a further check on statistical symmetry. This effort confirmed the close symmetry previously indicated for the FOTINI-L and implied for the SL-7 that the symmetry assumption is considerably better than was implied previously; apparently very much within engineering reason for the average magnitudes of stress, if not the extremes.

The several statistical tests performed on the adequacy of fit to the Rayleigh distribution of the samples of double amplitudes, and main extremes, are summarized in Appendix C-4.

With respect to the Rayleigh assumption for double amplitudes the tests performed on both data sub-sets for goodness-of-fit were failed at a rate 5 to 7 times the rate expected due to statistical variability. Essentially this result implied that blanket acceptance of the Rayleigh assumption for double amplitudes may result in incorrect conclusions between 20 and 35% of the time. The correctness of the assumption for double amplitudes has no direct bearing upon the prediction methods outlined since the real interest is in main excursions. However, it has a significant indirect bearing in that all or most existing methods have been verified against double-amplitude data.

The statistical tests on the fit to the Rayleigh distribution of the short-term wave-induced main extremes in the SL-7 data sub-set produced overall failure rates 7 or 8 times that expected on the basis of statistical variability. The samples of main extremes in tension or compression are badly fitted by the Rayleigh distribution 35% to 40% of the time. On the basis of these results it is difficult to accept the proposition that the short-term wave-induced stress maxima of the SL-7 always follow the Rayleigh distribution.

Similar tests on the fit of short-term wave-induced main extremes in the FOTINI-L data sub-set to the Rayleigh distribution produced failure rates 3 to 4 times that expected; that is, higher than would be desirable for an unconditional acceptance of the Rayleigh assumption but much lower than those for the SL-7.

By a subjective classification of the width of each of the FOTINI-L stress spectra it was possible to correlate the test failures with the spectral width. Failure rates for very narrow spectra were near enough to that expected so that the Rayleigh assumption could reasonably be accepted. The high overall rate was explained by higher rates of failure for broader spectra.

Exactly similar correlations were not made for the SL-7 results, but those that were implied that the problem there was with a high incidence of broad-band stress spectra.

It was apparent from the details of the SL-7 data sub-set that the ship slows to less than 15 knots speed only during extraordinarily severe wave conditions, and under these circumstances the ship heading is generally bow or head seas. Eleven such cases exist in the data sub-set. Examination of the tests of the Rayleigh assumption for these cases indicated that had the 11 low-speed cases been the only ones available there would have been little hesitation in accepting the Rayleigh assumption.

Since the results for the SL-7 at least had potentially serious implications with respect to the long-term prediction methods, and indirectly upon the validity of the basic short-term prediction procedure, it was of interest to see if the maxima and minima would, in general, fit the more complicated theoretical distribution cited earlier. In order to carry out these tests, all the maxima and minima in each record in the SL-7 data sub-set (not just main extremes) had to be found.

The testing procedures utilized in this effort were essentially similar to those on the main extremes. The overall failure rates of these tests were very much in line to the rate-of-failure expected. Thus the short-term statistics of the SL-7 stress records appear in general to be consistent with those expected under the linear random prediction theory for systems of arbitrary band width; that is, consistent with the two-parameter CLH distribution.

As in the earlier tests the procedure produced two sets of estimates of the distribution parameters, one from the samples of maxima, one from the minima. This afforded an opportunity for a third symmetry check. The first parameter of the distribution is the process RMS. Graphical comparisons of the values estimated from maxima with those from minima again indicated quite reasonable symmetry. The second parameter of the distribution is a non-dimensional broadness parameter which varies between zero and one. Graphical comparisons indicated quite good statistical symmetry for values of the parameter above 0.7, less good symmetry below. The sense of the result is that for the lower values of broadness parameter there tends to be more secondary oscillations in hogging-stress excursions than in sagging-stress excursions.

The majority of the problems with the Rayleigh assumption for the SL-7 data are explained by the incidence of the various values of broadness parameter. About half the time the derived broadness parameters were between 0.8 and 1.0; that is, the distribution of maxima or minima in the records is nearly normal. There is very little incidence of broadness parameter between 0.0 and 0.2; that is, very little incidence of nearly Rayleigh response in the data set.

It seems probable that the short-term statistical symmetry and the narrow-bandedness assumptions are within reason if not always true for relatively slow-speed ships. For a ship of the size and speed of the SL-7, which spends about half its sea time in quartering and following waves, it is difficult to accept the narrow-bandedness assumption, though it is probably within reason to accept symmetry.

Incorporation of the distribution for arbitrary band width (truncated so as to represent only positive maxima) into the expression for the long-term probability density, Eq 4.6 would be possible at the expense of an additional integration over the broadness parameter and the development of the joint distribution of the two distribution parameters.

However, it seems clear that the neglect of broad-band response, as would be the case when existing methods are used for the SL-7, will be on the conservative side. To illustrate, the upper tail of the CLH distribution, truncated to represent the positive values of the variate of interest, is smaller than the upper tail of the Rayleigh distribution regardless of broadness parameter (Ref 20). The effect would be that the probability of exceeding a given stress level will be higher under the Rayleigh assumption.

Regardless of the method utilized, it would appear that some care may be needed in interpreting the double-amplitude data in the data bases for purposes of validating prediction methods.

4.7 Investigation of Combined Stresses

4.7.1 Short-Term Distributions of Dynamic Increments to Wave-Induced Stress

Returning to the question of the amounts (σ_5) by which the combined dynamic stress exceeds the wave-induced stress, the details of the definition of this quantity in the short term, as well as of the investigations carried out, are noted in Appendix C-7. Briefly, a main combined stress extreme was defined as the maximum combined stress observed in a wave-induced stress excursion. The quantity σ_5 is defined as the difference between this combined main extreme and the wave-induced main extreme noted in the last section. This definition is exactly the same as that adopted in Ref. 1. The intended approach of the present work differed from that in Ref. 1 in that whereas 100 or so selected impact events were selected for analysis in the background work to that reference, it was the intent of the present work to look at all available events (stress excursions) in each record, and to repeat this for all the records available in the FOTINI-L and SL-7 data sub-sets.

Having developed the increment data (σ_5) for both tension and compression it was of interest to see if increments to tension and compression were symmetrical. This was carried out graphically for both the maximum increments in each record and the mean of the increments. The increments to wave-induced stresses for both ships appeared to be quite symmetrical statistically. In any given record there appears about an even chance that the maximum increment to wave-induced tension will be larger than the maximum increment to compression. This result, for both the FOTINI-L and the SL-7 is different from the result for the study ship of Ref 1 where assymetry was found; but in accordance with the qualitative nature of the vibration noted in Section 4.5 and Appendix C-3.

Following the general line of development of Ref 1, the next investigation involved the marginal distribution in the short term of the vibration-induced increments to wave-induced stresses. The implication in Ref 1 was that these increments might be distributed according to the Rayleigh or exponential distributions depending upon the nature of the response (slamming or whipping). Tests for goodness-of-fit of the short-term samples of increments to the exponential distribution were made for each record of each data sub-set. The hypothesis that the increments fit the exponential distribution was rejected in about 90% of each data set, a rate of rejection about 18 times that expected due to statistical variability. Similar tests were made for fit of the short-term samples of increments to the Rayleigh distribution. In this case the failure rates for both ships were 8 to 10 times that expected. Essentially, a reasonable fit to the Rayleigh distribution is not present 40% or 50% of the time. It appears that neither of the short-term marginal distributions of dynamic increments to wave-induced stress which were suggested in Ref 1 are particularly attractive assumptions for the FOTINI-L and the SL-7.

While statistical independence of short-term increments (σ_5) and wave-induced stresses (σ_4) does not vastly simplify the prediction problem (Section 4.2), it would help. Accordingly a brief investigation of statistical independence in the short-term was carried out. Because of the uncertainty about the distributions of both components, the test procedure used was distribution free.

The result for the SL-7 data sub-set was that statistical independence of short-term increments and wave-induced maxima appears to be a quite reasonable general assumption. In the case of the FOTINI-L the independence assumption appeared reasonable for increments to tensile stress but somewhat tenuous for compression. An examination of the individual cases where the independence assumption could not readily be accepted disclosed that in half of these cases the overall stress level was quite low.

The results of the investigations of the short-term marginal distributions of increments to wave-induced stress appear similar to those carried out upon isolated vibration (Section 4.5). It seems likely that the contributions of non-wave-related vibration excitation upset the various tests. All the tests were based upon expectations resulting one way or another from considerations of wave-induced phenomena.

4.7.2 An Alternate Approach to Short-Term Combined Stresses

Given the above results it seemed appropriate to cast about for some alternate approaches. One such approach involves combined stresses directly (Ref 8, for example). In this approach it is assumed that the vibration is a linear response of the ship to wave excitation that happens to occur at different frequencies than the wave-induced response. In this rationale the addition of vibration to wave-induced stress results in a new broader banded random-zero mean Gaussion short-term process. In terms of the development of Section 4.2, the variables σ_4 and σ_5 are combined in the short-term prediction procedure so that the conditional joint density $p_{45}(\sigma_4, \sigma_5, A_4 \ldots)$ is replaced by a conditional density $p_6(\sigma_6 A_4 \ldots)$ where σ_6 is the continuous sum of the wave-induced and vibratory stresses, not the sum of maxima as was previously implied. This approach has some very great practical attractions in that synthesis of both RMS wave-induced stress and RMS vibration, as well as the associated spectra, is considered to be within present state-of-art (Ref 8).

From the point of view of checking the applicability of this concept to the combined stress maxima it is first necessary to develop samples of all the maxima in the original stress record. It was convenient to do this in conjunction with one of the investigations noted in Section 4.6 (that which involved all the wave-induced stress maxima in the SL-7 data sub-set). Accordingly, tests for goodness-of-fit to the CLH distribution were made on samples of combined stress maxima from each record in the SL-7 data sub-set (details are noted in Appendix C-7).

The first results of this process were that the distribution parameters (RMS and broadness parameter) fitted to samples of maxima appeared symmetrical with those fitted to samples of minima, and that 94% of the broadness parameters were above 0.8. The rates of failure of the goodness-of-fit tests were nearly that expected due to statistical variability, and, accordingly, the results imply that the short-term maxima and minima of the combined stresses in the SL-7 data sub-set are quite generally nearly normally distributed, a result which would be expected as a consequence of the approach in Ref 8.

Two aspects of the just described investigation were disturbing. One was that the contribution of the vibration to the total variance of combined stress was extremely small, no reasonable check on the fundamental addition approach could be made. The second aspect was that the sample extremes were outside the range expected much more often than the good overall fits to the CLH distribution would imply. In most of the cases where the sample extremes were not within the expected range the extreme was larger than expected, and, moreover, these cases tended to be concentrated in head and bow-sea cases and in the severest weather. The implication is that while the combined maxima and minima may on average follow the expected distribution for a broad-band Gaussian process, severe wave-induced vibratory response (the item of real interest) may upset the tails of the distribution in a way not discernable with the fitting procedures utilized.

4.7.3 Composition of the Maximum Combined Stress in Twenty-Minute Records

Since the prospects for synthesis of combined wave-induced and dynamic stresses in the short-term appeared mixed at best, it appeared worthwhile to look at the combined stress problem in a much more purely empirical way. Since it was suspected that much of the confounding of results pertaining to vibration had to do with the influence of the many small vibrations which exist in every record, it was decided to consider only the maximum values of the various components of stress in each record. The detail of this effort is shown in the last two sections of Appendix C-7. Previously developed statistics from the FOTINI-L and SL-7 data sub-sets were used in this investigation.

The first question posed was about the magnitude of the maximum dynamic increment to wave-induced stress in relation to the magnitude of the maximum superimposed double amplitude of isolated vibration (Sections 4.4, 4.5). The first finding was as expected; that is, the maximum dynamic increment in a record is not generally exactly equal to half the maximum vibration double amplitude. It may be more or less. However, the results for the FONTINI-L suggested that it would not be terribly conservative to assume that the maximum dynamic increment in a record is equal to half the maximum vibration double amplitude (the most probable ratio between the two was about 0.9). The results for the SL-7 data were mixed. In this case the most probable value of the ratio of maximum increment to half the maximum vibration double amplitude was about 0.8 but the dispersion of the values was greater than that for the FOTINI-L.

The next question posed was essentially "does the maximum dynamic increment in a record increase the maximum wave-induced stress excursion in a record, or some other excursion?" The answer was that in general the maximum dynamic increment in a record is not added to the maximum wave-induced stress.

At this point it appeared that the addition of half the maximum double amplitudes of vibration to the maximum wave-induced main extremes in tension and compression would quite likely be an overly conservative procedure. Though this addition can and did occur, it does not appear highly probable. While the maximum dynamic increment in the record is approximately half the maximum double amplitude of vibration, the data indicate that it may increase wave-induced excursions of any magnitude.

These results implied that perhaps the problem was not being approached from an advantageous direction. In the present context the real interest is in the maximum combined stress in a record. The maximum combined stress in tension or compression is the sum of a wave-induced main extreme and a vibration-induced dynamic increment. Accordingly, it appeared reasonable to investigate the wave-induced stress and the dynamic increments "associated" with the maximum combined stress in each record.

In the case of the SL-7, in about 95% of all records in the data sub-set, the wave-induced main extreme associated with the maximum combined stress was found to be either within 5% of the maximum wave-induced main extreme in the record or exactly equal to it. In about 65% of the FOTINI-L records in the data sub-set, the wave-induced main extreme associated with the maximum combined stress was found to be within 10% of the maximum wave-induced main extreme in the record. The detailed results show that the associated wave-induced main extreme and the record maximum were identical in about 50% of the data sub-set. It appears that the maximum combined stress in a record may be generally assumed to result from the addition of vibration to the maximum wave-induced stress in the record. The assumption would involve very little conservation for the SL-7 and would appear within reason for the FOTINI-L.

Considering the increments due to vibration which are associated with the maximum combined stress, it was found that the ratio of this quantity to half the maximum vibration double amplitude in a record was more or less uniformly distributed between values of zero and about 1.1.

In summary, the results from the data sub-sets imply that it may be within reason, though somewhat conservative, to assume in the long term that the maximum combined main stress extreme in tension or compression in a record is the sum of the maximum wave-induced main extreme in the record and a dynamic increment which is a uniformly distributed fraction of half the maximum double amplitude of vibration in the record. Thus, an approach is suggested to the conversion of empirical long-term distributions of maximum vibration double amplitudes (Section 4.5) to long-term distributions of vibration increments associated with the maximum wave-induced stresses, since the uniform distribution just cited may be interpreted as a conditional distribution of σ_5, given the maximum vibration double amplitude.

5. CLASSIFICATION SOCIETIES AND HULL GIRDER DESIGN CRITERIA

5.1 Introduction

In general, it can be said that classification societies' rules represent current design practices. And, probably without exception, all merchant ships are designed, built and maintained at least to the minimum standards specified by the classification society in question.

Here, the hull girder design criteria of four of the leading classification societies are examined, compared and applied to the study ships. The organizations selected for the study have been steadily introducing rational design features in their rules based on results of research and development effort. They are:

- o American Bureau of Shipping (ABS) - USA
- o Lloyd's Register of Shipping (Lloyd's) - Brita
- o Bureau Veritas (BV) - France
- o Det Norske Veritas (DnV) - Norway

On the whole, all rules and requirements specified by these leading societies are similar, with differences only in details.

The primary elements of the rules are still-water bending moment, wave-induced bending moment, maximum permissible longitudinal bending stress and required minimum section modulus. The still-water and wave-induced moments are added directly. Estimation of dynamic moment is not a consideration. All unknowns, such as structural deviations, residual and thermal stresses, dynamic stress increments, etc., are reflected in the allowable stress.

5.2 Basic Approaches and Design Rules

American Bureau of Shipping - 1976[21]

a. Still-Water Bending Moment (SWBM)

Required - Calculations of SWBM for all the anticipated loaded and ballasted conditions are to be submitted.

Standard Design Formula - In case the detailed information of loading is not available, a "standard" SWBM as specified by the following equation may be used:

$$M_s = C_{st} L^2 \sqrt{L} B \quad (C_b + 0.5)$$

where

M_s = Standard SWBM

C_{st} = Emperical Constant dependent upon ship length and measurement system (SI or English)

L = Ship Length

B = Ship Breadth

C_b = Block Coefficient

b. Wave-Induced Bending Moment (WIBM)

Rule Equation: $M_w = C_2 L_1^2 B H_e$

where M_w = Wave-Induced Bending Moment

C_2 = Constant for Different Wave Conditions

L_1 = LBP

B = Ship Breadth

H_e = The Effective Wave Height of Standard Wave (derived from calculated long-term bending moment responses in North Atlantic Ocean waves).

c. Nominal Permissible Longitudinal Bending Stress - f_p

$$f_p = 10.56 + \frac{L-790}{2045} \text{ tons/in}^2 \text{ for } 790 < L \leq 1400 \text{ ft}$$

d. Minimum Required Section Modulus - SM

$$SM = M_t / f_p$$

where $M_t = M_{sw} + K_b M_w$ (Total Longitudinal Bending Moment)

M_{sw} = SWBM, $\geq 0.875\ M_s$, if calculated from loading information

M_w = WIBM

K_b = Constant dependent upon C_b

Lloyd's Register of Shipping - 1975[22]

a. SWBM

The design SWBM is the maximum, hogging or sagging, calculated for all the possible loading conditions

b. WIBM

The rule wave bending moment M_w can be calculated by using

$$M_w = \sigma_w C_1 L^2 B (C_b + 0.7) \times 10^{-3} \text{ (Metric System)}$$

where σ_w = Max. Permissible Stresses due to WIBM

C_1 = Factor dependent upon Ship Length

The above direct calculation equation was based on the derivation of response to regular waves by strip theory, short-term response to irregular waves using the sea spectrum concept, and long-term response predictions using statistical distributions of sea states.

c. Maximum Permissible Longitudinal Bending Stresses.

The maximum permissible stresses for still-water bending stress, wave bending stress and combined stress are tabulated in Table D.3.4 of Reference 22 for the appropriate ship type and different service conditions.

d. Min. Section Modulus Required - SM_m

$$SM_m = C_1 L^2 B (C_b + 0.7)\ cm^3$$

Bureau Veritas - 1975[23]

a. SWBM -

The most unfavorable loading condition is to be considered for SWBM calculation. If actual light ship weight distribution is not known, it may be based on statistical law approved by the head office.

b. WIBM -

The maximum rule value of wave bending moment (M_H) is given by the formula:

$$M_H = H L^2 B (C_b + 0.7) \times 10^{-3} \text{ (Metric System)}$$

where $H = 71.67 - 6.67 \left[\frac{300-L}{100}\right]^{3/2}$ if $L < 300^m$

$H = 71.67$ if $L \geq 300^m$

c. Maximum Permissible Stresses - 8.89 tons/in^2 (14 kg f/mm^2)

d. Minimum Section Modulus -

The midship section moduli at deck and bottom are not to be less than the greater of the two values:

$$W = W_m$$

$$W = \mu \frac{M_c + M_H}{14} 10^{-3}$$

with:

μ = 1.08 for oil tankers

μ = 1.05 for other ships

M_H = wave bending moment, in tm.

M_c = maximum value of still water bending moment, in tm.

W_m = minimum value of section modulus, in m^3, derived from

$$W_m = FL^2 B (C_b + 0.7) 10^{-6}$$

where:

$$F = 10.75 - \left[\frac{300-L}{100}\right]^{3/2} \quad \text{if } L < 300^m$$

$$F = 10.75 \quad \text{if } L \geq 300^m$$

Det Norske Veritas - 1975(24)

a. SWBM

As a first approximation - SWBM (M_{sv}) may be calculated by $M_{sv} = 0.5 \left[a (C_b + b) L \Delta n - (cLP + Mm + \sum px)\right]$

(Metric System)

where a, b, c = constants based on loading condition and ship type

$0.174 < a < 0.182$

$0.30 < b < 0.35$

$0.20 < c < 0.25$

Δn = The extreme displacement @ the actual draft

M = Weight of the machinery

P = Weight of light ship minus weight of machinery

m = The distance between the centre of gravity of the machinery and L/2

p = Individual weights which are included in the deadweight

x = The distance from L/2 to the centre of gravity of the individual weights

b. WIBM -

Equations for vertical wave bending moment - M_{BV}

$$M_{BV}(\text{sag}) = 0.325\ C_v\ L_1^2\ B\ (C_b + 0.2) \times 10^5 \text{ kg-cm}$$

$$M_{BV}(\text{hog}) = 0.43\ C_v\ L_1^2\ B\ C_b^2 \times 10^5 \text{ kg-cm}$$

where:

$$C_v = 0.3 - \left(\frac{250-L_2}{370}\right)^3$$

L_1 = LBP

L_2 = L_1 but need not be taken greater than 250^m

For horizontal wave bending moment - M_{BH}

$$M_{BH} = 0.94\left(0.23 - \left[\left(\frac{400-L_3}{650}\right)^3\right]\right)L_1^2\ d\ C_b \times 10^5 \text{ kg-cm}$$

where:

L_3 = L_1 but need not be taken greater than 400^m

d = mean moulded summer draft in meters

c. Max. Permissible Stress - 1900 kg/cm^2 (for ships intended to carry ore or similar heavy cargo)

The longitudinal compressive stress (σ_L) at a given location in midship section is to be taken as:

$$\sigma_L = 1.7\ \sigma_B + \sigma_{SV}$$

where:

$$\sigma_B = \sqrt{\left[\frac{M_{BV}\ (y-y_n)}{I_v}\right]^2 + \left[\frac{M_{BH}\ x}{I_H}\right]^2}$$ wave bending stress

$$\sigma_{SV} = \frac{M_{SV}\sqrt{(y-y_n)^2}}{I_v} \quad \text{-still-water bending stress}$$

I_v = moment of inertia in cm^4 of midship section about the horizontal neutral axis, corrosion allowance not deducted.

I_H = moment of inertia in cm^4 of midship section about the vertical centre line, corrosion allowance not deducted.

x and y = coordinates in cm of the plate panel location in relation to the intersection of of the ship's center line and keel line, see figure.

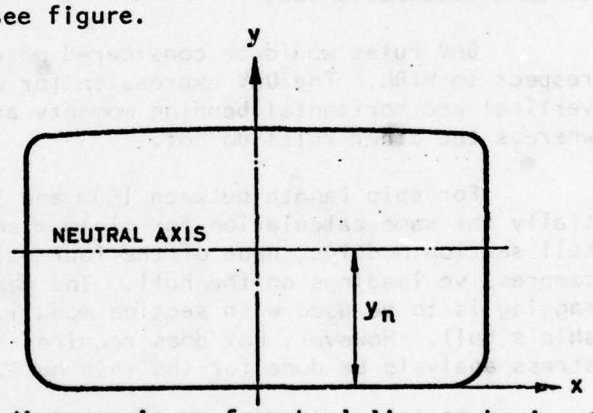

y_n = distance in cm from keel line to horizontal neutral axis.

d. Minimum Required Section Modulus

$$Z_o = \frac{C_1}{f_1} C_2 L_1^2 B (C_B + 0.7) \ cm^3$$

where

$$C_1 = 10.75 - \left(\frac{300-L_1}{100}\right)^{3/2} \qquad L < 300^m$$

$$= 10.75 \qquad L \geq 300^m$$

C_2 = 1.0 or 1.03 (depends on type of ship)

f_1 = 1.0 (Depends on material)

5.3 Application of Rules to Study Ships

The rules of the four societies (ABS, Lloyd's, BV and DnV) were applied to the SL-7, FOTINI-L and UNIVERSE IRELAND and calculations were made to determine the still-water bending moments, wave-induced bending moment, maximum permissible stress and minimum required section moduli. The numerical results are summarized in Table 5-1.

It can be seen that the requirements of longitudinal strength as specified by the four different classification societies are not very different from one another. All allow the use of calculated SWBM for anticipated loading condition. ABS further requires that a "standard" SWBM be calculated, and that any SWBM used in Section-Modulus calculations be at least 0.875 of the "standard" SWBM. The other rules make no similar restriction on SWBM. It is pertinent to note that the "standard" SWBM based on the ABS requirement are approximately the same as for the anticipated loading conditions for the SL-7 and UNIVERSE IRELAND. However, for the FOTINI-L, the "standard" SWBM appears to be considerably low.

DnV rules would be considered more detailed than other rules with respect to WIBM. The DnV expression for wave bending stress involves both the vertical and horizontal bending moments and moments-of-inertia explicitly, whereas the other rules do not.

For ship length between 150m and 300m, Lloyd's, BV and DnV have essentially the same calculation for minimum section modulus. In calculations for hull section modulus, none of the four rules distinguish between tensile and compressive loadings on the hull. The maximum bending moment due to hogging or sagging is to be used with section moduli for upper and lower portions of the ship's hull. However, DnV does require that a separate buckling (compressive) stress analysis be done for the ship hull.

Lloyd's distinguishes two ship types for the purpose of establishing the maximum permissible stress to be used in calculating the hull section modulus. Type 1 (ships with cargoes denser than fresh water) are allowed stress only 90% of that which is allowed for Type 2 (ships with cargoes less dense than fresh water). But it is known that many operators of dense cargo-carrying ships take special care to distribute the loads in a manner conducive to ship safety. If they wish to benefit from this practice, under the Lloyd's rules they must go the route of individual consideration for vessels of special or unusual design.

TABLE 5-1

Summary of Design Requirements of Classification for Three Study Ships

SHIP	Classification Societies	SWBM (FT-LT)	WIBM (FT-LT)	Max.Perm. Long Stress (TSI)	Min. Req. S.M. (FT-IN^2)
SL-7	ABS	688,183	870,857	10.60	153,652
	LLOYD'S	711,841 *	991.093	10.41	155,683
	BV	711,841 *	660.513	8.89	155.683
	DnV	711,841 *	M_{BV} = 533,977 M_{BH} = 267,944	12.06	155,683
FOTINI-L	ABS	M_t=214,040** 0.875M_t =184,484	1,027,809	10.56	164,289
	LLOYD'S	306,800*	986,815	Heavy Cargo 11.53 Coal,etc. 10.41	155,401
	BV	306,800*	763,656	8.89	155,401
	DNV	306,800*	M_{BV} = 628,997 M_{BH} = 442,654	12.06	155,401
UNIVERSE IRELAND	ABS	2,285,896	3,291.251	10.70	521,229
	LLOYD'S	2,355,000*	3,106,932	10.41	489,262
	BV	2,355,000*	2,071,216	8.89	489,262
	DnV	2,355,000*	M_{BV} = 1,914,589 M_{BH} = 1,584,478	12.06	489,262

* Max. SWBM from Loading Manual

** "Standard" SWBM

6. FINDINGS AND CONCLUSIONS

1. The Logbook information for the study ships related to deadweight distribution, and ballast changes and fuel consumption during voyages, is inadequate or unretrievable or too costly to retrieve. This situation precluded the reconstruction of the actual experienced loading conditions and the calculation of the corresponding still-water bending moments.

The correlation between the loading booklets and the full-scale stress data with respect to the still-water bending moment variation during voyages was poor.

2. Full-scale stress measurements lend themselves to the estimation of thermal stresses. The magnitude of the stress is dependent on the ship type, color of the deck or its protection from the sun and weather factor. No correlation is found between the magnitude of the stress and different geographical areas for the same ship.

3. The SL-7 full-scale stress data show maximum diurnal mean bending stress variation of 1 to 3 kpsi and variation throughout voyages of 1 to 6 kpsi.

The FOTINI-L full-scale stress data show maximum diurnal mean variation of 1 to 3 kpsi and voyage variation of 2 to 17 kpsi.

The UNIVERSE IRELAND full-scale stress data show maximum diurnal stress variation of 2 to 6 kpsi and voyage variation of 4 to 19 kpsi. The large variations in the mean stress do not correlate with the sample loading conditions, full load or ballast, in the loading booklet.

The implication of these variations is that the operating procedures of containerships require relatively small margin for still-water stress variation during voyages whereas those of the tankers and bulk carrier require large margins.

In general, the still-water bending stress variations appear to have a random nature and at the same time submit to the control of their extremes by the operators; this suggests that still-water bending moments can be expressed and estimated probabilistically with truncated distributions.

4. The UNIVERSE IRELAND experiences very little sea-related vibration and the magnitude of the associated vertical bending load appears nearly independent of heading or sea condition. In fact, for the purpose of design, at least in the near term, the effect of vibratory response from all causes could be conservatively accounted for by assuming an increment to wave-induced tension or compression of less than 2 kpsi.

5. A considerable portion of the high-vibration data for the FOTINI-L was found to be suspect; elimination of this data from the analysis tends to reduce the significance of vibration in the synthesis of extreme loads.

6. The maximum vibration in the SL-7 is induced both by forward bottom slamming and "flare shock" (the inception of vibration occurs at maximum wave-induced hogging as well as sagging). The maximum vibration increases gradually with wave severity and as the heading changes from following seas to head seas. Additionally, the general trends are functions of combinations of weather and speed parameters. There is a steep increase in the stress at Beaufort number 9 when the normal speed is still maintained but there is sharp decrease at Beaufort number 10 when the speed is reduced. Maximum vibration stress double amplitudes of 3 kpsi are exceeded in 12% of the records; peak stresses of 10 kpsi and 15 kpsi are present in the records.

7. The level of the maximum vibration of FOTINI-L is low. 98.6% of the double amplitudes of stress are below 3 kpsi and the remaining are below 9 kpsi; the higher values are associated with Beaufort numbers above 6 and beam seas. The trend in beam seas as well as the time histories suggest that the vessel experiences mostly springing.

8. The short-term maximum vibration stress data for both the SL-7 and FOTINI-L do not fit the Rayleigh or the exponential distributions, however, they are closer to the latter. This situation leaves a serious gap in the procedure to predict long-term trends from short-term RMS estimates and hinders the development of a rational method for the synthesis of loads.

9. The long-term distributions of the double amplitudes of the maximum vibration stress for the SL-7 and FOTINI-L fit (empirically) the Weibull distribution satisfactorily. This would aid in the development of a semi-empirical procedure for the long-term prediction of vibration loads, however, it would be constrained by the limited availability of full-scale data for various ship types.

10. The short-term wave-induced bending moment maxima for the SL-7 at slow speed fit the Rayleigh distribution reasonably well. At operating speed the data fit the Cartwright and Longuet-Higgins distribution with the broadness parameter approaching unity for over half of the data. A relatively small portion of the data fits the Rayleigh distribution. If it is assumed for the simplification of analyses that the short-term wave-induced bending moment maxima are always Rayleigh distributed, the resulting long-term prediction is likely to be conservative to a degree which is not possible to judge based on the work performed. The ratio of compression to tension of wave-induced bending moment maxima is approximately 1:1.2 for extremes and 1:1.06 for RMS.

In the case of the FOTINI-L, the assumption that the short-term wave-induced moment fit the Rayleigh distribution would be reasonable, if not always true. The magnitudes of compression and tension are symmetrical.

11. For the SL-7 and FOTINI-L the short-term distributions of the dynamic increment to wave-induced stress (which together form the combined dynamic stress) do not fit the Rayleigh or the exponential distributions. To use either form even with judicious corrections for engineering purposes does not appear advisable. The magnitude of the compression and tension are statistically symmetrical.

For purposes of estimating loads, the assumption that the dynamic increments and wave-induced bending moment maxima are statistically independent appears valid.

12. The combined short-term dynamic stress data for the SL-7 fits the Cartwright and Longuet-Higgins distribution with large broadness parameter; however, it is likely to underpredict the extremes.

13. The data suggest that in the long term the maximum combined dynamic stress extreme in tension or compression found in a record is the sum of maximum wave-induced main extreme and an increment which is a fraction of half the maximum double amplitude of vibration in the record. This fraction is approximately uniformly distributed between 0 and 1.1 over all records.

7. RECOMMENDATIONS

1. A very comprehensive program is required to establish the validity of making long-term predictions of still-water bending moments using a probabilistic approach and to determine the nature of the statistical distribution for different ship types. Three approaches should be considered.

   i) Collection of actual operating data on deadweight distribution, and fuel consumption and ballast changes during voyages for minimum of one year. In view of the difficulties experienced in this project, the data gathering, recording and communicating procedure must be worked out precisely in every detail and explained to every ship officer responsible for the task.

      Preliminary discussions should be held with the ship owners to obtain their view on the practicality of the program and the extent of the cooperation they would provide.

   ii) Derivation of all possible loading conditions (within practical limits of draft and trim) over the lifetime of a ship. It should include the derivation of fuel consumption and all possible ballast changes, including those during tank washing, for all possible voyages.

      The pitfall of this method is the requirement to employ subjective judgement to apply probabilities of occurrances to the different loading conditions and to establish the points of truncation of the distributions.

   iii) Installation of mechanical scratch gages which would record extreme stress variation during a designated time period. The still-water bending stress at time of the installation of the gage would be the reference stress for the duration of the instrumentation period.

      Results of this report indicated that the median of the stress extremes in each time period would be quite a reasonable estimate of the mean stress.

      Estimates of the still-water bending stress and thermal stress may be derived from the information on the means.

      It is believed that the scratch program could be cost-effective in the pursuit of rational design procedure.

2. The existing procedure for the estimation of wave-induced bending moment should be extended to incorporate the short-term broad-band response using the Cartwright and the Longuet-Higgins distribution. The response calculation for different ship types should be performed for both Rayleigh and broad-band distributions and compared with experimental and/or full-scale results. This comparison would indicate the magnitude of overestimation due to Rayleigh and the advisability of using it.

3. If the vibration is considered as a separate entity, the results of the long-term empirical predictions of the maximum vibration double amplitude may be applied to the classification society rules to determine the probable influence of vibration at varying risk levels in the estimation of the section modulus.

4. A study should be made to determine the advisability of converting the empirical long-term distributions of maximum vibration double amplitudes to long-term distributions of vibration increments associated with the maximum wave-induced stresses for inclusion in a design procedure.

8. REFERENCES

1. Lewis, E.V., Hoffman, D., MacLean, W.M., Van Hooff, R. and Zubaly, R.B., "Load Criteria For Ship Structural Design", SSC 240, Ship Structure Committee, 1973.

2. Boentgen, R.R., Fain, R.A., and Wheaton, J.W., "First Season Results from Ship Response Instrumentation Aboard the SL-7 Class Containership S.S. SEA-LAND McLEAN in North Atlantic Service", SSC-264, SL-7-8, 1976.

3. Wheaton, J.W. and Boentgen, R.R., "Second Season Results from Ship Response Instrumentation Aboard the SL-7 Class Containership S.S. SEA-LAND McLEAN in North Atlantic Service", SL-7-9, 1976, AD-A034162.

4. Kaplan, P., Sargent, T.P. and Cilmi, J. "Theoretical Estimates of Wave Loads on SL-7 Containership in Regular and Irregular Seas", Ship Structure Committee SSC-246, 1974.

5. Kim, C.H., "Theoretical and Experimental Correlation of Wave Loads for SL-7 Containership", Report SIT-DL-75-1829, 1975.

6. Dalzell, J.F. and Chiocco, M.J., "Wave Loads in a Model of the SL-7 Containership Running at Oblique Headings in Regular Waves", Ship Structure Committee SSC-239 (SL-7-2), 1974.

7. Little, R.S. and Lewis, E.V., "A Statistical Study of Wave-Induced Bending Moment on Large Oceangoing Tankers and Bulk Carriers", Society of Naval Architects and Marine Engineers Transactions, Volume 79, 1971.

8. Stiansen, S.G. and Mansour, A.E., "Ship Primary Strength Based on Statistical Data Analysis", Society of Naval Architects and Marine Engineers Transactions, Volume 83, 1975.

9. Hoffman, D., "A Comparison of Theoretical and Experimental Bending Moment Response in Regular Waves," American Towing Tank Conference, August 1971.

10. Chiocco, M.J. and Numata, E., "Vertical Wave Bending Moments in a Model of the Tanker S.S. UNIVERSE IRELAND Running at Oblique Headings in Regular Waves", Letter Report 1528, Davidson Laboratory, May, 1971.

11. Ivanov, L. and Madjarov, H., "The Statistical Estimation of SWBM for Cargo Ships", Shipping World and Shipbuilder, August 1975.

12. Mano, H., Kawabe, H., Iwakawa, K., Mitsumune, N., "Statistical Character of the Demand on Longitudinal Strength (Second Report) Long-Term Distribution of Still-Water Bending Moment", Journal of the Society of Naval Architects of Japan, Volume 142, December 1977.

13. Hogben, N. and Lumb, F.E., "Ocean Wave Statistics", H.M. Stationery Office, London, 1967.

14. Yamanouchi, Y. and Ogawa, A., "Statistical Diagram on the Winds and Waves on North Pacific Ocean", Ship Research Institute, Tokyo, Japan, March 1970.

15. Raff, A.I., "Program SCORES - Ship Structural Response in Waves", Ship Structure Committee SSC-230, 1972.

16. Johnson, A.E., Flaherty, J.A. and Walters, I.J., "A Method for Digitizing, Preparing and Using Library Tapes of Ship Stress and Environment Data", Ship Structure Committee SSC-236, 1973.

17. Jasper, N.H. and Church, J.W., "Structural Seaworthiness Studies," Trans., SNAME 71, 1963.

18. Nordenstrom, N., "A Method to Predict Long-Term Distributions of Waves and Wave-Induced Motions and Loads on Ships and Other Floating Structures". Det Norske Veritas, Publication No. 81, April 1973.

19. Ochi, M.K. and Bolton, W.E., "Statistics for Prediction of Ship Performance in a Seaway", International Shipbuilding Progress, 1973.

20. Ochi, M.K., "On Prediction of Extreme Values", Journal of Ship Research Volume 17, No. 1, March 1973.

21. American Bureau of Shipping, "Rules for Building and Classing Steel Vessels", Section 6-Longitudinal Strength, 1976.

22. Lloyd's Register of Shipping, "Rules and Regulations for the Construction and Classification of Steel Ships", Chapter D - Hull Construction, 1975.

23. Bureau Veritas, "Rules and Regulations for the Construction and Classification of Steel Ships", Section 5-2 - Criteria of Longitudinal Strength, 1975.

24. Det Norske Veritas, "Rules for the Construction and Classification of Steel Ships", Section 7 of Chapter II - Longitudinal Strength,,1975.

25. Fain, R.A., "Design and Installation of a Ship Response Instrumentation System Aboard the SL-7 Class S.S. SEA-LAND McLEAN", SSC-238, SL-7-1, 1973, AD-780090.

26. Boentgen, R.R., "Third Season Results from Ship Response Instrumentation Aboard the SL-7 Class Containership S.S. SEA-LAND McLEAN in North Atlantic Service", SL-7-10, 1976, AD-A034175.

27. Dalzell, J.F., "Correlation and Verification of Wavemeter Data from the SL-7, Report 1: Selection of Second Season Data Set, Digitization, Calibration, and Initial Results", SIT-DL-1865, Stevens Institute of Technology, 1977.

28. Dalzell, J.F., "Correlation and Verification of Wavemeter Data from the SL-7, Report 2: Analyses and Data Reduction Procedures", SIT-DL-77-1930, Stevens Institute of Technology, 1977.

29. Dalzell, J.F., Correlation and Verification of Wavemeter Data from the SL-7, Report 3: Reduced Results from Voyage 32", SIT-DL-77-1931, Stevens Institute of Technology, 1977.

30. Dalzell, J.F., "Correlation and Verification of Wavemeter Data from the SL-7, Report 4: Reduced Results from Voyage 33", SIT-DL-77-1933, Stevens Institute of Technology, 1977.

31. Dalzell, J.F., "Correlation and Verification of Wavemeter Data from the SL-7, Report 5: Reduced Results from Voyage 34", SIT-DL-77-1934, Stevens Institute of Technology, 1977.

32. Dalzell, J.F., "Correlation and Verification of Wavemeter Data from the SL-7. Report 6: Reduced Results from Voyages 35 and 36E", SIT-DL-77-1935, Stevens Institute of Technology, 1977.

33. Kaplan, P. and Sargent, T.P., "Further Studies of Computer Simulation of Slamming and Other Wave Induced Vibratory Structural Loadings on Ships in Waves", SSC 231, Ship Structure Committee, 1972.

34. Bendat, J.S. and Piersol, A.G., "Measurement and Analysis of Random Data" John Wiley & Sons, Inc., New York, 1966.

35. Cartwright, D.E., and Longuet-Higgins, M.S., "The Statistical Distribution of the Maxima of a Random Function", Proc. Royal Society, A,237, 1956.

36. Gumbel, D.E., "Statistics of Extremes", Columbia University Press, New York, 1958.

37. Dalzell, J.F., "Correlation and Verification of Wavemeter Data from the SL-7, Report 10, Summary, Discussion, Conclusions", SIT-DL-77-1944, Stevens Institute of Technology, 1977.

38. Cramer, H., "Mathematical Methods of Statistics", Princeton University Press, 1946.

39. Mood, A.M., "Introduction to the Theory of Statistics" McGraw-Hill, New York, 1950.

40. Gerassimov, A.V., "Energy Characteristics of Stationary Random Oscillations and Their Use in Statistical Linearization", Paper 41, International Symposium on the Dynamics of Marine Vehicles and Structures in Waves", University College London, April 1974.

ACKNOWLEDGEMENT

Research projects such as the "Load Criteria Study" are greatly dependent on the understanding and cooperation of private companies to provide proprietary information. Invariably it also involves demonstration of considerable personal interest and expenditure of valuable man-hours. The authors greatly appreciate such assistance from:

The American Bureau of Shipping

Bethlehem Steel Corporation, Marine Division, Edgemere Plant, Maryland

Sea -Land Service, Incorporated

National Bulk Carriers, Incorporated

Webb Institute of Naval Architecture

In addition, the authors wish to acknowledge the constructive guidance and opinion of the various members of the Project Advisory Committee.

APPENDIX A

STILL-WATER BENDING MOMENTS CALCULATIONS

TABLE A-1

SL-7, Summary of Sample Loading Conditions From Loading Manual

Condition / Item	Unit	A T L A N T I C				P A C I F I C			
		East Bound		West Bound		East Bound		West Bound	
		Depart New York	Arrive Europe	Depart Europe	Arrive New York	Depart Japan	Arrive U.S.A	Depart U.S.A	Arrive Japan
Displacement	LT	48504	47621	47880	46049	45112	41695	50374	49825
Light Ship Weight	LT	24671	24671	24671	24671	24671	24671	24671	24671
Dead Weight	LT	23833	22950	23209	21378	20441	17025	25703	25154
Containers	LT	18477	18477	17853	17833	12803	12803	18836	18836
Fuel Oil	LT	4036	1120	4036	1120	4998	948	4998	948
Diesel Oil	LT	138	60	138	60	138	60	138	60
Ballast	LT	606	2829	606	1881	1926	2750	1155	4846
Fresh Water	LT	576	464	576	464	576	464	576	464
Draft-Fore	FT	32.31	28.63	32.33	29.66	29.90	28.76	31.52	31.59
Draft-Aft	FT	33.56	35.55	32.95	33.24	32.13	29.62	35.97	35.48
Draft-Mean	FT	32.94	32.09	32.64	31.45	31.02	29.19	33.75	33.54
Trim	FT	1.25	6.92	0.62	3.58	2.23	0.86	4.45	3.89
Dead Weight Moment	LT-FT	1921494	1843776	1850450	1634112	1748750	1446084	2206986	2189014
Light Ship Moment	LT-FT	2357827	2357827	2357827	2357827	2357827	2357827	2357027	2357827
Disp. Moment	LT-FT	4279321	4201603	4208277	3991939	4106577	3803911	4564813	4546841
Stress Numeral		71	71	70	60	89	87	91	94
Buoy. Moment Hog	LT-FT	3731000	3590000	3602000	3535000	3450000	3155000	3875000	3835000
Net Buoy Moment	LT-FT	548320	611603	606277	456939	656577	648911	689813	711841
Stress	PSI	8388	9360	9280	6996	10045	9927	10554	10887
GM Corrected	FT	3.23	2.93	3.66	2.91	5.72	3.57	2.59	2.56
GM Required	FT	2.29	2.35	2.33	2.46	2.53	2.83	2.17	2.20

Section Modulus 184,521 IN^2 FT

TABLE A-2 (a)

FOTINI-L Summary of Sample Loading Conditions from Loading Manual

Item \ Condition	Unit	Heavy Cargo S.F. 20 €/LT				Coal Cargo S.F. 42 €/LT				Coal Cargo S.F. 48 €/LT			
		2	3	4	5	6	7	8	9	10	11	12	13
		Dep.	Arr.	Dep.	Arr.	Dep.	Arr.	Dep.	Arr.	Dep.	Arr.	Dep.	Arr.
Constants	LT	527	527	527	527	527	527	527	527	527	527	527	527
Provisions	LT	10	2	10	2	10	2	10	2	10	2	10	2
Fuel Oil	LT	2170	435	1339	226	2170	435	1339	226	2170	435	1339	226
Diesel Oil	LT	174	34	108	21	174	34	108	21	174	34	108	21
Fresh Water	LT	252	181	252	181	252	181	252	181	252	181	252	181
Ballast Water	LT	-	1950	-	1015	-	1920	1000	2015	1005	-	480	-
Cargo	LT	71070	71070	71967	71967	70509	70509	70509	70509	61696	61696	61696	61696
Deadweight	LT	74203	74199	74203	73939	73642	73608	73745	73481	65834	62875	64412	62653
Light Ship	LT	15950	15950	15950	15950	15950	15950	15950	15950	15950	15950	15950	15950
Displacement	LT	90153	90149	90153	89889	89592	89558	89695	89431	81784	78825	80362	78603
Equiv. Draft	FT-IN	44-6½	44-6½	44-6½	44-5	44-3½	44-3¼	44-4	44-2½	40-8¼	39-3½	40-¼	39-2¼
Draft-Fore	FT-IN	44-6¼	44-6½	44-6½	44-5	44-3	44-3¼	44-4	44-2½	40-8¼	39-3⅝	40-¼	39-3
Draft-Aft	FT-IN	44-6⅝	44-6½	44-6½	44-5	44-4	44-3¼	44-4	44-2½	40-8¼	39-3⅜	40-¼	39-1⅝
Draft-Mean	FT-IN	44-6½	44-6½	44-6½	44-5	44-3½	44-3¼	44-4	44-2½	40-8¼	39-3½	40-¼	39-2⅜
Trim	FT-IN	0-⅜	0	0	0	0-1	0	0	0	0	0-⅝	0	0-1⅜
Max SWBM	LT-FT	175000	173000	-155000	156600	-286100	-290600	-306800	-277800	-100800	-156900	-139500	-149800
Max SWB stress	PSI	2473	2444	-2190	2213	-4042	-4106	-4335	-3925	-1424	-2217	-1971	-2217

€ = cubic feet
(+) Hogging
(-) Sagging

Section Modulus = 158576 IN^2-FT

TABLE A-2 (b)

FOTINI-L Summary of Sample Loading Conditions from Loading Manual

Condition / Item	Unit	Bauxite S.F. 32 €/LT		Ballasted Condition			Ballast Condition			Summary from MARKA-L's Captain Abstract: Loaded Long Voyage		Loaded Short Voyage		
		14	15	16	17	18	Upper Bound	Lower Bound	Mean	Upper Bound	Lower Bound	Upper Bound	Lower Bound	Mean
		Dep.	Arr.	Dep.	Arr.	Arr.	Dep.	Dep.	Dep.	Dep.	Dep.			
Constants	LT	527	527	527	527	527	420	420	420	420	420	420	420	420
Provisions	LT	10	2	10	2	2								
Fuel Oil	LT	305	59	3905	2170	266	2663	640	553	1923	920	362	838	372
Diesel Oil	LT	25	5	314	174	21	148	74	100	105	83	68	29	93
Fresh Water	LT	252	181	252	181	181	30	60	50	30	100	20	50	30
Ballast Water	LT	-	305	34721	34721	34721	27000	26700	27553	-	-	-	-	-
Cargo	LT	73084	73084	-	-	-	-	-	-	69111	68713	61428	60590	61200
Deadweight	LT	74203	74163	39729	37775	35718	30261	27894	28676	71589	70236	62298	61927	62105
Light Ship	LT	15950	15950	15950	15950	15950	15950	15950	15950	15950	15950	15950	15950	15950
Displacement	LT	90153	90113	55679	53725	51668	46211	43844	44626	87539	86186	78248	77877	78055
Equiv. Draft	FT-IN	44-6½	44-6¼	28-3½	27-4	26-4⅛	-	-	-	-	-	-	-	-
Draft-Fore	FT-IN	44-6½	44-6¼	23-2¾	25-1¾	26-0¼	22-6	18-5	20-6	43-6	43-5	38-11	38-5	38-8
Draft-Aft	FT-IN	44-6½	44-6¼	33-7¼	29-7⅝	26-8⅝	28-6	27-9	27-4	44-8	43-10	39-10	39-3	39-8
Draft-Mean	FT-IN	44-6½	44-6¼	28-5	27-4⅜	26-4¾	25-6	23-1	23-11	44-1	43-7	39-4	38-10	39-2
Trim	FT-IN	0	0	10-4½	4-6	0-8½	6-0	9-4	6-10	1-2	0-5	0-11	0-10	1-0
Max. SWBM	LT-FT	-228600	-232500	266700	213100	198600	227112	238867	-176133	-366571	-	-	-	-116882
Max SWB Stress	PSI	-3230	-3285	3768	3011	2806	3209	3375	-2488	-5179	-	-	-	-1651

(+) Hogging
(-) Sagging

TABLE A-3

UNIVERSE IRELAND Summary of Sample Loading Conditions from Loading Manual

Condition	Unit	Full Load (Summer) Long Voyage				Full Load Short Voyage		Dirty Ball.	Normal Ballast		Heavy Ballast		Bet. 8&9
		2	3	4	5	6	7	8	9	10	11	12	13
Item		Dep.	Arr.	Dep.	Arr.	Dep.	Arr.	Dep.	Dep.	Arr.	Dep.	Arr.	Dep.
Constants	LT	-	-	-	-	-	-	-	-	-	-	-	-
Provisions	LT	-	-	-	-	-	-	-	-	-	-	-	-
Fuel Oil	LT	12943	6707	12943	6707	4895	2855	6707	6707	1118	6707	1118	6707
Diesel Oil	LT	-	-	-	-	-	-	-	-	-	-	-	-
Fresh Water	LT	605	248	605	248	363	232	605	605	248	605	248	605
Ballast Water	LT	-	-	-	-	-	-	-	28370	29530	33378	33378	26000
Cargo	LT	312702	312702	312702	312702	320992	320992	145469	45388	50174	86661	92607	34554
Deadweight	LT	326250	319657	326250	319657	326250	324079	152781	81070	81070	127351	127351	67866
Light Ship	LT	49561	49561	49561	49561	49561	49561	49561	49561	49561	49561	49561	49561
Displacement	LT	375811	369218	375811	369218	375811	373640	202342	130631	130631	176912	176912	117427
Draft-Fore	FT-IN	81-5	80-1	80-7 1/8	80-1	81-5	81-2 5/8	37-8 1/4	27-10 3/4	28-1 1/2	37-1	38-1/2	20-8 3/8
Draft-Aft	FT-IN	81-5	80-1	82-3 1/4	80-1	81-5	80-8 7/8	54-1/2	32-9	32-5 7/8	43-10 3/8	42-5 1/2	34-8 1/2
Draft-Mean	FT-IN	81-5	80-1	81-5 1/2	80-1	81-5	80-11 3/4	45-10 3/8	30-3 7/8	30-3 3/4	40-5 3/4	40-3	27-8 1/2
Trim	FT-IN	0	0	1-8 1/8	0	0	F0-5 3/4	16-4 1/4	4-10 1/4	4-4 3/8	6-9 3/8	4-5	14-0 1/8
Max SWBM	LT-FT*	-1050	-1940	-770	-1790	-2220	-2355	-1960	1858	1640	-1709	-1770	-2017
Position	FR.NO.	107	84	108	82	81	80	100	80	83 1/2	101 1/2	101	98
Max.SWB Stress	PSI	-4150	-7667	-3043	-7074	-8774	-9307	-7746	-7343	6481	-6718	-6995	-7971

Section Modulus = 566,794 FT-IN^2

(+) Hogging
(-) Sagging

TABLE A -4

SL-7 - Maximum, Minimum, and Maximum Difference of

Relative SWBS for the Voyages and Normality Tests

Voyage Leg. *	TMR Tape No.	Date	Rel. SWBS Stress (PSI)		
			Max.	Min.	Diff.
25E	101,103	9/23/73-9/26/73	2161	-1994	4155
25W	105,107	10/1/73-10/5/73	25	-4119	4144
26E	109,111	10/9/73-10/13/73	5620	-118	5738
26W	113,115	10/17/73-10/21/73	1122	-1136	2258
27E	117,119	10/22/73-10/27/73	736	-2099	2835
28E	121,123	11/29/73-12/03/73	4404	0	4404
28W	125,127	12/6/63-12/10/73	549	-1120	1669
29E	129,131	12/11/73-12/15/73	298	-1497	1795
29W	133,135,137	12/18/73-12/24/73	2520	-2199	4719
32E	139,141	12/30/73-1/4/74	870	-1270	2140
32W	143,145,147	1/8/74-1/14/74	1654	-3083	4737
33E	149,151	1/17/74-1/21/74	835	-2064	2899
33W	153,155	1/23/74-1/27/74	588	-2285	2873
34E	157,159	1/29/74-2/2/74	3754	-1411	5165
34W	161,163	2/5/74-2/9/74	3734	-100	3834
35E	165,167	2/12/74-2/17/74	695	-3012	3707
35W	169,171,173	2/20/74-2/25/74	2416	-1492	3908
36E	175,177	2/27/74-3/3/74	897	-1352	2249
37E	185	3/17/74-3/18/74	264	-879	1143
37W	187,189	3/21/74-3/25/74	1023	-2543	3566

Normality Tests: (5% Level of Significance)

		Mean	σ
Max:	Fail	1708	1527
Min:	Pass	-1689	1023
Diff:	Pass	3397	1236

* E - North Atlantic Eastbound
  W - North Atlantic Westbound

TABLE A-5

FOTINI-L - Maximum, Minimum, and Maximum Difference of Relative SWBS for the Voyages and Normality Tests

Voyage Leg	Date	TMR Tape No.	Rel. SWBS (PSI)		
			Max.	Min.	Diff.
Peru-Japan	10/17/67-11/1/67	1FL2-3	0	-1809	1809
U.S.A.-Peru	12/4/67-12/10/67	2FL1-3,2FL1-3R	1493	-3278	4771
Peru-Japan	12/14/67-1/5/68	2FL2-3,2FL2-3R	3455	-2411	5866
Japan-U.S.A.	1/13/68-1/24/68	3FL1-3,3FL1-3R	7450	-2726	10176
U.S.A.-Peru-Japan	2/9/68-3/2/68	3FL2-3,3FL2-3R	5231	-2548	7779
Japan-Peru	3/12/68-4/20/68	4FL1-3,4FL1-3R	3199	-3727	6926
Japan-Peru	5/5/68-5/15/68	5FL1-3	4424	- 464	4888
Peru-Japan	6/4/68-6/27/68	5FL2-3,5FL2-3R	93	-5013	5106
Japan-Peru	7/5/68-7/28/68	6FL1-3,6FL1-3R	4034	-6713	10748
Peru-Japan	8/1/68-8/27/68	6FL2-3,6FL2-3R	2166	-3472	5638
Japan-Peru	9/2/68-9/13/68	7FL1-3	3316	-3352	6668
Japan-U.S.A.	11/13/68-11/26/68	8FL1-3,8FL1-3R	6167	-9143	15310
U.S.A.-Peru	11/28/68-12/2/68	8FL2-3	0	-14686	14686
Japan-Peru	1/12/69-1/31/69	9FL1-3,9FL1-3R	4880	-10377	15257
Peru-Japan	2/6/69-2/17/69	9FL2-3,9FL2-3R	12066	-5057	17123
Japan-Peru	3/5/69-3/24/69	10FL1-3,10FL1-3R	9971	-3652	13623
Japan-Peru	10/24/69-11/13/69	14FL1-3,14FL1-3R	1368	-4629	5997
Peru-Japan	11/22/69-12/3/69	14FL2-3,14FL2-3R	0	14439	14439

Normality Tests: (5% Level of Significance)

		Mean	σ
Max:	Pass	3851	3339
Min.	Fail	-5416	4007
Diff.	Fail	9267	4651

TABLE A-6

UNIVERSE IRELAND - Maximum, Minimum, and Maximum Difference

Relative SWBS for the Voyages and Normality Tests

Voyage Leg	Date	TMR Tape No.	Rel. SWBS (PSI)		
			Max.	Min.	Diff.
Japan-Persian Gulf (B)*	9/7/68-9/21/68	1U12-3,1U12-3R	2552	-1634	4186
Persian Gulf-Western Europe (L)	9/27/68-10/29/68	1U12-3R,1U13-3,1U13-3R	623	-6066	6689
Western Europe-Persian Gulf (B)	11/1/68-11/29/68	2U11-3,2U11-3R,2U12-3	8578	-5416	13994
Persian Gulf-Western Europe (L)	12/3/68-1/2/69	2U12-3,2U12-3R,2U13-3	1605	-2787	4392
Western Europe-Persian Gulf (B)	1/17/69-2/2/69	3U11-3,3U11-3R	4344	-3728	8072
Persian Gulf-Western Europe (L)	2/6/69-3/8/69	3U11-3R,3U12-3,3U12-3R	6394	-928	7322
Western Europe-Persian Gulf (B)	3/11/69-4/8/69	4U11-3,4U11-3R,4U12-3	10232	-3917	14149
Persian Gulf-Western Europe (L)	4/16/69-5/22/69	4U12-3,4U12-3R,4U13-3,4U13-3R	15512	-1905	17417
Western Europe-Persian Gulf (B)	7/21/69-8/15/69	5U11-7,5U11-7R,5U12-7	7519	-4690	12209
Western Europe-Persian Gulf (B)	11/22/69-12/21/69	7U11-7,7U11-7R,7U12-7	17831	-977	18808
Persian Gulf-Western Europe (L)	12/24/69-1/23/70	7U12-7R,7U13-7,7U13-7R	12416	-1829	14245
Western Europe-Persian Gulf (B)	1/27/70-2/23/70	8U11-7,8U11-7R,8U12-7	12157	-650	12807
Persian Gulf-Western Europe (L)	2/26/70-3/14/70	8U12-7,8U12-7R,8U13-7	4724	-13788	18512

Normality Tests: (5% Level of Significance)

			Mean	σ
Max:	In Ballast	Pass	9030	4707
	Full Load	Pass	6879	5432
	All	Pass	8037	5167
Min:	Ballast	Fail	-3000	1754
	Full Load	Pass	-4551	4440
	All	Fail	-3709	3371
Diff:	All	Pass	11750	4931

* B = Ballast, L = Full Load

APPENDIX B

WAVE-INDUCED BENDING MOMENTS CALCULATIONS

TABLE B-1

Summary of Wave Data for SL-7 - Number of Observations in North Atlantic

Ref: "Ocean Wave Statistics" by N. Hogben & F.E. Lumb
Area No. 6 & 7 are used for SL-7 Wave Spectra Calculation

Wave Height Code	Wave Period Code 2	3	4	5	6	7	8	9	TOTALS	FEET	Wave Height (Ft)
00	2074	65	41	22	7	3	8	3	2223	1.0	
01	5446	625	168	75	28	6	5	4	6357	1.5	
02	10924	5031	1142	351	125	38	24	10	17645	3.0	
03	5914	10226	3585	912	287	107	30	12	21073	5.0	
04	1627	6929	5065	1597	404	119	39	15	15795	6.5	
05	691	3855	4465	2112	614	184	47	18	11986	8.0	
06	271	1838	3076	1997	708	229	59	14	8192	9.5	
07	178	1129	2112	1605	736	246	70	24	6100	11.0	
08	72	610	1264	1169	629	221	75	26	4066	13.0	
09	73	484	1032	1032	584	248	96	25	3574	14.0	
10	11	60	184	190	118	54	16	1	634	16.0	
11	16	64	167	177	112	71	18	3	628	17.5	
12	13	102	247	289	175	79	22	10	937	19.0	
13	22	84	220	318	182	90	32	5	953	21.0	
14	3	33	116	116	79	31	10	1	389	22.5	
15	3	48	106	136	94	55	21	3	466	24.0	
16	3	22	82	91	107	30	21	2	358	25.5	
17	2	17	38	64	52	38	17	2	230	27.0	
18	1	11	30	52	56	22	18	1	191	29.0	
19	3	15	54	106	78	53	30	18	357	30.5	
Totals	27347	31248	23194	12411	5175	1924	658	197	102154		

0 5 7 9 11 13 15 17 19 (Sec)

Wave Period (Second)

TABLE B-2

Summary of Wave Data For SL-7 - Percentage of Observations in North Atlantic

Wave Height (Ft)	Wave Period (Sec.) 0 5	7	9	11	13	15	17	19	Total
1.0	2.03	.06	.04	.02	.01	--	.01	--	2.17
1.5	5.33	.61	.16	.07	.03	.01	--	--	6.22
3.0	10.69	4.92	1.12	.34	.12	.04	.02	.01	17.27
5.0	5.79	10.01	3.51	.89	.28	.10	.03	.01	20.63
6.5	1.59	6.78	4.96	1.56	.40	.12	.04	.02	15.46
8.0	.68	3.77	4.37	2.07	.60	.18	.05	.02	11.73
9.5	.27	1.80	3.01	1.95	.69	.22	.06	.01	8.02
11.0	.18	1.11	2.07	1.57	.72	.24	.07	.02	5.97
13.0	.07	.60	1.24	1.14	.62	.22	.07	.03	3.98
14.0	.07	.48	1.01	1.01	.57	.24	.09	.03	3.50
16.0	.01	.06	.18	.19	.12	.05	.02	---	.62
17.5	.02	.06	.16	.17	.11	.07	.02	---	.61
19.0	.02	.10	.24	.28	.17	.08	.02	.01	.92
21.0	.02	.08	.22	.31	.18	.09	.03	.01	.93
22.5	---	.03	.11	.11	.08	.03	.01	---	.38
24.0	---	.05	.10	.13	.09	.05	.02	---	.46
25.5	---	.02	.08	.09	.10	.03	.02	---	.35
27.0	---	.02	.04	.06	.05	.03	.02	---	.23
29.0	---	.01	.03	.05	.05	.02	.02	---	.19
30.5	---	.02	.05	.10	.08	.05	.03	.02	.22
	26.77	30.59	22.70	12.15	5.07	1.88	.65	.19	100%

Selection For Wave Spectra

Wave Height	4.0	5.5	7.0	7.5	8.0	8.5	11.0	13.0	14.0	16.0
Wave Period	4	6	7	8	9	10	12	14	16	18

TABLE B-3

Summary of Wave Data for FOTINI-L Number of observations between Japan, Peru and San Pedro, California

Ref. "Ocean Wave Statistics" by Hogben & Lumb Route between California and Peru:

AREAS 5, 14, 22, 32 are included

Wave Period Code

Wave Height Code	X	2	3	4	5	6	7	8	9	Totals	Feet	Wave Height (Ft.)
00	1055	1246	29	4	3	0	2	1	0	2340	1.0	
01	60	2628	235	83	31	6	2	2	0	3047	1.5	
02		5035	1948	412	113	43	12	4	0	7567	3.0	
03		1951	3050	793	249	70	36	9	0	6158	5.0	
04		290	1166	754	238	79	17	3	0	2547	6.5	
05		54	343	380	168	46	14	7	1	1013	8.0	
06		10	103	158	85	50	11	4	3	424	9.5	
07		3	40	68	59	25	10	3	0	208	11.0	
08		3	12	27	28	17	0	4	3	94	13.0	
09		2	8	22	17	11	2	6	3	71	14.0	
10		2	1	2	5	1		0		11	16.0	
11		2	2	1	2	1		1		9	17.5	
12		3	4	5	2	4		1		19	19.0	
13			1	5	2	1		1		10	21.0	
14			2	1	0	1				4	22.5	
15				3	1					4	24.0	
16				1						1	25.5	
17											27.0	
18											29.0	
19											30.5	
20												
Totals	1115	11229	6944	2719	1003	355	106	46	10	23527		

0 5 7 9 11 13 15 17 19 (Sec)

Wave Period (Seconds)

TABLE B-4

Summary of wave data for FOTINI -L- Percentage of observations between Japan and California

Ref. "Statistical diagrams on the winds and waves on the North Pacific Ocean" by Y.Yamanouchi and A.Ogawa March 1970. Ship research institute. Tokyo, Japan.

Area 6 5 2 15 16 17 18
% 4.1% 66% 12.2% 12.0% 32.6% 22.5% 10%

Summary of above areas

Wave Height (M)	Wave Period (Sec.) 0 5	5 7	7 9	9 11	11 13	13 15	15	TOTAL
	12.30	1.58	.55	.14	.02	.02	5.92	20.53
1-	16.06	18.75	5.44	.84	.14	.03	.85	42.11
2-	1.33	6.23	10.23	4.31	.66	.12	.44	23.32
3-	.25	.95	1.98	2.24	1.54	.48	.21	7.65
4- 5-	.13	.32	.71	.72	.47	.35	.21	2.91
6- 7-	.03	.10	.18	.17	15	.10	.58	1.31
8- 9- 10-	--	.02	.06	.09	.08	.07	.09	.41
TOTAL	30.10	27.95	19.15	8.51	3.06	1.17	8.30	1.76

Calm Water

TABLE B-5

Summary of wave data for FOTINI-L
Percentages of observation

Route Between California And Peru

		Wave Period (Sec) 0	5	7	9	11	13	15	Total
	1	16.47 29.69	1.12 21.24	.37 5.12	.15 1.54	.03 .48	.02 .20	.01 .06	18.17 58.33
	2	1.46	6.41	4.82	1.73	.53	.13	.05	15.13
Wave Height (M)	3	.06	.61	.96	.61	.32	.09	.04	2.69
	4 5	.04	.10	.22	.22	.13	.01	.07	.79
	6 7	.01	.03	.06	.02	.02	---	.01	.15
	8 9 10								
Total		47.73	29.51	11.55	4.27	1.51	.45	.24	4.74

Calm water

Route Between Japan - California - Peru

		Wave Period (Sec) 0	5	7	9	11	13	15	Total
	1	14.39 22.88	1.35 20.0	.46 5.28	.14 1.19	.03 .31	.02 .11	2.96 .45	19.35 50.22
Wave Height (M)	2	1.40	6.32	7.52	3.03	.60	.12	.24	19.23
	3	.15	.78	1.47	1.43	.93	.28	.13	5.17
	4 5	.08	.21	.47	.47	.30	.18	.14	1.85
	6 7	.02	.06	.12	.10	.09	.05	.29	.73
	8 9 10	---	.01	.03	.05	.04	.03	.04	.20
Total		38.92	28.73	15.35	6.41	2.30	.79	4.25	3.25

Calm Water

Conclusion: Wave Period Range (SEC) 0～11 15～
Wave Height Range (M) 0～5.75 (1～17.5)

TABLE B-6

SL-7 WIBM For Heavy Load And Zero Speed Condition

Sig. Vertical Wave Bending Moment / Sig. Wave Height (FT-TON/FT)

Ship Headings (Degree)	Wave Periods Tw (Second)									
	4	6	7	8	9	10	12	14	16	18
0	792	4244	7900	11000	12846	13714	13278	11619	9818	8231
30	1030	5378	8909	11417	12692	12929	11944	10190	8500	7077
60	2300	8222	9636	9750	9308	8500	6778	5381	4286	3465
90	3067	4278	4145	3875	3554	3229	2639	2148	1755	1438
120	1933	6756	7973	8250	7923	7357	6000	4810	3859	3131
150	787	6022	9636	12000	13154	13357	12278	10476	8682	7231
180	567	4856	8673	11750	13538	14286	13722	12000	10136	8462

TABLE B-7

SL-7 - HEAVY LOADED CONDITION

ZERO SPEED

FRACTION OF WAVE DAMPING = .1

VERTICAL BENDING MOMENT RESPONSE OPERATORS AT MIDSHIP CALCULATED FROM SCORES SHIP MOTION PROGRAM (FT/TONS/FT)

ANGLE FREQ.	0.0	30.0	60.0	90.0	120.0	150.0	180.0
.31790	11200	8130	1590	1960	1640	8200	11300
.36880	18700	14000	3420	2630	3500	14100	18900
.41970	27000	21100	6090	3410	6170	21400	27300
.47060	34600	28600	9590	4290	9580	28900	35100
.52150	38700	34300	13900	5210	13600	34900	39700
.57240	36900	36400	18600	6140	17400	37100	38400
.62330	28200	33300	23000	7090	20700	34700	31000
.67420	14700	24300	26900	7880	22100	27200	19700
.72510	1560	11300	28800	8420	21600	17800	9570
.77600	7090	1570	27200	8500	19600	9040	6470
.82690	6570	8230	21600	8560	17800	5180	7440
.87780	3900	7610	13500	9420	15700	7300	5070
.92870	4890	4020	6900	10900	11600	6220	338
.97960	3690	4380	6400	11400	5420	1670	2290
1.03050	2570	4500	8800	11300	1420	1940	933
1.08140	2480	2910	9160	10800	5370	1880	1940
1.13230	1110	2630	7020	9780	6800	1070	1500
1.18320	1900	1710	3760	8640	5430	1830	416
1.23410	1500	1360	2530	7410	2500	677	1030
1.28500	840	1800	3700	6100	487	742	821
1.13359	588	1200	3520	4910	2020	880	531
1.38680	1060	731	2310	3860	1840	543	267
1.43770	600	603	1890	3000	653	329	680
1.48860	161	800	2100	2340	670	119	611
1.53950	564	447	1690	1880	999	339	193
1.59040	503	236	1200	1540	589	329	451

TABLE B-8

FOTINI-L WIBM For Ballast Load And 16 Knots Speed Condition With 0.1 Fraction Of Critical Roll Damping

Sig. Vertical Wave Bending Moment / Sig. Wave Height (FT - TON/FT)

Ship Headings (Degree)	Wave Periods Tw (Second)									
	4.0	5.5	6.5	7.5	8.5	9.5	10.5	12.0	14.0	16.0
0	1618	3320	6717	10300	12750	14057	14375	13800	12083	10200
30	1748	4340	8250	11514	13375	14029	13875	12900	11000	9200
60	2380	8400	10850	11643	11413	10686	9750	8340	6692	5400
90	1764	2940	3050	2857	2563	2243	1963	1600	1233	975
120	2840	8360	11833	13286	13250	12500	11425	9740	7783	6250
150	1758	4700	9283	13571	16125	17000	16875	15500	13167	10950
180	1504	3780	7717	12371	15625	17286	17750	16900	14667	12350

TABLE B-9

FOTINI-L WIBM For Ballast Load And 16 Knot Speed Condition With 0.2 Fraction Of Critical Roll Damping

Sig. Vertical Wave Bending Moment (FT - Ton/FT)
Sig. Wave Height

Ship Headings (Degree)	Wave Periods (Second)									
	4.0	5.5	6.5	7.5	8.5	9.5	10.5	12.0	14.0	16.0
0	1613	3322	6720	10273	12750	14077	14357	13813	12105	10219
30	1750	4333	8260	11545	13333	14000	13929	12875	11000	9188
60	2388	8400	10900	11636	11417	10692	9786	8313	6684	5375
90	1763	2944	3060	2864	2558	2246	1957	1600	1232	972
120	2850	8367	11800	13273	13250	12462	11429	9750	7789	6250
150	1763	4700	9280	13545	16083	17000	16786	15500	13211	10938
180	1500	3767	7720	12364	15667	17308	17714	16875	14684	12344

TABLE B-10

FOTINI-L WIBM For Full Load (20€ / ton) And 15 Knot Speed Condition

Sig. Vertical Wave Bending Moment / Sig. Wave Height (FT - Ton/FT)

Ship Headings (Degree)	Wave Periods Tw (Second)									
	4.0	5.5	6.5	7.5	8.5	9.5	10.5	12.0	14.0	16.0
0	1344	2800	6083	9757	12488	14029	14625	14200	12583	10750
30	1076	3600	7383	10757	12875	13800	13875	13100	11333	9500
60	1532	6280	8783	9943	10100	9700	9025	7870	6417	5200
90	1692	3080	3717	3914	3775	3457	3100	2590	2025	1605
120	2660	6760	10567	12786	13250	12686	11700	10000	8058	6500
150	1684	4080	7933	12486	15500	16857	16875	15700	13417	11200
180	1450	3520	6583	11243	15000	17000	17625	17000	14917	12600

TABLE B-11

FOTINI-L WIBM For Full Load (20€ per ton) And 16 Knot Speed Condition

Sig. Vertical Wave Bending Moment / Sig. Wave Height (FT - Ton/FT)

Ship Headings (Degree)	Wave Periods Tw (Second)									
	4.0	5.5	6.5	7.5	8.5	9.5	10.5	12.0	14.0	16.0
0	1146	2740	5950	9529	12200	13700	14250	13900	12333	10450
30	1166	3580	7250	10557	12625	13529	13625	12800	11083	9300
60	1554	6320	8783	9900	10038	9629	8950	7800	6358	5150
90	1678	3020	3667	3914	3788	3486	3125	2610	2050	1625
120	2720	6780	10667	12986	12943	12943	11938	10200	8208	6600
150	1708	4100	7950	12629	15750	17143	17250	16000	13667	11400
180	1468	3540	6600	11371	15250	17289	18000	173000	15167	12750

TABLE B-12

FOTINI-L WIBM For Full Load (42€ / ton) and 15 Knot Speed Condition

Sig. Vertical Wave Bending Moment (FT-Ton/FT)
Sig. Wave Height

Ship Headings (Degree)	Wave Periods Tw (Second)									
	4.0	5.5	6.5	7.5	8.5	9.5	10.5	12.0	14.0	16.0
0	998	2640	5883	9557	12350	13957	14625	14300	12750	10900
30	928	3440	7133	10514	12750	13714	13875	13200	11417	9650
60	1362	5760	8283	9571	9875	9614	9038	7980	6575	5400
90	2020	3980	4983	5500	5488	5157	4713	4010	3192	2560
120	2680	7300	11733	14286	14875	14286	13250.	11500	9250	7500
150	1600	4320	8417	13271	16500	17857	18000	16800	14500	12100
180	1336	3640	6917	11786	15750	17857	18500	17900	15833	13400

AD-A072 910 ROSENBLATT (M) AND SON INC NEW YORK F/G 13/10
EXAMINATION OF SERVICE AND STRESS DATA OF THREE SHIPS FOR DEVEL--ETC(U)
APR 79 J F DALZELL, N M MANIAR, M W HSU N00024-75-C-4324
UNCLASSIFIED SSC-287 NL

2 OF 3
ADA 072910

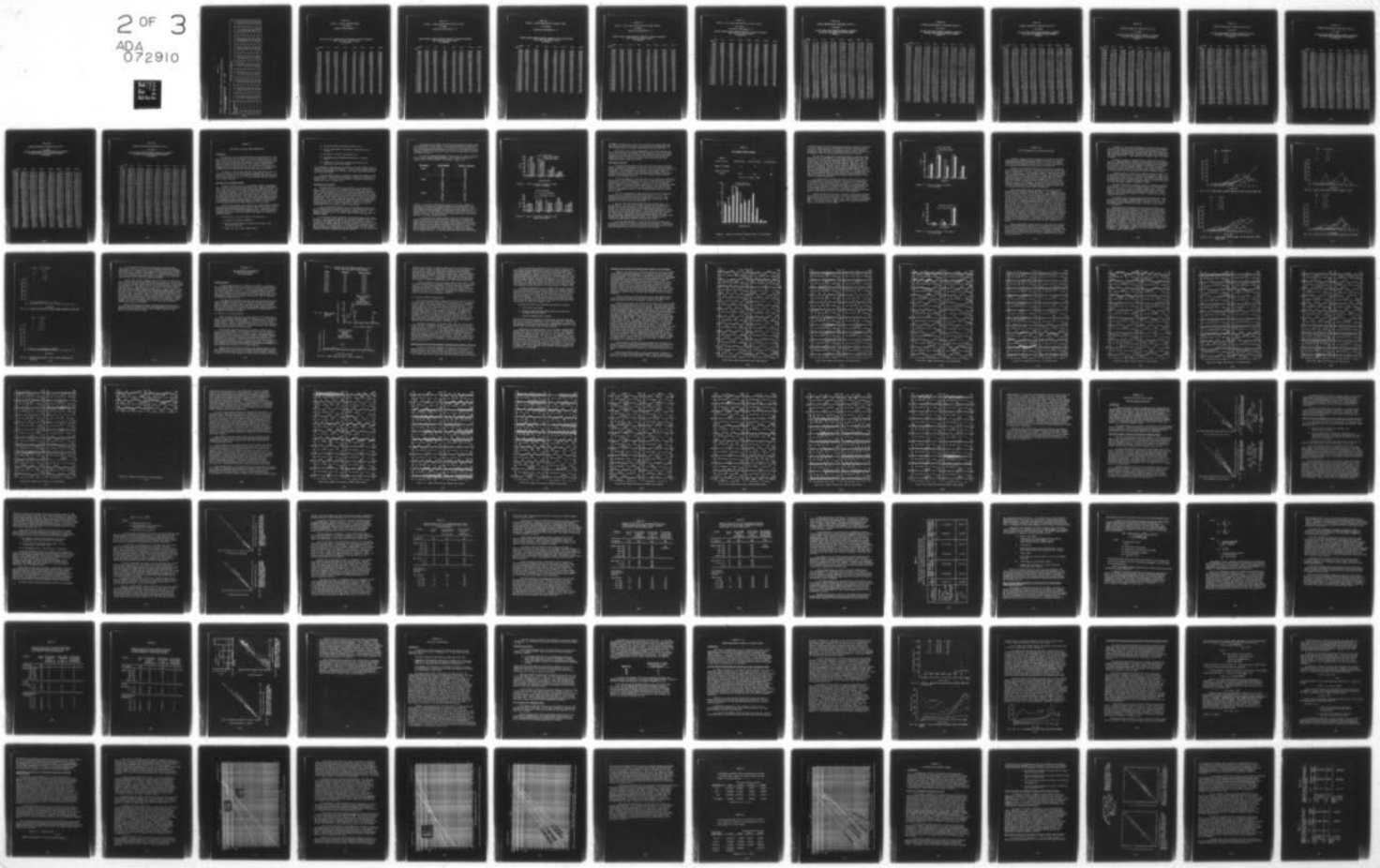

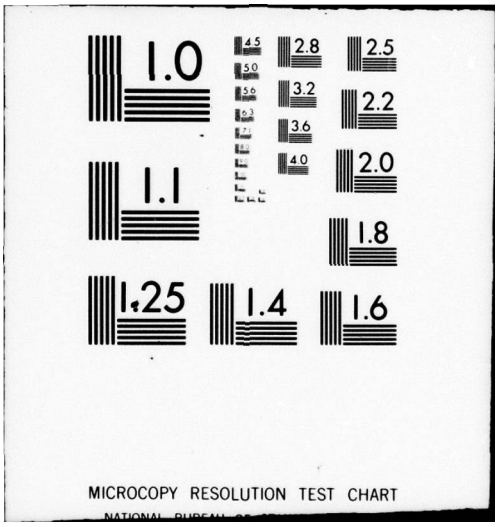
1.0
1.1
1.25
1.4
1.6
1.8
2.0
2.2
2.5
2.8
3.2
3.6
4.0
4.5
5.0
5.6
6.3
MICROCOPY RESOLUTION TEST CHART

TABLE B-13

FOTINI-L WIBM For Full Load (42€/ton) And 16 Knot Speed Condition

Sig. Vertical Wave Bending Moment (FT - TON/FT
Sig. Wave Height

Ship Headings (Degree)	Wave Periods Tw (Second)									
	4.0	5.5	6.5	7.5	8.5	9.5	10.5	12.0	14.0	16.0
0	1122	2680	5783	9357	12063	13629	14250	13900	12417	10600
30	1028	3420	7033	10329	12463	13443	13625	12900	11250	9540
60	1362	5800	8283	9529	9813	9529	8950	7890	6500	5300
90	2020	3920	4917	5457	5463	5157	4713	4020	3208	2570
120	2720	7300	11850	14571	15250	14714	13625	11700	9500	7650
150	1620	4340	8433	13486	16875	18429	18500	17300	14833	12350
180	1350	3660	6950	11971	16125	18286	19000	18400	16167	13650

TABLE B-14

FOTINI-L - BALLAST CONDITION (MEAN)

16.0 KNOTS

FRACTION OF WAVE DAMPING = .2

VERTICAL BENDING MOMENT RESPONSE OPERATORS AT MIDSHIP CALCULATED FROM SCORES SHIP MOTION PROGRAM (FT/TONS/FT)

ANGLE FREQ.	0.0	30.0	60.0	90.0	120.0	150.0	180.0
.31790	12000	9240	3480	486	3600	10000	13100
.36880	19200	15200	5880	749	6130	17000	21900
.41970	27700	22600	9110	1110	9690	25800	32300
.47060	35300	30155	13100	1590	14400	36000	43400
.52150	39900	36300	17900	2200	20300	46000	52000
.57240	38700	39100	22700	3010	27600	51600	50400
.62330	31000	36900	27100	4070	35400	44300	32900
.67420	18100	29100	30400	5340	40800	26100	11700
.72510	5840	17300	32000	6690	38600	9080	8300
.77600	6930	6330	31200	7800	30000	9730	11000
.82690	7680	6310	27900	8210	19300	11200	5470
.87780	3140	7460	22200	7900	10700	5630	8900
.92870	1880	3830	15100	7440	10600	7820	9840
.97960	3630	1100	8240	7070	13800	10100	2630
1.03050	6960	3180	4600	6590	13200	4200	7070
1.08140	7240	3800	5440	6010	8410	4970	6470
1.13230	3240	4790	5520	5230	3170	7410	1300
1.18320	1810	2860	3500	4480	5760	2800	3400
1.23410	4370	1590	4790	3710	7220	2780	173
1.28500	6190	330	2020	3000	4510	2270	2530
1.33590	2600	6640	2700	2040	587	1390	1180
1.38680	936	9640	1570	1940	4070	2230	827
1.43770	1130	2700	298	1630	4090	496	429
1.48860	1620	1780	1320	1440	981	1030	1140
1.53950	732	1640	957	1280	2360	303	1040
1.59040	181	1810	250	1100	3100	900	189

TABLE B-15

FOTINI-L - LOADED CONDITION ORE (20 CUBIC FT/TON)

15.0 KNOTS

FRACTION OF WAVE DAMPING = .2

VERTICAL BENDING MOMENT RESPONSE OPERATORS AT MIDSHIP CALCULATED
FROM SCORES SHIP MOTION PROGRAM
(FT/TONS/FT)

ANGLE FREQ.	0.0	30.0	60.0	90.0	120.0	150.0	180.0
.31790	13600	10600	3920	750	4070	11100	14600
.36880	21600	17000	6570	1200	6730	18000	23000
.41970	30200	24700	1000	1870	10200	26100	32700
.47060	37400	32100	14100	2840	14200	36000	45000
.52150	40600	37200	18400	4380	19200	53600	59200
.57240	37300	38300	22700	6710	33300	52000	42000
.62330	27700	34000	25800	10100	46000	31400	19000
.67420	14000	24400	27300	12600	37300	12600	6220
.72510	3220	12200	26900	8780	27100	8490	12200
.77600	7620	3120	24200	6130	16700	13000	9310
.82690	6970	6910	19300	7790	8700	9390	7100
.87780	1780	6870	13600	8100	10000	6400	11200
.92870	3270	2480	7610	7670	14300	10600	7200
.97960	3100	2630	3530	6990	14900	8030	5420
1.03050	1980	3800	3700	6220	11000	3710	8130
1.08140	3320	1410	4660	5440	5360	7370	3610
1.13220	1950	2070	4080	4690	4700	5120	3190
1.18320	971	2380	2180	4010	6830	2060	1710
1.23410	5480	490	167	3410	5690	2700	1680
1.28500	7060	876	1680	2910	2400	841	922
1.33590	1110	2200	1890	2500	3110	1830	133
1.38680	2000	2490	903	2200	4110	446	982
1.43770	2190	2480	1564	1960	2420	793	541
1.48860	1660	4220	1180	1770	1770	1140	882
1.53959	1250	3070	831	1660	2960	864	1300
1.59040	626	2800	522	1480	2020	1220	1130

TABLE B-16

FOTINI-L - LOADED CONDITION ORE (20 CUBIC FT/TON)

16.0 KNOTS

FRACTION OF WAVE DAMPING = .2

VERTICAL BENDING MOMENT RESPONSE OPERATORS AT MIDSHIP CALCULATED FROM SCORES SHIP MOTION PROGRAM (FT/TONS/FT)

ANGLE FREQ.	0.0	30.0	60.0	90.0	120.0	150.0	180.0
.31790	13200	10300	3860	771	4000	11000	14300
.36880	21000	16800	6440	1240	6630	17900	22900
.41970	29400	24100	9830	1910	10000	26000	32600
.47060	36600	31300	14000	2910	14000	37000	46900
.52150	39600	36400	18200	4490	19300	56700	61200
.57240	36400	37600	22300	6890	36000	51700	41200
.62330	27000	33300	25600	10400	46400	30900	18200
.67420	13600	24000	27200	12800	37100	12000	6510
.72510	3130	12000	26900	8720	26900	8930	12500
.77600	7710	3070	24200	5360	16400	13400	9220
.82690	7270	6940	19800	7330	8430	9330	7300
.87780	2480	7070	13800	7830	10400	6530	11600
.92870	2990	2920	7600	7500	14900	10900	7180
.97960	2980	2460	3230	6890	15100	8100	5540
1.03050	2540	3620	3700	6160	11100	3740	8260
1.08140	4020	1410	4800	5400	5290	7510	8580
1.13230	2940	2240	4100	4670	4840	5140	3220
1.18320	3290	2660	2060	4010	7040	2080	1690
1.23410	4380	769	563	3420	5800	2720	1700
1.28500	3640	1040	1910	2930	2400	864	873
1.33590	5220	4000	2000	2530	3220	1840	142
1.38680	1210	5190	988	2230	4230	470	1030
1.43770	1300	1670	822	2000	2470	807	543
1.48860	1110	2320	1380	1800	1840	1200	916
1.53950	837	1680	1040	1640	3070	870	1400
1.59040	342	1820	761	1510	2100	1260	1160

TABLE B-17

FOTINI-L - FULL LOADED CONDITION COAL (42 CUBIC FT/TON)

15.0 KNOTS

FRACTION OF WAVE DAMPING = .2

VERTICAL BENDING MOMENT RESPONSE OPERATORS AT MIDSHIP CALCULATED FROM SCORES SHIP MOTION PROGRAM (FT/TONS/FT)

ANGLE FREQ.	0.0	30.0	60.0	90.0	120.0	150.0	180.0
.31790	14300	11200	4690	1690	5670	13200	16700
.36880	22400	18000	7500	2520	9000	20700	25800
.41970	31000	25400	11000	3710	13100	28700	34700
.47060	37900	32600	15100	5430	17100	36700	46400
.52150	40400	37300	19300	8040	18800	59100	63600
.57240	36800	37900	23000	12000	39300	54700	42000
.62330	26700	33000	25700	17000	53000	31400	18700
.67420	12900	23200	26600	16600	41000	13800	10900
.72510	2540	11000	25200	6520	28700	12300	15000
.77600	7690	2340	21900	8820	17700	15200	10600
.82690	7030	6980	17000	11700	10500	10200	7400
.87780	2060	6900	11600	11300	12000	6610	10800
.92870	3300	2690	6600	10100	15300	9980	6010
.97960	3530	2620	3340	8670	15000	6900	5180
1.03050	1210	3940	3280	7410	10800	3690	6900
1.08140	3300	1630	4070	6290	5080	6800	2320
1.13230	2530	1800	3760	5290	4870	3820	3270
1.18320	1960	2800	2230	4444	6590	2620	1580
1.23410	4240	1070	194	3740	5100	2600	2590
1.28500	2740	2100	1380	3180	2270	1970	1240
1.33590	1990	1210	1760	2710	3460	2280	1100
1.38680	58	1770	967	2330	3960	1330	1460
1.43770	1070	1920	372	2020	2190	1300	910
1.48860	513	996	1040	1770	2020	1540	1160
1.53950	511	1060	814	1540	2810	1080	1060
1.59040	464	1500	392	1360	1730	1400	921

TABLE B-18

FOTINI-L - FULL LOADED CONDITION COAL (42 CUBIC FT/TON)

16.0 KNOTS

FRACTION OF WAVE DAMPING = .2

VERTICAL BENDING MOMENT RESPONSE OPERATORS AT MIDSHIP CALCULATED FROM SCORES SHIP MOTION PROGRAM (FT/TONS/FT)

ANGLE FREQ.	0.0	30.0	60.0	90.0	120.0	150.0	180.0
.31790	14000	11000	4600	1700	5630	13100	16600
.36880	21900	17500	7340	2560	8960	20600	25600
.41970	30200	24900	10900	3760	13000	28400	34400
.47060	37000	31900	14900	5500	16800	37700	49300
.52150	39400	36600	19000	8130	18400	63100	65700
.57240	35900	37100	22800	12100	43400	54000	41400
.62330	26000	32300	25300	17200	53700	30900	18200
.67420	12400	22900	26300	16700	40600	13300	11000
.75210	2500	10900	25300	5920	28200	12700	15100
.77600	7680	2300	22100	8170	17100	15500	10300
.82690	7300	6930	17300	11300	10200	10100	7500
.87780	2740	7090	11800	11100	12200	6670	11000
.92870	3090	3140	6330	10000	15800	10200	5960
.97960	3570	2480	2820	8600	15300	6910	5300
1.03050	1590	3900	3380	7390	10800	3640	6990
1.08140	4060	1740	4230	6270	5000	6910	2260
1.13230	3840	1910	3630	5290	5000	3790	3310
1.18320	4540	3300	1870	4470	6760	2690	1570
1.23410	3500	1490	324	3780	5190	2610	2610
1.28500	1780	2720	1620	3200	2270	2010	1230
1.33590	1230	2220	1780	2740	3560	2270	1100
1.38380	430	2810	913	2370	4070	1400	1500
1.43770	520	1240	686	2060	2200	1320	903
1.48860	470	970	1270	1800	2100	1600	1190
1.53950	457	347	1030	1570	2910	1090	1090
1.59040	239	1100	690	1380	1770	1430	906

TABLE B-19

UNIVERSE IRELAND-BALLAST (MEAN DRAFT 39.59 FT.)

10.0 KNOTS

VERTICAL SHEAR FORCE RESPONSE OPERATORS AT AMIDSHIP
CALCULATED FROM SCORES SHIP MOTION PROGRAM
(TONS/FT)

ANGLE REQ.	0.0	30.0	60.0	90.0	120.0	150.0	180.0
0.200	15.560	14.490	12.570	12.450	15.130	19.150	21.240
0.250	27.300	24.690	20.050	19.590	25.260	34.750	40.280
0.300	45.100	38.960	29.250	28.420	38.500	58.550	71.550
0.325	57.620	48.250	34.410	33.460	46.210	74.590	93.650
0.350	73.630	59.600	39.870	38.890	54.510	94.110	121.050
0.375	93.940	73.610	45.570	44.700	63.290	117.620	154.110
0.400	119.020	90.900	51.450	50.860	72.370	145.230	192.390
0.425	148.670	111.660	57.460	57.310	81.590	176.660	234.200
0.450	181.610	135.620	63.500	63.970	90.700	210.330	276.250
0.475	215.380	162.710	69.560	70.720	99.310	243.600	313.900
0.500	248.300	191.000	76.230	77.410	106.740	273.040	342.260
0.525	275.770	218.650	82.730	83.780	112.000	295.700	357.280
0.550	293.790	243.050	89.360	89.430	113.990	309.460	354.270
0.575	299.080	261.410	96.080	93.920	112.940	310.600	327.780
0.600	289.460	271.060	102.800	96.740	111.990	294.740	280.260
0.625	265.020	269.940	109.400	97.460	114.990	261.920	212.460
0.650	228.600	257.150	115.810	95.490	121.550	208.940	133.450
0.675	186.020	233.380	121.890	91.010	131.520	147.010	67.070
0.700	145.440	201.240	127.560	84.600	135.040	90.100	46.120
0.750	97.300	131.320	136.840	69.040	123.910	74.340	60.200
0.800	77.700	88.060	139.980	55.980	107.510	77.090	24.140
0.850	70.710	66.870	130.720	45.620	89.640	34.360	60.930
0.900	81.970	52.540	105.290	38.100	93.410	55.230	66.470
0.950	78.030	60.220	70.670	31.740	96.990	59.300	93.590
1.000	64.320	59.380	44.420	26.230	75.240	75.810	70.300
1.050	49.230	46.960	35.980	19.260	32.980	66.190	47.910
1.100	45.020	32.290	25.940	14.060	12.390	33.610	50.390
1.200	25.920	21.640	15.340	5.530	11.660	27.590	32.460
1.300	12.100	6.720	13.770	6.360	23.530	13.900	13.130
1.400	6.590	2.740	16.110	6.020	24.700	9.260	4.980
1.500	29.910	5.340	12.460	2.610	5.360	5.500	23.600
1.600	74.860	6.840	5.290	1.610	4.530	4.300	43.220
1.700	167.660	2.940	3.550	3.130	4.390	9.290	83.490
1.850	331.790	8.590	7.210	2.650	3.150	12.380	191.430

TABLE B-20

UNIVERSE IRELAND-BALLAST. (MEAN DRAFT 39.59 FT.)

15.0 KNOTS

VERTICAL SHEAR FORCE RESPONSE OPERATORS AT AMIDSHIP
CALCULATED FROM SCORES SHIP MOTION PROGRAM
(TONS/FT)

ANGLE / FREQ.	0.0	30.0	60.0	90.0	120.0	150.0	180.0
0.200	14.640	13.650	12.170	12.590	15.950	20.720	23.160
0.250	26.080	23.760	19.470	19.390	27.070	38.510	44.930
0.300	42.380	37.530	28.610	28.950	42.050	66.150	80.800
0.325	53.120	46.120	33.820	34.140	51.000	84.300	105.370
0.350	66.390	56.250	39.390	39.750	60.860	107.370	136.560
0.375	82.970	68.370	45.220	45.770	71.560	134.100	172.830
0.400	103.450	83.010	51.460	52.150	83.030	164.630	213.310
0.425	128.010	100.640	57.940	58.340	95.020	197.410	254.430
0.450	156.060	121.510	64.490	65.760	107.090	228.760	290.920
0.475	186.100	145.370	71.290	72.300	118.140	254.270	316.580
0.500	215.600	171.250	78.330	79.770	126.310	273.100	330.460
0.525	241.250	197.360	85.640	87.420	128.640	278.310	349.040
0.550	259.320	221.510	93.260	92.400	123.530	300.300	345.240
0.575	266.340	240.990	101.220	97.270	113.360	300.340	307.650
0.600	260.050	253.000	109.490	100.640	103.200	278.090	248.480
0.625	240.330	255.200	118.000	102.190	112.480	233.740	176.150
0.650	210.140	246.270	126.530	101.370	122.170	178.480	93.950
0.675	176.130	226.580	134.730	98.370	127.600	111.180	42.830
0.700	147.210	198.670	142.210	93.500	131.390	63.460	59.510
0.750	131.190	139.860	152.730	79.980	121.080	93.060	70.210
0.800	126.350	113.850	153.290	66.310	93.790	87.140	27.150
0.850	118.550	104.220	139.830	54.920	92.220	34.440	65.230
0.900	125.680	87.790	111.750	45.870	109.740	60.510	73.250
0.950	133.430	84.260	75.000	38.350	113.040	63.690	105.820
1.000	126.690	81.700	43.300	32.080	83.810	86.900	72.200
1.050	123.590	70.470	30.810	24.900	31.080	69.620	51.450
1.100	136.740	57.930	23.600	19.710	17.780	33.700	54.220
1.200	103.200	47.040	12.470	11.970	11.640	30.330	32.560
1.300	63.150	18.260	12.380	9.950	24.420	15.140	13.270
1.400	15.600	19.440	15.440	7.770	28.650	10.430	5.210
1.500	36.480	20.810	12.110	3.930	5.550	6.560	23.690
1.600	49.260	22.370	6.580	2.540	5.340	3.350	43.030
1.700	63.890	8.480	5.090	3.710	6.500	9.020	80.560
1.850	123.370	5.000	8.730	3.970	3.670	13.310	191.630

TABLE B-21

UNIVERSE IRELAND-FULL (MEAN DRAFT 81.70 FT.)

10.0 KNOTS

VERTICAL SHEAR FORCE RESPONSE OPERATORS AT AMIDSHIP
CALCULATED FROM SCORES SHIP MOTION PROGRAM
(TONS/FT)

ANGLE FREQ.	0.0	30.0	60.0	90.0	120.0	150.0	180.0
0.200	8.470	8.970	10.310	12.050	14.580	18.400	20.530
0.250	12.530	12.630	15.590	19.430	25.600	37.460	44.480
0.300	25.310	19.630	21.470	29.360	43.520	73.420	90.310
0.325	38.290	27.050	24.580	35.640	56.750	100.620	124.340
0.350	56.350	38.320	27.840	43.080	74.480	135.770	166.420
0.375	79.180	53.570	31.270	52.110	93.750	180.080	216.450
0.400	105.730	72.450	34.930	63.570	133.080	235.530	272.050
0.425	134.140	93.940	39.380	77.900	181.590	285.790	293.420
0.450	161.590	116.540	44.080	95.090	235.890	269.310	214.140
0.475	185.000	138.140	49.150	110.630	274.030	147.960	80.500
0.500	200.500	156.040	54.670	117.270	262.660	33.370	130.210
0.525	204.900	167.920	61.660	124.590	197.390	96.550	178.870
0.550	196.690	171.440	72.690	131.720	126.880	136.340	181.280
0.575	175.650	165.190	87.900	129.150	75.400	143.090	149.360
0.600	144.100	149.180	100.210	112.580	54.020	122.570	98.190
0.625	106.590	124.750	102.780	93.170	53.630	83.650	44.810
0.650	69.350	95.470	96.720	75.070	61.210	56.900	43.020
0.675	40.110	66.960	86.550	61.760	65.230	25.800	75.010
0.700	25.170	45.770	77.810	51.570	63.430	61.120	90.150
0.750	15.050	30.130	68.470	37.260	44.400	90.300	64.060
0.800	10.490	17.110	61.730	27.780	27.050	59.570	33.940
0.850	25.470	7.520	57.940	21.160	43.200	29.380	18.160
0.900	25.120	25.100	53.560	16.520	54.640	15.880	36.560
0.950	17.310	29.790	42.680	13.060	46.060	24.760	38.810
1.000	6.410	21.200	28.260	10.480	24.750	30.190	14.480
1.050	8.540	8.270	16.120	8.480	7.400	11.510	9.440
1.100	8.850	5.570	9.130	6.930	7.450	1.950	15.200
1.200	1.430	5.810	6.380	4.640	3.790	6.650	3.490
1.300	1.540	2.180	1.680	3.240	1.980	2.250	1.890
1.400	1.470	0.730	2.770	2.030	3.480	2.180	2.340
1.500	2.440	0.350	1.020	1.310	1.540	4.770	2.670
1.600	4.540	0.510	0.560	0.810	1.310	3.110	1.270
1.700	6.470	0.920	0.270	0.480	1.040	0.560	1.480
1.850	9.390	1.540	0.060	0.200	1.040	0.660	2.250

TABLE B-22

UNIVERSE IRELAND-FULL (MEAN DRAFT 81.70 FT.)

15.0 KNOTS

VERTICAL SHEAR FORCE RESPONSE OPERATORS AT AMIDSHIP
CALCULATED FROM SCORES SHIP MOTION PROGRAM
(TONS/FT)

ANGLE / FREQ.	0.0	30.0	60.0	90.0	120.0	150.0	180.0
0.200	7.390	8.010	9.580	12.060	16.060	21.500	24.360
0.250	7.810	9.570	13.940	19.380	29.040	44.350	53.510
0.300	11.620	9.750	18.060	29.180	51.120	90.240	110.960
0.325	20.720	12.780	19.770	35.350	68.140	126.600	156.350
0.350	35.020	20.440	21.140	42.630	91.950	177.250	218.420
0.375	54.110	32.600	22.140	51.560	126.540	250.140	302.790
0.400	77.310	48.690	22.820	62.780	173.270	333.250	362.430
0.425	103.300	67.890	23.430	76.770	245.450	347.710	287.160
0.450	129.990	89.090	24.370	93.290	308.970	217.120	98.780
0.475	154.610	110.660	26.570	108.120	321.850	58.330	92.990
0.500	174.060	130.610	29.770	116.420	253.370	62.690	157.820
0.525	185.320	146.740	34.440	126.730	163.750	119.630	182.630
0.550	186.040	156.830	40.610	135.200	98.100	143.120	170.310
0.575	175.220	159.230	48.090	133.500	56.790	137.910	129.560
0.600	153.670	153.080	56.240	115.990	43.890	106.960	73.550
0.625	124.510	138.680	63.550	95.410	51.490	64.570	31.210
0.650	92.090	117.630	68.000	76.550	60.860	18.280	60.690
0.675	63.540	92.820	68.610	62.810	64.790	43.260	91.800
0.700	45.300	68.190	66.860	52.340	62.010	79.980	99.550
0.750	34.570	36.400	68.300	37.960	40.140	98.130	58.830
0.800	24.950	27.050	74.710	23.540	29.910	55.360	30.650
0.850	31.170	15.290	72.020	22.120	53.070	25.410	17.330
0.900	33.930	18.760	58.160	17.600	63.540	13.990	43.020
0.950	27.010	21.800	40.860	14.240	50.830	29.890	39.530
1.000	17.880	16.180	27.570	11.690	24.530	32.200	11.450
1.050	17.600	9.340	17.970	9.650	6.820	9.150	10.020
1.100	21.750	4.070	10.540	8.000	9.640	0.560	16.730
1.200	17.630	6.170	7.680	5.440	5.390	6.890	4.330
1.300	12.710	3.120	2.620	3.790	3.220	3.510	5.170
1.400	6.990	3.940	2.530	2.410	4.480	8.180	4.640
1.500	4.150	4.880	0.520	1.600	2.430	1.100	1.770
1.600	2.110	5.960	0.230	1.050	2.240	0.860	1.160
1.700	1.150	2.580	0.460	0.680	4.150	0.640	1.500
1.850	1.320	0.450	0.270	0.320	0.280	0.710	2.200

TABLE B-23

UNIVERSE IRELAND-BALLAST (MEAN DRAFT 39.59 FT.)

10.0 KNOTS

VERTICAL BENDING MOMENT RESPONSE OPERATORS AT AMIDSHIP
CALCULATED FROM SCORES SHIP MOTION PROGRAM
(FT-TONS/FT)

ANGLE	0.0	30.0	60.0	90.0	120.0	150.0	180.0
FREQ.							
0.200	11834.5	8630.4	2087.1	1429.9	1810.3	8219.6	11398.1
0.250	27655.5	20628.2	5364.9	2235.4	5378.7	20054.7	27133.4
0.300	52165.5	39789.4	12421.1	3274.7	11919.7	39636.0	52327.8
0.325	67190.6	51965.7	16903.7	3900.5	16590.0	52416.3	68156.4
0.350	83270.3	65490.6	22222.8	4595.7	22315.5	66879.3	85394.7
0.375	99426.3	79618.5	28348.7	5368.2	29144.6	82411.5	103677.8
0.400	114374.1	94150.5	35181.6	6223.7	37059.4	98111.9	119080.6
0.425	126570.7	107422.2	42604.6	7165.4	45930.6	112703.8	132023.1
0.450	134363.0	118498.3	50413.9	8202.9	55718.0	124667.6	139544.6
0.475	136341.6	126169.3	58334.3	9355.4	65987.3	132005.0	139187.7
0.500	131474.4	129306.5	66050.4	10643.2	76311.2	132634.1	129072.7
0.525	119430.5	127023.3	73208.9	12097.6	85319.2	124884.6	108553.8
0.550	100346.0	118677.0	79432.2	13605.1	93452.7	107913.1	79340.8
0.575	77500.9	105103.0	84346.1	15342.7	98211.9	83084.5	46036.3
0.600	52574.0	86704.6	87630.9	17207.9	98315.0	54124.2	15141.6
0.625	31416.5	65569.0	89045.3	19579.3	94620.0	25744.5	9327.2
0.650	23314.9	44675.3	88516.0	21485.9	85922.4	6149.0	24855.7
0.675	27895.7	28833.5	85939.7	23035.4	74184.7	19331.1	27730.9
0.700	31035.2	24262.2	81435.5	24131.9	59999.2	28171.2	19890.0
0.750	18605.6	29654.9	67565.0	24878.2	28676.6	18267.6	12072.8
0.800	9429.9	19265.8	49357.7	23600.5	16754.2	11796.1	26770.7
0.850	19045.6	8643.7	31746.4	22439.7	29454.9	25058.8	6327.2
0.900	12880.2	17304.8	21679.9	19835.8	29606.7	8344.3	21608.8
0.950	10384.7	13502.1	20743.4	16661.2	14998.9	17794.4	12780.3
1.000	5125.0	10068.6	18330.3	13156.5	4494.5	16279.4	10787.0
1.050	3542.3	7871.5	10854.1	10028.5	14437.0	5826.9	7565.2
1.100	4604.1	2139.1	7049.0	7505.2	11110.1	11057.7	9893.1
1.200	2636.7	2355.4	8968.3	4929.1	8930.2	8136.1	6038.8
1.300	1565.9	2102.0	6376.9	3079.0	3120.3	4426.7	3508.7
1.400	3572.6	3031.6	3759.5	1854.1	3159.6	662.0	1961.5
1.500	8587.8	2558.4	3570.8	5022.6	3945.5	2323.1	2384.5
1.600	7606.9	1647.1	3283.2	6092.4	3117.0	2909.0	5541.6
1.700	8474.0	4272.8	3101.8	4036.9	1890.0	353.0	9480.4
1.850	10007.7	8930.3	616.0	948.5	1959.5	2442.3	11044.7

TABLE B-24

UNIVERSE IRELAND-BALLAST (MEAN DRAFT 39.59 FT.)

15.0 KNOTS

VERTICAL BENDING MOMENT RESPONSE OPERATORS AT AMIDSHIP
CALCULATED FROM SCORES SHIP MOTION PROGRAM
(FT-TONS/FT)

ANGLE FREQ.	0.0	30.0	60.0	90.0	120.0	150.0	180.0
0.200	10770.1	7875.1	1914.0	1375.9	1564.1	7423.4	10360.
0.250	25427.5	19043.8	5496.1	2131.3	4376.3	18620.1	25318.
0.300	48284.1	37009.0	11760.9	3177.1	11178.0	37776.5	50095.
0.325	62347.5	48475.9	16063.8	3812.1	15798.3	50644.5	66149.
0.350	77430.7	61252.4	21190.9	4533.4	21583.6	65526.5	84027.
0.375	92615.9	74825.9	27130.5	5353.2	28631.9	81973.1	102773.
0.400	106691.4	88469.3	33805.0	6234.3	37008.5	99171.6	120856.
0.425	118232.7	101258.3	41099.7	7337.7	46704.6	115914.6	136161.
0.450	125731.8	112098.0	48850.3	8523.5	57595.6	130062.1	145334.
0.475	127801.3	119612.0	56833.0	9331.6	69498.7	138717.2	144759.
0.500	123399.5	123247.6	64757.5	11413.2	81522.5	138581.1	131131.
0.525	112160.8	121510.5	72286.4	13169.0	92507.1	126906.9	104565.
0.550	94610.6	114135.2	79065.8	14942.9	101157.0	104066.9	70529.
0.575	72412.5	101232.3	84727.2	16926.1	105414.8	74921.7	35933.
0.600	48611.2	83655.3	88912.0	18932.6	103690.1	43418.0	3711.
0.625	28680.4	63143.1	91297.1	21390.1	96484.3	13463.4	19780.
0.650	22674.4	42575.4	91627.8	23103.7	84761.5	12623.6	31009.
0.675	28777.7	26978.5	89748.1	24249.0	69196.9	28218.0	30001.
0.700	32712.8	23483.9	85629.5	24780.3	52241.6	33946.4	17501.
0.750	21102.7	31052.8	71258.8	24309.0	19748.4	14591.6	19587.
0.800	3154.7	20646.2	51463.8	22337.5	23910.2	19592.6	29819.
0.850	16420.2	2669.3	31940.6	21120.4	37767.1	29429.5	3920.
0.900	13973.9	15571.9	21924.6	18638.5	32902.4	5458.8	25672.
0.950	10985.2	12668.9	21673.2	15518.3	13336.3	22880.6	12408.
1.000	9466.5	8990.5	18899.3	12127.6	8929.8	17201.8	13644.
1.050	7803.6	8773.9	10546.9	9091.9	13611.3	8257.1	7797.
1.100	11057.3	1841.7	7565.3	6707.2	12202.4	12176.6	11134.
1.200	11126.6	1077.6	8905.1	4454.3	11562.3	3826.7	6935.
1.300	11209.3	8502.0	7546.4	2749.8	4459.7	4933.2	3791.
1.400	11305.6	7215.0	4874.9	1533.8	3400.8	974.8	1695.
1.500	10150.4	5719.4	3926.6	4990.6	4613.9	2362.9	2353.
1.600	4006.1	4015.3	4144.7	6106.5	3639.9	3149.1	3273.
1.700	4924.2	3464.1	4105.9	4071.7	2121.2	733.5	3617.
1.850	41176.6	7364.5	2816.2	1243.3	2291.6	2381.8	49037.

TABLE B-25

UNIVERSE IRELAND-FULL (MEAN DRAFT 81.70 FT)

10.0 KNOTS
VERTICAL BENDING MOMENT RESPONSE OPERATORS AT AMIDSHIP
CALCULATED FROM SCORES SHIP MOTION PROGRAM
(FT-TONS/FT)

ANGLE	0.0	30.0	60.0	90.0	120.0	150.0	180.0
FREQ.							
0.200	17393.9	13672.0	6092.8	2378.9	6421.7	14222.2	18046.2
0.250	37267.0	29370.5	12800.3	4419.5	13122.8	29761.0	37700.0
0.300	65385.2	52265.6	23173.1	7801.9	23341.3	51495.5	64097.6
0.325	81110.0	65665.5	29778.9	10327.2	29378.5	63420.1	77611.0
0.350	96471.5	79380.7	37226.7	13725.6	37473.7	74815.1	89351.5
0.375	109934.3	92402.7	45321.5	18457.6	46357.7	84835.9	98343.0
0.400	119302.3	103456.1	53764.1	25386.3	57213.2	91348.3	100265.5
0.425	124426.3	111203.9	62154.6	35659.3	68982.4	74936.0	74276.0
0.450	122490.2	114367.1	69827.3	50704.9	69417.5	38010.8	67719.7
0.475	113345.3	111987.8	75939.7	68798.5	51432.5	71877.1	102435.5
0.500	97313.6	103647.8	79221.1	79637.3	36538.0	96513.8	102122.6
0.525	75334.7	89716.6	78073.4	80662.8	48291.4	90728.3	79069.5
0.550	51483.5	71448.9	71828.7	79821.9	59111.8	71441.2	52438.2
0.575	27761.5	51026.7	64626.1	75456.5	60983.3	49040.0	34049.6
0.600	10727.0	31474.8	62923.9	67070.9	57264.3	32023.8	33010.2
0.625	13721.1	16704.8	64058.0	57778.6	49517.2	29294.6	37373.4
0.650	19764.5	12894.8	61675.3	48777.7	39014.9	34225.9	35810.8
0.675	19917.5	16877.0	55779.3	42035.2	27573.4	35887.2	27540.7
0.700	15315.4	19845.3	48817.6	36596.8	16632.6	31264.3	18211.0
0.750	8373.7	15903.7	37162.7	27470.6	14843.0	14726.2	21040.5
0.800	12176.5	9347.5	29617.7	20622.6	24574.1	17983.6	13176.7
0.850	8022.3	12954.0	23652.9	15024.5	23690.2	11445.2	9002.9
0.900	6439.8	9223.3	17521.4	10646.6	14265.8	6124.8	11518.9
0.950	3788.6	8095.5	12055.9	7150.3	5235.8	9665.3	2125.4
1.000	3053.1	5945.9	8330.3	4576.4	6354.2	1914.2	3541.3
1.050	2743.1	4158.5	5766.4	2758.2	5075.1	3410.5	2329.5
1.100	1991.4	3830.5	4405.5	1614.4	1618.4	1005.9	1233.2
1.200	1351.9	2083.5	2535.2	717.4	2321.0	1285.2	1785.8
1.300	723.4	1142.1	1767.0	867.2	2121.0	1649.2	1476.2
1.400	669.8	463.7	933.6	919.0	1127.9	1025.5	858.4
1.500	1160.1	181.1	451.2	787.7	702.4	2065.7	1658.1
1.600	1597.2	237.9	211.0	503.7	524.0	1494.8	1100.0
1.700	3459.3	505.4	85.4	252.5	430.0	191.3	244.7
1.850	6752.3	798.8	42.6	86.3	492.6	291.5	609.8

TABLE B-26

UNIVERSE IRELAND-FULL (MEAN DRAFT 81.70 FT.)

15.0 KNOTS

VERTICAL BENDING MOMENT RESPONSE OPERATORS AT AMIDSHIP
CALCULATED FROM SCORES SHIP MOTION PROGRAM
(FT-TONS/FT)

ANGLE FREQ.	0.0	30.0	60.0	90.0	120.0	150.0	180.0
0.200	16077.9	12692.5	5811.1	2502.3	6465.5	13924.4	17571
0.250	34620.9	27395.0	12211.4	4655.4	13211.7	29133.1	36693
0.300	60943.2	48904.0	22072.1	8262.0	23686.8	50388.7	62121
0.325	75759.9	61505.3	28315.9	10935.8	30638.7	62356.3	75479
0.350	90329.0	74489.5	35316.4	14684.9	39302.2	75521.4	90014
0.375	103307.7	86944.4	42861.7	19895.2	50336.2	89437.0	99571
0.400	113194.7	97774.2	50717.6	27635.7	65229.0	75111.7	62883
0.425	118510.5	105794.1	58439.8	39179.7	74523.5	21140.9	61752
0.450	118039.9	109904.8	65561.3	55918.1	61471.5	78653.7	113890
0.475	111094.2	109239.5	71548.0	75246.2	45727.4	107734.9	115734
0.500	97772.3	103342.0	75566.6	86531.1	54760.8	103544.8	95084.
0.525	79033.7	92324.4	77335.3	87657.4	65088.9	85469.5	67117.
0.550	56970.4	76926.8	75914.7	83969.6	83075.5	61496.8	42076.
0.575	34221.6	58570.5	71209.9	79592.0	65077.3	39537.0	32426.
0.600	14663.9	39248.0	63873.1	69250.7	57836.0	29061.6	37604.
0.625	10552.3	21583.7	55956.9	58596.1	47645.0	33706.0	40983.
0.650	17615.6	10624.6	49895.7	48792.6	35221.1	39319.5	35754.
0.675	20421.1	13103.1	45[illegible].1	41677.6	22263.4	34413.6	24259.
0.700	17261.3	17484.7	41527.9	36063.9	12295.2	30556.6	15648.
0.750	3247.4	14395.8	30056.9	26839.3	20144.4	13164.8	23999.
0.800	9520.0	4093.3	22370.6	20015.5	29613.2	20623.1	11677.
0.850	7351.2	6260.1	21328.1	14470.3	26170.7	10557.8	11468.
0.900	3947.4	6841.3	18891.9	10165.6	14043.5	8153.8	11696.
0.950	2914.2	3597.2	13950.9	6731.1	5058.2	10360.4	2314.
1.000	1035.3	3487.9	9266.6	4211.3	7912.2	1196.4	3318.
1.050	3551.5	1199.6	6651.3	2463.9	5859.1	3831.7	3238.
1.100	1555.2	2190.4	5612.9	1419.1	2111.1	1600.9	791.
1.200	1995.7	1431.3	2855.2	801.8	3023.9	1872.1	2254.
1.300	2520.5	2039.6	1693.6	1003.7	2788.0	2262.3	3123.
1.400	3130.6	2165.9	924.1	1016.3	1608.2	3748.2	2336.
1.500	1904.6	2312.8	313.6	864.8	1071.4	693.9	1012.
1.600	652.3	2480.1	138.9	575.7	916.9	456.8	874.
1.700	905.4	1296.8	241.7	325.8	1393.0	224.0	287.
1.350	574.2	339.9	177.0	135.2	146.4	339.2	792.

APPENDIX C-1

DATA BASES: FULL-SCALE STRESS OBSERVATIONS

Introduction

The available full-scale observations on the three ships of interest in the current work were all gathered by Teledyne Materials Research. The basic techniques used were the same, as were the recordings and, to a great extent, the initial data-reduction procedures. The stress data examined under the present project were confined to a response termed "Midship Longitudinal Vertical Bending Stress". This response is effectively the average of port and starboard deck edge stresses; that is, the deck stress response due only to body-vertical bending loads near midship (Ref.7).

The extent of the available data base varies from ship to ship. In addition, the extent to which these data were examined also varies. It is accordingly the objective of this appendix to document that which was available in each case as well as the way in which the data were partitioned for various special analyses.

Data Base for the UNIVERSE IRELAND

The data collection effort for the UNIVERSE IRELAND is summarized in Ref.7. Briefly, the ship was instrumented from July 1968 through December 1970, during which time the ship made eleven voyages (648 days at sea). The ship's trade route during this time was between Europe and the Persian Gulf via the Cape of Good Hope. Some 2700 30-minute stress records were obtained by the automatic data-acquisition system which was set primarily to record one record per four-hour watch. About 1900 of these records pertain to midship longitudinal bending stress. Since there were almost 3900 sea-watches in the data-taking period, the data base for longitudinal bending stresses of the UNIVERSE IRELAND corresponds roughly to a sample of conditions in half the sea-watches naturally occurring over a 2-1/2 year period.

The basic data reduction was carried out by Teledyne Materials Research according to the methods described in Ref. 16. Most of the results of this reduction process were analyzed and reported in Ref.7. Among those results are the statistics of wave-induced stresses and most of the information on the mean stress levels. Much less reporting was made on the magnitude of vibratory stresses.

The data base for this ship involves, for each record:

1) A summary of log-book information

2) Mean stress level relative to stress at the start of the analog recording tape

3) Number of cycles of wave-induced stress

4) The maximum peak-to-trough wave-induced stress

5) The root-mean-square of the peak-to-trough wave-induced stresses

6) The number of "bursts" (see Appendix C-2)

7) The maximum double amplitude of vibration, or maximum "burst".

8) A 12000 point time series representing the actual time history of stress for 20 minutes.

This information is contained on two varieties of digital magnetic tape retained at Teledyne Materials Research: a "Library" tape containing all the information noted above, and a "Summary" tape containing everything except the time series (item 8).

Only the summary data for the UNIVERSE IRELAND were examined in the present project. Teledyne Materials Research furnished listings of the summary tape for this purpose, and carried out a parametric correlation of the maximum "burst" stresses as well.

Data Base for the FOTINI-L

The data-collection effort for the FOTINI-L is also summarized in Ref.7. Briefly, the ship was instrumented from September 1967 through November 1970, during which time the ship made 17-1/2 voyages (834 days at sea). The ship's trade route at the time was between West Coast USA, Peru and Japan. Some 2800 30-minute stress records were obtained by the automatic data-acquisition system which was set primarily to record one record per 4-hour watch. About 1550 of these records pertain to midship longitudinal bending stress. Since there were about 5000 sea-watches in the data-taking period, the data base for longitudinal bending stresses of the FOTINI-L corresponds roughly to a sample of conditions in about 1/3 of the sea-watches naturally occurring over a nearly 3-year period.

As with the UNIVERSE IRELAND, the basic data reduction was carried out by Teledyne Materials Research according to methods described in Ref.16 and most of the results of this reduction were reported in Ref 7. The details of the data for FOTINI-L are the same as those noted previously for UNIVERSE IRELAND.

In the present project the FOTINI-L data were examined at two levels of detail. The first level of detail involved only the summary data. As in the case of the UNIVERSE IRELAND, Teledyne Materials Research furnished listings of the summary tape and carried out a parametric correlation of the maximum "burst" stresses observed in the 1550 vertical longitudinal bending stress records. At a later stage in the present project the same summary data were obtained on punched cards by the investigators so that correlations alternate to those by Teledyne could be carried out.

The second level of detail in the present examination of FOTINI-L data involved analyses of some digital time series representing the observed midship longitudinal bending stresses. The selection of the actual sub-set of data to be considered was made largely on the basis of the prevalence of high-vibratory response since some quite surprisingly high magnitudes are quoted for FOTINI-L in Ref.7.

All data for midship longitudinal bending stress for FOTINI-L are contained in three digital tapes as follows: (the "B" and "L" suffixes in voyage numbers indicate "ballast" and "loaded", respectively):

Tape Number	Voyage Numbers	Number of Intervals
FOTN01	2B	18
	6L	135
	9L	35
	2L	139
	4B	56
	3L	132
FOTN02	1L	17
	4L	80
	14B	110
	3B	103
	10B	88
	5L	87
	9B	101
FOTN03	6B	128
	7B	68
	8B	119
	14L	67
	5B	68

A scan of the summary listing indicated that the third tape (FOTN03) contained the most evidence of vibratory response which was unusually large with respect to wave-induced response, and a copy of this tape was obtained from Teledyne Materials Research. As may be noted, four voyage legs in ballast and one in loaded condition are involved. There are a total of 450 records in the tape. One record was found to be short and was discarded so the total for present purposes was 449.

For purposes of the present analysis a sub-set of 168 records was chosen so that all records with significant vibration were included (95 records out of 449), the remaining intervals were chosen so that the incidence of Beaufort wind strength and heading angles contained in the sub-set would resemble the corresponding incidences in the entire data base. The extent to which this was possible is indicated in Figures C-1 and C-2. The percentages quoted are of the total number of records where Beaufort wind or heading was given. In the entire data base only 5% of records have

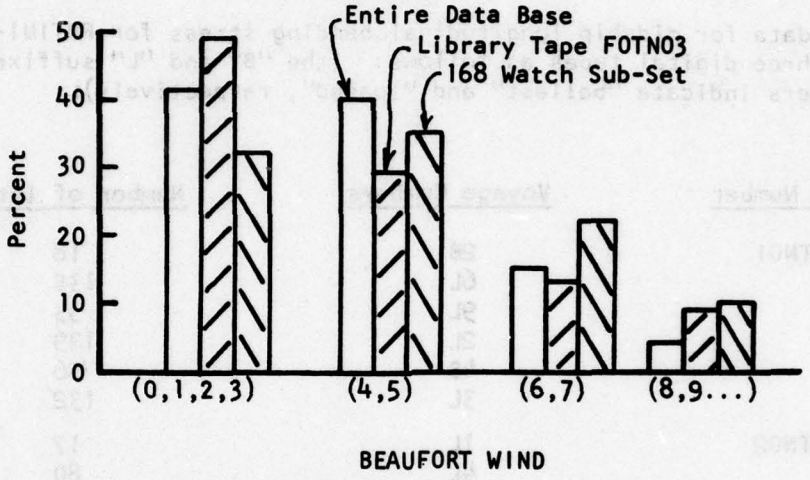

FIGURE C-1 Relative Incidence of Beaufort Winds, FOTINI-L Data Bases

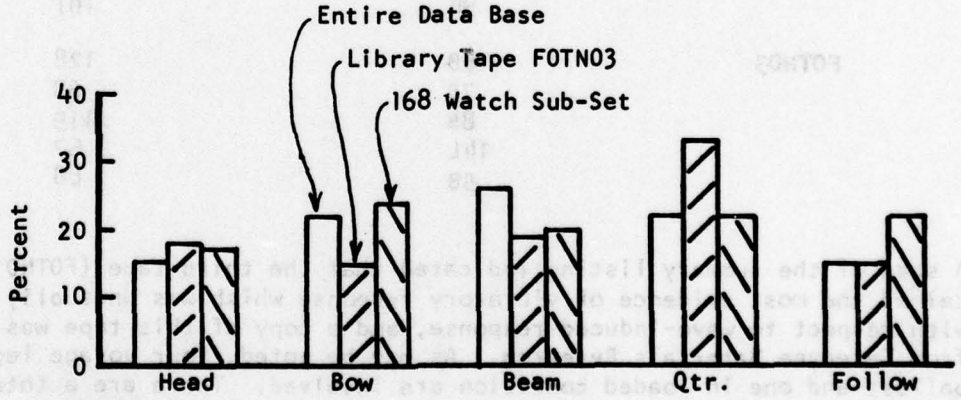

FIGURE C-2 Relative Incidence of Headings In The FOTNI-L Data Bases

no Beaufort wind noted, while 46% of the records have no heading noted. The 168 record data sub-set may be seen to be somewhat biased toward the higher wind strengths and thus presumably toward more severe wave conditions.

Ship speed in the intervals represented in the library tape and the data sub-set were typically between 14.5 and 16 knots with extreme variations of 13.5 to 16.9 knots. Only one case of zero speed was noted in the summary. However the other log book entries imply that it could have been zero. All told there are only 7 records in the entire 1550 record data base where speeds were quoted at less than 10 knots.

Data Base for the SL-7

The data-collection effort for the SL-7 class containership SEA-LAND McLEAN is summarized in References 2,3,25 and 26. Briefly, data were acquired during three winter seasonswhile the ship was in service between East Coast U.S.A. and Europe. The instrumentation was attended in each season. Table C-1 indicates the inclusive dates, number of voyages and the number of records of midship longitudinal bending stress reduced by Teledyne Materials Research according to the methods of Ref. 16.

In-so-far as sampling is concerned there are two significant differences between the SL-7 data gathering effort and that for the other ships. Owing to the enormous burden of instrumentation in the SL-7 program four records of bending stress per watch were obtained instead of one. Thus the 5000 odd records noted in Table C-1 correspond to about 1200 watches. In the terms noted for the other ships, the SL-7 data base involves a sample of conditions in about 2/3 of the sea-watches occuring in 270 or 280 days exposure to winter North Atlantic weather.

This last interpretation suggests the second significant differences between the SL-7 data base and that of the other ships. It is that the data base must be taken as being biased toward severe conditions, rather than being representative of conditions experienced in normal year-round operation (as is the case for the other ships).

The SL-7 data base was also examined at two levelsof detail. As for the FOTINI-L, the first level of detail involved only the summary data. Because the third-season data had not been reduced at the outset of the project, the initial examinations of the Teledyne summary data were carried out only for the first and second-season data (about 4200 records). Listings and parametric correlations were carried out by Teledyne Materials Research. At a later stage in the present project the summary data for first and second season were transmitted to the present investigators via punched cards, and the third season data by magnetic tape so that in the end all the Teledyne data base was available for alternate correlations.

As in the case of FOTINI-L, it was desired to make some analyses of selected time histories of midship longitudinal bending stress. The selection of the actual sub-set of records for the present work was made on the entirely practical grounds that at the time the analysis was initiated,

TABLE C-1

SL-7 Recording Season Summary

Season	1	2	3
Inclusive Dates	10/8/72-4/4/73	9/23/73-3/25/74	1/17/75-3/17/75
Number of Voyages	12	13	3
Number of Records Reduced	2078	2112	864

(Total: All Seasons, 5054)

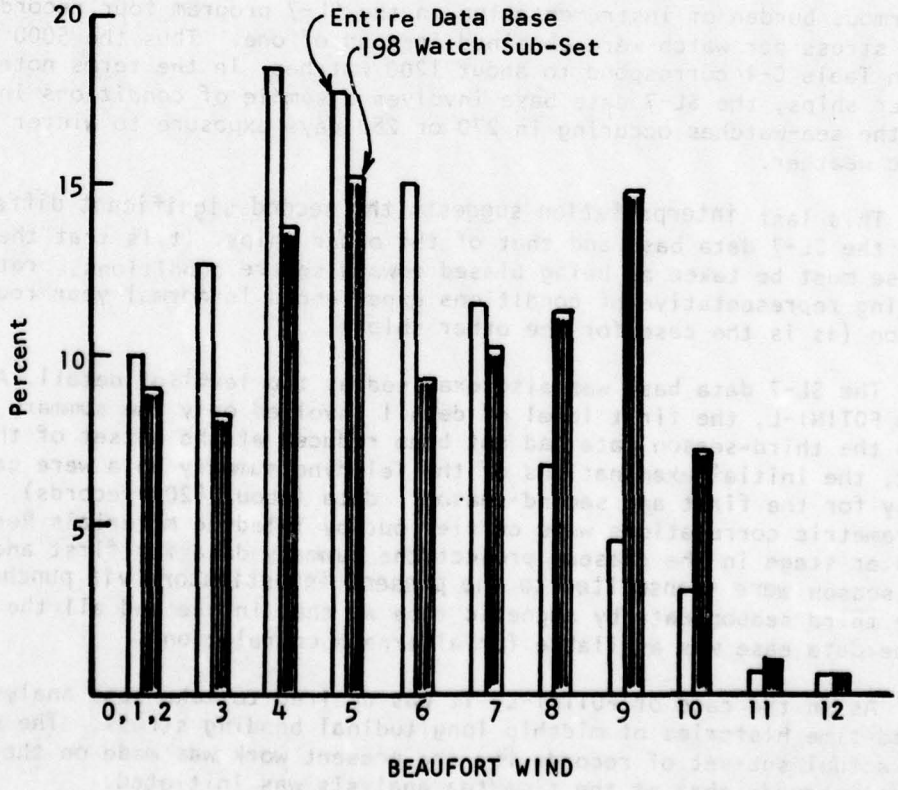

FIGURE C-3 Relative Incidence of Beaufort Winds: SL-7 Data Bases.

a 198 record sub-set from the second-season records was immediately available for direct computer access as a by-product of the work reported in Refs 27 through 32. These 198 digital time histories of stress were produced at Davidson Laboratory according to procedures generally similar to those in use by Teledyne. Details of the procedures are to be found in Ref 27.

The selection of particular records for analysis in Ref 27 was based almost entirely on requirements in that work for reducing other data. The net result of the selection procedure was 198 digitized records from nine-voyage legs during the period 30 December 1973 to 3 March 1974. For this period, roughly one record per watch was digitized. Records at beginning and end of voyage legs and those in which electronic malfunction was suspected were discarded. The 198 intervals finally resulting co-respond to 75% of all sea-watches during the nine-voyage legs (about 85% of all watches where the ship was apparently not in protected waters). The data sub-set corresponds to approximately 33 24-hour days at sea. In reviewing the stress data it was noted that the stress-time series for one of the 198 records contained some sort of electronic malfunction and actual analyses of stress from this interval were excluded.

It is appropriate to consider the extent to which the data sub-set is representative of the entire data base. Figure C-3 is a comparison of the incidence of various Beaufort winds in the sub-set with the incidence in the entire (three-season 1200 watch) data base. It is apparent that the sub-set is more conservatively biased than the data base (more Beauforts 8 to 10 and fewer Beauforts 3 through 6). The sub-set is thought to more closely resemble the second-season data since milder weather conditions were apparently experienced in the first and third recording seasons.

Figures C-4 and C-5 indicate the incidence of headings and ship speeds for the sub-set and the entire data base. The sub-set has proportionately fewer beam and more following-sea cases, and a lower incidence of intermediate speeds. Again, the sub-set is thought to more closely resemble second-season data. It is believed that ship speeds tended to be lower during the first season for non-weather related reasons.

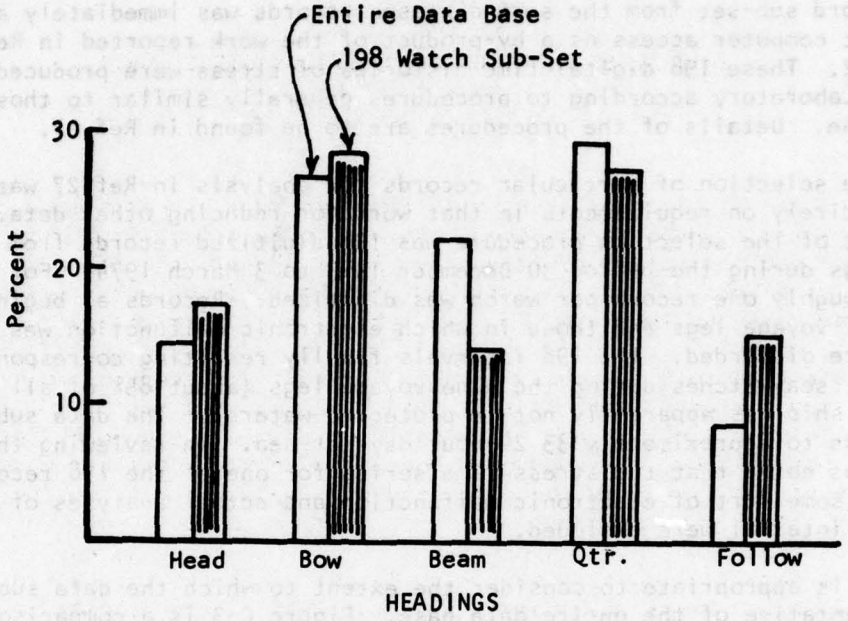

FIGURE C-4 Relative Incidence of Headings: SL-7 Data Bases

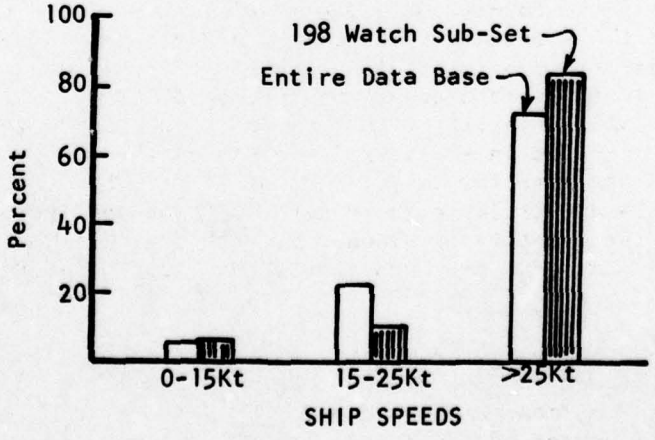

FIGURE C-5 Relative Incidence of Ship Speeds: SL-7 Data Bases

APPENDIX C-2

INITIAL EXAMINATION OF VIBRATORY-STRESS DATA

Insofar as midship stresses in the main hull girder are concerned, vibratory-stress response has been observed to be primarily at the two-noded longitudinal hull mode frequency (Ref.1, 7, 17, 33, for example). This empirical observation colors much of what is done in the processing of the raw data and indeed influences some of the definitions.

Referring to the methods of Ref.16, the first step in processing the raw stress signal is to pass it through a low-pass filter which effectively eliminates most if not all signal content at frequencies more than about an octave above the two-noded mode frequency. The vibratory content of the resulting signal is then isolated by a second filtering operation involving a fairly narrow-band pass filter centered nearly on the two-noded mode frequency. The wave-induced component of the stress is isolated by a parallel low-pass filtering in which nearly all the content above 0.2 or 0.3 Hz is eliminated. The validity of the results of these operations depends upon a reasonable separation between the highest wave encounter frequency and the first-mode frequency, a condition fulfilled in the cases of the ships under present consideration.

The processing done upon the isolated vibration signal involves determination of successive "double amplitudes". In this context a double amplitude is defined as the difference in stress between a maximum and the succeeding minimum--the terminology comes about because this difference is very nearly twice the local amplitude for a narrow-band process. In the system of Ref.16, the succeeding double amplitudes of vibration are scanned in order to determine if their magnitude exceeds a certain threshhold (1000 psi for UNIVERSE IRELAND and FOTINI-L, 600 psi for the SL-7). When one does, the initiation of a "burst" of vibration is assumed and the scan continues until the double-amplitude level falls below the threshold, whereupon the "burst" is assumed to be over. A given record may have no "bursts" (no vibration above threshold), one "burst" (either <u>all</u> vibration double amplitudes in the record above the threshold, or as few as one), or a great many fluctuations in vibration level above and below the threshold. The summary data described in Appendix C-1 includes the number of "bursts" in each record. Along with the scanning to determine "bursts", the maximum vibration double amplitude in the record is found and included in the summary. This latter quantity is synonomous with "maximum burst stress" or "maximum first-mode peak-to-trough stress" as used in References 2, 3 and 26.

Given the existence of these measures of vibration within the database libraries described in Appendix C-1, the obvious first and simplest step was to access the "maximum burst" data and attempt to develop statistical trends with measures of sea conditions, ship speed and heading. The process used by Teledyne Materials Research for developing such trends is described in Ref.2 and was exercised by them to develop data used in the initial examination.

The Beaufort wind strength was taken as a measure of wave severity, and two two-way classifications of the maximum burst data were carried out; the first classification was by Beaufort wind and ship speed, the second was by Beaufort wind and heading. The mean value, mean of 1/3 highest and RMS values were computed for the vibration double amplitudes falling within each classification cell. (Each combination of Beaufort number and heading or speed.)

Figures C-6 through C-11 summarize part of the results of the correlation. Figures C-6 and C-7 pertain to second-season SL-7 data (computations were also made for the first season but indicated similar trends and are not shown). Figures C-8 and C-9 pertain to the FOTINI-L, and Figures C-10 and C-11 are for the UNIVERSE IRELAND. In all cases the numbers plotted are the mean value of all the maximum burst stresses falling within the classification cell formed by Beaufort number and speed or heading.

Considering the SL-7 results first (Figures C-6 and C-7) there is an obvious overall upward trend of vibration level with Beaufort number, and by implication with wave severity. Similarly there appears an upward trend as heading goes from following to head seas. The picture with speed is confused due to the lower incidence of low ship speeds, but overall the vibration magnitude appears somewhat independent of speed.

The results for FOTINI-L (Figures C-8 and C-9) indicate a confused picture overall. There is so little speed variation in the data base that practically all data is in the 12 to 16-knot classification. Thus the results in Figure C-8 indicate a mild overall upward trend with Beaufort number, as do the beam, bow and head-sea results in Figure C-9. There is a tendency for the vibration levels to be lower in quartering and following seas, Figure C-9.

In contrast, there is not much which can be concluded about trends of the vibration levels on UNIVERSE IRELAND, Figures C-10 and C-11. The mean values of the largest vibration double amplitudes are all less than the 1000 psi analysis threshold, and there is no obvious trend with any of the parameters.

The mean value of the maximum vibration double amplitudes within each classification cell was selected for trend analysis in hopes that it was the most stable statistic available. Considering all the individual data points for a particular Beaufort number, there is typically an enormous scatter about the mean--individual values ranging from below the threshold to values typically three times the mean. In the case of SL-7 there are a quite significant number of peak vibration double amplitudes between 3000 and 10000 psi and a few isolated points (5 points exactly) to 15000 psi. The data for FOTINI-L show a significant number of points between 3000 and 8000 psi, with four points falling between 8000 and 11000 psi. In contrast, all the data for UNIVERSE IRELAND except for four points are less than 3400 psi. These latter four points lie between 6500 and 9500 psi. Interestingly, there are no points in excess of 1000 psi for Beaufort numbers greater than 7.

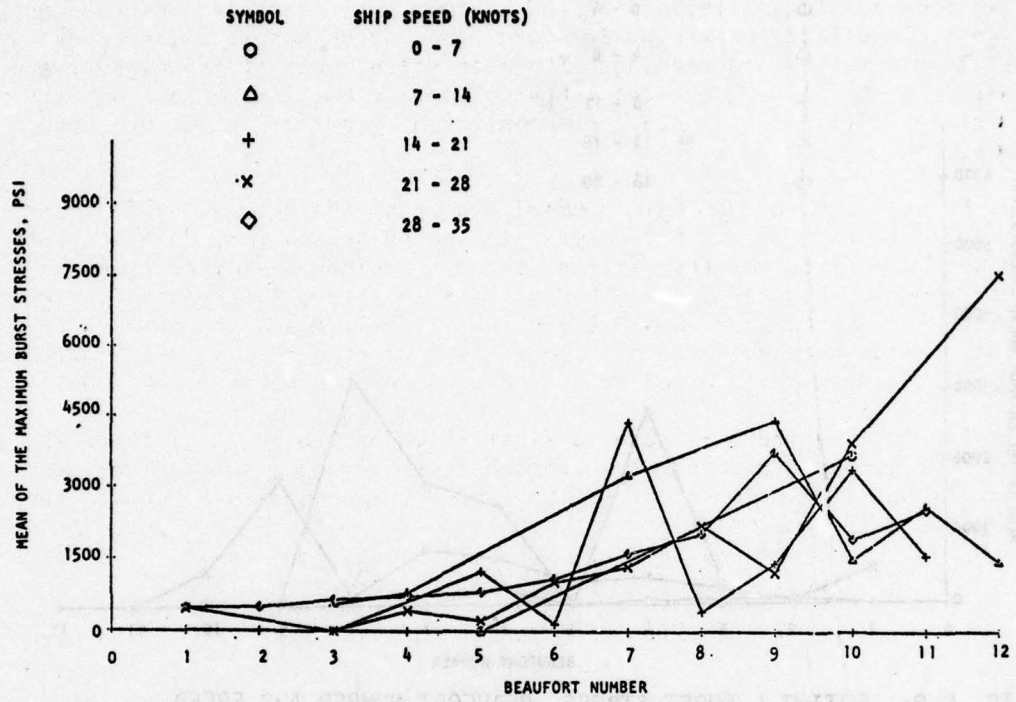

FIG. C-6: SL-7 BURST STRESS, BEAUFORT NUMBER AND SPEED (SECCIND SEASON DATA)

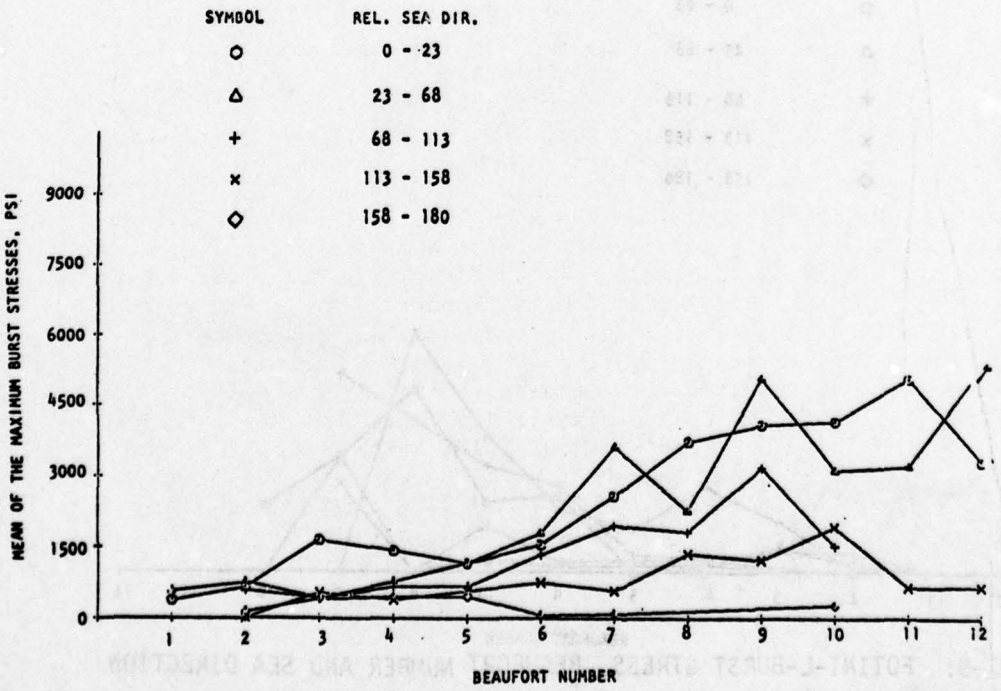

FIG. C-7: SL-7 - BURST STRESS, BEAUFORT NUMBER AND SEA DIRECTION (SECOND SEASON DATA)

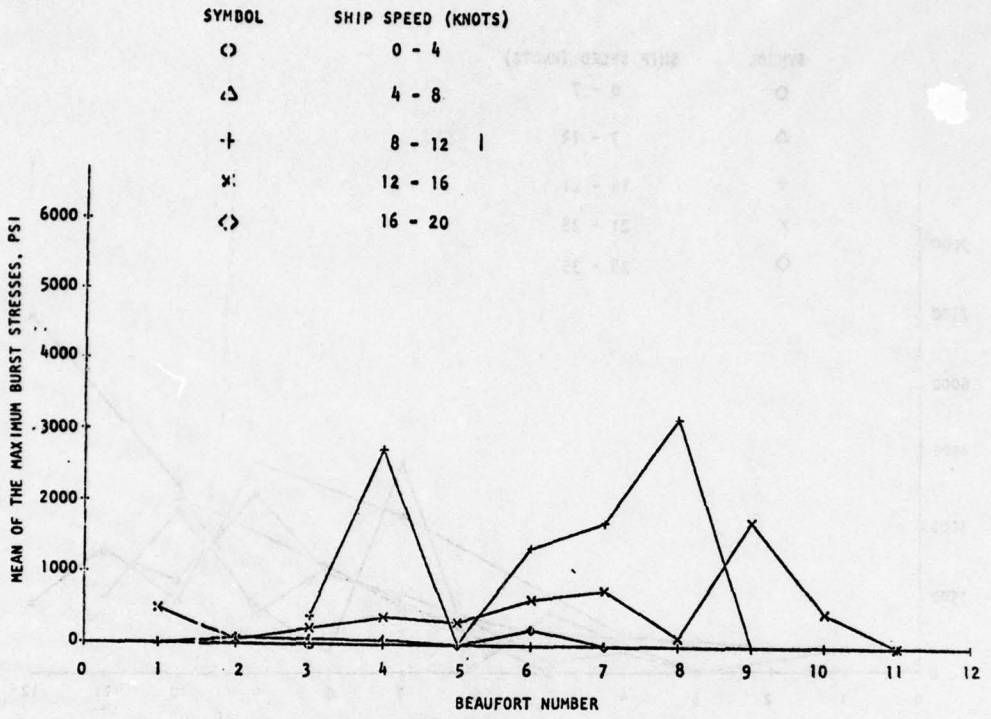

FIG. C-8: FOTINI-L-BURST STRESS, BEAUFORT NUMBER AND SPEED

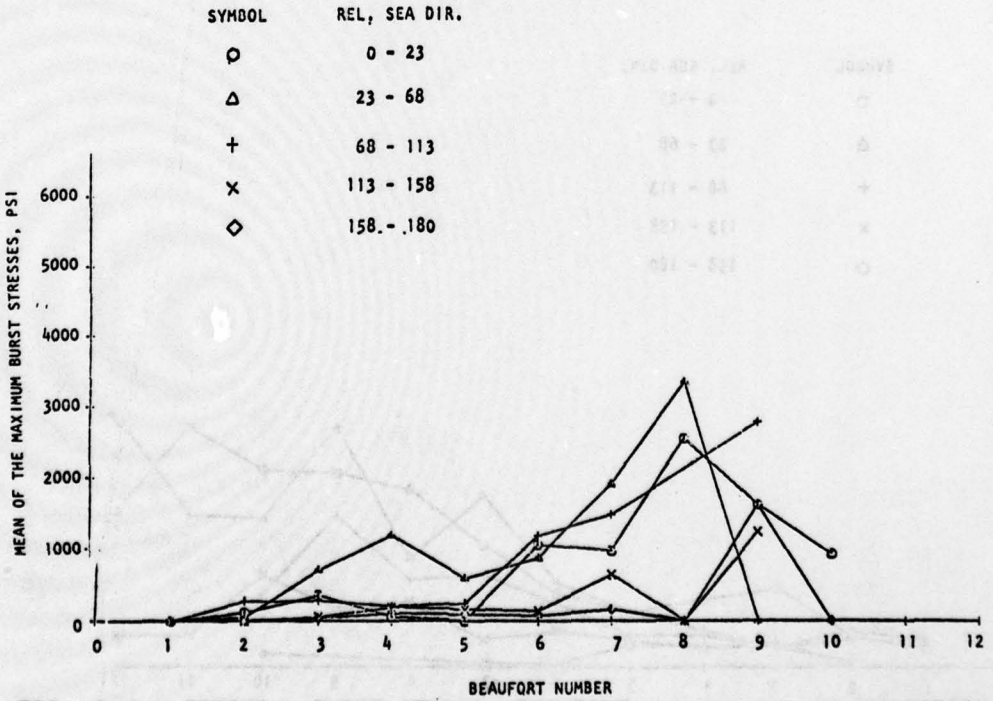

FIG. C-9: FOTINI-L-BURST STRESS, BEAUFORT NUMBER AND SEA DIRECTION

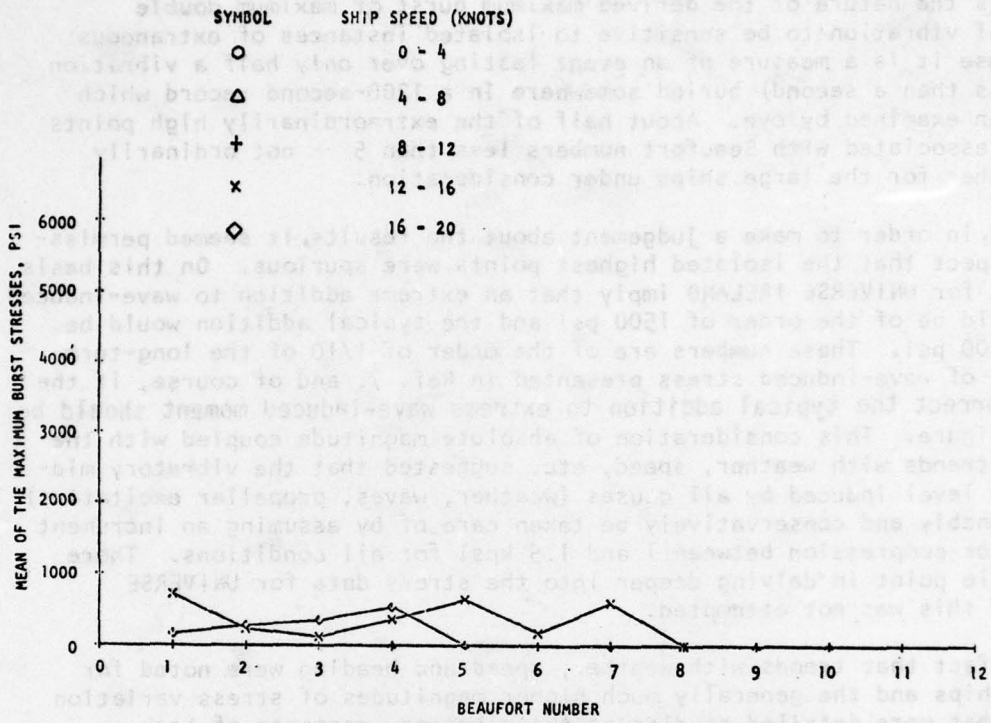

FIG. C-10: UNIVERSE IRELAND-BURST STRESS, BEAUFORT NUMBER AND SHIP SPEED

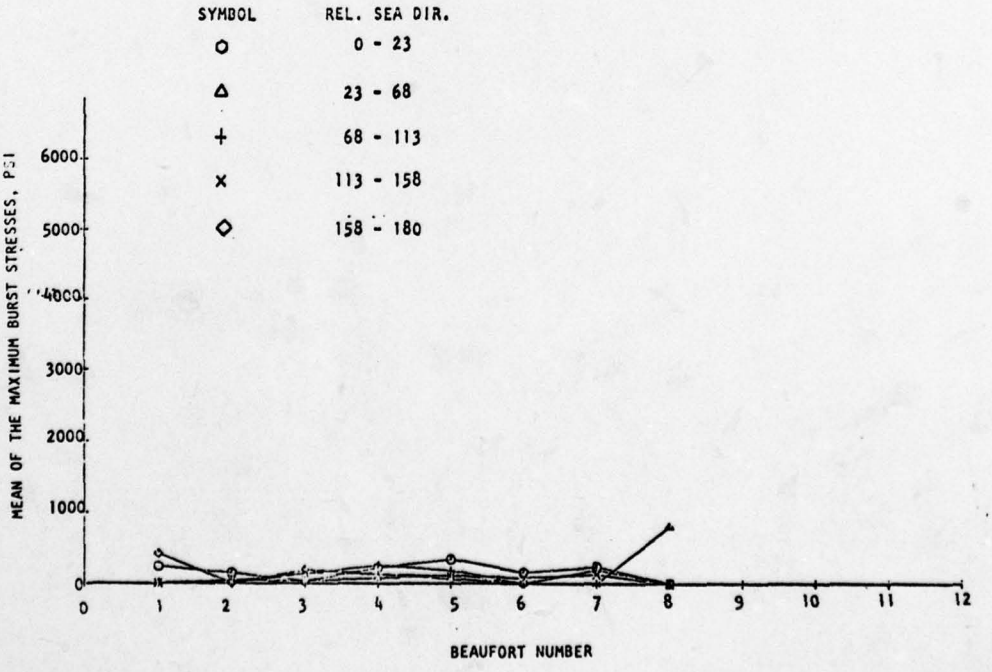

FIG. C-11: UNIVERSE IRELAND-BURST STRESS, BEAUFORT NUMBER AND SEA DIRECTION

It is the nature of the derived maximum burst or maximum double amplitude of vibration to be sensitive to isolated instances of extraneous noise because it is a measure of an event lasting over only half a vibration period (less than a second) buried somewhere in a 1200-second record which has not been examined by eye. About half of the extraordinarily high points cited were associated with Beaufort numbers less than 5 -- not ordinarily severe weather for the large ships under consideration.

Thus, in order to make a judgement about the results, it seemed permissible to suspect that the isolated highest points were spurious. On this basis the results for UNIVERSE IRELAND imply that an extreme addition to wave-induced stress should be of the order of 1500 psi and the typical addition would be less than 500 psi. These numbers are of the order of 1/10 of the long-term predictions of wave-induced stress presented in Ref. 7, and of course, if the data are correct the typical addition to extreme wave-induced moment should be the lower figure. This consideration of absolute magnitude coupled with the absence of trends with weather, speed, etc. suggested that the vibratory midship stress level induced by all causes (weather, waves, propeller excitation) could reasonably and conservatively be taken care of by assuming an increment to tension or compression between 1 and 1.5 kpsi for all conditions. There seemed little point in delving deeper into the stress data for UNIVERSE IRELAND and this was not attempted.

The fact that trends with weather, speed and heading were noted for the other ships and the generally much higher magnitudes of stress variation indicated that more detailed studies of the vibratory response of both FOTINI-L and the SL-7 were in order.

APPENDIX C-3

INITIAL EXAMINATION AND ANALYSIS
OF STRESS-TIME HISTORIES IN
THE DATA SUB-SETS

Spectrum Analysis

Though a sample spectrum of stress for the FOTINI-L is included in Ref 8, it became apparent that not too many stress spectra had been computed from the FOTINI-L data. As of the initiation of the present work, none at all had been computed for the SL-7. It was therefore decided to estimate the stress spectrum for all the records in the FOTINI-L and SL-7 data sub-sets, both to allow a quantitative description of the expected peak at first-mode bending frequency, and to identify the important range of frequencies corresponding to wave excitation.

The spectra were estimated with one of the many variations of the FFT method, the details of which are noted in Ref.28. Because the time series sampling interval for the SL-7 data is different from that of the FOTINI-L data the frequency resolution of the spectra had to be slightly different. The SL-7 stress spectra were resolved at 0.0511 Rad/Sec intervals (36 degrees-of-freedom per estimate), and those for the FOTINI-L at 0.0614 Rad/Sec (48 degrees-of-freedom per estimate).

a) Analysis of SL-7 Stress Spectra

The first analysis of the SL-7 stress spectra was to locate peaks in the vibratory frequency range and assess the frequency range of wave-induced stress. On the average, the data suggest a first-mode bending frequency of (0.78 ± 0.03) Hz. This is in reasonable accord with the value of 0.80 Hz quoted in Ref.3. Table C-2 summarizes the estimates of the lowest vibratory bending frequency for each voyage leg. These are averages of the frequencies estimated from the spectrum for each interval.

The frequency range of significant low-frequency spectral density was assessed to be between 0.0 Hz and about 0.3 Hz with the vast majority of response laying below 0.2 Hz. For practical purposes the stress response below 0.3 Hz was thus considered to be wave induced. No prominent peak was noted between 0.3 and 0.75 Hz where the first-mode bending spectral density peak began, but occasionally something around 0.5 Hz was observed just breaking through the noise. In this latter case the level was considered so low as to have negligible effect on subsequent operations. The SL-7 data are evidently also in accord with previously found indications (Appendix C-2) that vibration occurs primarily at first-mode frequency.

Qualitatively the relative magnitudes of the spectrum peak at first-mode frequency and the wave-induced (low-frequency) spectrum peak were found to be quite different than that for the FOTINI-L shown in Ref.8. Typically the peak at this vibration frequency was found to be less than 10% of the low-

TABLE C-2 - AVERAGE FIRST-MODE BENDING FREQUENCIES OF SL-7 IN NINE VOYAGE LEGS FROM SPECTRAL ANALYSES

VOYAGE	MEAN DRAFT	AVERAGE FREQUENCY
32 East	34.0	0.80 Hz
32 West	31.8	0.81 Hz
33 East	34.0	0.78 Hz
33 West	35.2	0.80 Hz
34 East	34.1	0.80 Hz
34 West	32.2	0.75 Hz
35 East	33.2	0.78 Hz
35 West	33.8	0.77 Hz
36 East	35.2	0.76 Hz

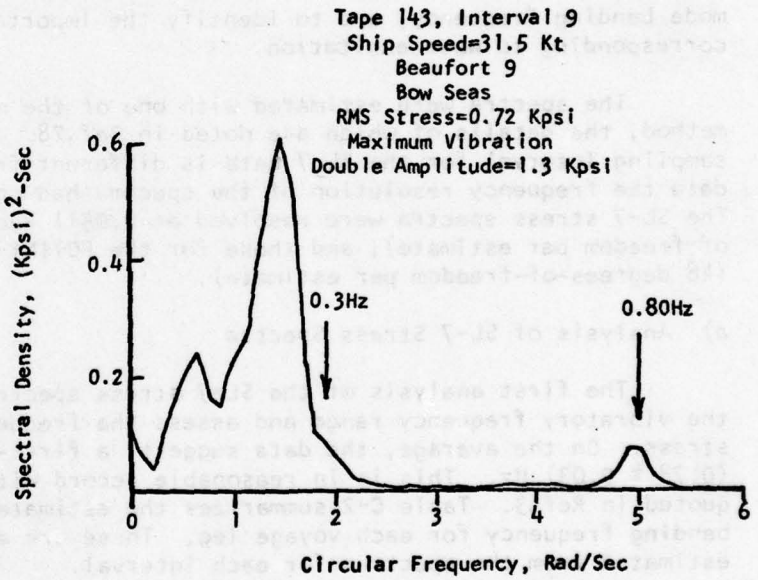

FIG. C-12 - SAMPLE STRESS SPECTRUM: SL-7

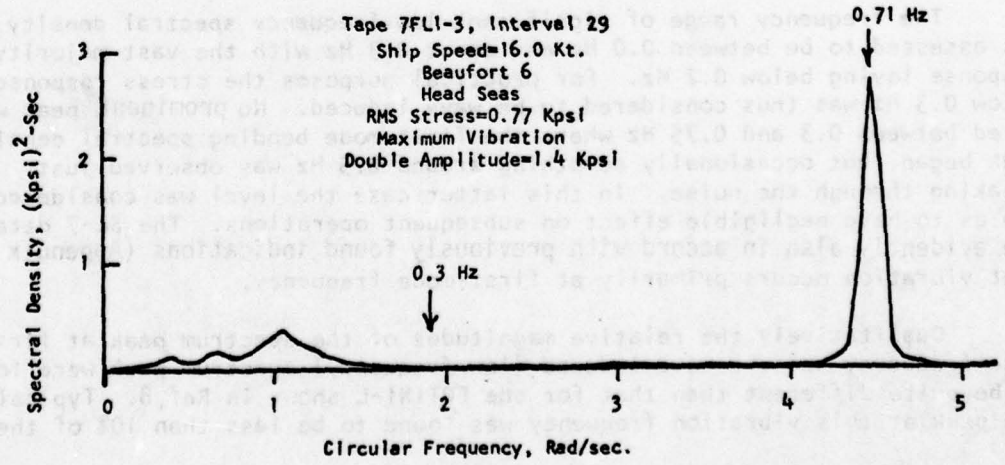

FIG. C-13 - SAMPLE STRESS SPECTRUM; FOTINI-L, VOYAGE 7B

frequency spectrum peak. A vibration peak of 20% of the low-frequency peak was quite rare. Figure C-12 shows one of these relatively rare cases in which a spectral peak at first-mode bending frequency was sufficiently prominent to be visible when plotted to a linear scale. The case chosen is also one of the rare cases in which wave-induced stress content is visible above a frequency of 0.3 Hz. The overall stress level for this particular record is relatively low. Interestingly, first-mode vibration peaks were not prominent in spectra corresponding to very high overall stress levels.

The wave-induced portion of the stress spectra varied widely in shape from cases of obvious very narrow-band reponse to cases of quite wide-band response. The wave-induced portions of all spectra have been plotted in References 29 through 32. Roughly half of the spectra indicate significant stress response at very low frequencies (less than the frequency of roll resonance, in fact). This is rougly in accordance with the portion of time spent in quartering and following seas, Figure C-4.

b) Analysis of FOTINI-L Stress Spectra

The analysis of the FOTINI-L spectra was similar to that for the SL-7. All spectra were scanned to locate the lowest prominent peak in the bending vibration range. The average frequency of vibration for the four-ballast legs was found to be 0.74 ± 0.03 Hz, about as expected from Ref 7. In the loaded voyage (14L) that vibration which could be identified from the spectrum appeared to be at 0.66 Hz. In two of the four ballast voyages there were noticeable changes in the frequency of vibration. In voyage 6B the vibration frequency at the start of the leg appeared to be about 0.73 Hz, increased to 0.77 Hz at the middle of the leg and ended at 0.74 Hz. In voyage 5B the frequency increased from 0.72 Hz at the start to 0.76 at the end of the voyage. No spectral peaks other than that corresponding to first-mode bending were discernable above a frequency of 0.3 Hz. The frequency range of wave-induced stress appeared well below 0.3 Hz.

The general appearance of the spectra when significant vibration was present was about as expected from Ref 7. There was very little vibration in the intervals corresponding to the loaded case. In this case the spectra resembled those for the SL-7. In the ballast voyages the qualitative features of the wave-induced part of the stress spectra were somewhat different from those for the SL-7 in that a much lower incidence of low-frequency spectral density was observed, perhaps only in 30 out of the 168 cases. The first-mode vibration peak was generally quite prominent. Figure C-13 shows one of the most extreme FOTINI-L stress spectra. In this case the vibration constitutes most of the response, in contrast to the extreme example for the SL-7 shown in Figure C-12.

Separation of Wave-Induced and Vibratory Stresses Using the Digital Time Series

In order to discriminate between wave-induced and vibratory stresses, some variation of filtering is required. In the analysis by Teledyne Materials Research, real analog filters were used, one to low pass the data and eliminate vibration; and one to band pass the data and isolate vibration. In the present case digital filters were required to perform the same functions.

The first filtering problem was to realize digital filters which pass the wave-induced components and reject the vibratory components. For this purpose various recursive digital 6-pole Sine-Butterworth low-pass filters were designed. Recursive filters have phase lags and, to some extent, the designs were based on the possibility of achieving a near-zero effective phase lag by shifting the output of the filter backwards in time. For each of the filters, a time shift was chosen so as to result in a net phase lag smaller than 4° throughout the frequency range of dominant wave excitation. This magnitude of phase shift was felt to be small enough that the filtered and unfiltered stress time series could be treated as though there had been no phase distortion in the wave-excitation frequency range.

The design of band-pass filters to isolate the vibration turned out not to be very promising for a variety of reasons. The method ultimately used was to subtract the low-pass filtered time series from the unfiltered time series as a first estimate, and then smooth the result with another six-pole low-pass digital filter having a cut off about twice the first-mode bending frequency. Although the subtraction is theoretically equivalent to a high-pass filter, rounding and quantization errors were magnified in low-level vibration time series. This made the additional filtering necessary to remove high-frequency noise.

The result of the filtering operations was three time series:

1. The original raw stresses.

2. Low-pass filtered stresses (wave-induced) which were time correlated with the original.

3. A series representing the vibration.

The size of the resulting arrays for the entire data sub-sets would have been much too large for convenience in storing for future use. Accordingly, these arrays existed only for a short time in the computer as scratch files. The remainder of the various data-reduction procedures were started for each record as soon as the above arrays had been generated.

There were, in all, three low-pass filters utilized to separate wave-induced stress, one for the FOTINI-L and two for the SL-7. The amplitude response of all three was unity $\pm$ 0.5% from D.C. to 0.25 Hz and (depending upon cut-off frequency) no lower than 0.95 at 0.3 Hz, the upper limit of wave-induced stress frequencies. The filter for the FOTINI-L had a nominal cut-off of 0.40 Hz which resulted in a 97% attenuation of first-mode vibration components. The first of the two SL-7 filters had a cut-off of 0.44 Hz, resulting in a 96-1/2% attenuation of first-mode vibration. This filter was used for the bulk of the SL-7 data reduction. The second SL-7 filter was utilized in some special analyses of wave-induced stresses to be described in Appendix C-4. Its cut-off was 0.36 Hz and the filter attenuated first-mode vibration by almost 99%.

Characteristics of Midship Longitudinal Stress Records in the Time Domain

Because it was easy to do, a great many analyses of the stress records in the data sub-sets were done prior to the time that serious consideration was given to a qualitative assessment of the behavior of the stress records in the time domain. In effect, it was initially assumed that the wave-induced and superimposed vibratory stresses in the records behaved as the implied definitions of slamming response, whipping, springing, etc. in Ref 1. Ultimately, there appeared to be so many oddities in the results of these analyses (especially with the FOTINI-L data) that it appeared necessary to go back to basics. By this is meant the old fashioned (but still valid) idea that before performing moderately complicated statistical analyses on records, at least a portion of each should be inspected by eye. (All of the records in the present two data sub-sets had been examined, but at a time compression in which not even individual wave-induced fluctuations could be discerned.)

Thus with respect to the chronology of the work the contents of the present section are purposely out of order--no particularly good purpose would be served by a strictly chronological account of the work.

Figures C-14a through C-14i contain plots of short portions of the 198 digital stress time series in the SL-7 data sub-set. Both the original series and the filtered (wave-induced) series are plotted. (The wave-induced stress is shown as a dashed line.) The origin of the data in each frame is identified by the Teledyne analog tape and interval number as well as by a "run number" which was assigned at Davidson Laboratory for convenience in handling the data. The vertical scale for each frame is adjusted to suit the data; in general, the scales vary from frame to frame. Positive stress is deck tension, corresponding to a hogging moment. "Zero" stress corresponds to the sample mean. The horizontal scale is time. In all cases the duration of the plotted time history is about 76 sec. The number in the upper right corner of each frame is the number of the last plotted point of the time series. The particular portion of time history shown was determined by the position of the maximum vibration double amplitude found in the entire record. In the process of developing vibration double amplitudes from the vibration time series described in the last section, the position of the largest in the array was retained. For purposes of making Figure C-14 then, the portion of time series selected was such as to make the maximum vibration double amplitude appear in the center of the time axis unless it happened to be observed at the beginning or end of the time series. In terms of the conventions of the Figures, if the last point number is greater than 512 or less than 8192 the maximum vibration is somewhere left of center, and if the last point number is 8192 the maximum vibration is to the right of center.

The rationale for the above selection procedure was the sensitivity (noted earlier) of the maximum vibration double amplitude to extraneous noise, and the corresponding high probability that if anything was amiss in the records it would be observed in conjunction with the perceived maximum vibration.

Scanning the time histories in the SL-7 data sub-set, Figure C-14, there are six records noted as being questionable. Each is indicated by an asterisk in the right or left hand margin. The item questioned is marked by

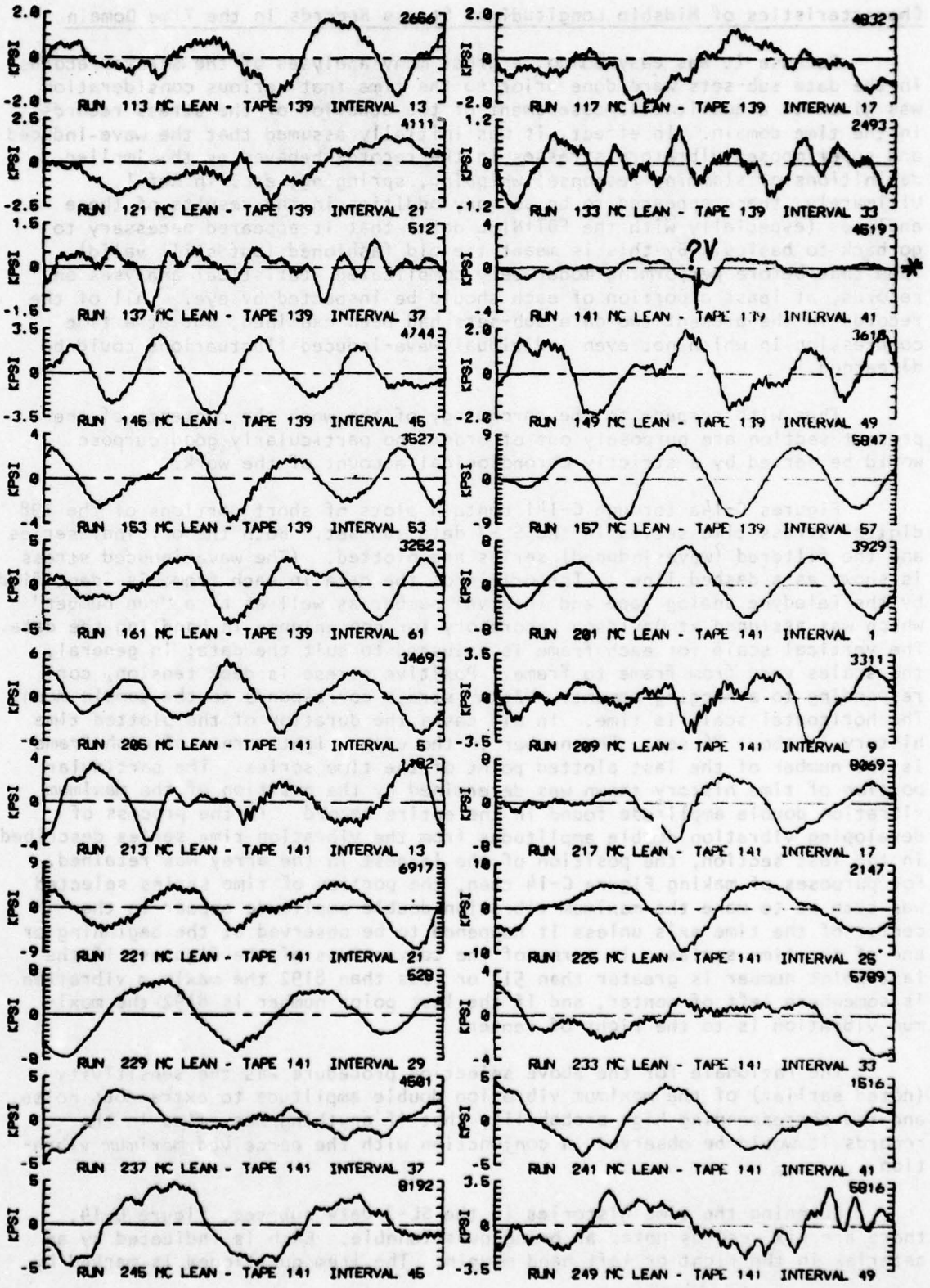

Figure C-14a Sample Time Histories, SL-7 Data Sub-Set

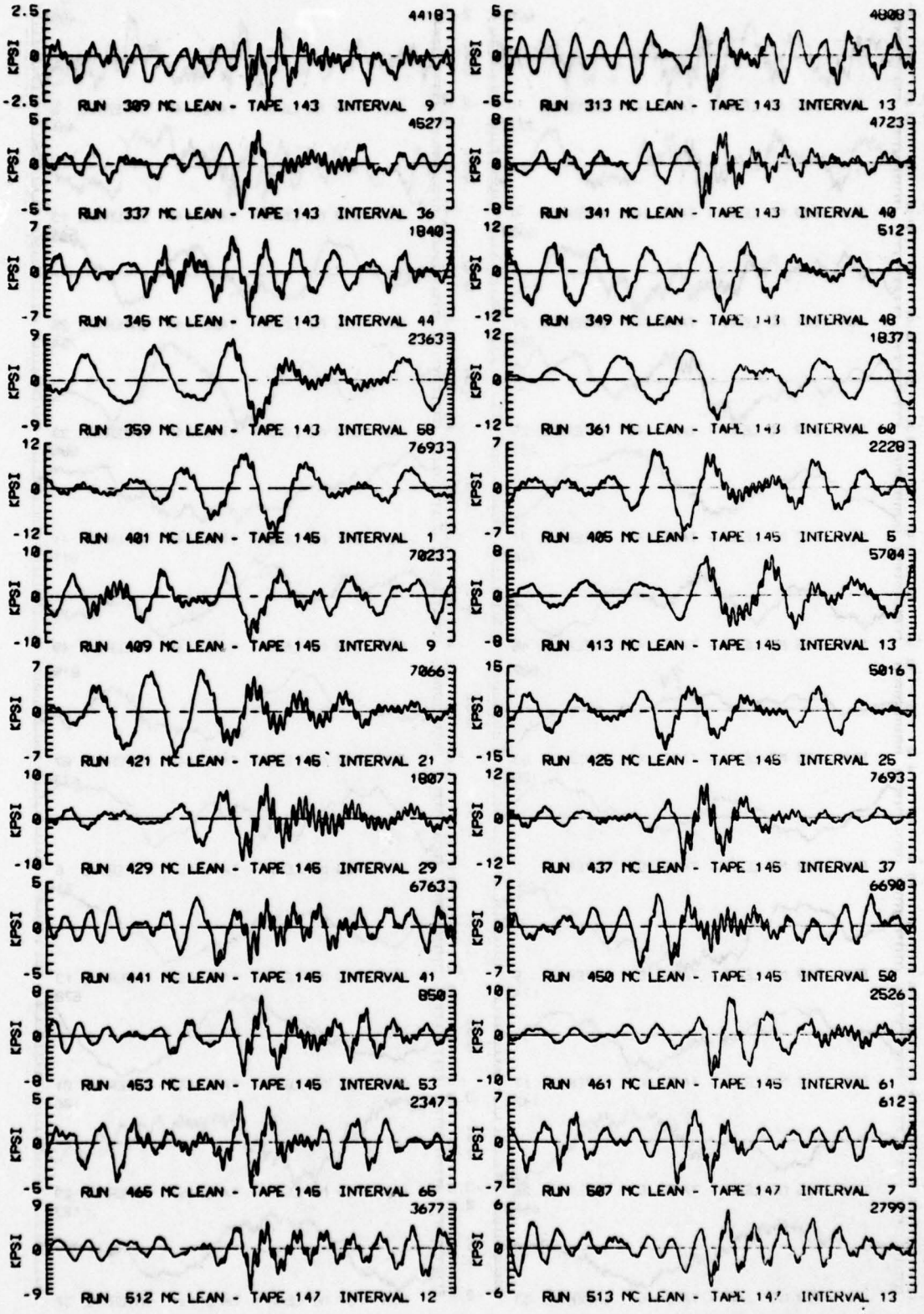

Figure C-14b Sample Time Histories, SL-7 Data Sub-Set

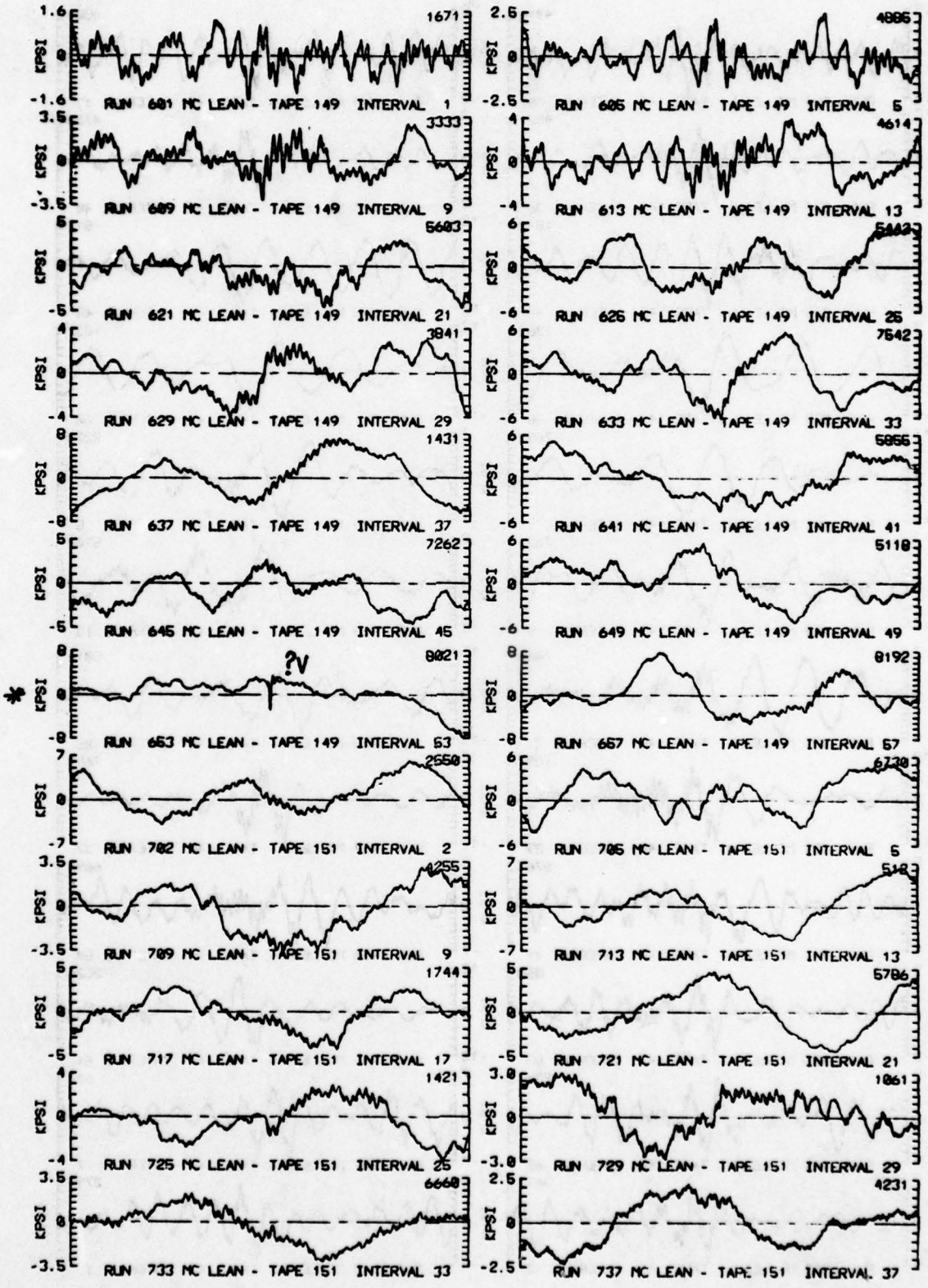

Figure C-14c Sample Time Histories, SL-7 Data Sub-Set

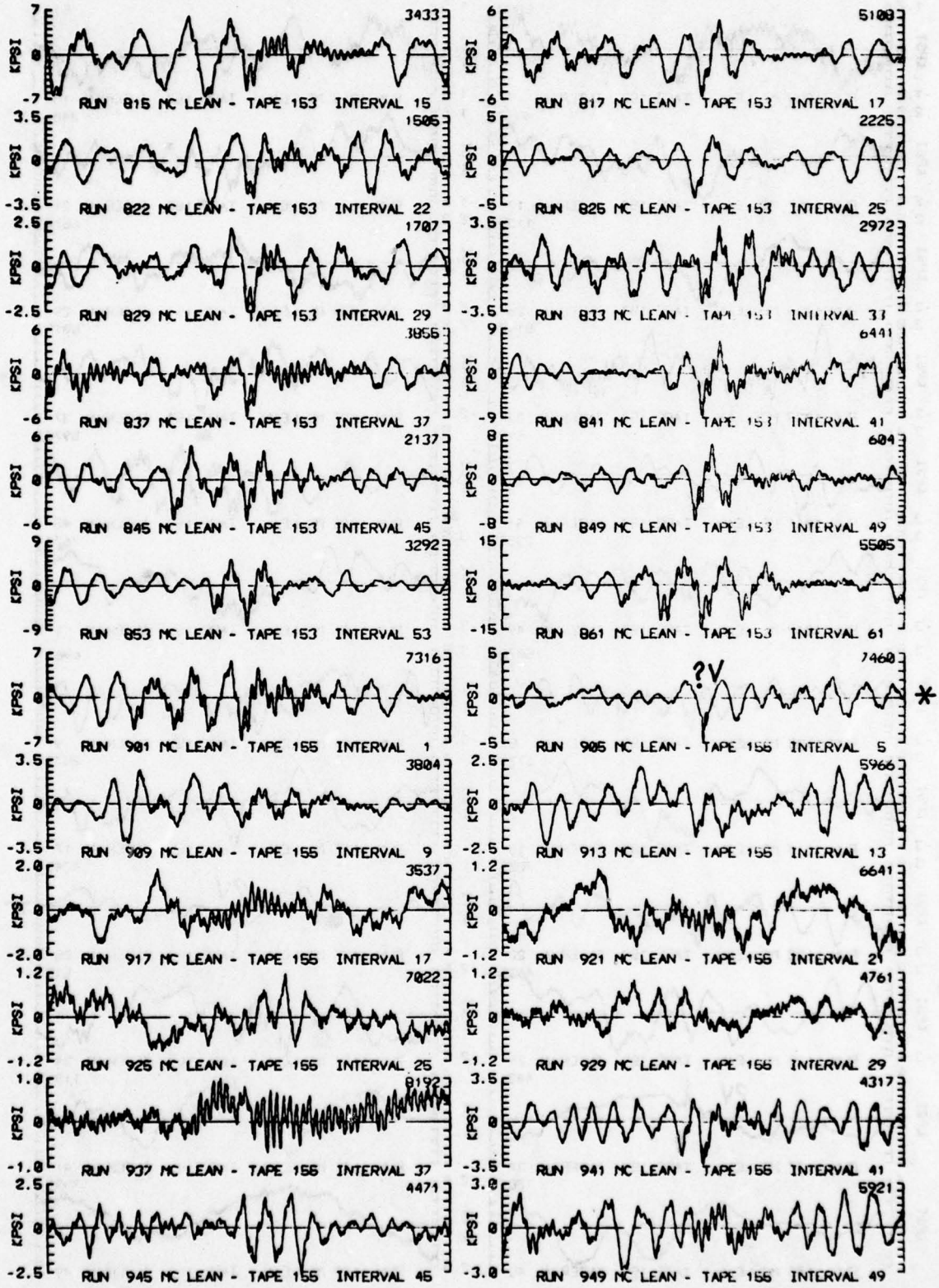

Figure C-14d Sample Time Histories, SL-7 Data Sub-Set

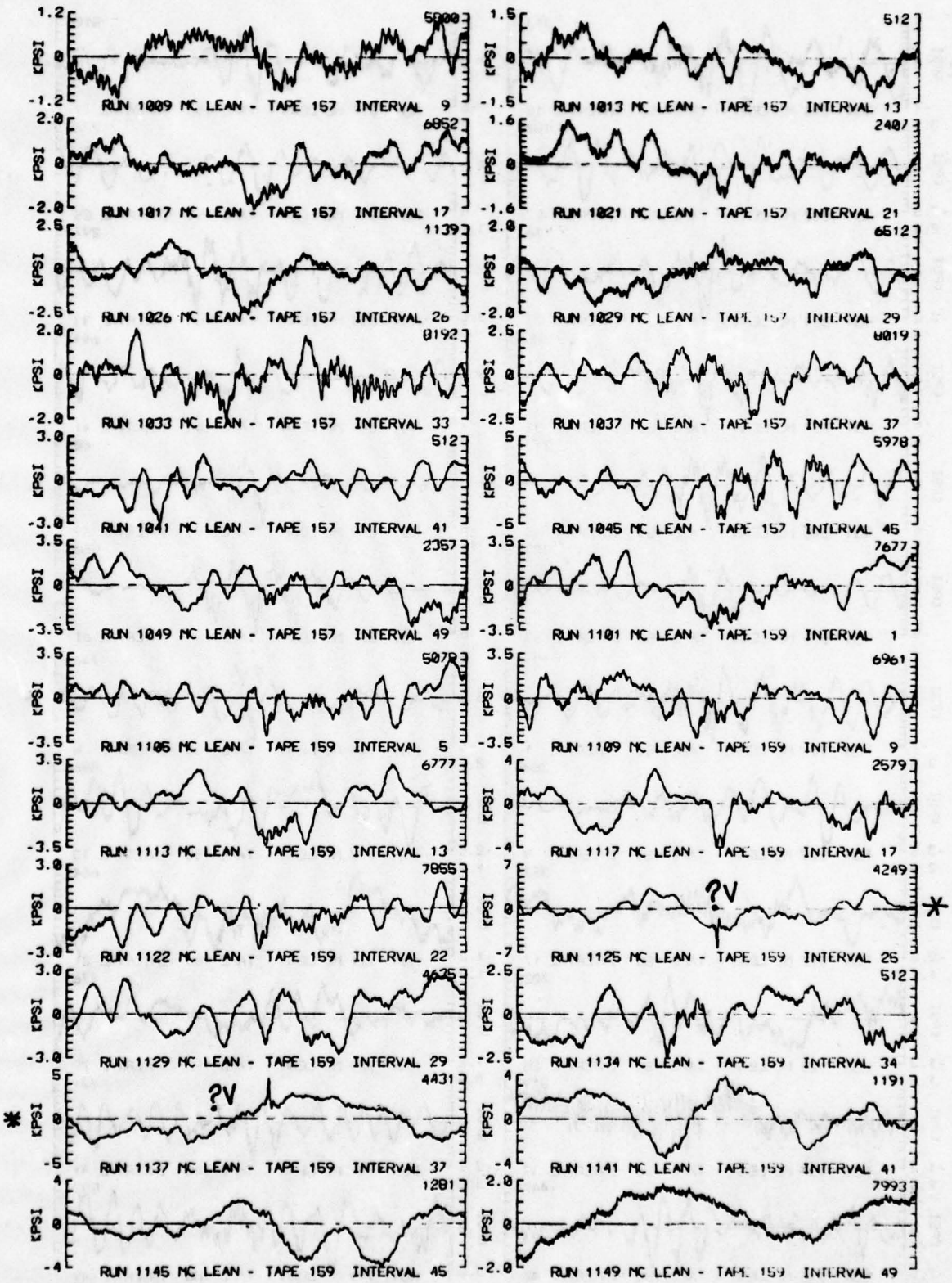

Figure C-14e Sample Time Histories, SL-7 Data Sub-Set

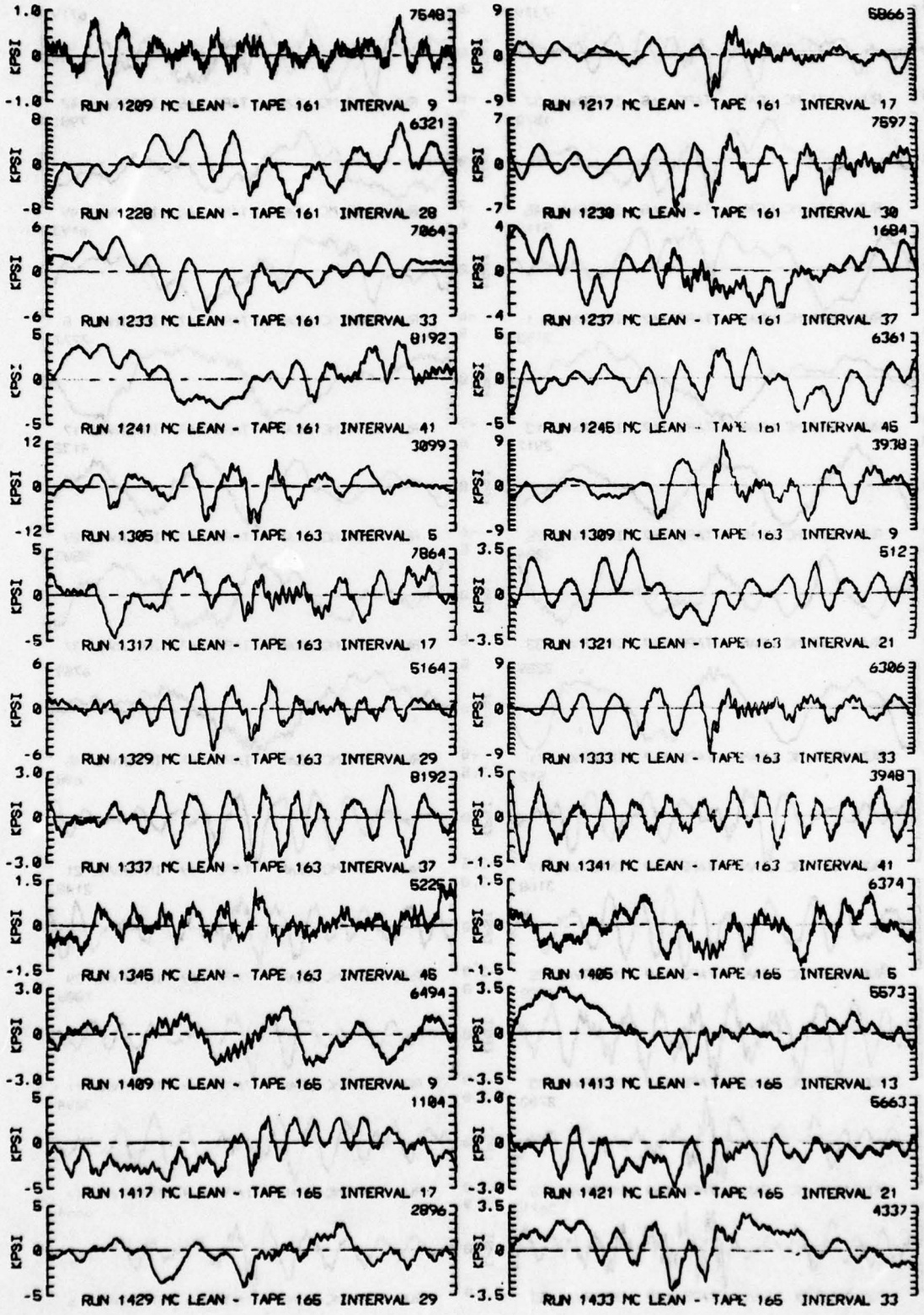

Figure C-14f Sample Time Histories, SL-7 Data Sub-Set

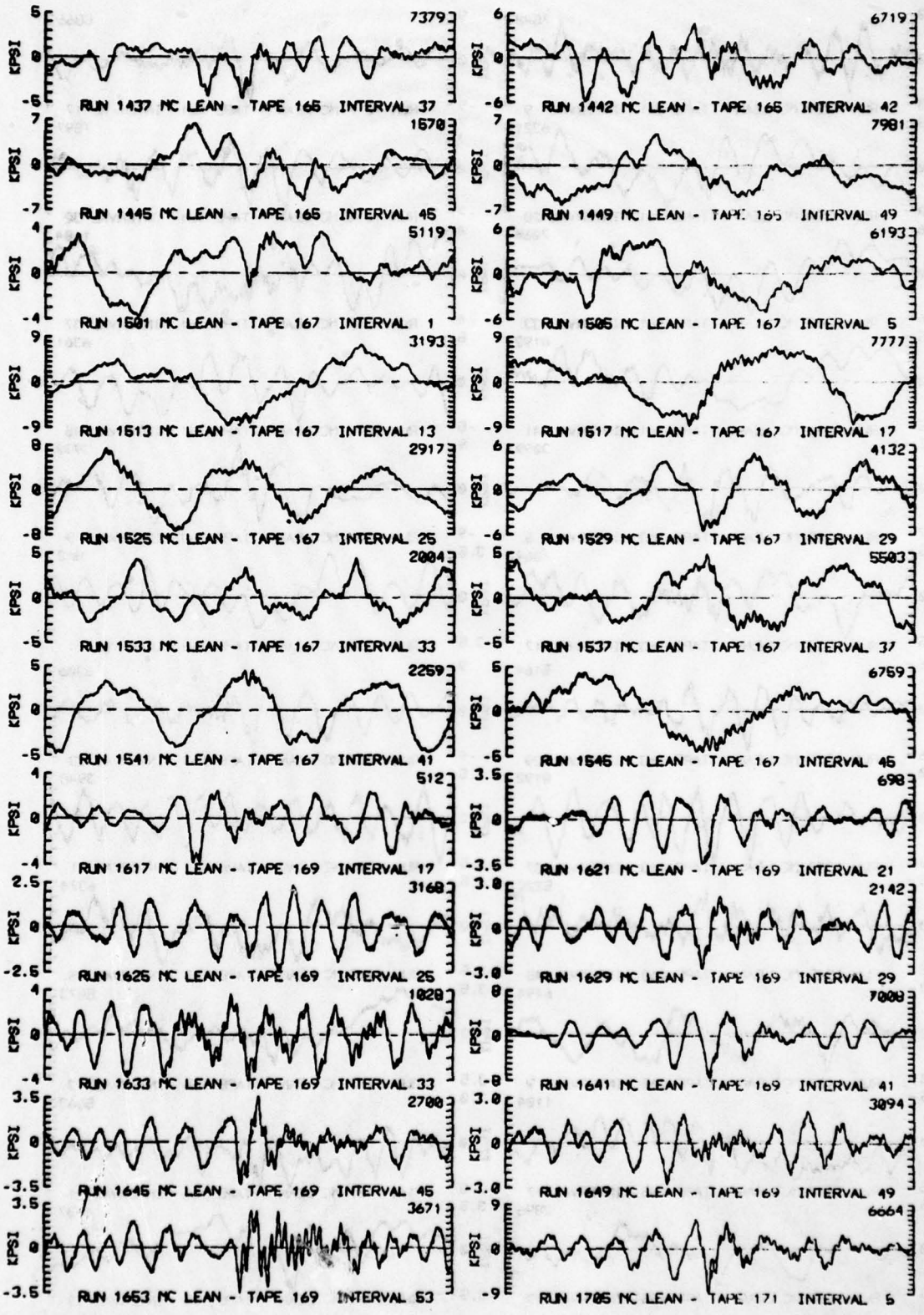

Figure C-14g Sample Time Histories, SL-7 Data Sub-Set

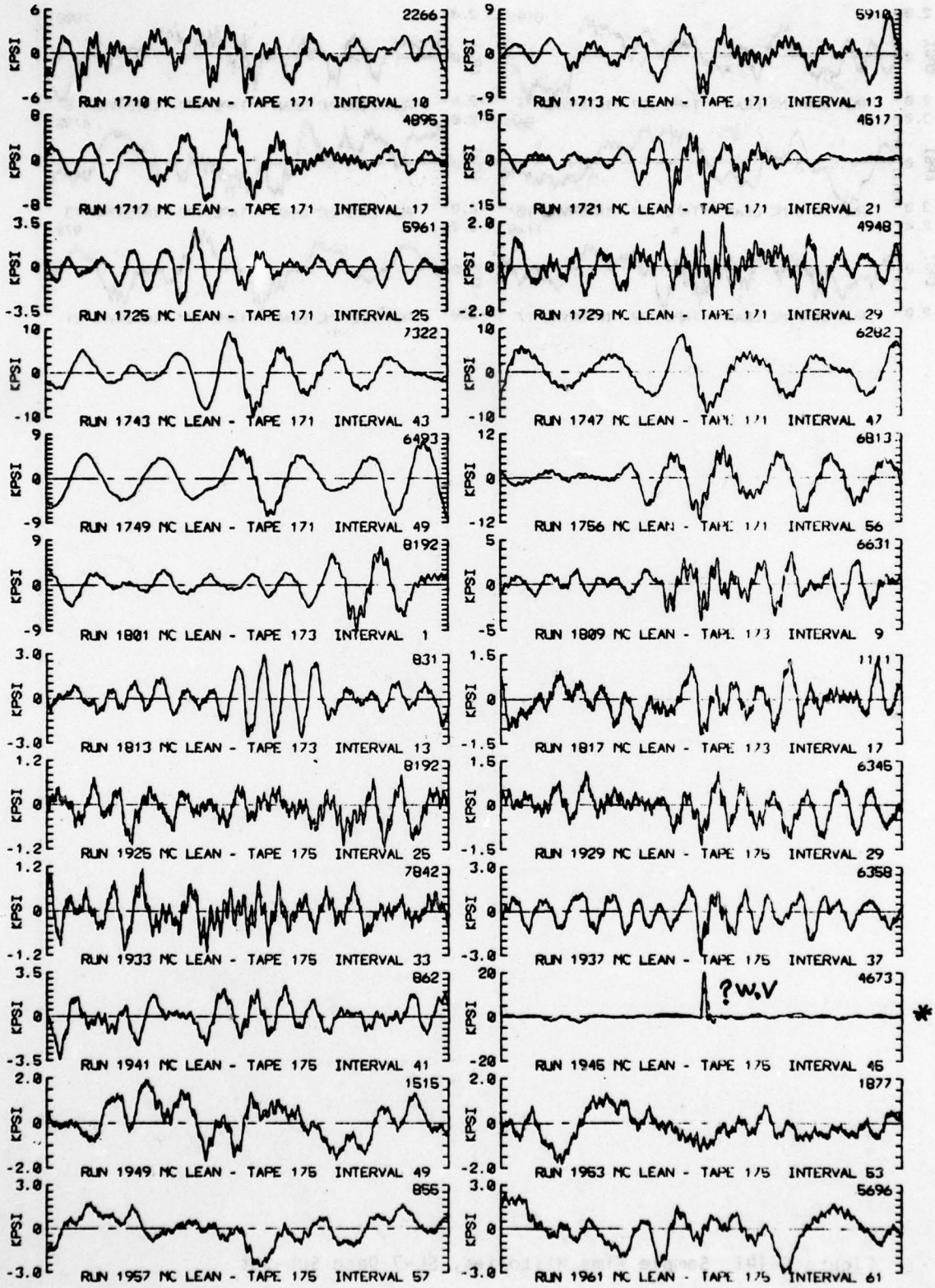

Figure C-14h Sample Time Histories, SL-7 Data Sub-Set

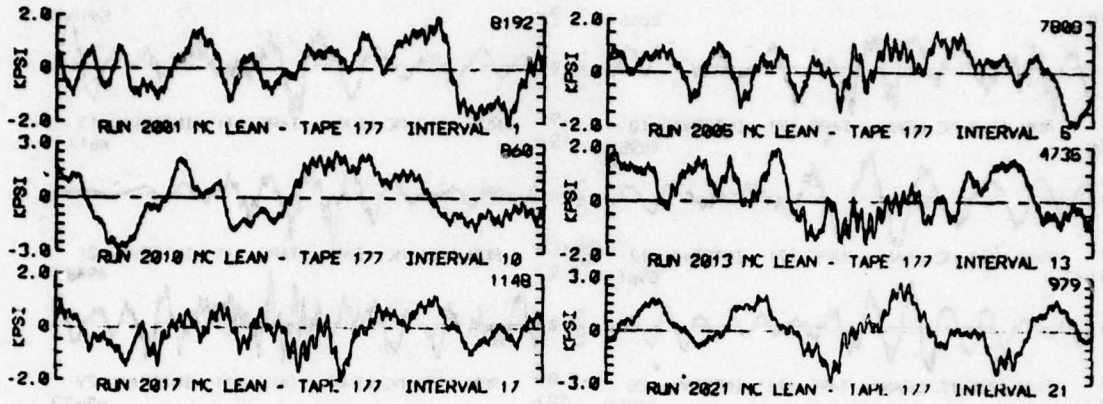

Figure C-14i Sample Time Histories, SL-7 Data Sub-Set

a question mark and the letters "V" for "questionable vibration response" and/or "W" for "questionable wave-induced response". Runs 141, 653, 905, 1125 and 1137 are questioned on the grounds that the maximum "vibration" cannot be believed as representing something which actually happened aboard ship. Sudden pulses without subsequent vibratory decay are considered to be stray electronic transients introduced somewhere in the necessarily large amount of analog data processing. In Run 1945 (Figure C-14h) something has saturated badly and the result is a questionable record for analyses of both the maximum vibration and the wave-induced component. In subsequent analyses, Run 1945 was omitted from all consideration and the five runs noted were omitted when considering vibration. The SL-7 data sub-set on the whole appears relatively free of unbelievable data.

As far as superimposed vibrations are concerned there are many instances of more or less continuous low level vibration, but only one instance (Run 937, Figure C-14d) where the presence of "springing" could be argued. When the vibration is large, it appears to be impact induced with the subsequent "whipping" decay. In quite a number of cases, the inception of vibration appears to be nearer to the time of maximum wave-induced compression (sagging) than the time of wave-induced tension (hogging). This is in some contrast to the result for the slower speed cargo ship of Ref.1 where it was indicated that inception of vibration always occurred near the time of maximum wave-induced tension. Given that the SL-7 is generally of the size and nearly of the speed of an aircraft carrier, the "flare shock" mechanism noted in Ref.17 can be expected in addition to forward bottom slamming so that impact inception may also reasonably be expected near times of maximum compression (sagging).

With respect to the wave-induced (longer period) stresses there are a good number of cases where very long period and relatively short period components superimpose to form a short-term process which cannot possibly be considered narrow banded.

Turning attention to the FOTINI-L data sub-set, Figures C-15a through C-15g contain portions of the 168 digital stress time series in the set. With some minor exceptions, the plotting conventions are the same as those used for the SL-7 data sub-set. Because the records were taken from the Teledyne digital library tape, the basic time sampling interval is 0.1 sec so that the duration of the plotted time histroy is 51 seconds. The "Run number" was arbitrarily assigned at Davidson Laboratory, and the Teledyne analog tape identification, interval and index numbers are indicated for each record. As before, stresses are plotted relative to the sample mean, positive stress is deck tension (hogging). The FOTINI-L time series have 12000 points so that this number replaces "8192" in the discussion of conventions for Figure C-14. Questionable records are marked as previously described.

In the data set, there is a very large incidence of questionable "vibration" and a number of questionable wave-induced stress records. Out of the 168 records, 78 are marked questionable leaving 90 records. The vast majority of the questions involve isolated pulses or a train of pulses which often occur in the absence of first-mode vibration. These are not considered believable super-

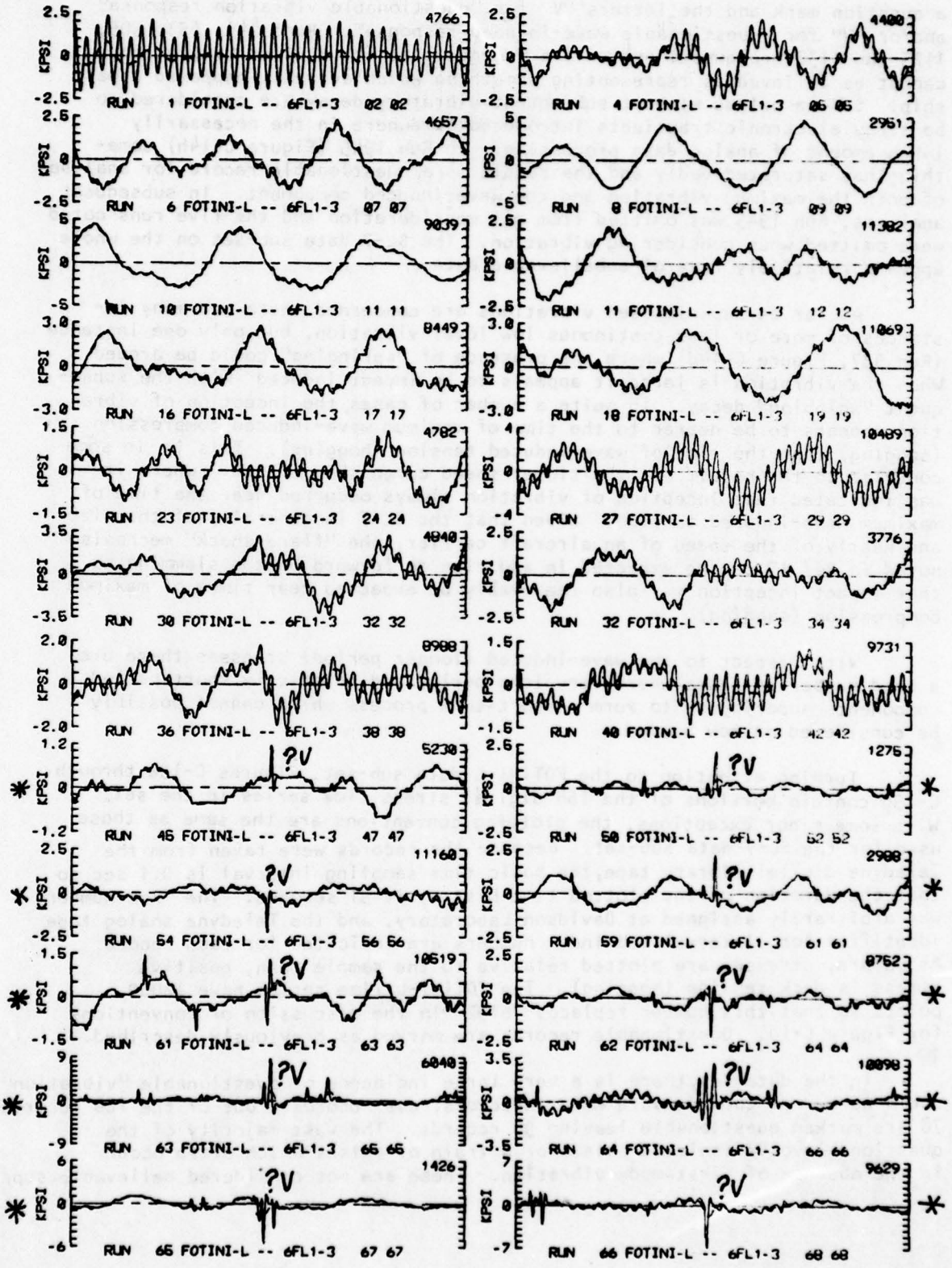

Figure C-15a Sample Time Histories, FOTINI-L Data Sub-Set

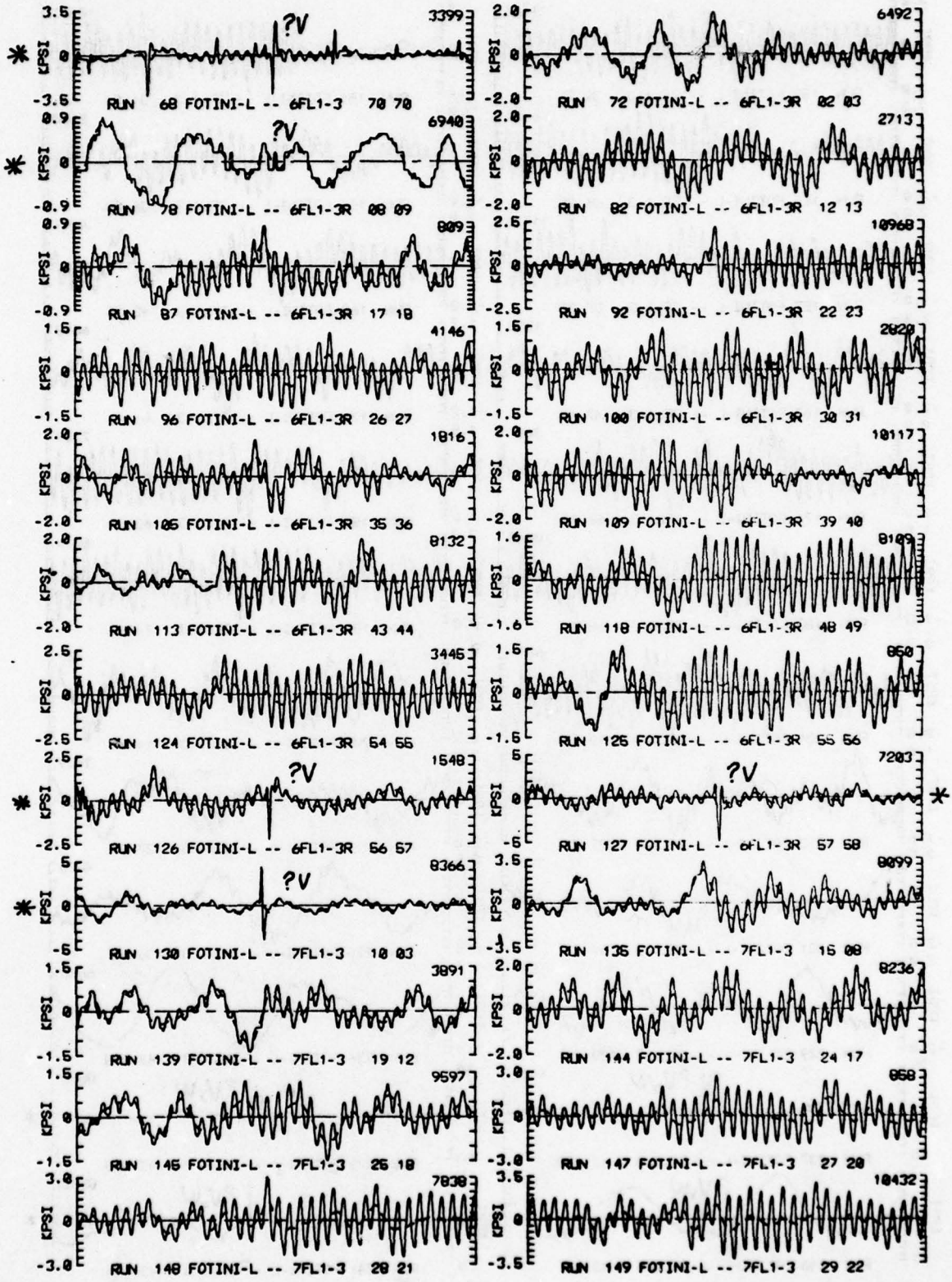

Figure C-15 Sample Time Histories, FOTINI-L Data Sub-Set

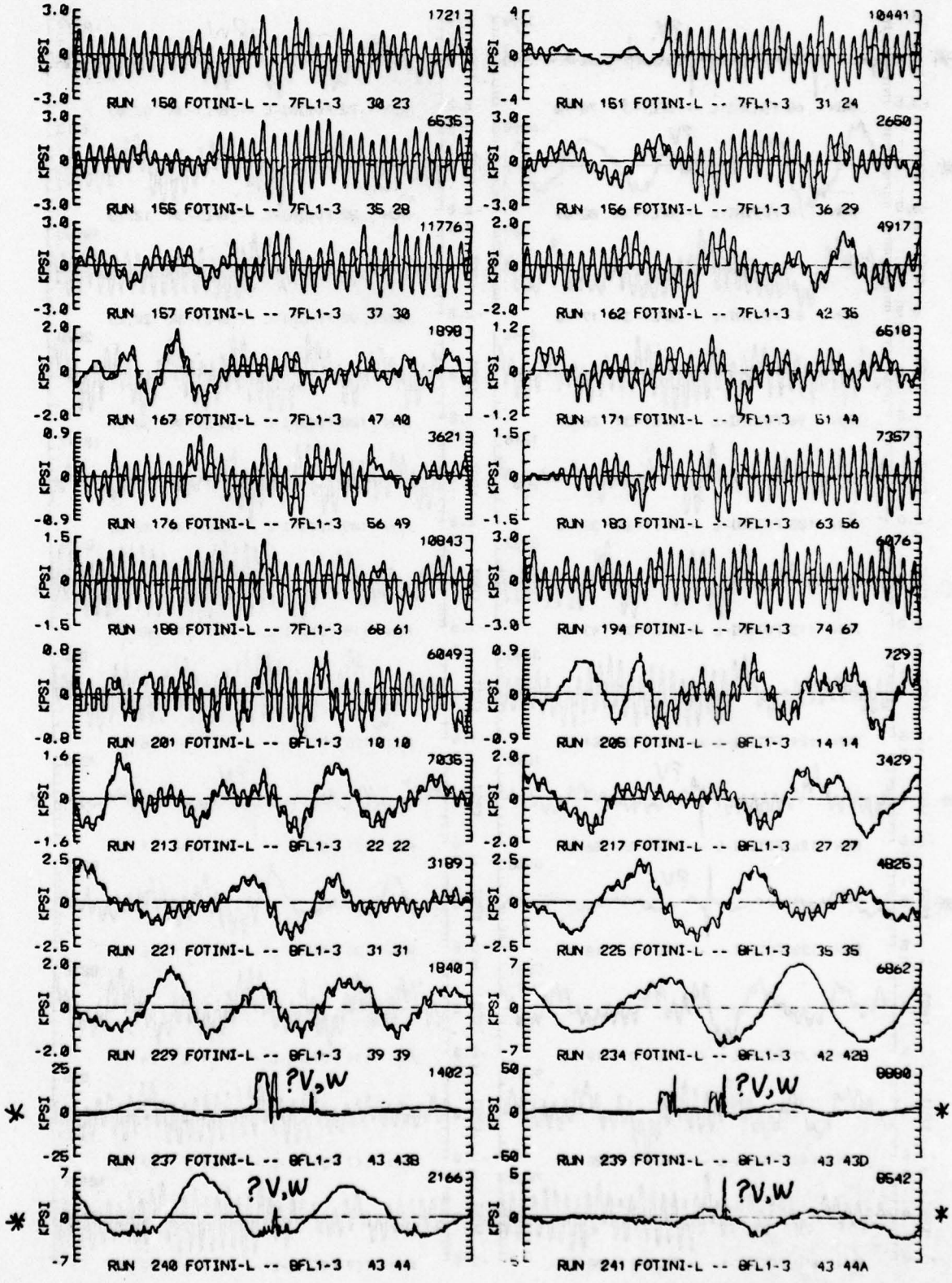

Figure C-15C Sample Time Histories, FOTINI-L Data Sub-Set

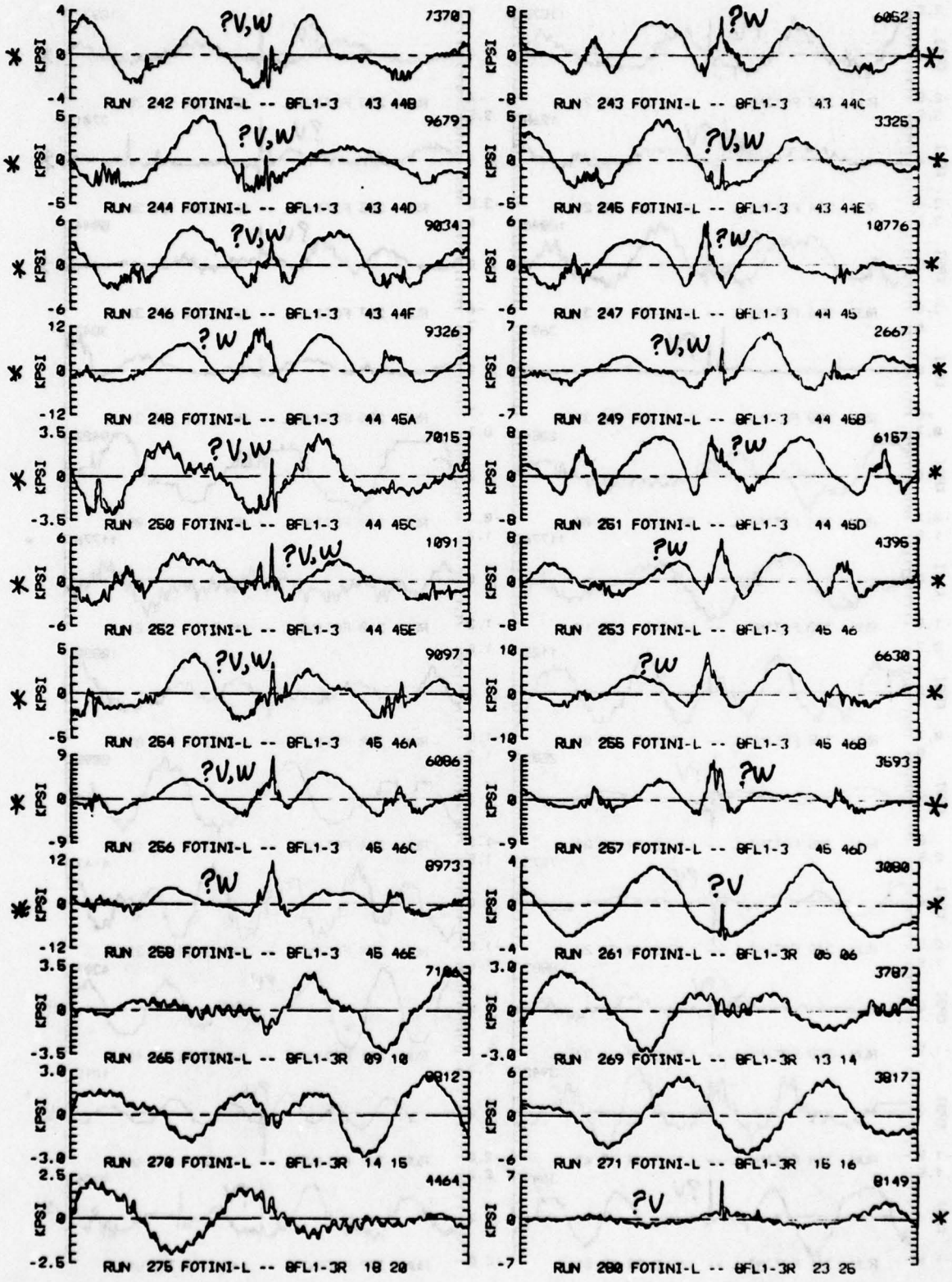

Figure C-15d Sample Time Histories, FOTINI-L Data Sub-Set

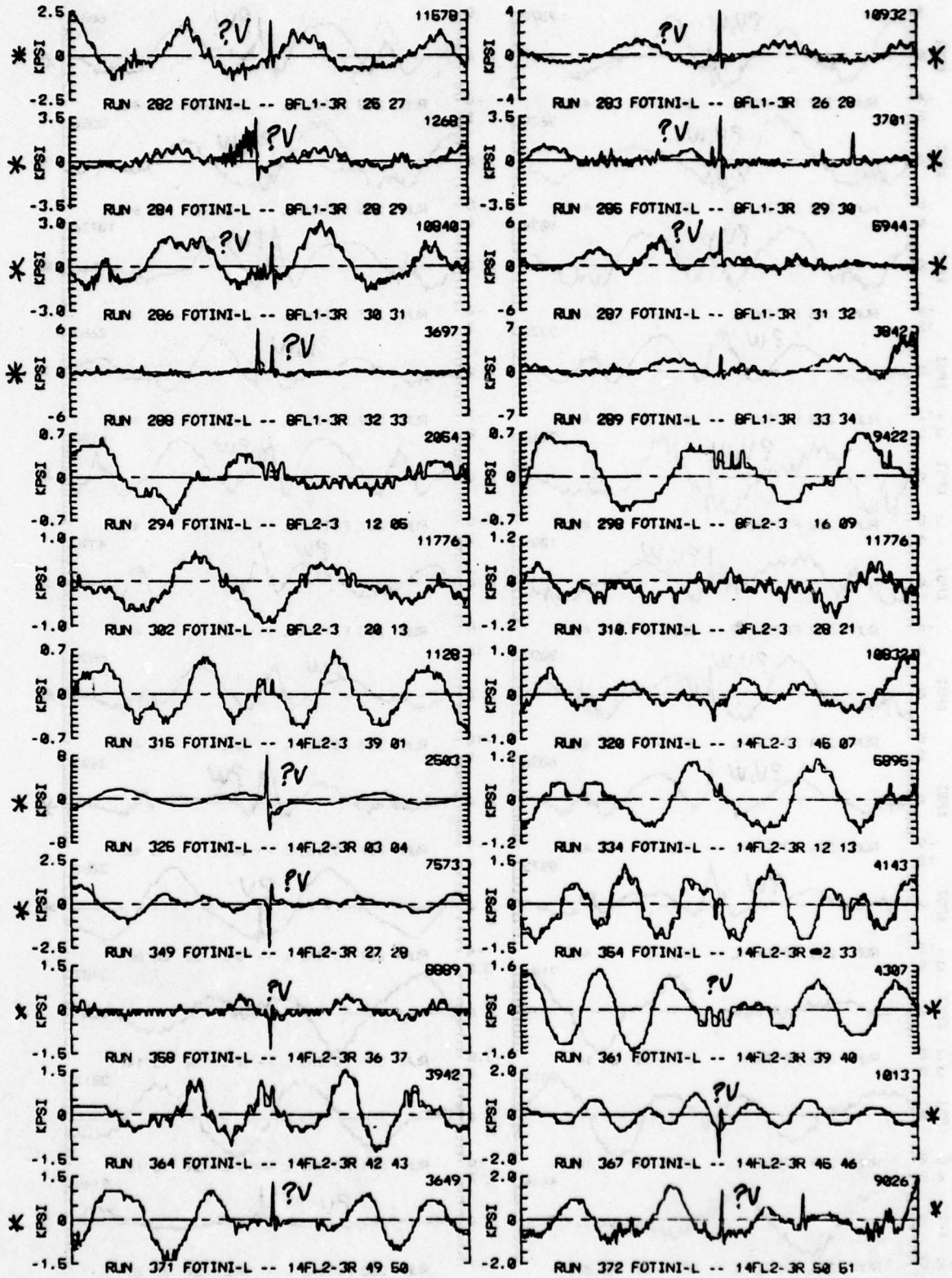

Figure C-15e Sample Time Histories, FOTINI-L Data Sub-Set

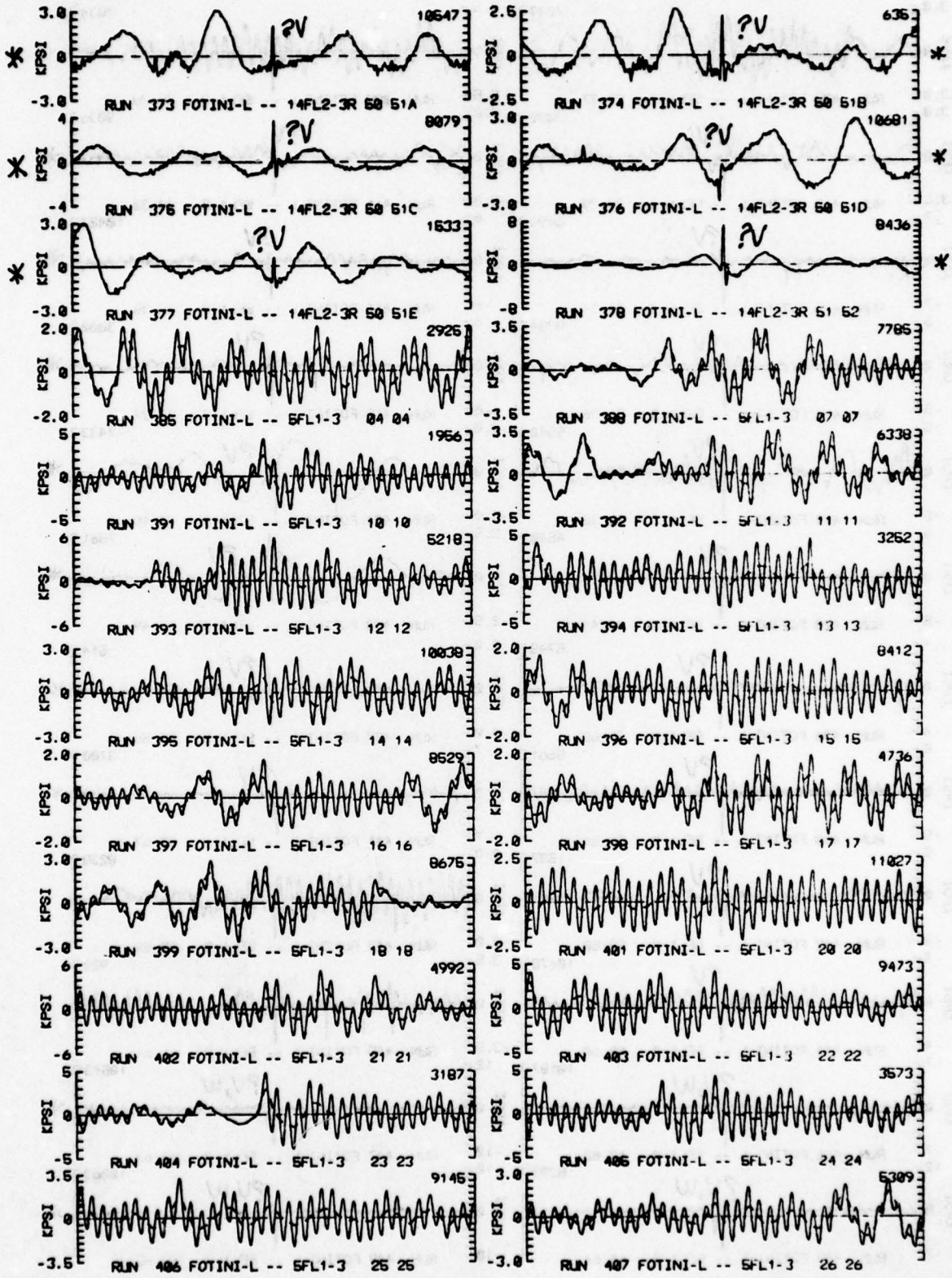

Figure C-15f Sample Time Histories, FOTINI-L Data Sub-Set

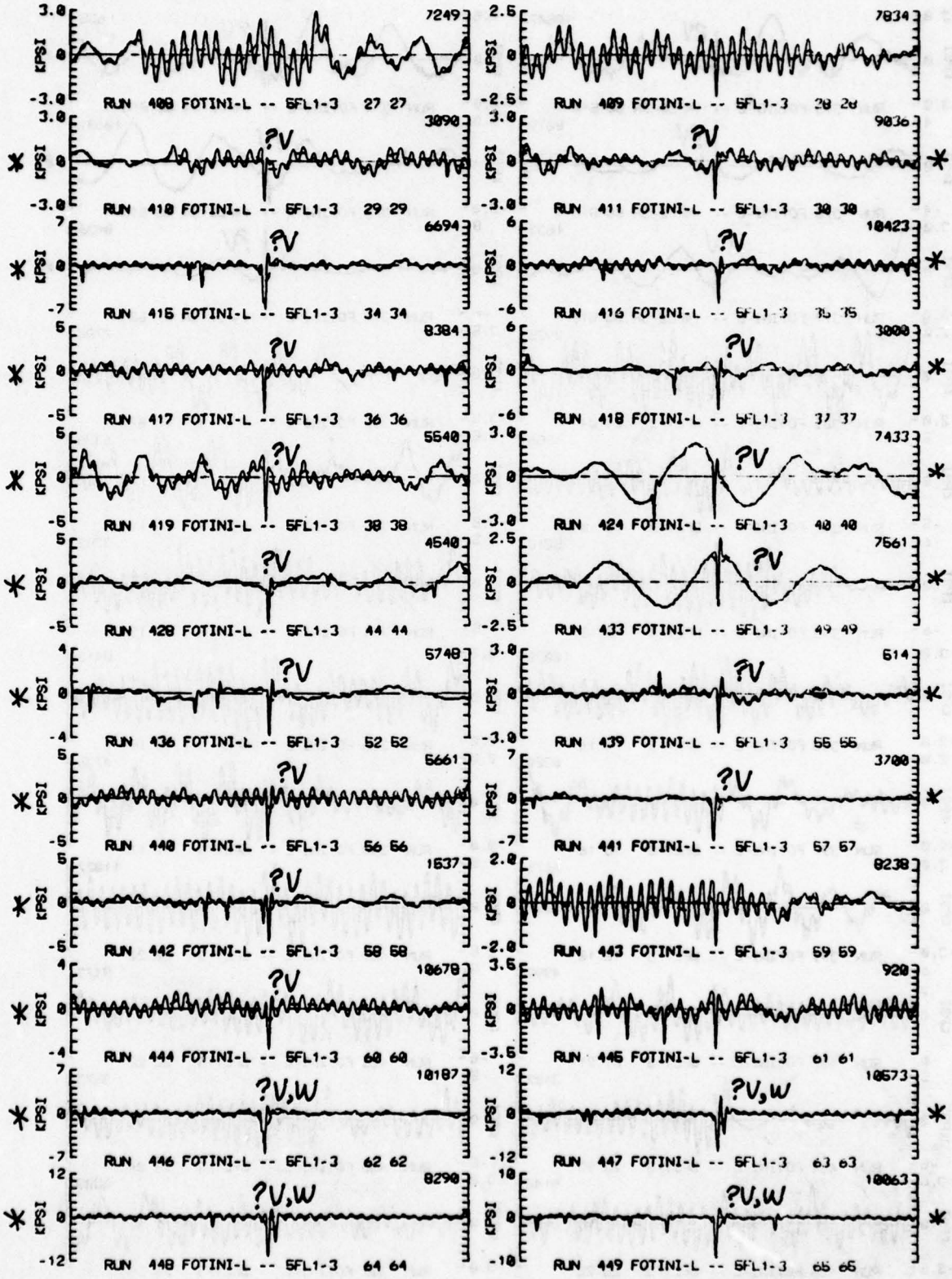

Figure C-15g Sample Time Histories, FOTINI-L Data Sub-Set

posed vibration. In a few cases, the pulse was of sufficient duration that the filter partially followed it-- thus introducing a spurious "wave-induced" extreme. One such extreme is noted in Run 237, Figure 15C. In this case, a saturation existed for sufficient time to make the filtered signal indicate a 27 Kpsi "wave-induced" double amplitude. This, the highest "wave-induced" double amplitude in the entire data base, agrees reasonably with the determination by Teledyne, but is almost certainly false. The records following Run 237 are qualitatively similar. Some further investigation disclosed that the mean stress (corresonding to zero in the plot) was approximately 18 Kpsi compression apparently due to ballast changes. According to descriptions of the instrumentation, Ref. 7, it would appear that the mean-stress signal was at or beyond the nominal distortion free range of the analog magnetic-tape unit. This means that further compression could easily cause the erratic behavior characteristic of magnetic-tape recorders driven into hard saturation. It also means that the signals were probably in the range where the tape recorder calibration was highly non-linear. The assymetry of records 240 through 258 is consistent with this hypothesis. According to the listings of the basic Teledyne data-reduction process, serious tape saturation could be expected for nearly all of tape 8FLi-3 and on this basis the wave-induced part of records 237 through 258 is questioned.

Considering those records with no questions, there are few instances in which vibration appears to be suddenly initiated, and of these, virtually none where the vibration decays rapidly. In most cases where the vibratory stress is appreciable, the records have the appearance of "springing" response. Though there is some evidence of broad-band wave-induced response in the records, none are comparable to the extreme examples of such response in the case of the SL-7 (Figure C-14).

APPENDIX C-4

ANALYSIS OF THE STATISTICS OF SHORT-TERM WAVE-INDUCED STRESS DATA

Introduction

There were two basic reasons for embarking upon an examination of the statistics of the short- term wave-induced stress data contained in the FOTINI-L and SL-7 data subsets. The first is that the state-of-art procedure for prediction of long-term stress distributions (Ref.1) depends to a great extent upon general assumptions about the statistics of the short-term response. These general assumptions follow directly from the basic linear narrow-band random process model, and have been extensively checked in the cases of the relatively small general cargo ships which were studied in Ref.1. In the present case, both ships are significantly larger, and the SL-7 is of course significantly faster.

The second reason was in relation to the analysis of the superimposed vibratory response. It was considered unlikely that the short-term statistics of the increase in stress due to vibration could be rationalized without some assurance that the wave-induced components were understood.

Statistical Symmetry: Comparisons of Hogging and Sagging Stresses

One of the consequences of the linear random or "linear superposition" model is that the predicted wave-induced loads and resulting stresses must be statistically symmetrical; that is, the magnitude of wave-induced peak compressive (sagging) stresses are assumed to be the same as the magnitude of the tensile (hogging) stresses. A simple first analysis is to compare the maximum values of tension and compression observed in each record.

In none of the available records was the actual mean stress level known. Accordingly, the filtered (wave-induced) stress records were corrected to zero record mean. Using this sample as a reference, the maximum "wave-induced" tension and the maximum compression were found from each record. The resulting values are shown plotted against one another in Figure C-16 for the SL-7 and in Figure C-17 for the FOTINI-L for all the records not questioned in Appendix C-3. The dashed line at 45° is the expected relation. Two things might be noted. The maximum tension and compression are not necessarily found in the same encounter cycle. The maximum value in a sample scatter is to be expected.

Considering Figure C-16 for the SL-7, the maximum compressive wave-induced stress in a 20-minute record can be less than or as much as twice the maximum tensile stress. The average ratio of maximum compressive (sagging) stress to maximum tensile (hogging) stress is in the vicinity of 1.2. This is in the direction typically expected but not so large as is implied (for instance) by the DetNorske Veritas Rules where the ratio for the SL-7 block coefficient works out to be nearly 2.

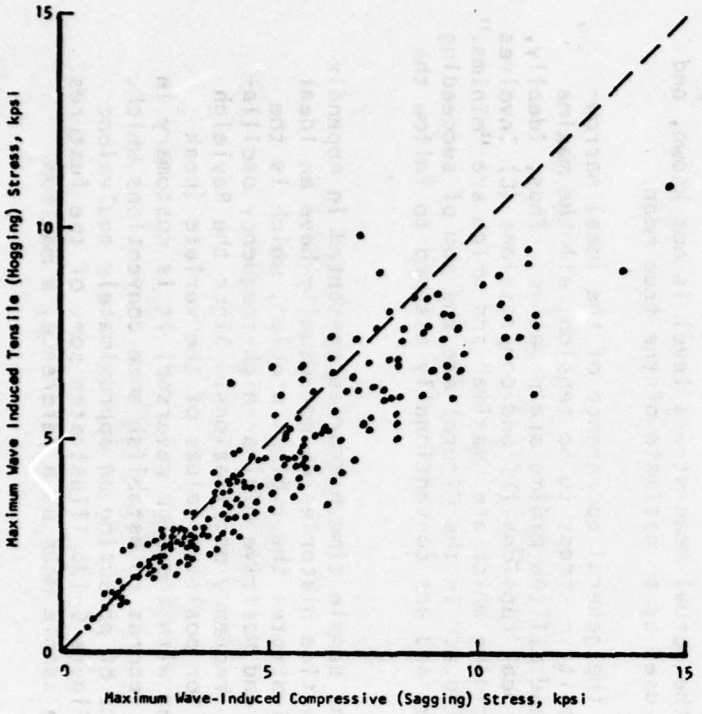

FIG. C-16 - COMPARISON OF MAXIMUM SHORT-TERM WAVE-INDUCED HOGGING AND SAGGING STRESSES: SL-7

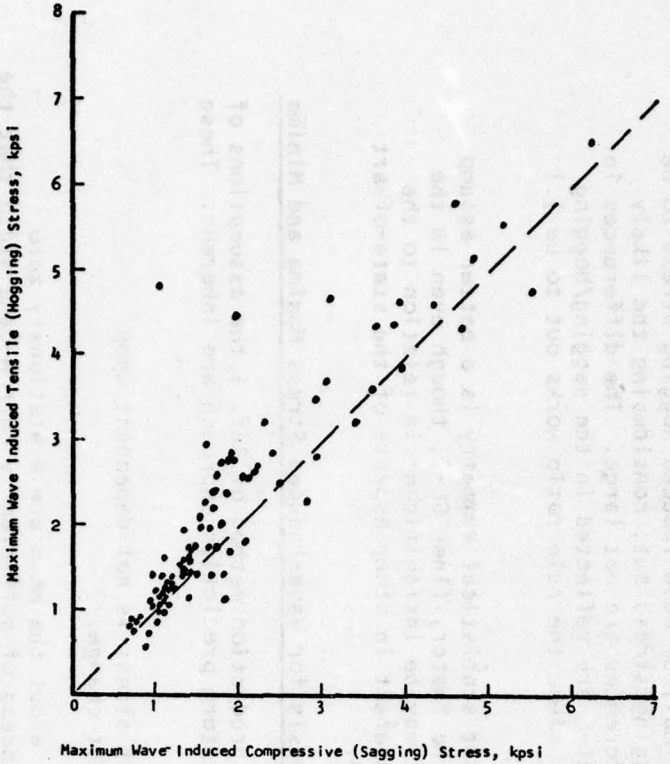

FIG. C-17 - COMPARISON OF MAXIMUM SHORT-TERM WAVE-INDUCED HOGGING AND SAGGING STRESSES: FOTINI-L

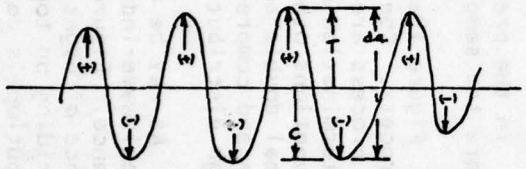

FIG. C-18a - MAXIMA AND MINIMA OF THE IDEAL NARROW-BAND PROCESS

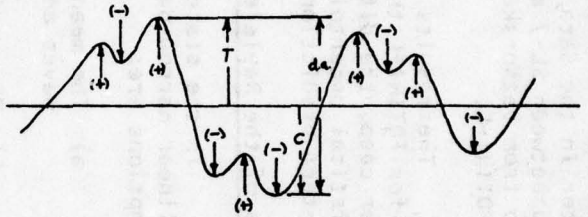

FIG. C-18b - MAXIMA AND MINIMA OF TYPICAL RECORDS

A somewhat different situation is found for FOTINI-L, Figure C-17. There appears a tendency for maximum wave-induced hogging stress to be larger than wave-induced sagging stress but, considering the likely scatter in the data, the differences are not large. The differences in trend between SL-7 and FOTINI-L are reflected in the sagging/hogging ratio from DetNorske Veritas, since the rule ratio works out to be 1.1 for FOTINI-L.

The results imply that statistical symmetry is a better assumption for FOTINI-L than for the faster, finer SL-7, though even in the latter case, the differences may be insignificant in relation to the statistical uncertainties inherent in other aspects of the state-of-art long-term prediction methods.

Tests of the Rayleigh Hypothesis for Wave-Induced Stress Maxima and Minima

In the state-of-art prediction method of Ref. 1, the assumptions of the linear narrow-band short-term prediction approach are inherent. These assumptions are:

a) The mean value of stress is not dependent upon waves and does not change.

b) The oscillations about the mean are a stationary zero mean Gaussian process of sufficiently narrow-band width that the maxima and minima follow the Rayleigh distribution, and are statistically symmetrical.

In the present case the actual mean-stress level is not known, and therefore the sample mean is used as an estimate of the true mean.

Figure 18a indicates the general appearance of the ideal narrow-band process. Considering positive stress to be tension, all the maxima of the process are positive and all the minima are negative. Thus, ideally, the determination of all the peak tensions (T) and compressions (C) involves no conventions other than deciding which are "maxima" and which are "minima." The ideal double amplitudes ("d.a." in the Figure) are the sum of succeeding tension and compression peaks, and are conventionally assumed to follow the Rayleigh distribution also.

As may be noted in the sample time histories presented in Appendix C-3, real wave-induced stress time histories do not usually have an ideal appearance. Figure C-18b illustrates the typical problem, which is the existance of negative maxima and positive minima--high-frequency oscillations riding on top of lower frequency oscillations. Since the Rayleigh distribution is defined only for positive values of the variate (peak tensions, or peak compressions with the sign reversed) it is customary in the interpretation of actual records to establish some conventions which, it is thought, have the effect of producing an approximately equivalent ideal narrow-band process. Figure C-18b illustrates some of the features of this procedure. Using the sample mean as a reference, a maximum

(tension) is defined as the largest filtered (wave-induced) stress digitized during a positive stress excursion, and a minimum (compression) as the smallest stress during a negative stress excursion. Thus the existence of "maxima" and "minima" depend upon zero crossings. Negative maxima and secondary positive maxima are ignored. What is being defined by this procedure is the "main extreme" in an excursion. The double amplitude (defined as "d.a.") in the Figure is thus the sum of the main positive and the main negative extremes in an excursion. These conventions are basically those used in the available reduction of data for the entire data bases, Ref. 16.

These conventions were followed in developing data for a further check on the short - term (wave-induced) stress statistics of the FOTINI-L and SL-7 data sub-sets. The filtered (wave - induced) digital stress records were processed to the end that, for each record, there was available:

a) The number of filtered stress excursions from tension to compression which were contained in the record.

b) An array of the wave-induced main extremes in tension in each record, in the order found.

c) A corresponding array for main extremes in compression.

It was the intention to use various "goodness-of-fit" techniques to test the conformity of these samples with the Rayleigh hypothesis. Some details of the testing procedures used are given in Appendix C-5. The first operation was to perform run tests on all the basic arrays of maxima and minima. The result of these tests for each record was a parameter "j" such that if every jth extreme was considered, the resulting decimated sample would pass the run test at the 95% level of confidence. For reasons outlined in Appendix C-5, only the decimated samples were used in subsequent testing.

Noting that the most often used measure of magnitude of oscillatory wave-induced stresses is the double amplitude, samples of wave-induced double amplitude were formed by adding algebraically the adjacent main extremes in tension and compression. (As previously noted the maxima and minima found in the data reduction were stored in the order found in order to allow this operation). It was found that the level of sequential correlation of the double amplitudes according to the run test was very nearly the same as that for the main extremes in tension or compression.

For these purposes the Rayleigh probability density was represented as:

$$p(\eta) = \eta \; E \; x \; p \; (- \eta^2/2)$$

Where:

η = Reduced variate = X/R

X = the dimensional variate (tensile or compressive main excursions)

R = the distribution parameter.

In fitting the distribution to the sample, the distribution parameter was estimated by the maximum likelihood approach. In the present case the fitted parameter, R, is the root mean square of the sample points divided by $\sqrt{2}$. The distribution parameter for the Rayleigh distribution may also be estimated as equal to process root-mean-square (the root mean square of the entire record, an operation involving the entire sample time history).

In carrying out the various tests on the short-term data samples, there were thus generated two new estimates of the process root-mean-square; one from the main tension extreme data, and one from the compression data. These estimates were considered much more stable statistics with which to check statistical symmetry. Accordingly, the pairs of estimates resulting from each record were plotted in the same way as had been done for the maxima of each record (Figures C-16 and C-17). The results are shown in Figure C-19 for the SL-7 and Figure C-20 for FOTINI-L. In the case of FOTINI-L, all records questioned in Appendix C-3 were disregarded. Only the single SL-7 record where wave-induced stresses were questioned was disregarded.

As might be expected, the scatter in Figures C-19 and C-20 is much reduced relative to that in Figures C-16 and C-17. Figure C-19 implies that the wave-induced sagging stresses for the SL-7 are, on average, much closer to being statistically symmetrical with the wave-induced hogging stresses-- a mean line through the scatter implies a 6% rather than a 20% difference. In the case of the FOTINI-L, Figure C-20, the symmetry appears to be very close. With respect to the state-of-art short-term linear-random process approach, the only thing estimated is the "process" rms and it has to be assumed that the distribution of short-term maxima

is the same as that for short-term minima. Though the data implies that the symmetry is not exact, the results in Figures C-19 and C-20 indicate that the symmetry assumption is very much within engineering reason for the average magnitude of stress if not for the extremes.

Because it seemed probable that the statistics of short-term stresses had not previously been examined for ships of the size and speed of the SL-7, the initial concentration of effort and development of techniques was upon the wave-induced data for this ship. The first series of tests were upon the decimated samples of double amplitudes which could be formed from the 197 records in the SL-7 sub-set for which no questions about wave-induced stress response could be raised in Appendix C-3. Both the tests on sample

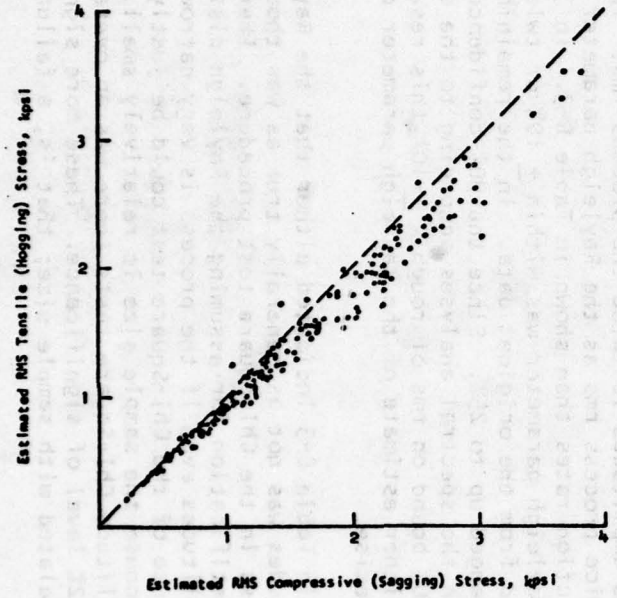

FIG. C-19 - COMPARISON OF SHORT-TERM PROCESS RMS HOGGING AND SAGGING STRESSES ESTIMATED FROM THE MAIN EXTREMES IN THE SL-7 STRESS RECORDS

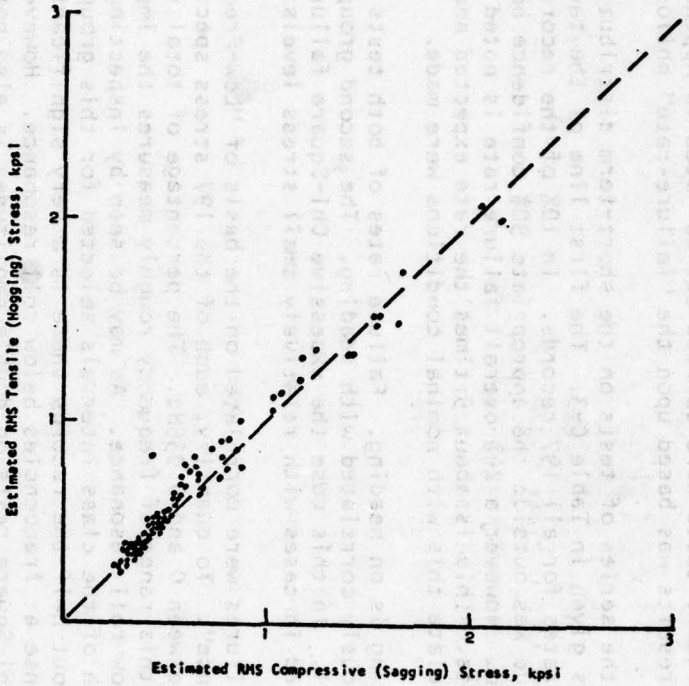

FIG. C-20 - COMPARISON OF SHORT-TERM PROCESS RMS HOGGING AND SAGGING STRESSES ESTIMATED FROM THE MAIN EXTREMES IN THE FOTINI-L STRESS RECORDS

extremes and the Chi-Square tests were carried out as noted in Appendix C-5, and evaluation of the results was based upon the "failure-rate" philosophy.

The results of the series of tests on the short-term distributions of double amplitudes is given in Table C-3. The first line of the table indicates the failure rates for all 197 records. In 10% of the records, the maximum sample value was outside the appropriate 90% confidence bounds as would be anticipated. However, a 24% overall failure rate is noted for the Chi-Square tests. This is about 5 times the rate expected and three attempts to correlate this with nominal conditions were made.

The first grouping is on heading. Failure rates of both tests do not seem to be obviously correlated with heading. The second grouping was on rms stress level. In this case the excessive Chi-Square failure rate seems to be concentrated in cases with relatively small stress levels.

Finally, the failures were correlated on the basis of "Low-Frequency Contributions to Variance". To quantify, each of the 197 stress spectra was partially integrated between 0 and 0.035Hz. The percentage of total variance originating from this range of frequency roughly measures the importance of stress response below roll resonance. As may be seen by inspecting the number of tests in each of the class intervals selected for this grouping of failure rate, in about half the records there is a very significant amount of stress response at frequencies below roll resonance. However, the failure rate for the Chi-Square tests on double amplitudes is also not obviously explained by this correlation.

According to the usual approximation, the parameter of the Rayleigh distribution for double amplitudes is twice the process rms. The same tests were run with twice process rms as the Rayleigh parameter and the result was higher rejection rates than shown in Table C-3. In 75% of the intervals, the fitted Rayleigh parameter was within $\pm$ 10% of twice the process rms as computed from the original data. In the remaining 25% of cases, the difference ranged up to 25%. Since the 90% confidence bound on variance as computed in the spectral analyses according to the spectral band width implies a 90% bound on rms of roughly $\pm$ 10%, this result was not too surprising; neither estimate of the Rayleigh parameter can be taken as being very precise.

The results in Table C-3 indicated either that the Rayleigh assumption for double amplitudes was not as generally true as was thought, or that something was amiss in the Chi-Square test procedure. There is no strict mathematical justification for assuming the Rayleigh distribution of apparent double amplitudes even if the process is very narrow banded. On the other hand the use of the Chi-Square test could be justly criticized in this application because the sample size is relatively small. In the case of the double-amplitude Chi-Square tests there was an overall rate of failure of 15% at the 2% level of significance. These more significant failures were not correlated with sample size; that is, a failure at the

Table C-3

Summary of Tests for Fit to the Rayleigh Distribution of Wave-Induced Stress Double Amplitudes Found in the SL-7 Data Sub-Set.

Grouping	No. of Tests	Failure Rate on Maximum Value (10% Expected)	Failure Rate on Chi-Square Tests (5% Expected)
All Records	197	10%	24%
Nominal Head Seas	32	12%	22%
Bow Seas	62	10%	27%
Beam Seas	22	18%	27%
Qtr. Seas	54	6%	20%
Follow. Seas	27	10%	22%
Rms Stress < 1.0	59	10%	44%
1.0 < 2.0	81	10%	13%
> 2.0	57	10%	6%
Low-Frequency Contribution to Variance			
Less than 4%	67	16%	20%
4 to 9%	14	0	42%
9 to 16%	10	0	30%
16 to 25%	7	0	15%
over 25%	99	9%	23%

2% or lower level of significance was as apt to occur with a 100 point sample as with a 50 point sample.

The maxima and minima of stress (main excursions) are more to the point for structural purposes. Also, there is less lack of justification mathematically for assuming the Rayleigh distribution. Accordingly, the tests on the extreme sample value, the Chi-Square tests, and the Kolmogorov-Smirnov tests were run on both the main extremes in tension and those in compression. The distribution parameter for the tests on extreme sample value and the Chi-Square test was fitted to the data. The distribution parameter for the Kolmogorov-Smirnov test was the process rms as computed from the filtered time series. The results of these tests are shown in Tables C-4 and C-5.

As far as the test on sample extremes is concerned, the failure rate for tension (Table C-4) appears about as expected and in line with that for double amplitudes. The failure rate for compression (Table C-5) is about twice that expected, with no consistent indication of correlation with heading, stress or portion of low-frequency variance.

The overall rates of failure of the Chi-Square tests shown in Table C-4 and C-5 are much higher than the rate for double amplitudes (Table C-3). Correlation of failure rate with heading is as inconclusive as with the double amplitudes. The apparent correlation with stress level noted for double amplitudes is not borne out. However, something approaching significance appears in the correlation with the portion of low-frequency variance. In effect, it appears that 60% of all the cases, in which low-frequencies contribute more than 25% to variance, failed.

Since on average the cases in which 25% or more of variance is attributable to low-frequencies are also the cases with the smallest sample size, the Kolmogorov-Smirnov tests were also correlated on this basis. The advantage of the Kolgomorov-Smirnov tests is that it is considered more applicable to small samples if the distribution parameter is known. The parameter (process rms) is estimated to within ± 10%, and the results shown in the tables were produced with the process rms as the distribution parameter. As may be noted, the failure rates for the Kolmogorov-Smirnov tests confirm the failure rates for the Chi-Square tests very closely.

Some perturbations of the Kolmogorov-Smirnov tests were also made. The tests were run with the distribution parameter fitted to the data as had been done for the Chi-Square tests. In this case, the failure rates were even closer to those for the Chi-Square tests, and there were relatively few cases where the two tests did not agree at the 5% level of significance. The next perturbation of the Kolmogorov-Smirnov test was to test with distribution parameters 90% and 110% of the process rms. In 21 cases, the result of one perturbation or the other increased the level of significance of the result to above 5%. However, in only 5 cases (2-1/2% of the total) did this fail to agree with the Kolmogorov-Smirnov test results where the distribution parameter was fitted to the data.

TABLE C-4

Summary of Tests for Fit to the Rayleigh Distribution of Wave-Induced Main Extremes in Tensile (Hogging) Stress Found in the SL-7 Data Sub-Set

Grouping	No. of Tests	Failure Rate on Maximum Value (10% Expected)	Failure Rate on Chi-Square Test (5% Expected	Failure Rate on Kolmogorov-Smirnov Test (5% Expected)
All Records	197	10%	34%	38%
Nominal Head Seas	32	6%	6%	Not Evaluated
Bow Seas	62	8%	29%	
Beam Seas	22	10%	36%	
Qtr. Seas	54	13%	56%	
Follow. Seas	27	10%	37%	
Rms Stress < 1.0	59	8%	27%	
1.0 < 2.0	81	13%	45%	
> 2.0	57	7%	28%	
Low-Frequency Contribution to Variance				
Less than 4%	67	7%	9%	7%
4 to 9%	14	0%	7%	0%
9 to 16%	10	10%	20%	20%
16 to 25%	7	0%	16%	43%
over 25%	99	13%	59%	66%

TABLE C-5

Summary of Tests for Fit to the Rayleigh Distribution of Wave-Induced Main Extremes in Compressive (Sagging) Stress Found in the SL-7 Data Sub-Set

Grouping	No. of Tests	Failure Rate on Maximum Value (10% Expected)	Failure Rate on Chi-Square Test (5% Expected)	Failure Rate on Kolmogorov-Smirnov Test (5% Expected)
All Records	197	25%	39%	37%
Nominal Head Seas	32	30%	25%	Not Evaluated
Bow Seas	62	29%	26%	
Beam Seas	22	14%	64%	
Qtr. Seas	54	30%	54%	
Follow. Seas	27	10%	33%	
Rms Stress < 1.0	59	6%	29%	
1.0 to < 2.0	81	30%	47%	
> 2.0	57	30%	39%	
Low-Frequency Contribution to Variance				
Less than 4%	67	31%	18%	7%
4 to 9%	14	21%	14%	0%
9 to 16%	10	10%	20%	10%
16 to 25%	7	10%	40%	14%
over 25%	99	24%	60%	60%

Of most significance with respect to the results of both Chi-Square and Kolmogorov-Smirnov tests is that, in each case, in about 25% of all the sets of data, the goodness-of-fit tests were failed at less than a 2% level of significance. Interpreting the Kolmogorov-Smirnov tests in the most liberal way, the perturbation on the distribution parameter would not decrease the percentage of very significant failures to less than 15%. In at least 15% of all intervals either goodness-of-fit test failed very badly.

A final correlation of failure rates was attempted by examining the test results for the 11 records where ship speed was less than 15 knots. In this case, all the Chi-Square tests on main extremes in tension were passed at 10% or higher levels of significance, and in only one case was the Kolmogorov-Smirnov test failed at the 5% level. Similarly, all the Kolmogorov-Smirnov tests on the main extremes in compression were passed at 10% or higher levels of significance, three out of the 11 Chi-Square tests were failed at the 5% level. Had the 11 low ship speed records been the only ones available, there would have been little hesitation in accepting the general Rayleigh hypothesis. It is apparent from the documentation (ref 27) of the data sub-set that the SL-7 slowed down to less than 15 knots only when the sea conditions were extraordinarily severe and, under these circumstances, the ship heading was altered, if necessary, to the head or bow-sea case.

With respect to the SL-7 data, the above evidence appeared to cast considerable doubt on the general Rayleigh assumption. Failure rates, approaching 8 times that expected, seemed quite significant. The correlations carried out suggested that the large incidence of mathematically broad-band stress response was at the root of the problem. A high incidence of exceptionally broad-band response may be expected for a 30-knot ship which spends half its sea time in quartering or following waves.

Given the above results for the SL-7, it was of interest to use the same procedures on the 90 good records available for the FOTINI-L. Since the FOTINI-L is a much slower ship, and since a much smaller incidence of ultra broad-band response was noted in the records, it was expected that a much lower failure rate would be experienced if the problems with the SL-7 data had been correctly diagnosed.

All the same procedures as noted above for SL-7 were applied to the FOTINI-L data. Table C-6 summarizes the failure analysis for both Chi-Square and Kolmogorov-Smirnov tests as applied to main extremes in tension, main extremes in compression, and to "double amplitudes" as defined in Figure C-18. In all cases, the expected failure rate was 5%. In the table the Chi-Square test is abbreviated "X^2 test" and the Kolmogorov-Smirnov test is abbreviated "K-S Test".

Considering the results in Table C-6, the overall failure rates for maximum tensions and compressions are higher than would be desirable for unconditional acceptance of the Rayleigh hypothesis but much lower than

TABLE C-6

Summary of Tests for Fit to the Rayleigh Distribution of Wave-Induced Stress Maxima and Minima Found in the FOTINI-L Data Sub-set (Expected Failure Rate 5% in All Cases)

Grouping	No. Tests	Maximum Tensions Failure Rate (%) On X^2 Test	Maximum Tensions Failure Rate (%) On K-S Test	Maximum Compressions Failure Rate (%) On X^2 Test	Maximum Compressions Failure Rate (%) On K-S Test	"Double Amplitudes" Failure Rate (%) On X^2 Test	"Double Amplitudes" Failure Rate (%) On K-S Test
All Good Records	90	20	13	20	14	34	31
Spectrum Shape:							
Very Narrow	33	10	10	12	6	15	3
Normal, Single Peak	41	24	10	22	17	54	47
Double Peak	13	18	18	23	31	54	54
Containing Very Low Frequency Energy	3	100	100	66	33	0	33
RMS Stress							
< .5	26	27	15	31	27	65	58
.5 <1.0	46	20	13	18	13	30	28
1.0 <	18	11	11	11	6	16	0

the corresponding rates for the SL- 7. The overall failure rate for double amplitudes is quite high--higher than would justify blanket acceptance of the Rayleigh hypothesis. Some auxiliary groupings of the failures were made and these illuminate the sources of the problem. One grouping was upon rms stress. There is a tendency for the Rayleigh hypothesis to fall down for low-stress levels.

Because the "low-frequency contribution" grouping used to correlate the SL-7 results was not considered an entirely successful gambit, an alternate classification of stress spectrum shape was made. The FOTINI-L stress spectra were classified by inspection into four qualitative groups:

a) "Normal, single peak"

These spectra were single peaked and were about as broad relative to modal frequency as are most published wave and response spectra.

b) "Very narrow"

Wave-induced spectral density concentrated in a very narrow band as would be the case for a swell spectrum.

c) "Double peak"

Two or more well defined peaks but no very low-frequency components.

d) "Containing very low-frequency energy"

Spectra with significant or at least some energy content near zero frequency.

Under this grouping the failure rates are better understood. The failure rate for very narrow spectra are near enough the expected value that the Rayleigh hypothesis would be accepted. Failure rates of records having broad spectra are higher and appear to be the main reason for the overall somewhat high failure rate. It is notable that even in the case of FOTINI-L the assumption that stress double amplitudes are Rayleigh distributed might well be used with care.

Tests of a More General Hypothesis For the Distribution of Wave-Induced Stress Maxima and Minima

With respect to state-of-art predictions of loads or stresses, the results of the tests just described had serious implications with respect to both the extrapolations of short-term predictions to long-term predictions and indirectly the validity of the linear-random short-term predicition method. The tests, of course, could not shed light upon what the short-term distribution was if it was Rayleigh, but the symptoms clearly indicated non-narrow bandedness to be at the root of the problem, and it appeared sufficient to

concentrate upon the SL-7 data where the worst of the problem appeared to be.

Clearly, the next step was to hypothesize that the stress maxima followed the theoretical distribution (Ref 35) for the maxima of a linear random Gaussian zero mean process of arbitrary band width. For present purposes the distribution will be called the "Cartwright-Longuet-Higgins distribution" or "CLH" distribution after the authors of Ref. 35. Under this hypothesis the probability density of the maxima of the process may be represented as:

$$p(\eta) = \left(\epsilon \operatorname{Exp}\left[-\eta^2/2\epsilon^2\right] + \sqrt{1-\epsilon^2}\,\eta \operatorname{Exp}\left[-\eta^2/2\right] \cdot \Phi\left(\eta\sqrt{(1-\epsilon^2)/\epsilon^2}\right)\right)/\sqrt{2\pi}$$

where:

η = normalized variate

$= Xi/\sigma$

Xi = the maxima of the process

σ = process rms or square root of variance

ϵ = spectrum broadness parameter

$$\Phi(a) = \int_{-\infty}^{a} \operatorname{Exp}\left[-t^2/2\right]dt$$

The maxima and minima of the non-narrow-band process are also theoretically statistically symmetric so that if the minima are denoted γ, the normalized variate becomes $\eta = -\gamma/\sigma$

When the broadness parameter approaches unity (zero) the CLH distribution approaches the normal (Rayleigh).

In making a fit of this distribution to a sample, two approaches are possible. The first involves knowledge of the stress spectra from which both of the distribution parameters required may, in principle, be computed. Computation of the broadness parameter from the spectrum is numerically troublesome however, and, in the tests to be described, the second alternate approach was utilized. In this approach the distribution parameters are fitted directly to the sample of maxima or minima as follows:
Given a sample of "N" maxima, Xi, (i= 1...N)

Form:

$$\bar{S}_2 = \frac{1}{N}\sum_{i=1}^{N} Xi^2$$

$$\bar{S}_1 = \frac{1}{N}\sum_{i=1}^{N} Xi$$

Then:

$$\hat{\sigma} = \text{fitted process RMS} = \sqrt{\bar{S}_2 - 2\,(\bar{S}_1)^2/\pi}$$

$$\rho = (S_1)^2/\bar{S}_2$$

$$\epsilon = \text{fitted broadness parameter} = \sqrt{1 - [2\rho/(\pi - 2\rho)]}$$

The procedures noted in Appendix C-5 which were used in making the various "goodness-of-fit" tests to the CLH distribution are no different in principle from those for the Rayleigh. There is more computation involved and it is necessary to allow for the extra fitted parameter in the degrees of freedom associated with the sample statistics.

There is a fundamental difference in checking the applicability of this distribution to the short-term stress data. It is that the sample must be composed differently. Referring to Figure C-18, all the maxima and minima must be found instead of just the main extreme, and no zero crossing convention is assumed. The process of finding all the maxima of the wave-induced records is more sensitive to minor components of vibration left after filtering than the process to find main extremes. Accordingly, in re-processing the SL-7 records the digital filter used in developing the main extremes was replaced by one which rejected almost 99% of the first-mode vibration instead of 96 1/2%. Apart from this, the end product of the process was quite similar to that which produced the

main extremes in that an array of the maxima (tension) and an array of minima (compression) in each record was obtained and stored in the order found. As expected, the process resulted in more maxima per 20-minute record than main excursions. The differences were largest in quartering and following-sea cases where there were typically found to be three times as many maxima as main excursions.

Run tests were performed on this data as before; each sample of maxima and minima was decimated to minimize the effects of sequential correlation, and the three hypothesis tests described in Appendix C-5 were performed on each sample.

The failure analyses are summarized in Tables C-7 and C-8. Table C-7 pertains to the wave-induced-maxima (tensile peaks) and Table C-8 pertains to the minima. The first line of the tables shows overall failure rates much more in line with those expected if the distribution hypothesis is generally true. The Kolmogorov-Smirnov test results failed less than expected, the Chi-Square tests somewhat more. Inspection of the detail of the tests disclosed that the majority of failure of the tests on compressive extremes (Table C-8) involved sample extremes just outside the 90% confidence bounds so that this failure rate is not perhaps of too much concern. In the case of the Chi-Square tests on compressive minima, there was a much lower incidence of failures at very low significance levels than was the case with the tests on main extremes.

As before, the failures were classified into several groupings; on nominal heading, on the fitted rms stress ($\hat{\sigma}$) and on the fitted broadness parameter (ε). The rates of failure appear relatively uniform across these groupings.

Those results indicate that the statistics of the SL-7 short-term stress records are consistent with those expected under the linear-random prediction theory for arbitrary band-width; that is, consistent with the two parameter CLH distribution.

Again, the testing procedure produced two estimates of the process rms ($\hat{\sigma}$), one from all the maxima of each record and one from all the minima. These pairs of estimates are plotted for all the records in Figure C-21. The degree of symmetry is virtually the same as that obtained in the analysis of main extremes, Figure C-19. On the average the process rms estimated from the minima (maxima in the compressive or sagging sense) is again shown to be about 6% more than the results obtained from the maxima.

TABLE C-7

Summary of Tests for Fit to the CLH Distribution of Wave-Induced Maxima (Tensions) of Short-Term Stress Records in the SL-7 Data Sub-Set.

Grouping	No. of Tests	Failure Rate on Maximum Value (10% Expected)	Failure Rate on Chi-Square Test (5% Expected)	Failure Rate on Kolmogorov-Smirnov Test (5% Expected)
All Records	197	9	7	1
Nominal Head Seas	32	9	3	3
Bow Seas	62	6	5	0
Beam Seas	22	10	0	0
Qtr. Seas	54	11	15	0
Follow. Seas	27	7	7	0
Fitted Rms Stress < 1.0	62	8	3	0
1.0 < 2.0	82	10	6	1
> 2.0	53	7	13	0
Fitted Broadness Parameter, ϵ 0 < .2	9	11	0	11
.2 < .4	33	9	12	0
.4 < .6	36	5	3	0
.6 < .8	29	14	14	0
.8 <1.0	90	8	6	0

TABLE C-8

Summary of Tests for Fit to the CLH Distribution of Wave-Induced Minima (Compressions) of Short-Term Stress Records in the SL-7 Data Sub-Set

Grouping	No. of Test	Failure Rate on Maximum Value (10% Expected)	Failure Rate on Chi-Square Test (5% Expected)	Failure Rate on Kolmogorov-Smirnov Test (5% Expected)
All Records	197	18	12	1
Nominal Head Seas	32	22	19	0
Bow Seas	62	19	14	3
Beam Seas	22	9	13	0
Qtr. Seas	54	20	7	0
Follow. Seas	27	15	4	0
Fitted Rms Stress < 1.0	56	18	11	2
1.0 < 2.0	77	14	12	0
> 2.0	64	20	10	1
Fitted Broadness Parameter, ϵ 0 < .2	1	0	0	0
.2 < .4	5	20	0	0
.4 < .6	59	15	18	3
.6 < .8	38	29	13	0
.8 < 1.0	94	16	7	0

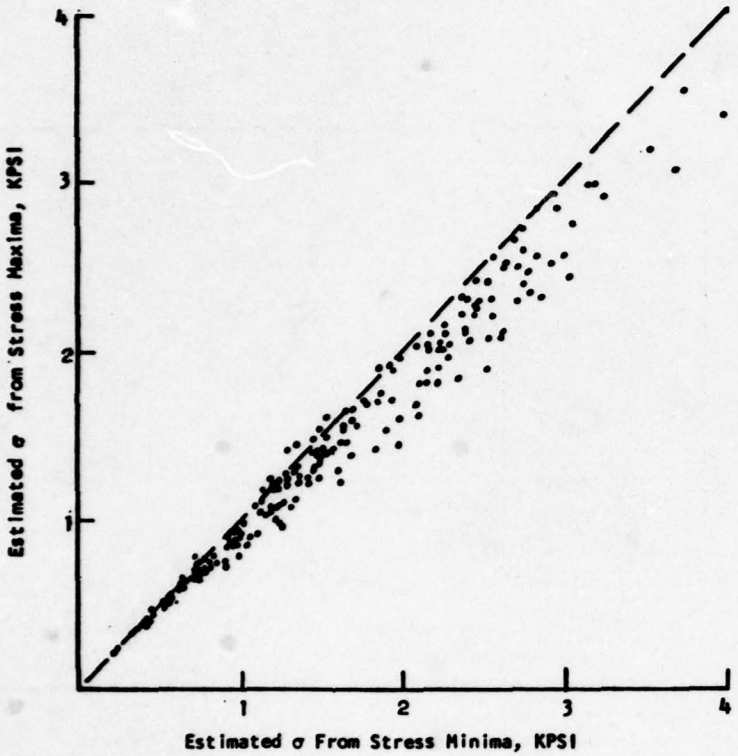

FIG. C-21 - COMPARISON OF SHORT-TERM PROCESS RMS STRESSES ESTIMATED FROM THE MAXIMA AND MINIMA IN THE SL-7 STRESS RECORDS

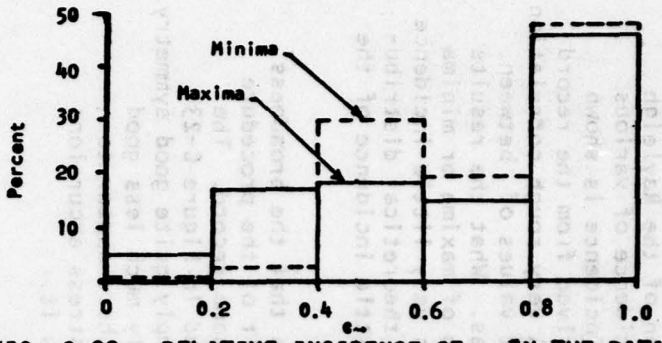

FIG. C-22 - RELATIVE INCIDENCE OF ε IN THE DATA SUB-SET

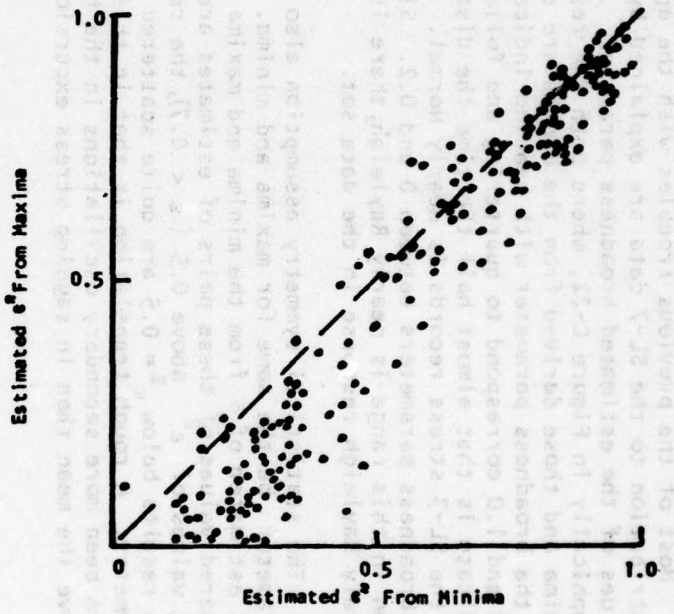

FIG. C-23 - COMPARISON OF SQUARED BROADNESS PARAMETER ESTIMATES FROM THE MAXIMA AND MINIMA IN THE SL-7 STRESS RECORDS

Most of the previous troubles with the application of the Rayleigh distribution to the SL-7 data are explained by the incidence of various values of the estimated broadness parameter . This incidence is shown graphically in Figure C-22, where both the results derived from the record maxima and those derived from the minima are shown. A very rough correlation of the broadness parameter with heading indicates that values of between 0.8 and 1.0 correspond to quartering and following seas. What the results indicate is that almost half the time the distribution of maxima or minima in the SL-7 stress records is nearly Normal. There is very little incidence of broadness parameters between 0 and 0.2. Since the theoretical distribution in this range is nearly Rayleigh, there is very little incidence of the purely Rayleigh response in the data set.

The statistical symmetry assumption also requires that the broadness parameter be the same for maxima and minima. A result of the procedure was estimated of ε from the minima and maxima of the same record. The squared values of these pairs of estimates are compared in Figure C-23. For values of ε^2 above 0.5 ($\varepsilon < 0.7$), the results imply quite good symmetry. The results below $\varepsilon^2 = 0.5$ are quite scattered but imply much less good symmetry. A rough translation is that in this range there appear to have been more secondary oscillations in the hogging stress excursions above the mean than in sagging stress excursions below it.

APPENDIX C-5

STATISTICAL TESTING TOPICS

Introduction

In analyses of the data sub-sets for FOTINI-L and the SL-7, it was desired to make various tests of "goodness-of-fit" to data drawn from each individual record.

The type of question it was desired to answer was of the form:

Regardless of environmental conditions, ship speed, etc., can a given component of the stress data be reasonably considered as having been drawn from a population having a particular distribution?

The broadness of the question is dictated by the breath of the overall problem which is the prediction of loads and stresses over periods of time equivalent to ship lives.

The large volume of data in the various data bases previous discussed necessitated a certain amount of automation of the analyses. The tests involved were all statistical hypothesis test procedures and it is in order to discuss some of the caveats. No hypothesis test can indicate with absolute certainty that something is true or false. In all cases, there is a "level of significance" of some sort designed into the test. The level of significance can be interpreted as the probability of rejecting a hypothesis on the basis of an individual sample when it is really true. Unfortunately, a designed zero level of significance corresponds to an automatic acceptance of the hypothese regardless of its truth. The usual philosophy is to design the test for a 5 or sometimes 10% probability of failure, and to make pass/fail determinations rigorously on this basis for each individual case. If an individual case is failed at the nominal level of significance, the meaning of the failure is assessed in terms of the level of significance at which the test would be passed. Thus if a particular sample fails at the 5% level of significance but would have passed had the test been designed for 4%, the failure is not considered too significant. On the other hand if the test could only be passed if the test had been designed for 0.1% level of significance, the failure must be considered highly significant.

However, it can be noted that if repeated tests of independent samples truly drawn from a hypothesized population are made at the 5% level of significance, it would be expected that the rate of failure of the tests should approach 5%. This point of view was espoused in the present work in order to attempt to interpret the results of the large number of tests which were made. To illustrate, for a particular case of interest it may be presumed that the data sub-sets are a reasonable representation of all nominal conditions. If the hypothesis is made that the maxima of tensile stresses are always distributed in the short term according to the Rayleigh distribution, and this hypothesis is tested at the 5% level of significance for all of the available sets of short-term data, it would be expected that a roughly 5% failure rate would be experienced if the hypothesis is always true, and a much larger failure rate would be observed if the hypothesis is not always (or never) true.

Given this overall philosophy, the remainder of the present appendix is given over to a documentation of some of the detail of the various tests utilized.

Sequential Correlation

The various hypothesis tests to be described are predicated upon a statiscally independent sample, and such tests are failed for various reasons, principally:

a. If the sample does not fit the hypothesized distribution.
b. Due to sampling variability even if the sample is actually drawn from a population having the hypothesized distribution.
c. If the data contain trends or are not statistically independent samples.

Items a and b are taken care of by the testing procedure; item c is not. Sequences of maxima or minima from band-limited processes are often sequentially correlated. In the limit of an ideally narrow-band process, succeeding maxima are almost perfectly correlated.

One way to assess the magnitude of sequential correlation is to perform a "Run" test, Ref. 34. The run test is a non-parametric test used to to indicate fluctuating trends. In this test, it is hypothesized that each observation is independent of its neighbors. Under this hypothesis, the probability of a sample point being greater or less than the sample median does not change from observation to observation, and this makes possible the construction of a confidence interval on the number of "runs" of data greater or less than the sample median.

In application to short-term stress data (sequences of maxima, minima, or the like), the tests were repeated using every j^{th} data point in the sequence ($j=1,2,3\ldots$). From these results, it was possible to develop a data increment (j, say) for each record such that when every j^{th} piece of data was used to form a sample, that sample would pass the run test at the 95% confidence level. This procedure does not guarantee success of course, but does seem to remove the worst effects of sequential correlation.

Test Procedures for "Goodness-of-Fit"

Three types of tests were used to test the hypothesis that the data fit some particular distribution. In all cases the data to be checked were decimated to remove serial correlation according to the results of the run tests just discussed.

The first type of test is not a conventional goodness-of-fit test. It was simply a determination if the largest element in the sample lay within the 90% confidence bounds on the maximum in a sample of the given size from a population having the hypothesized distribution.

The second test is the conventional Chi-Square Test. In this test, the parameters of the hypothesized distribution are fitted to the sample data, the data are sorted into class intervals and the sample chi-square statistic computed in the usual way. Except as noted, all tests were performed using the equi-probability class interval method. In this approach, the boundaries of the class interval are chosen so that the expected sample frequency is the same in all intervals (and equal to 1/(number of class intervals). The number of class intervals was chosen according to the sample size according to an extrapolation of recommendations given in Ref. 34. for the optimization of Chi-Square tests at the 5% level of significance. The expected number of sample points per class interval resulting from this method is as follows:

Sample Size	Expected Number of Sample Points Falling in Each Class Interval
200	13
100	8
50	5
20	3

To evaluate the adequacy of the fit, an evaluation was made of the percentage point of the Chi-Square distribution with (number of class intervals-2) degrees of freedom corresponding to the sample Chi-Square statistic.

The third test was the Kolmogorov-Smirnov test as outlined in Ref. 19. In this test the maximum deviation between the sample cumulative distribution and the hypothesized cumulative distribution is computed. A statistic, approximately Chi-Square distributed with 2 degrees of freedom, is formed by multipyling the squared maximum deviation by four times the sample size. The percentable point of the Chi-Square distribution with 2 degrees of freedom corresponding to this statistic is then evaluated, and this, in turn, is used to interpret the test.

APPENDIX C-6

FURTHER DEVELOPMENT OF TRENDS OF VIBRATORY STRESS

Introduction

The results in Appendicies C-2 and C-3 suggested that some further examination of the statistics of the maximum vibration (maximum burst) data contained in the Teledyne data bases would be in order for the FOTINI-L and SL-7. In the case of FOTINI-L, the influence of the apparently spurious data noted in Appendix C-3 was of interest. It was also of interest to combine the maximum SL-7 vibration data from all the three recording seasons since this was not possible in the early stages of the work. Finally, it was desirable to see if a fit of the maximum vibration data could be made in some sense to some analytical distribution .

Revised Trends of Maximum Vibration Double Amplitudes with Beaufort Number

As noted in Appendix C-1, the maximum vibration data for all three SL-7 measurement seasons was available in a later stage of the work. The combined three-seasons data base involves nearly 5000 records so that the elimination of the few spurious records noted in Appendix C-3 had no visible affect upon the scatter of maximum vibration data. Since the incidence of problems in the data sub-set is quite low, it appeared likely that the incidence in the entire data base was also quite low. As in the description of the first two-seasons data in Appendix C-2, there are in the combined three-seasons data base a large number of maximum vibration double amplitudes between 3000 and 10000 psi. The addition of third-season data increased the number of vibration double amplitudes above 1000 psi from 5 to 7. All seven of these instances appear to be associated with either severe Beaufort winds or high wave-induced stresses. Though there are undoubtedly spurious pieces of maximum vibration double-amplitude data remaining in the combined data base, there appeared no reasonable alternative to assuming that the incidence was too low to affect subsequent operations.

Essentially the same two-way classification of data described in Appendix C-2 was carried out upon the combined SL-7 data base. The means in each classification cell were computed and compared with the results in Figure C-6 and C-7.

A graphical presentation of these results is omitted since no clarification of the trends relative to those already shown for the second season (Figures C-6 and C-7) was apparent.

In the case of the FOTINI-L data, the data sub-set had been selected on the basis that it contained most of the unusually high vibratory response.

As noted in Appendix C-3 a good deal of this vibratory response was spurious. Accordingly, the FOTINI-L data base was revised by first discarding the 78 records questioned in Appendix C-3, and twelve additional records which were not in the sub-set but which had been recorded just before or after records in which nearly continuous malfunction was noted in Appendix C-3. This action reduced the FOTINI-L data base from 1550 records to 1455, and had the effect of significantly reducing the incidence of very high vibration amplitudes. In the revised data base, there are just 19 points falling between 3000 and 8000 psi, and only one in excess of 8000 psi--- effectively 98.6% of the vibration amplitudes are below 3000 psi.

A two-way classification of vibration double amplitudes for FOTINI-L was done in nearly the same way as indicated in Appendix C-2. Because there are only 46 instances of Beaufort 8 and above in the revised data base, all base data were grouped. Similarly, Beauforts 0 and 1 were grouped. The second part of the classification was upon ship-wave heading as in Figure C-9, with the additional class "no heading given" included. The mean vibration in each classification cell was computed, counting vibration below the 1000 psi threshold as 500 psi, and the revised trends with Beaufort number and speed are shown in Figure C-24. Relative to Figure C-9, the revised trends have somewhat less scatter, and the means of the maximum burst data are below the 1000 psi threshold for all Beaufort numbers below 6. The relatively high means for beam and quartering seas for Beaufort numbers of 6 and higher arise from the average of very few points. The revised averages of all data indicate a milder upward trend with Beaufort number than might be inferred from Figure C-9.

It was seen from the results of the two-way classification that much of the confusion in the trends with heading and Beaufort number resulted from too few members in each classification cell. In the FOTINI-L data base, there are 822 records where heading was recorded. The two-way classification requires 8 x 5= 40 cells, so that, on average, there are expected to be only about 20 records in each cell. In the event, there were typically 4 to 7 records in each of the classification cells for the high Beaufort numbers--possibly too few for firm generalizations. Accordingly, it appeared worthwhile to examine trends with Beaufort number alone, that is, to ignore heading and speed. A one-way classification allows more detail for the statistics of the maximum vibration to be indicated. An attempt in this direction is shown in Figure C-25. The Beaufort number classification is as in the previous figure and the mean of all vibration amplitudes for each Beaufort number is given. In addition, for each Beaufort number, the single maximum vibration double amplitude is plotted along with approximate contours of constant empirical probability. The convention followed is that the stated percentage of all

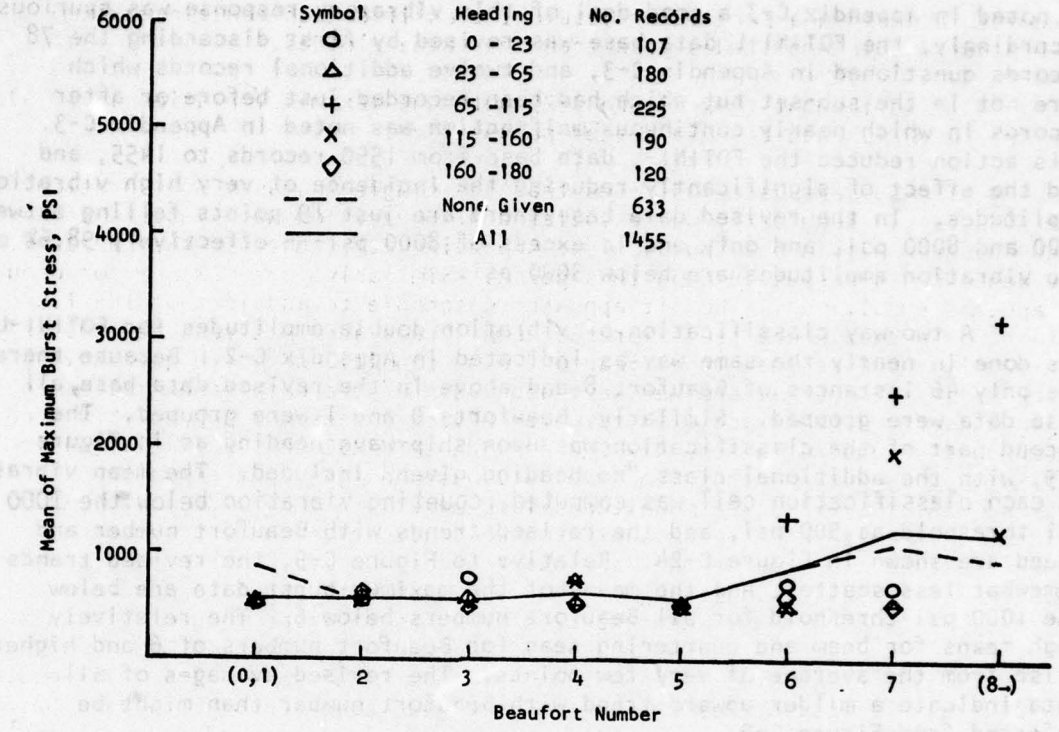

FIG. C-24 - FOTINI-L: REVISED BURST STRESS TRENDS, BEAUFORT NUMBER AND SEA DIRECTION

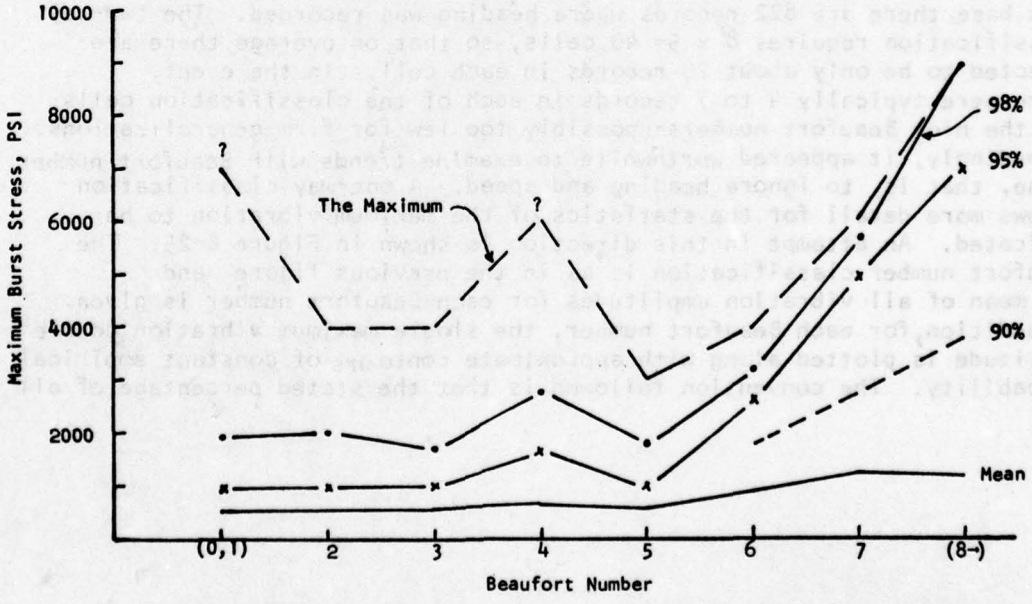

FIG. C-25 - FOTINI-L: REVISED MAXIMUM BURST STRESS TRENDS WITH BEAUFORT NUMBER

records falling in à particular Beaufort classification contain maximum vibratory double amplitudes less than the value plotted.

It is thought that Figure C-25 puts the maximum vibration amplitudes in the FOTINI-L data base in better perspective.

The summary data indicates that the single instance of vibration of 7000 psi in Beaufort 1 was associated with very low wave-induced stress and occurred within one "burst" (see Appendix C-2), that is, the surrounding evidence casts suspicion upon this point. Similarly, the maximum for Beaufort 4 appears suspicious. Thus it appears reasonable to assume that the 1.4% of the data base where real vibration amplitudes are in excess of 3000 psi primarily involves the higher Beaufort wind conditions (and higher waves). Looking at the problem another way, about 98% of the data base implies an allowance for dynamic addition to wave-induced stress not appreciably greater than that suggested in Appendix C-2 for the UNIVERSE IRELAND. Elimination of 90 questionable records from the data base has the apparent effect of making FOTINI-L vibration magnitudes look more like the UNIVERSE IRELAND vibration magnitudes. This conclusion does not solve the problem since there must be concern for the rare occurrences. However, these rare occurrences appear associated for the most part with the more severe wave conditions as would have been expected prior to an inspection of the data.

In order to treat the SL-7 data in a similar way, a one-way (Beaufort Number) classification was run on the combined three-season SL-7 data base, and means and approximate probability contours were computed as had been done for FOTINI-L. The results are shown in Figure C-26. At comparable levels of probability, the SL-7 vibration magnitudes are clearly higher than those of FOTINI-L. With the exception of the maximum values experienced in Beaufort 2 and 3, the relation between the maximum, the various probability contours and the mean for each Beaufort grouping are consistent in appearance. The approximately 12% of time that vibration exceeded 3000 psi is not associated as exclusively with high Beaufort winds as in the case of FOTINI-L, Figure C-25. Since the arbitrary 3000 psi level was exceeded 12% of the time, maximum vibration double amplitudes in excess of 3000 psi appear to be 8 or 10 times more likely in SL-7 than in FOTINI-L. Part of this must be attributed to the bias in the SL-7 data base (winter North Atlantic only) relative to the year round service experience in the FOTINI-L data base.

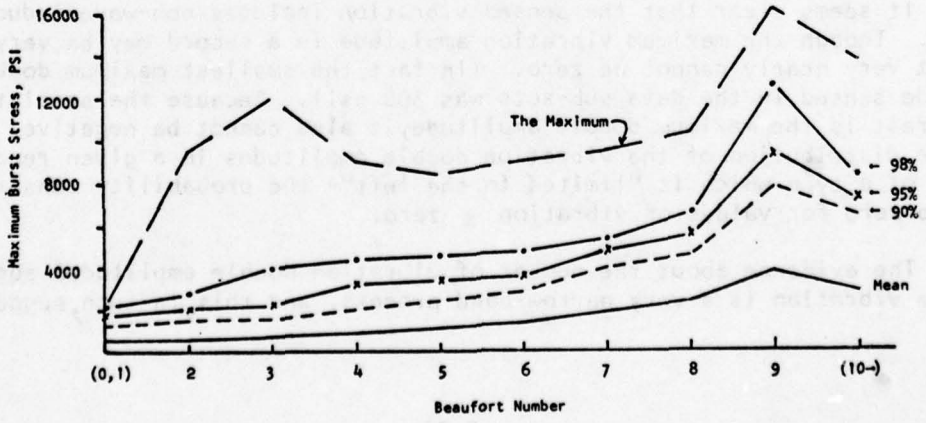

FIG. C-26 - SL-7: MAXIMUM BURST STRESS TRENDS WITH BEAUFORT NUMBER

Investigation of the Form of the Distribution of Short-Term Vibratory Stress

The description of the statistics of the maximum vibratory stress double amplitudes by means of some semi-analytical expression has obvious advantages. The process of arrival at an expression based upon the data can take many forms, but in the end, all may be classified as "curve fitting". Since success in practical curve fitting depends more upon the assumed analytical model than upon nearly anything else, any investigation must start with some educated guess-work on the nature of the process. The first effort in this direction was to investigate the short-term situation.

Re-capitulating from the descriptions in previous appendices, the primarily first-mode vibration is isolated from the combined stresses by a band-pass filtering process. Each piece of data in the data base is the single maximum double amplitude of this vibration which was experienced in one 20-minute record. No other measure of the magnitude of vibration is available in the data bases.

The vibration observed is the net result of all excitation-- wave-induced due to slamming, flare shock, etc. as well as propeller-induced vibration. Propeller-induced vibration is ordinarily of small magnitude-- often small enough to be disregarded by ship's personnel. However strain-gage bridges are not discriminatory. Given that the first-mode frequencies of the SL-7 and FOTINI-L ranged from 0.66 to 0.8Hz; if more or less continuous vibration due to non-wave-related sources was large enough to be sensed, it would be expected that between 800 and 1000 vibration double amplitudes would be sensed in each 20-minute record regardless of surrounding environmental conditions. The detailed time histories available in the data sub-sets make possible a check of this hypothesis. The digital time histories of vibration described in Appendix C-3 were accessed and a count was made of the number of vibration amplitudes in each record. The results were almost precisely as expected. Each vibration record in the data sub-sets from both the FOTINI-L and the SL-7 contained between 820 and 1050 vibration double amplitudes. The number of amplitudes seemed not to vary with Beaufort wind or speed or any of the other parameters.

It seems clear that the sensed vibration includes non-wave-induced effects. Though the maximum vibration amplitude in a record may be very small, it very nearly cannot be zero. (In fact, the smallest maximum double amplitude sensed in the data sub-sets was 300 psi). Because the statistic of interest is the maximum double amplitude, it also cannot be negative. Thus, the distribution of the vibration double amplitudes in a given record must be of a type which is "limited to the left"- the probability density equal to zero for values of vibration $\leq$ zero.

The evidence about the number of vibration double amplitudes suggests that the vibration is a very narrow-band process, and this, in turn, suggests

the assumption that the vibration double amplitudes are Rayleigh distributed; that is, the density of the double amplitudes (V) would be given by:

$$p(V) = V \, Exp[-V^2/8\sigma^2]/4\sigma^2$$

(For $V > o$)

Where:

σ^2 = The variance of the vibration time history. (The extra factor of two is to compensate for double amplitudes).

Though not explicitly stated in Ref 8, the above assumption seems implict in the part of that work which deals with springing.

If the assumption is made, the probability distribution of the highest double amplitude (Vmx) in a sample of N becomes (Ref 19, 36):

$$P(Vmx < X) = \left[1-Exp(-X^2/8\sigma^2)\right]^N$$

Essentially, under these assumptions, the value of extreme is "scaled" by σ, the process rms value of vibration. This fact makes the assumption quite attractive in view of the probability that rms vibration may be computed (Ref 8). The foregoing equation implies that in 90% of repeated samples of 800 to 1000 double amplitudes the ratio Vmx/0 should lay within the approximate range:

$$6.6 < Vmx/\sigma < 8.8$$

Employing the failure rate philosophy of Appendix C-5, it is thus expected that only about 10% of observed ratios will be outside the above range if the assumption is generally true for all combinations of speed, heading etc, and if the 800 or 1000 amplitudes in each record are chosen at random. This last is unlikely to be true, however. The number of fluctuations in the envelope of the vibration in each of the SL-7 records was computed. This number ranged from 100 to 200. The result implies that the extreme in each record should be interpreted as the maximum in a sample of no more than 100 or 200. In samples of 100 or 200 the extreme ratio (Vmx/σ) should lay within the approximate range:

$$5.2 < Vmx/\sigma < 8.1$$

in 90% of all samples.

The data sub-sets for FOTINI-L and the SL-7 were used to gain a first idea of the validity of the short-term Rayleigh assumption. The rms of the vibration, σ was computed from the time series described in Appendix C-3, as was the maximum double amplitude in each record, and the ratio Vmx/σ was formed for each record. The results were compared with the foregoing 90% confidence bounds, for samples of 100 or 200, and the rates of failure were found.

The result of this operation was that all failures for both ships were of the high limit of the confidence bound -- the maximum vibration double amplitude was higher than expected relative to the rms when the test was failed. The failure rate for the SL-7 was 64%, that for the FOTINI-L 37% versus an overall expectation of 10%. The data in the sub-sets clearly do not, in general, conform to the short-term Rayleigh assumption.

The consistent failures of the high limit suggested that the short-term distribution of vibration amplitudes might be closer to exponential. A physical or mathematical rationale for such an assumption is not available, but if it is made the distribution of double amplitudes becomes:

$$P(V<X) = 1-\text{Exp}[\ -X/2_{\sigma}]$$

$$(V>0)$$

and the distribution of the highest double amplitude (Vmx) in a sample of N becomes:

$$P(Vmx < X) = (1-\text{Exp}[\ -X/2\sigma])^{N}$$

Using this last expression, the extreme ratio of double amplitude to rms ($Vmx/^{\sigma}$) in samples of 100 or 200 double amplitudes would be expected to lie within the following range in 90% of repeated samples:

$$7.0< Vmx/\sigma <16.5$$

This criterion was applied to the computed sample ratios for both ships as had been done under the Rayleigh assumption.

The results were:

a) When a failure occurred it was always of the lower bound in the data sub-sets for both ships.

b) The failure rate for the SL-7 data was 15% that for the FOTINI-L was 27%.

It thus appears that the short-term distribution of vibration double amplitudes may, in general, be closer to exponential than to Rayleigh, but neither assumption is particularly convincing -- something in between may be appropriate. The results imply that the construction of long-term trends

of vibration from estimates of short-term rms may not be within current state-of-art. In the case of the suspected springing response of the FOTINI-L, the current state-of-art implies a zero mean Gaussian vibratory response, and consequently a Rayleigh distribution of maxima. For suspected slamming or flare shock response as for the SL-7, it is not clear what distribution current state-of-art implies. In either case it may be suspected that vibrations due to propeller excitation are confusing the situation.

Investigation of the Form of the Long-Term Distribution of Maximum "Burst" Stresses

The alternate to the synthesis of a long-term distribution of maximum double amplitudes of vibration is to treat the entire mass of data empirically. The problem is again one of making assumptions and checking the fit. The data of interest is the extreme vibration double amplitude observed in a 20-minute sample. From the discussion in the previous section, the short-term distribution is limited to the left. If the assumption is made that there exists an initial long-term distribution of vibration amplitudes, then the data available can be thought of as the result of the examination of a large number of samples from the (unknown) long-term process. Clearly, construction of the long-term initial distribution seems beyond the present state of art. However, it seems quite certain that the type of this distribution will also be limited since, by definition, no member of the entire population of vibration double amplitudes which could be experienced by the ship can be negative. Extrapolating the discussion of the last section slightly, the presence of propeller-excited vibration implies also that the lower limit of the long-term initial distribution is nearly zero.

In the absence of an explicit form for the initial long-term distribution the exact distribution of the extremes in 20-minute samples cannot be constructed. However, the asymptotic distribution of largest values (for large samples) has been known to depend only upon the general type of initial distribution (Ref 36). Accordingly, if the sample from which the extreme value of vibratory stress is taken is "large", it may be hypothesized that the distribution of these date may be approximated by the appropriate asymptotic form.

For limited distributions the "third asymptote" of Ref 36 is appropriate. If the limit parameter is assigned the value zero, both the second and third asymptotes (Ref 36) are of the same form, and are equivalent to the two-parameter Weibull distribution extensively used in Ref. 18. For present purposes this distribution is written.

$$P(Vmx < X) = 1-Exp[-(X/a)^m] \qquad (X > 0)$$

Where the parameters m and a are, in general, unknown.

To try out this assumption, the semi-graphical approach of Ref. 18 was utilized. This involves constructing an empirical probability distribution, plotting it on a specially constructed probability paper, fitting a straight line and making a judgement upon the deviations of the empirical data from this straight line to assess the fit. First, all the maximum vibration data in the SL-7 and FOTINI-L data bases were sorted into class intervals, the cumulative count was computed, and the results were divided by one plus the total number of records to produce the empirical cumulative distribution. (Division by $N+1$ allows the maximum double amplitude in the data base to be plotted.)

Uniform class intervals were utilized. In the case of FOTINI-L, vibration amplitudes below 1000 psi are classed as zero in the basic data reduction (Appendix C-2). Thus class intervals 1000 psi in width were dictated by this fact. This results in 90% of the data being classified in the lowest class -- not an optimum situation, but one which had to be accepted. A choice of 1200 psi intervals for the SL-7 (twice the original analysis threshold) resulted in 14 non-null class intervals with reasonable numbers of points in the upper intervals, and roughly 60% of data in the lowest class interval. After plotting on the probability paper, straight lines were fitted by a least-squares method to the empirical data which corresponded to probability levels of 0.999 and lower.

The results of this analysis are shown in Figure C-27 for both ships. The large spots indicate the maximum values in the data sets. The fitted values of the two Weibull parameters are indicated in the figure. Visually, the fits of the data to the straight lines appears as adequate as the examples of similar fits shown in Ref. 18.

Chi-Square tests for goodness-of-fit of these empirical distributions to the fitted Weibull distributions were made with the result that the FOTINI-L data passed at the 34% level of significance and the SL-7 data at the 2% level of significance. Inspection of the fits in Figure C-27 would have suggested the opposite results; the SL-7 fit essentially fails the Chi-Square test though the visual fit looks better than that for FOTINI-L which passes the test handily. What the results would have been had it been possible to sort the data into equi-probability class intervals is problematical. It is thought, however, that a serious problem with the Chi-Square test in the SL-7 data has to do with independence of the data itself. Since four data samples per watch were recorded, a significant amount of sequential correlation could be present. The techniques noted in Appendix C-5 could not, for various reasons, be run on the entire SL-7 data base. It is suspected that decimation of the SL-7 data base to about every fourth record would be sufficient to produce a passing Chi-Square test. It seems reasonable to accept the Weibull distribution first shown in Figure C-27 as a reasonable long-term representation of the empirical data.

It was of interest to see if the fits to the Weibull distribution could be made for various sub-groupings of the data base -- that is for the various headings, Beaufort numbers, etc.; and whether the parameters of the fitted distributions would make any sense. Efforts were made in this direction. The results for each of the two ships must be discussed separately.

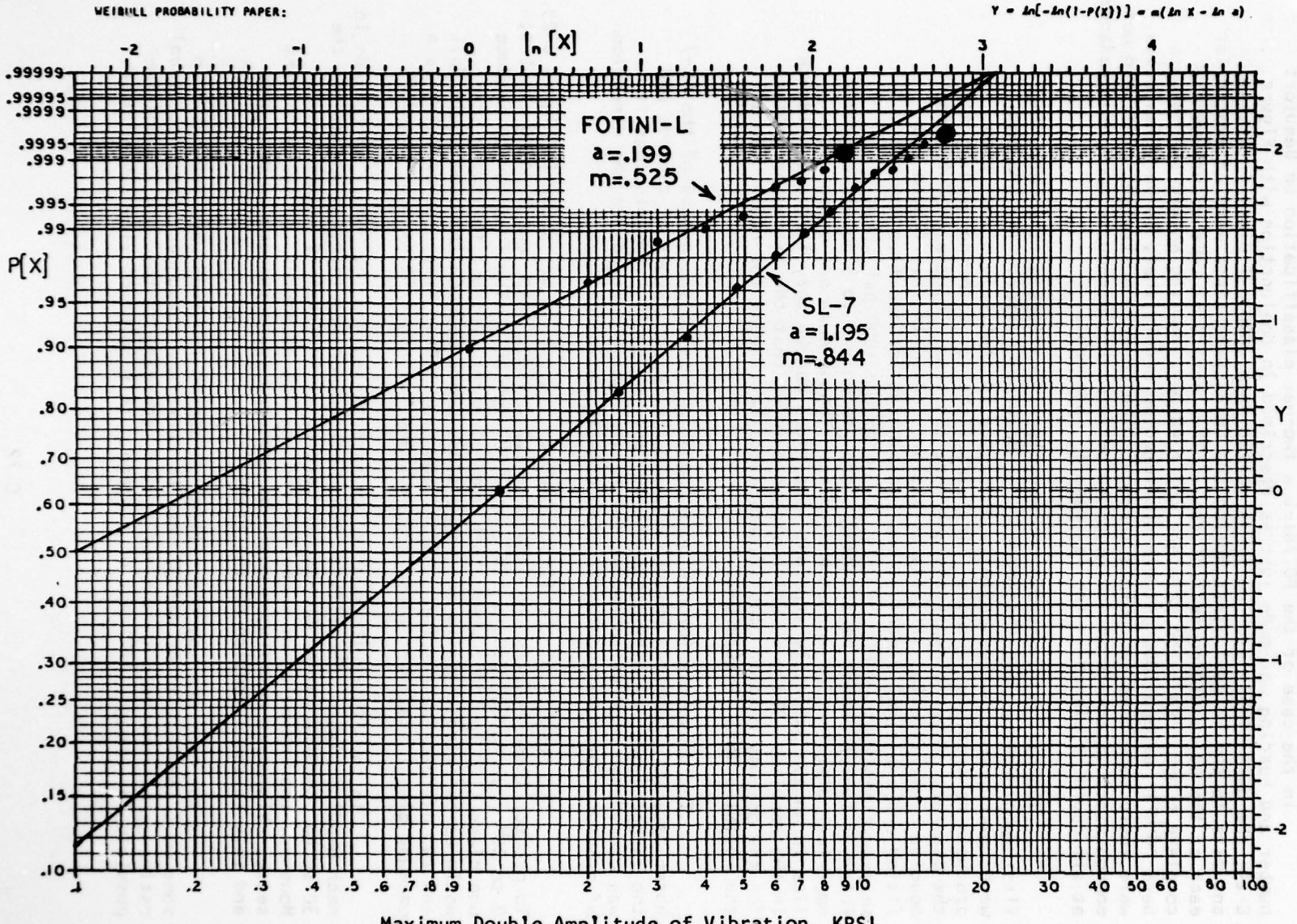

Figure C-27 Long-Term Distributions of Maximum "Burst" Stresses for SL-7 and FOTINI-L

In the case of the FOTINI-L, a two-way classification on Beaufort number and heading was made just as described in conjunction with Figure C-24; the data within each cell was sorted into 1000 psi class intervals, and fits to the Weibull distribution and Chi-Square tests were attempted for each of the 40 resulting sets of data. The results of this effort were a complete blank. When the data are split 40 ways, the 140 points in the data base which exceed 1000 psi are scattered so widely that, in very few cases, were there more than two points through which to draw a straight line, and not enough class intervals were present to perform the Chi-Square test. No credance at all could be placed in the few results obtainable.

The next trial was two one-way classifications of the data, the first upon heading, and the second upon Beaufort number. The problems were ameliorated but essentially persisted so that this effort also produced no credible answers. The situations for both the heading and the Beaufort number classifications were the same. Figure C-28 for the heading classification illustrates the problems. In this figure the fitted and empirical distributions are plotted for the five nominal ship-wave headings in Figure C-24. Owing to the 1000 psi class interval (which cannot be altered), there are only 3 to 5 points on the empirical distribution for each heading. Though each set of points lies in an approximately straight line, there can be very little confidence in the results. The most which may be said is that the fitted parameters for the one-way heading classification scatter around the result for all the FOTINI-L data, Figure C-27.

The prospects for making reasonable fits to sub-groups of the SL-7 burst data were somewhat better owing to the larger number of records and the larger amount of data above the 600 psi threshold. Nevertheless it was considered prudent to revise the classification methods in the direction of providng for more records in each classification cell.

The results of the first attempt at grouping are shown in Figure C-29. To produce these results, the data were sub-divided into four heading classes; 0 to 30^{o}, 30 to 60^{0}, 60 to 120^{0}, and 120^{0} to 180^{0}. The idea was to produce one class (120 to 180^{0}) where both nominal quartering and following seas would be expected to fall, one broad class where seas on the beam would fall and two narrower ranges for head and bow seas. This first sub-division is a one-way classification-- all ship speeds and wave severities are included.

In the figure, the numbers in parentheses are the number of records in each heading class. The fits to the distribution are fair, only that for the 30 to 60^{0} heading passes Chi-Square testing at 5% level of significance. However, the variation of slope (m) and scaling parameter (a) seems to make sense. Vibration magnitudes would be expected to be largest in head seas and this is the direction of the trend.

The next one way classification scheme involved wave severity. In some ways the results of Ref 37 can be construed to suggest that the visual estimates of wave height made during the recording of the data are not impossibly far wrong-- at least on average. This point of view was adopted

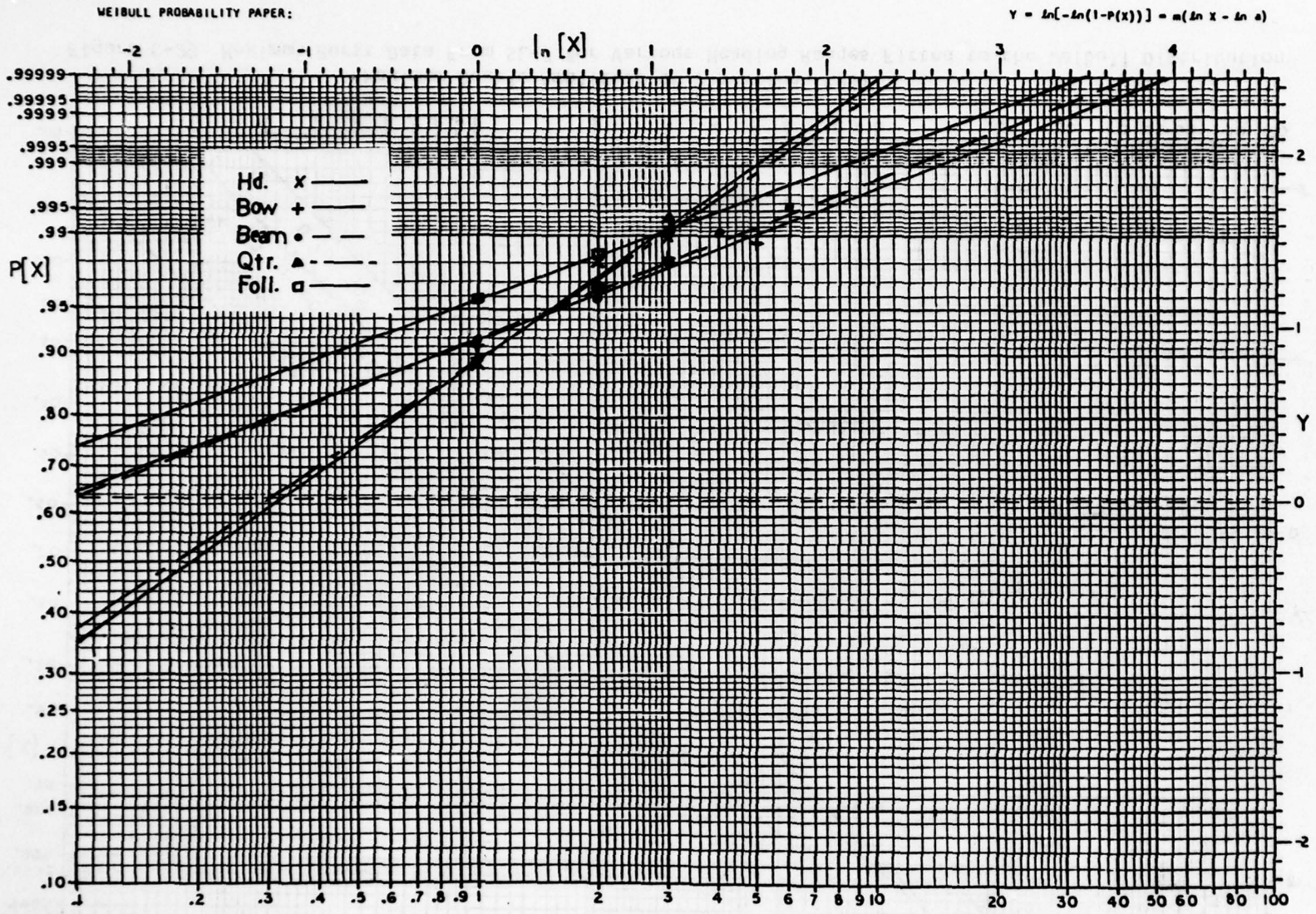

Figure C-28 Distributions of Maximum "Burst" Stresses for FOTINI-L According to Ship-Wave Heading

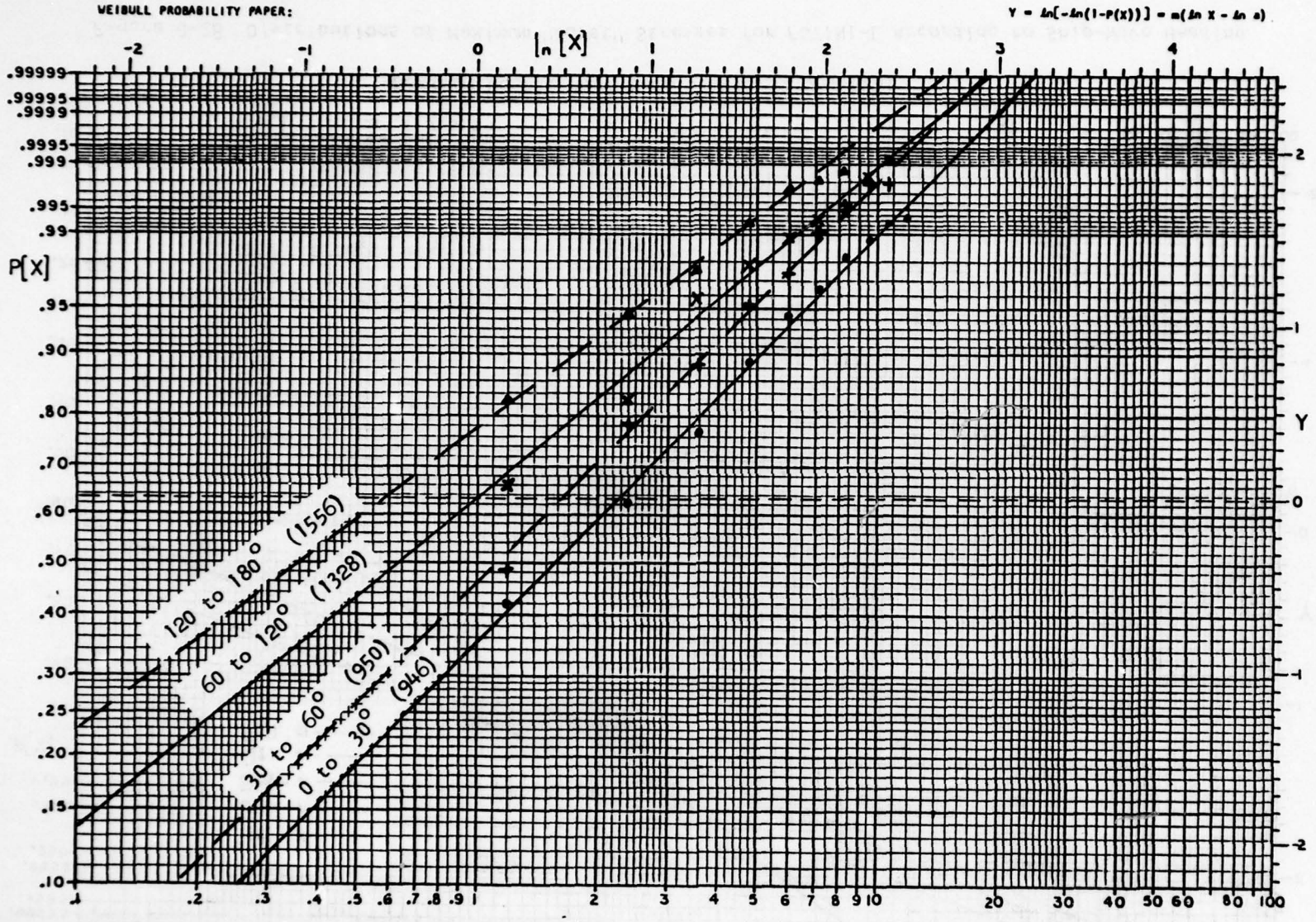

Maximum Double Amplitude of Vibration, KPSI

Figure C-29 Maximum Burst Data From SL-7 for Various Heading Ranges Fitted to the Weibull Distribution

and the data were separated into five visual wave height classes; wave heights 0 to 5 feet, 6 to 14 feet, 15 to 24 feet, 25 to 34 feet, and above 34 feet. Empirical distributions were computed and fitted to the Weibul distribution with the result shown in Figure C-30. As before, the total number of records is shown in parentheses after each label. To a point, the trends are as would be expected; the slope (m) and scaling parameter (a) increase with wave height. The results for the highest waves are significantly out of trend. Examination of the detail of the results indicates practically no ship speeds above 15 knots in the above 34-feet class while ship speeds in excess of 15 knots are about half the total in the 25-34-feet class, and are practically non-existant in the lower classification.

These results suggested that the parameters of the fitted distributions vary with ship speed as well as heading and wave height. A three-way classification of data was accordingly attempted by adding three speed groups to the wave and heading groups just described. The three speed ranges adopted were; 0 to 15 knots, 15 to 25 knots and over 25 knots. As in the previous analyses, the data were sorted into the resulting (5 x 4 x 3=60) cells, the data within each cell were sorted into class intervals and fits to the Weibull distribution and Chi-Square tests were attempted for each of the 60 subs-sets of data. The results of this effort were not too credible for the same reasons discussed in conjunction with the FOTINI-L data.

The best that could be done in this direction was to make two, two-way classifications. The first was speed-heading for all wave conditions and the second was wave height-heading for all ship speeds. The resulting fitted values of slope (m) and scale (a) are summarized in Table C-9 and C-10. The majority of the fits shown are as good or better than those shown in Figures C-29 and C-30 when the smaller amount of data are taken into account. The dashes in Table C-10 indicate cases where no remotely credible fit could be obtained. In both tables, a consistent upward trend of slope and scale is shown as heading tends to head seas, as speed reduces, and as wave height increases.

TABLE C-9

Fitted Weibull Parameters (m/a) for Maximum Burst Stresses in SL-7 Data Base: Results for Various Heading and Speed Ranges in all Wave Condtions:

	Ship- Wave Headings, Degrees			
Speed Range, kt	0-30	30-60	60-120	120-180
0-15	1.46/3705	1.55/2879	.60/417	.59/227
15-25	1.44/2969	1.14/2014	.85/960	.75/589
≥ 25	0.92/1934	0.94/1460	.85/1037	.77/612
All Speeds	1.03/2259	1.01/1623	.83/980	.77/590

(Dimension of "a" is psi)

TABLE C-10

Fitted Weibull Parameters (m/a) for Maximum Burst Stresses in SL-7 Data Base: Results for Various Heading and Visual Height Ranges for All Ship Speeds.

	Ship-Wave Heading, Degrees			
Visual Wave Height Range	0-30	30-60	60-120	120-180
0-5 Ft	1.09/1179	.76/682	.62/416	.51/210
6-14 Ft	1.35/3529	1.35/2098	.95/1315	.83/717
15-24 Ft	1.71/5395	2.15/4620	1.13/1828	.89/1124
25-34 Ft	2.61/4661	4.89/3877	-	1.52/1574
> 34 Ft	2.20/4235	-	-	-

(Dimension of "a" is psi)

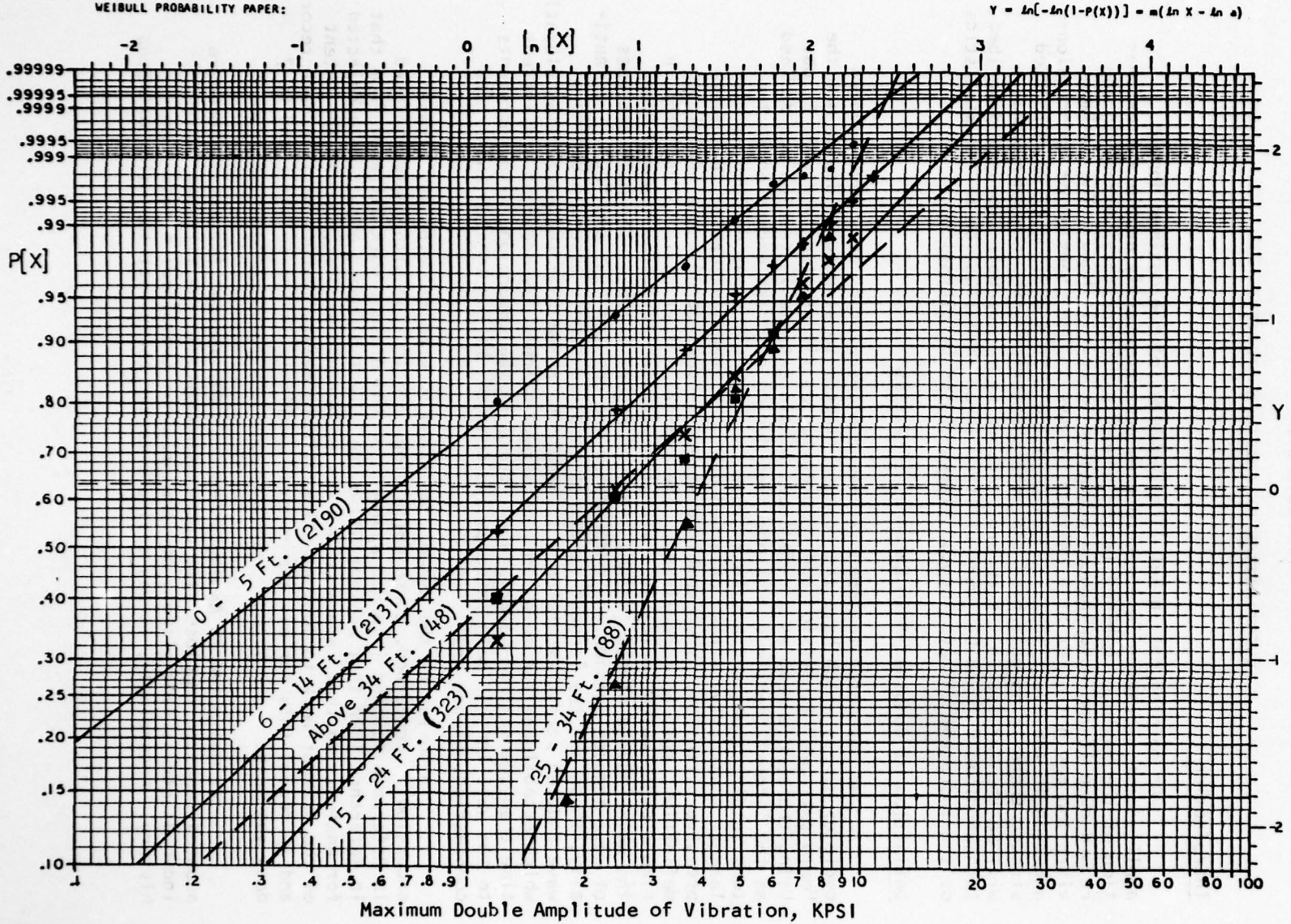

Figure C-30 Maximum Burst Data From SL-7 for Various Wave Height Ranges Fitted to the Weibull Distribution

APPENDIX C-7

INVESTIGATION OF COMBINED STRESSES

Introduction

As pointed out in Ref. 1, a knowledge of the maximum double amplitude of vibration in a record does not necessarily enable the estimation of the maximum combined (wave-induced plus vibratory) stress in the record even if the wave-induced situation is well in hand. The maximum vibration may not occur at a maximum in wave-induced tension or compression--and even in the event that it does coincide with a maximum of wave-induced stress, there is no guarantee that the particular wave-induced maximum will be the largest in the record. Accordingly, the data sub-sets described in Appendices C-1 and C-3 were utilized in an investigation of the statistics of the increment to wave-induced stress caused by vibration.

Definition of Combined Main Extremes of Stress

As was noted in Appendix C-4, the descriptors of a wave-induced cycle of stress which have the most pertinence to structural design are the "main extremes" in tension and compression as illustrated in Figure C-18b. Using the sample mean as a reference, a main extreme in tension was defined as the largest tensile stress observed during a stress excursion in the tensile direction, and a main extreme in compression was defined as the largest compressive stress observed during a stress excursion in the compressive direction. When combined stress is considered, some additional definitions must be established. The typical situation is illustrated in Figure C-31, which indicates a vibration (solid line) superimposed upon the wave-induced stress (dashed line) of Figure C-18b. The main extremes of wave-induced tension and compression are denoted "T_W" and "C_R". Essentially, these are the largest values of combined stress observed during a wave-induced stress excursion. It should be noted that the particular vibration which establishes the main combined stress extreme may occur at a different time than the maximum wave-induced stress in the excursion. The increments to the wave-induced main extremes are denoted $\delta+$ for tension and $\delta-$ for compression, Figure C-31.

In-so-far as the dynamic addition to stress during any stress excursion is concerned, these definitions are in line with those employed in Reference 1. The intended approach of the present work differed from that in Reference 1 in that whereas 100 or so selected impact events were selected for analysis in that reference and its background studies, it was the intent of the present work to look at all available events (excursions) in each record, and to repeat this for all the records available in the FOTINI-L and SL-7 data sub-sets.

It was noted in Appendix C-3 that the digital filtering procedure adopted resulted in close time correlation between the filtered (wave-induced) stress time history and the original (combined) stress time history. Accordingly, it was a simple matter to extract the main extremes

of combined stress at the same time as the main extremes of wave-induced stress described in Appendix C-4 were developed. At the end of the process, there was available (to the computer) for each record of the data sub-sets:

a. An array of main extremes of combined tensile stress (T_R) in the order found.

b. An array of main extremes of combined compressive stress (C_R) in the order found.

c. An array of wave-induced main extremes in tension (T_W) correspnding to a.

d. An array of wave-induced main extremes in compression (C_W) corresponding to b.

Statistical Symmetry of Dynamic Increments to Wave-Induced Stresses

The analysis of dynamic increments to wave-induced stresses in Reference 1 indicated that the increments to tension are not statistically symmetrical with those in the compressive direction for the relatively small cargo ships studied. In the case of the present ships, inspection of the portions of the records in the data sub-sets shown in Figures C-14 and C-15 suggested an opposite conclusion. (The valid vibratory response for the FOTINI-L appears similar to springing, and that for the SL-7 appears to be a combination of slamming and flare shock.)

The results of a simple investigation into the symmetry of the dynamic increments (δ + and δ -) to wave-induced stress are summarized in Figures C-32 for the FOTINI-L and C-33 for the SL-7. The maximum dynamic increments to wave-induced stress were found for each record, and the maximum for tension was plotted against the maximum for compression on logarithmic scales. Without attempting any arithmetic, the maximum dynamic additions to wave-induced stress appear to be quite symmetric for both ships. In any given record in the sub-sets, there appears to be roughly an even chance that the maximum increment to compression will be greater than that to tension. As in the case of similar comparison plots of maximum wave-induced stresses, Figure C-16, C-17, there is likely to be a significant scatter due to the fact that isolated maxima are being compared. The mean increments to tension and compression were computed for each record and plotted in a similar fashion. As expected, the scatter was much reduced and the apparent symmetry confirmed.

Short-Term Distributions of the Dynamic Increment to Wave-Induced Stresses

The implication in Reference 1 is that the dynamic increment to compression may be exponential in the short term while the dynamic increment

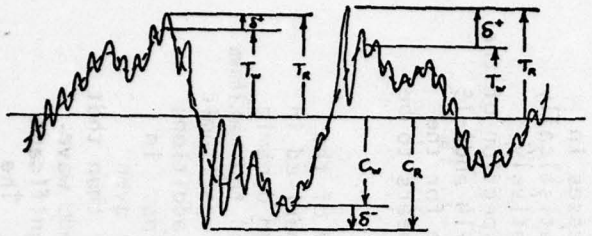

Figure C-31 Definition of the Combined Main Extremes in Tension and Compression, and the Increments to Wave-Induced Stress

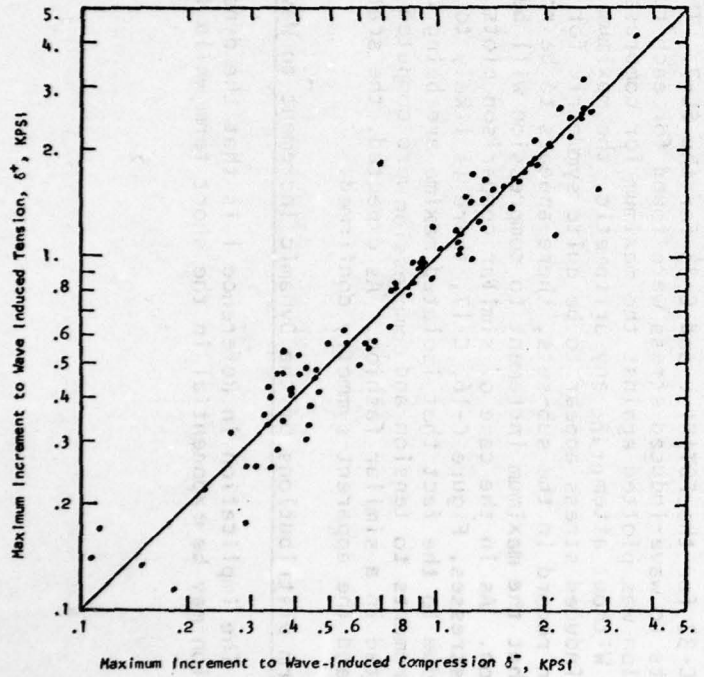

Figure C-32 FOTINI-L: Comparison of the Maximum Dynamic Increment to Wave-Induced Tension with the Maximum Increment to Wave-Induced Compression

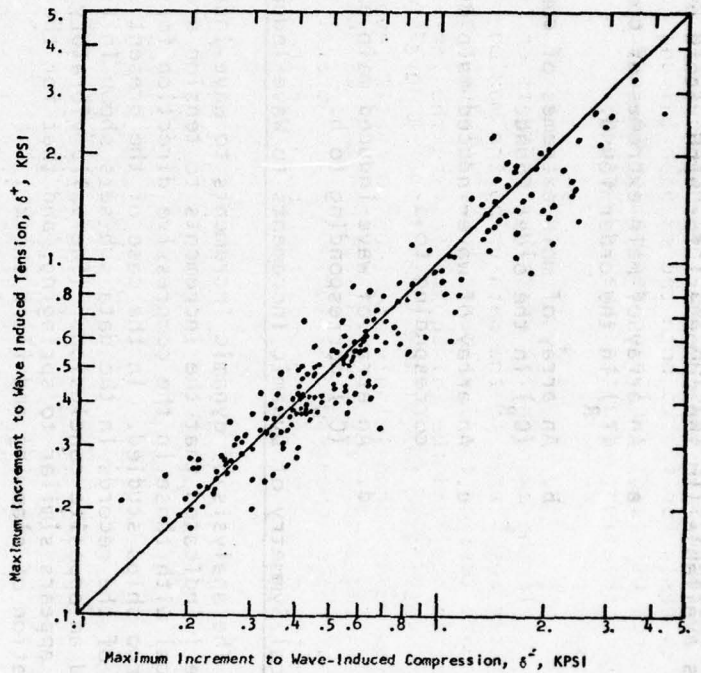

Figure C-33 SL-7: Comparison of the Maximum Dynamic Increment to Wave-Induced Tension with the Maximum Increment to Wave-Induced Compression

to tension may be Rayleigh. However, previously presented data indicate the increment to be statistically symmetrical in the present case. Accordingly, the increments to tension and the increments to compression were subjected to tests for fit to both the exponential and Rayleigh distributions. The procedures utilized, including decimation to reduce the effects of sequential correlation, were the same as those described in Appendices C-4 and C-5.

In the exponential distribution tests on the SL-7 data, the distribution parameter was fitted to the data using the maximum likelihood method. The Chi-Square test on the increments to wave-induced tension was failed in 92% of the records, and the Chi-Square test on the increments to wave-induced compression was failed 84% of the time at the 5% level of significance. The failures were overwhelmingly at or below the 1% level of significance. The tests on the sample extremes failed in 60% of all cases. The results suggest that the exponential distribution is, in general, not a reasonable assumption for either the increments to tension or the increments to compression found in the SL-7 data.

Next the dynamic increment data were checked for fit to the Rayleigh distribution. The distribution parameter was fitted to the data. Failure rate results are summarized in Tables C-11 and C-12. The failure rate with respect to the Rayleigh distribution is quite high. In this case, a pattern different than that for wave-induced main extremes (Appendix C-4) is apparent; that is, the Rayleigh assumption for the increments improves for following seas rather than degrades, the failure rate for head seas appears very high, and no significant correlation with stress level is apparent. There are a great many instances of failure at 1% level of significance in these results. With overall failure rates 8 to 10 times that expected, it is also quite difficult to accept the short-term Rayleigh hypothesis as being generally applicable to the dynamic increments to the wave-induced stresses in the SL-7 data sub-set.

The dynamic increments found in the 90 valid records of the FOTINI-L data sub-set was checked for fit to the exponential and Rayleigh distributions in the same way as had been done in the case of the SL-7. The results of this procedure were essentially the same. The dynamic increments to tension and compression failed the Chi-Square tests at the 5% level of significance for fit to the exponential distribution in more than 90% of the records. The failures in the FOTINI-L tests were also overwhelmingly or below the 1% level of significance. In checking the fits of the dynamic increments to the Rayleigh distribution, both the Chi-Square and Kolmogorov-Smirnov tests were performed. Overall failure rates of these tests were in the range of 55 to 60% at the 5% level of significance. With failure rates 10 times that expected, correlation of failures with the various known parameters was not attempted.

It appears that the distributions of vibratory stress additions found applicable for the small cargo ships of Reference 1 are not overwhelmingly attractive assumptions in the cases of the FOTINI-L and the SL-7.

TABLE C-11

Summary of Tests for Fit to the Rayleigh Distribution of Dynamic Increments to Tension Found in the SL-7 Data Sub-Set

Grouping	No. of Tests	Failure Rate on Maximum Value (10% Expected)	Failure Rate on Chi-Square Tests (5% Expected)
All Intervals	192	39%	39%
Nominal Head Seas	30	90%	70%
Bow Seas	62	45%	50%
Beam Seas	22	27%	23%
Qtr. Seas	54	18%	18%
Follow. Seas	23	17%	35%
Rms Stress < 1.0	54	20%	44%
1.0 < 2.0	81	50%	37%
> 2.0	57	37%	35%
Low Frequency Contribution to Variance			
Less than 4%	65	76%	61%
4 to 9%	14	21%	21%
9 to 16%	10	40%	40%
16 to 25%	7	29%	43%
Over 25%	95	17%	25%

TABLE C-12

Summary of Tests for Fit to the Rayleigh Distribution of Dynamic Increments to Compression Found in the SL-7 Data Sub-Set

Grouping	No. of Tests	Failure Rate on Maximum Value (10% Expected)	Failure Rate on Chi-Square Test (5% Expected)
All Intervals	192	48%	46%
Nominal Head Seas	30	96%	91%
Bow Seas	62	53%	67%
Beam Seas	22	36%	32%
Qtr. Seas	54	31%	9%
Follow. Seas	23	26%	37%
Rms Stress < 1.0	54	35%	50%
1.0 < 2.0	81	58%	52%
> 2.0	57	47%	33%
Low Frequency Contribution to Variance			
Less Than 4%	65	82%	82%
4 to 9%	14	50%	64%
9 to 16%	10	50%	20%
16 to 25%	7	57%	57%
Over 25%	95	24%	20%

AD-A072 910 ROSENBLATT (M) AND SON INC NEW YORK F/G 13/10
EXAMINATION OF SERVICE AND STRESS DATA OF THREE SHIPS FOR DEVEL--ETC(U)
APR 79 J F DALZELL, N M MANIAR, M W HSU N00024-75-C-4324
UNCLASSIFIED SSC-287 NL

3 OF 3
ADA 072910

END
DATE FILMED
9-79
DDC

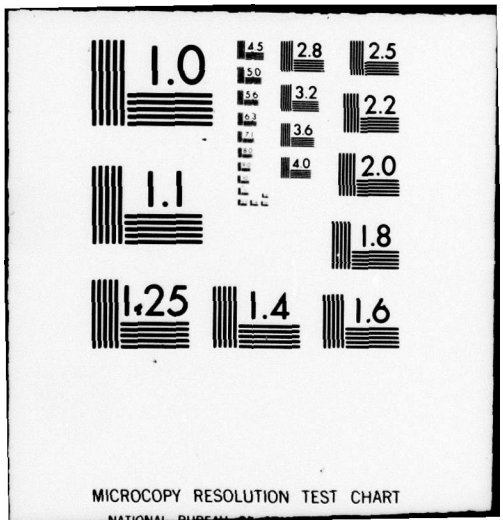
1.0
1.1
1.25
1.4
1.6
1.8
2.0
2.2
2.5
2.8
3.2
3.6
4.0
4.5
5.0
5.6
6.3
7.1
MICROCOPY RESOLUTION TEST CHART

Independence of Wave-Induced Main Extremes and Dynamic Increments in the Short Term

One of the operations in the background work to Reference 1 was an examination of the correlation of slam-induced stresses with wave-induced stresses for a small cargo ship. It was of interest to perform a somewhat parallel investigation in the current case. In previous work herein, it was found that the maximum vibration amplitude tends to increase with wave severity. If the vibration is a direct result of individual wave cycles it would be more or less expected that the dynamic increment to wave-induced stress would vary in the short term with the magnitude of wave-induced main extremes.

The simplest first check on the short-term interdependence of the wave-induced main extremes and the dynamic increments is to compute the correlation coefficients of the data for each record. This was done for all the good records in the SL-7 and FOTINI-L data sub-sets. The great majority of the correlation coefficients computed were within the range $\pm$ 0.20 with the largest magnitude in either data set being about 0.5.

This result suggested that the dynamic increments and the wave-induced main extremes tended to be independent in the short term. A further check on this was attempted by means of standard contingency table analysis techniques (Reference 38,39). In order to avoid the problems which arise because the short-term distributions of neither the dynamic increments or the main extremes are known with any certainty the distribution-free approach suggested in Reference 39 was used. This approach amounts to finding the median of the increments and main extremes in each record and then classifying each of the increment-main extreme pairs into one of four classes: 1) both elements above their respective medians, 2) both below, 3) the first of the pair above, the second below, and 4) the reverse of third category. The result of this operation is the number of pairs falling in each cell of a 2 x 2 contingency table which may be analyzed with standard methods. In these methods, the hypothesis is made that the two sets of data are independent; a statistic is computed, which is approximately Chi-Square distributed with one degree of freedom in the case of a 2 x 2 table, and the acceptance or rejection of hypothesis is made in much the same way as described for the goodness-of-fit tests in Appendix C-5.

The results of carrying out this procedure on all good records in the SL-7 data sub-set were that the hypothesis of independence of increments to tension and main tensile extremes was rejected in only 9% of the records at the 5% level of significance. The corresponding rejection rate of increments to compression and main compressive extremes was 12%. In the case of FOTINI-L, the rejection rates at the 5% level of significance were 14% for tension and 26% for compression. As in the previous tests, an approximately 5% rejection rate at the 5% level of significance can be accepted as the result of variability. An inspection of the details of the results disclosed that highly significant failures (corresponding to levels of significance below 2% say) were involved in less than half the total, and that in about half the cases of failure, the vibratory stress levels were extremely low.

If the failures for extremely low-stress levels are discounted, the rejection rates for the SL-7 data may be considered in line with that expected, and it seems reasonable to accept the proposition that the dynamic increments and wave-induced main extremes in the SL-7 data are statistically

independent in the short term. On the same basis, the short-term independence of dynamic increments to tensions and main extremes in tension for the FOTINI-L may be accepted. Independence of compressive increments and compressive main extremes in the case of FOTINI-L is apparently a more tenous assumption.

Short-Term Distribution of Combined Stresses

Concurrent with the investigation of wave-induced main extremes noted in Appendix C-4, it was convenient to test the main extremes of combined stress (T_R,C_R, Figure C-31) for fit to Rayleigh distribution. This was carried out on the possibility, as asserted in Reference 40 on the basis of a fairly elaborate phase-plane argument, that the main extremes as derived herein follow the Rayleigh distribution regardless of spectral broadness. The tests were carried out in an identical manner to those described in Appendix C-4. Failure rates of the tests on the SL-7 combined stress main extremes were very nearly the same as those shown in Tables C-4 and C-5 for the wave-induced main extremes. Overall failure rates for the combined-stress main extremes of the FOTINI-L data were in the neighborhood of 50%; a significant increase over those shown for wave-induced main extremes in Table C-6. Including the vibration of the FOTINI-L data produces an apparent broad-band process. The results do not bear out the philosophy of Reference 40.

Another possible approach to the short-term distribution of combined-stress amplitudes is to consider the combined stress as a zero mean Gaussian process which is the sum of two like processes, the wave-induced stress and the vibratory stress. (This is the point of view implied in the analysis of short-term vibration in Appendix C-6).

As in the case of the increments to stress, it was convenient to investigate this assumption concurrently with the tests of the SL-7 wave-induced maxima against the CLH distribution, Appendix C-4. The procedure involved finding all the maxima and minima of the combined-stress records in the SL-7 data sub-set. The results were decimated to reduce serial correlation, a fit to the CLH distribution was made, and the Chi-Square, and Kolmogorov-Smirnov tests as well as the tests on the extreme in the sample were carried out as in Appendix C-4.

The first result of the procedure was not too surprising. Ninety-four percent of the fitted broadness parameters were above 0.8, the remaining six percent were between 0.7 and 0.8. The fitted values of RMS and broadness parameters appeared symmetrical in that the values derived from maxima and minima were nearly the same. The overall failure rates of the Chi-Square tests at the 5% level of significance were 9% for maxima and 12% for minima. Those for the Kolmogorov-Smirnov tests were 3% for maxima and 5% for minima. There were no particularly significant differences in failure rate between head or bow seas and quartering or following seas. The failure rates of the goodness-of-fit tests are near enough to that expected, and the broadness parameters are so high in general that the results imply that the short-term maxima and minima of the combined stresses in the SL-7 data sub-set are generally nearly normally distributed.

On the other hand, the tests on the sample extremes of the short-term minima (compressive stress or sagging moment) implied a somewhat different conclusion. The overall failure rates on the tests on the extremes of the samples were 32% for combined minima and 15% for combined maxima. The former is three times the rate expected. In the tests on sample extremes, there are four possible modes of failure: the largest element of the sample can be either larger or smaller than expected , as can the smallest element in the sample. It was found that the failure mode in the tests on extremes of the minima was such that the largest value was larger than expected in 80% of the failures. (The largest compressive (sagging) combined stress was larger than expected). These failures were, moreover, concentrated in the head and bow-sea cases and in the severest nominal weather in the data sub-set. The implication is that while the combined maxima may be nearly normally distributed, severe wave-induced vibratory response may upset the upper "tail" of the distribution. This indication is consistent with the analysis of the isolated vibration in Appendix C-6. There, it was found that the maximum vibration was also fairly consistently higher than expected relative to the RMS vibration.

As has been noted previously, the idea that the RMS combined stress may be synthesized in the short-term by adding the squares of RMS wave-induced stress and vibratory stress is most attractive. The results for the SL-7 just cited are encouraging in this respect, at least for average conditions. However, the data do not provide a very good check on the idea of addition because the difference between process RMS wave-induced stress computed from the data and the correspondingly computed process RMS combined stress are extremely small.

Statistical Relationships Between the Maximum Vibration Double Amplitudes and the Maximum Dynamic Increments in Each Record

Since the prospects for the synthesis of the combined stresses in the short-term for the two ships appeared mixed at best, it was of interest to investigate possible relationships between the maximum vibration double amplitude in each record and the maximum dynamic increments.

The results in Appendix C-6 include empirical approximations to the distribution of the maximum double amplitude of (isolated) vibration in the relatively long term (over the data bases for each ship). If the data sub-sets for each ship are reasonable samplies of the long-term situation (as suggested in Appendix C-1), then it might be hoped that relationships between maximum vibration double amplitudes and maximum dynamic increments observed in the data-sub-sets would be applicable in the long term.

Perhaps the most conservative attitude in developing the extremes of combined stress in a record is to postulate that half the (isolated) maximum vibration double amplitude is added to the maximum main extremes of wave-induced tension and compression . If this is true, the maximum dynamic increments to wave-induced stresses would be equal in magnitude to half the vibration double amplitude. Thus, half the maximum vibration double amplitude appears to be a reasonable scaling parameter for the maximum dynamic

increments to stress. Similarly, a reasonable scaling parameter for the wave-induced main extremes which are associated with the maximum dynamic increments in the record appeared to be the maximum wave-induced main extremes in the record.

The procedure implied above was carried out upon each valid record in the data sub-sets for both the SL-7 and the FOTINI-L. For each record, the maximum dynamic increments to tension and compression were found and divided by half the maximum vibration double amplitude in the record. To each of these maximum increments there corresponded wave-induced main extremes. These main extremes in tension and compression were divided by the maximum wave-induced main extremes in the record.

The first question to try to answer from the above results was that of the relative magnitude of maximum dynamic increments. Histograms were formed for each of the two data sub-sets of the ratio: (the maximum dynamic increment) half the maximum vibration double amplitude). These results are shown in Figure C-34 for the FOTINI-L and in Figure C-35 for the SL-7.

Considering the results for the FOTINI-L, Figure C-34, it appears that the maximum increment to tension or compression may be expected to range from about 0.5 to 1.2 times half the maximum vibration double amplitude. The most probable value of the ratio appears to be about 0.9. Since there is no guarantee that the maximum vibration double amplitude as derived from data involves a symmetrical oscillation, the ratio need not be unity or less. It should be noted that the 3% of records which produced the non-zero histogram values between ratios of 1.3 and 1.6 involved very low overall stress magnitudes or very low level vibration, and accordingly their validity is discounted. On the whole, the results in Figure C-34 for the FOTINI-L suggest that it would not be terribly conservative to assume that the maximum dynamic increment to tension or compression in a record is approximately equal to half the maximum vibration double amplitude.

The corresponding results for the SL-7 (Figure C-35) show that the maximum increment to tension or compression may be expected to range from about 0.5 to 1.3 times half the maximum vibration double amplitude. The few records which produced non-zero values of the histogram between ratios of 1.3 and 1.6 involve low stress levels and, as in the case of the FOTINI-L, are discounted. The shape of the histogram for the SL-7 (Figure C-35) is clearly different from that for the FOTINI-L (Figure C-34). The most probable value of the SL-7 maximum dynamic increment ratio appears to be slightly lower but the dispersion appears greater. In about 25% of the records the maximum dynamic increment to tension or compression was greater than half the maximum vibration double amplitude. It appears reasonable to assume that the differences in shape of the histograms for the two ships reflect the probable differences in origin of the vibration. (Springing for FOTINI-L slamming or flare shock for the SL-7).

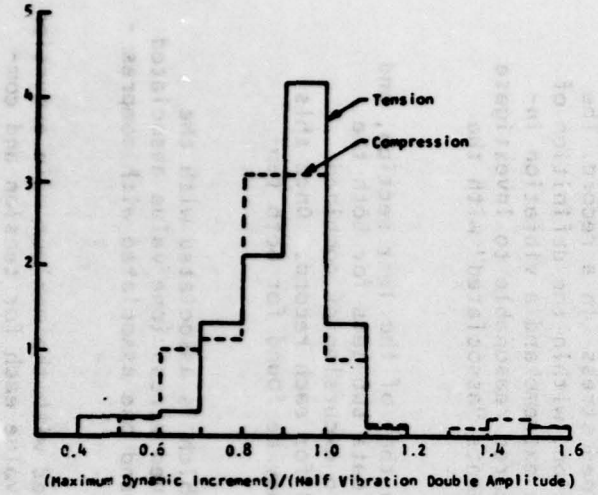

Figure C-34 FOTINI-L Data Sub Set, Histogram of the Ratio: (Maximum Dynamic Increment)/(Half the Maximum Vibration Double Amplitude).

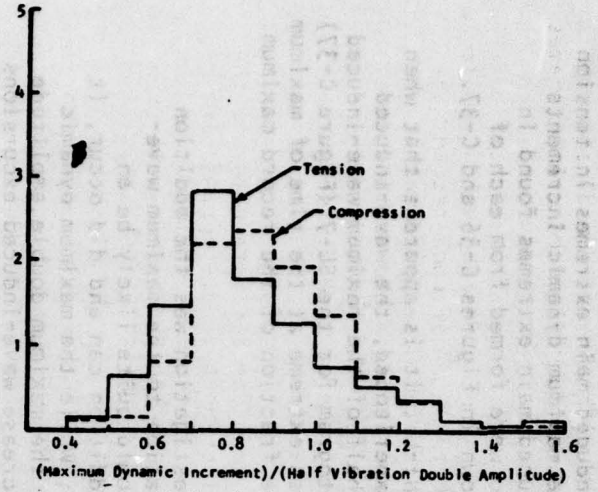

Figure C-35 SL-7 Data Sub-Set, Histogram of the Ratio: (Maximum Dynamic Increment)/(Half the Maximum Vibration Double Amplitude)

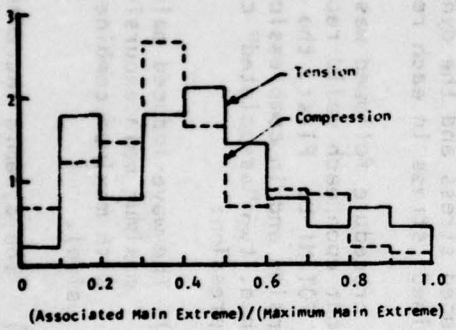

Figure C-36 FOTINI-L Data Sub-Set, Histogram of the Ratio: (Wave-Induced Main Extreme Associated with the Maximum Dynamic Increment)/Maximum Wave-Induced Main Extreme).

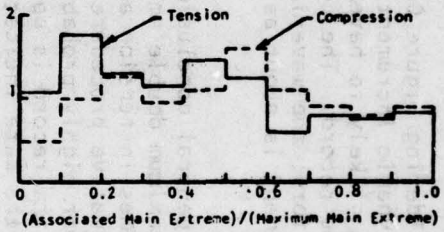

Figure C-37 SL-7 Data Sub-Set, Histogram of the Ratio: (Wave-Induced Main Extreme Associated with the Maximum Dynamic Increment)/(Maximum Wave-Induced Main Extreme)

The next part of the maximum combined stress problem is the question of the magnitudes of wave-induced main extremes when the maximum dynamic increments occur. As previously noted, the wave-induced main extremes in tension and compression which were associated with the maximum dynamic increments were found and divided by the maximun wave-induced main extremes found in the record. Histograms of the resulting ratio were formed from each of the two data sub-sets, and the results are shown in Figures C-36 and C-37.

Considering Figure C-36 for the FOTINI-L , it is apparent that when the maximum dynamic increment to stress was experienced, the wave-induced stress was most likely to have been less than half of the maximum wave-induced extreme in the record. The corresponding histogram for the SL-7 (Figure C-37) is nearly uniform; the wave-induced main stress extreme at the time of maximum dynamic increment is about as likely to be one fraction of the record maximum as another.

The general conclusion from this investigation was the addition of half the maximum double amplitudes of vibration to the maximum wave-induced extremes in tension and compression would quite likely be an overly conservative procedure. Though this addition can and did occur, it does not appear highly probable. Essentially, while the maximum dynamic increment in the record is approximately half the maximum double amplitude of vibration, the data indicate that it may increase wave-induced excursions of any magnitude.

The Composition of the Maximum Combined Stress in the Record

The results of the last section implied that perhaps the problem was not being approached from an advantageous direction. In the present context, the real interest is in the maximum combined stress in a record. The maximum combined stress in tension or compression, within the definition of Figure C-31, is the sum of a wave-induced main extreme and a vibration induced dynamic increment. Accordingly, it appeared reasonable to investigate the wave-induced stress and the dynamic increments "associated" with the maximum combined stress in each record.

The procedure followed was similar to that of the last section, and was carried out upon each valid record in the data sub-sets for both the SL-7 and the FOTINI-L. First, the maximum main excursion of combined stress in tension and in compression was found for each record. Once this is accomplished, two "associated" components may be found for both tension and compression:

1) The wave-induced main extreme which is associated with the maximum main excursion of combined stress (one value associated with maximum combined tension, and one associated with compression).

2) The dynamic increment associated with the maximum main excursion of combined stress (again, one value each for tension and compression).

The sum of items 1) and 2) for tension and compression is, by definition the maximum main extreme of combined tensile or compressive stress in the record. In order to compare the results from all records; the associated wave-induced extremes in tension and compression were divided by the maximum wave-induced main extremes found in the record; and the associated dynamic increments were divided by half the maximum isolated vibration double amplitude.

As before, histograms of the various ratios were formed for each of the two data sub-sets. Figures C-38 for the SL-7 and C-39 for the FOTINI-L indicate the statistics of the ratio of the wave-induced main extremes associated with maximum combined stresses, to the maximum wave-induced main extremes in the record.

In the case of the SL-7, Figure C-38, the conclusion is obvious. In about 95% of all records in the data sub-set, the wave-induced main extreme associated with the maximum combined stress is either within 5% of the maximum wave-induced main extreme in the record or exactly equal to it. (Actually, the associated wave-induced main extreme and the maximum were identical in 85% of the data sub-set). No values of the ratio were found to be less than 0.85. The results indicate that, with very little conservatism, the maximum combined stress in a record could be generally assumed to result from the addition of vibration to the maximum wave-induced stress.

The situation for the FOTINI-L, Figure C-39, is similar but not as clear cut. In about 65% of the records in the data sub-set, the wave-induced main extreme associated with the maximum combined stress is within 10% of the maximum wave-induced main extreme in the record. The detailed results show that the associated wave-induced main extreme and the record maximum were identical in about 50% of the data sub-set. In the case of the FOTINI-L, the assumption appears within reason, though somewhat conservative, that the maximum combined stress in a record is, in general, the result of the addition of vibration to the maximum wave-induced stress.

The corresponding histograms of the dynamic increments associated with the maximum combined stress main extremes are shown in Figures C-40 and C-41. In the case of the FOTINI-L, Figure C-40, the ratio of the associated dynamic increment to half the maximum vibration double amplitude scatters reasonably uniformly between zero and just above unity. The two records in the data set which produced ratios between 1.2 and 1.3 involved very low stress levels and are discounted as before. The results for the SL-7, Figure C-41, show a reasonably uniform distribution of ratios between zero and about 0.7, and a lessening of incidence of higher ratios. Figures C-40 and C-41 suggest that it may be reasonable to assume that the ratio of the associated dynamic increment to half the maximum vibration double amplitude is uniformly distributed between zero and about 1.1 for both ships. As may be noted from the figures, the assumption is conservative, but not overly so.

*U.S. GOVERNMENT PRINTING OFFICE: 1979-281-568/137

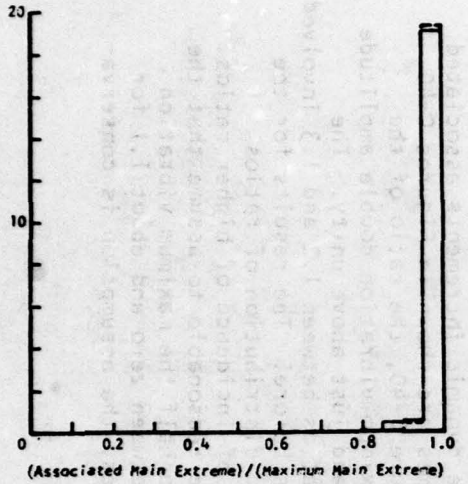

Figure C-38 SL-7 Data Sub-Set, Histogram of the Ratio: (Wave-Induced Main Extreme Associated with the Maximum Combined Stress)/ Maximum Wave-Induced Main Extreme)

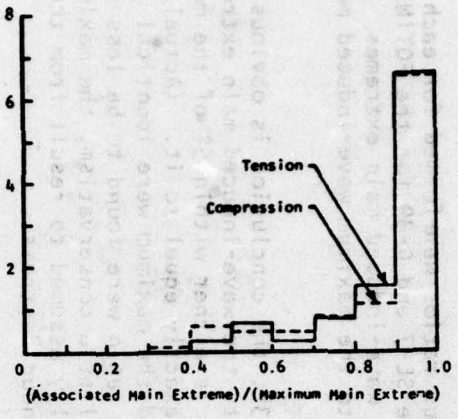

Figure C-39 FOTINI-L Data Sub-Set, Histogram of the Ratio: (Wave-Induced Main Extreme Associated with the Maximum Combined Stress)/(Maximum Wave-Induced Main Extreme)

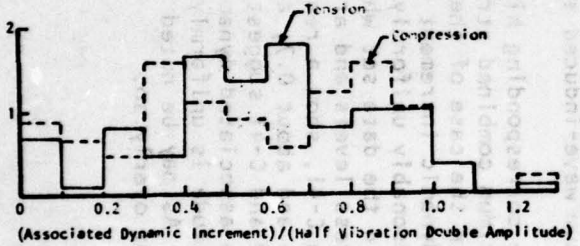

Figure C-40 FOTINI-L Data Sub-Set, Histogram of the Ratio: (Dynamic Increment Associated with the Maximum Combined Stress)/(Half of the Maximum Vibration Double Amplitude)

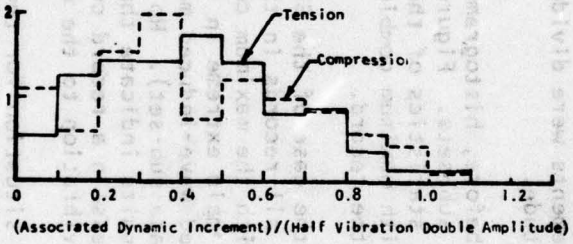

Figure C-41 SL-7 Data Sub-Set, Histogram of the Ratio: (Dynamic Increment Associated with the Maximum Combined Stress)/(Half the Maximum Vibration Double Amplitude)

SHIP RESEARCH COMMITTEE
Maritime Transportation Research Board
National Academy of Sciences-National Research Council

****

The Ship Research Committee has technical cognizance of the interagency Ship Structure Committee's research program:

Mr. O. H. Oakley, Chairman, *Consultant, McLean, VA*
Mr. M. D. Burkhart, *Naval Oceanography Division, Department of the Navy, Washington, D.C.*
Dr. J. N. Cordea, *Senior Staff Metallurgist, ARMCO INC., Middletown, OH*
Mr. D. P. Courtsal, *Vice President, DRAVO Corporation, Pittsburgh, PA*
Mr. W. J. Lane, *Consultant, Baltimore, MD*
Mr. A. C. McClure, *Alan C. McClure Associates, Inc., Houston, TX*
Dr. W. R. Porter, *Vice Pres. for Academic Affairs, State Univ. of N.Y. Maritime College*
Prof. S. T. Rolfe, *Civil Engineering Dept., University of Kansas*
Mr. R. W. Rumke, *Executive Secretary, Ship Research Committee*

****

The Ship Design, Response, and Load Criteria Advisory Group prepared the project prospectus, evaluated the proposals for this project, provided the liaison technical guidance, and reviewed the project reports with the investigator:

Mr. W. J. Lane, Chairman, *Consultant, Baltimore, MD*
Prof. A. H.-S. Ang, *Dept. of Civil Engineering, University of Illinois*
Prof. S. H. Crandall, *Dept. of Mech. Engrg., Massachusetts Inst. of Technology*
Mr. L. R. Glosten, *L. R. Glosten Associates, Inc., Seattle, WA*
Mr. P. M. Kimon, *EXXON International Company, N.J.*
Dr. O. H. Oakley, Jr., *Project Engineer, GULF R&D Company, Houston, TX*
Prof. R. H. Scanlan, *Dept. of Civil & Geological Engrg., Princeton University*
Prof. H. E. Sheets, *Chairman, Dept. of Ocean Engrg., Univ. of Rhode Island*
Mr. J. E. Steele, *Naval Architect, Quakertown, PA*

****

SHIP STRUCTURE COMMITTEE PUBLICATIONS

These documents are distributed by the National Technical Information Service, Springfield, Va. 22151. These documents have been announced in the Clearinghouse journal U. S. Government Research & Development Reports (USGRDR) under the indicated AD numbers.

SSC-272, *In-Service Performance of Structural Details* by C. R. Jordan and C. S. Cochran. 1978. AD-A057212.

SSC-273, *Survey of Structural Tolerances in the U.S. Commercial Ship-Building Industry* by N. S. Basar and R. F. Stanley. 1978. AD-A057597.

SSC-274, *Development of an Instrumentation Package to Record Full-Scale Ship Slam Data* by E. G. U. Band and A. J. Euler. 1978. AD-A059549.

SSC-275, *The Effect of Strain Rate on the Toughness of Ship Steels* by P. H. Francis, T. S. Cook, and A. Nagy. 1978. AD-A059453.

SSC-276, *Fracture Behavior Characterization of Ship Steels and Weldments* by P. H. Francis, T. S. Cook, and A. Nagy. 1978. AD-A058939.

SSC-277, *Original Radar and Standard Tucker Wavemeter SL-7 Containership Data Reduction and Correlation Sample* by J. F. Dalzell. 1978. AD-A062394.

SSC-278, *Wavemeter Data Reduction Method and Initial Data for the SL-7 Containership* by J. F. Dalzell. 1978. AD-A062391.

SSC-279. *Modified Radar and Standard Tucker Wavemeter SL-7 Containership Data* by J. F. Dalzell. 1978. AD-A062393.

SSC-280, *Results and Evaluation of the SL-7 Containership Radar and Tucker Wavemeter Data* by J. F. Dalzell. 1978. AD-A062392.

SSC-281, *Bibliography for the Study of Propeller-Induced Vibration in Hull Structural Elements* by O. H. Burnside and D. D. Kana. 1978. AD-A062996.

SSC-282, *Comparison of Stresses Calculated Using the DAISY System to Those Measured on the SL-7 Containership Program* by H. Y. Jan, K. T. Chang, and M. E. Wojnarowski. 1979.

SSC-283, *A Literature Survey on the Collision and Grounding Protection of Ships* by N. Jones. 1979.

SSC-284, *Critical Evaluation of Low-Energy Ship Collision-Damage Theories and Design Methodologies - Volume I - Evaluation and Recommendations* by P. R. Van Mater, Jr., and J. G. Giannotti. 1979.

SSC-285, *Critical Evaluation of Low-Energy Ship Collision-Damage Theories and Design Methodologies - Volume II - Literature Search and Review* by P. R. Van Mater, Jr., and J. G. Giannotti. 1979.

SSC-286, *Results of the First Five "Data Years" of Extreme Stress Scratch Gauge Data Collection Aboard Sea-Land's SL-7's* by R. A. Fain and E. T. Booth. 1979.